TESTICULAR NEOPLASIA: FUNCTIONAL POLARIZATION OF MACROPHAGES AND DENDRITIC CELLS

INAUGURAL-DISSERTATION

submitted in partial fulfilment

of the requirements for the degree of

Dr.rer.nat./ Ph.D.

to the Faculty of Biology

at the Justus-Liebig-University, Giessen

as part of the joint award Ph.D. program

with Monash University

Submitted by

Dana Püschl,

M.Sc. (Biology) from Zeitz

Gießen, 2018

Mit Genehmigung des Fachbereiches Biologie
der Justus-Liebig-Universität Gießen
Dekan/Dean: Prof. Dr. Jürgen Janek_____

Gutachter/Reviewer:
Prof. Dr. Martin Bergmann

Gutachter/Reviewer:
Prof. Dr. Tina Trenczek

Tag der Disputation/date of disputation:

28.01.2019

TABLE OF CONTENTS

LIST OF FIGURES

CHAPTER 1

CHAPTER 2

CHAPTER 3

CHAPTER 4

ABBREVIATIONS

acc/decc acceleration/deceleration
ACTB ß-actin
AD assay diluent (ELISA)
AEC 3-Amino-9-Ethylcarbazole
AFP alpha fetoprotein
APC antigen-presenting cell
APES 3-aminopropyltriethoxysilane
BSA bovine serum albumin
CCL C-C motif ligand (chemokine)
CCR chemokine receptor
CD cluster of differentiation
cDP common dendritic cell progenitor
cDNA complementary DNA
CIS carcinoma in situ
Cq quantification cycle
Ct threshold cycle
DAB 3,3′-Diaminobenzidine
DAPI 4′,6-diamidino-2-phenylindole
DC dendritic cells
ddH2O Bidistilled water
DNA deoxyribonucleic acid
DNase deoxyribonuclease
dNTP deoxyribonucleosid triphosphate
EDTA ethylenediaminetetraacetic acid
FACS fluorescence-activated cell sorting
FasL Fas ligand
FCS fetal calf serum
g gram
GAPDH glyceraldehyde 3-phospate dehydrogenase
GCNIS germ cell neoplasia in situ
Gas6 growth arrest-specific 6
GILZ Glucocorticoid-Induced Leucine Zipper
h hour

HCC hepatocellular carcinoma
hCG human chorion gonadotropin
HE hematoxylin/eosin staining
HLA human leukocyte antigen
HMGB1 High mobility group box 1 protein
IDO Indoleamine-pyrrole 2,3-dioxygenase
IFNγ interferon gamma (cytokine)
IL interleukin (cytokine)
KO knock-out
L litre
ly lymphocytic infiltrate
µg microgram
µl microliter
µM micromolar
M-CSF macrophage colony-stimulating factor
MCT mast cell tryptase
mDC myeloid dendritic cells
MHC major histocompatibility complex
min minute
ml millilitre
mM millimolar
mRNA messenger RNA
NF-κB nuclear factor of kappa light polypeptide gene enhancer
NK natural killer
nsp normal spermatogenesis
PBMC peripheral blood mononuclear cells
PBS phosphate buffered saline
PCR polymerase chain reaction
PD-1 programmed cell death protein
PD-L1 programmed death-ligand 1
pDC plasmacytoid dendritic cells
PMA phorbol 12-myristate 13-acetate
ProS protein S
PGE2 prostaglandin E2

PTGES prostaglandin E synthase
rcf relative centrifugal force
RNA ribonucleic acid
RNase ribonuclease
RPLP0 60S ribosomal protein, large, P0
rpm revolutions per minute
RT reverse transcription
RT-PCR reverse transcription polymerase chain reaction
RT-qPCR reverse transcription quantitative polymerase chain reaction
Se seminoma
sec second
SOCS1 suppressor of cytokine signaling 1
STAT signal transducers and activators of transcription
TAE Tris-acetate EDTA buffer
TAM tumour-associated macrophages
TBS Tris-buffered saline
TC tumour cell
TGCT testicular germ cell tumour
TGF-β tumour growth factor beta (cytokine)
Th1 T helper cell type 1
Th2 T helper cell type 2
TIDC tumour infiltrating Dendritic cells
TIL tumour infiltrating lymphocytes
TLR Toll-like receptor
TIM-3 T cell Ig and mucin domain 3
TNFa tumour necrosis factor alpha (cytokine)
Treg T regulatory
Tris Tris(hydroxymethyl)-amino-methane
VEGF vascular endothelial growth factor (
vol. volume
W Watt
WB western blot
WT wildtype

CHAPTER 1

Literature Review

CHAPTER 1: Literature Review: The Contribution of Innate Immune Cells to Testis Function in the Healthy Testis and Testicular Neoplasia

INTRODUCTION

Dendritic cells (DCs) and macrophages are cells of the innate immune system that are the first responders in cases of inflammation caused by pathogens and other insults such as neoplasia. These are called antigen-presenting cells (APC), serving as sentinels that capture, recognise and phagocytise pathogens, with the capacity to process and present antigens on their surface via human leukocyte antigen (HLA) molecules (Palucka and Banchereau, 1999; Janeway, 2001; Steinman and Hemmi, 2006). The processed antigens can be presented to T-cells, leading to strong immune reactions by the activation of pathogen-specific lymphocytes that are part of the adaptive immune system (Janeway, 2001).

There are distinct subtypes of APCs; macrophages can be classified into classically activated M1 and alternatively activated M2 subpopulations, and their differentiation into one or the other depends on the local environment (Sica and Mantovani, 2012; Martinez and Gordon, 2014; Zhang et al., 2016). M1 macrophages typically produce high amounts of pro-inflammatory cytokines and are considered tumour-destructive (Sica et al., 2006; Sica et al., 2008 a)/b); Allavena et al., 2008; Biswas and Mantovani, 2010). In contrast, M2 macrophages can produce anti-inflammatory cytokines, promote angiogenesis and facilitate matrix remodelling that support tumour progression and metastasis (Sica et al., 2006; Sica et al., 2008 a)/b); Allavena et al., 2008; Biswas and Mantovani, 2010). M2 macrophages present in neoplastic tissue may be classified as tumour-associated macrophages (TAMs), which express CD163 and CD206 and modulate immune-suppressive properties by producing anti-inflammatory cytokines such as TGF-β and IL-10 (Grivennikov et al., 2010; Zhang et al., 2011; Mantovani et al., 2004; Martinez et al., 2008; Sica et al., 2006; Yang and Zhang, 2017). Importantly, in different cancer types in which these TAMs are detectable, their presence is primarily associated with poor patient outcomes (Yang and Zhang, 2017; Zhang et al., 2011; Ryder et al., 2008; Lee et al., 2008; Shieh et al., 2009). In human testicular germ cell cancers, TAMs have yet to be characterised, and Chapter 2 of this thesis presents a characterisation of these cells.

Immune privileged organs are defined as organs in which foreign tissue grafts are tolerated without evoking detrimental immune responses resulting in rejection (Streilein, 1995; Fijak & Meinhardt, 2006). Following this definition, the mammalian testis is an immune privileged site, where immune attack of meiotic and postmeiotic germ cells that first arise in puberty after self-tolerance has developed and is suppressed to support normal spermatogenesis (Fijak et al., 2018). In the human testis, resident M2 macrophages are important contributors to maintenance of the immune-suppressive local milieu through the secretion of anti-inflammatory cytokines, such as IL-10 and TGF-β (Zhao et al., 2014; Chapter 2). Remarkably, the functional polarization of M2 macrophages has been observed in associated with infections and tumours whereas in the human testis, M2 macrophages seem to be a resident immune cell type (Martinez et al., 2009; Cassetta et al., 2011; Zhao et al., 2014, Chapter 2).
In addition to the presence of macrophages, infiltrating DCs are commonly observed in cancers; the outcome for patients, either good or poor, depends on which DC subset is present (Tran Janco et al., 2015). Myeloid and plasmacytoid dendritic cells (pDC, mDC; described further in Sectons 1.3.3 and 1.3.4) are dendritic cell subsets that arise from myeloid progenitors that form common DC progenitors (CDPs), then give rise to pDCs and pre-DCs that are progenitors of these two myeloid subsets (Tran Janco et al., 2015). DC subsets, pDCs and mDCs, can induce different immune responses during an inflammation depending on environmental factors (Kadowaki, 2009). Different DC subsets have been reported to possess synergistic immune-stimulatory as well as immune-suppressive properties, due to the expression of regulatory molecules, receptors and their capability for cross-presentation, all of which are critical for an effective immune response (Haniffa et al., 2013; Mildner and Jung, 2014; Da Silva and Barton, 2016; Tran Janco et al., 2015).

This Chapter addresses the function of the testis as an immune-privileged organ, and describes the immune cells that are present and contribute to this unique environment. Furthermore, the features of different macrophage and DCs subsets and their functional polarization associated with testicular neoplasia, specifically GCNIS and seminoma, are discussed. Additionally, markers used to delineate DC and macrophage subsets are presented.

1.1 Introduction to cells of the innate and adaptive immune system

The immune system comprises a complex interaction of cells and molecules that serves as a protective mechanism against foreign substances, cells and pathogens, including bacteria, viruses and parasites (Murphy and Weaver, 2017). The immune system is divided into innate and adaptive response mechanisms (Fig. 1). Cells of the innate immune system are mast cells, macrophages, dendritic cells, natural killer cells (NK cells) and granulocytes (basophils, eosinophils and neutrophils), whereas cells of the adaptive immune system are B cells and T cells, NK cells and γδ T cells are defined as cells of both the innate and adaptive immune system (Fig. 1) (Dranoff et al., 2004). Innate immune system cells are predominantly derived from the myeloid lineage during hematopoiesis, whereas T cells and B cells are derived from the lymphoid lineage.

The adaptive immune system is characterized by immunological memories, a hallmark feature that leads to strong and antigen-specific immune reactions. The orchestrated reaction of all components is defined as an immune reaction. Immune reactions are orchestrated through antigen-antibody complexes, initiated by phagocytic cells that belong to the innate immune system which present antigens to T cells. The innate immune system can nonspecifically and rapidly develop immune responses against pathogens. It contains the complement system of soluble proteins, as well as phagocytic, antigen-presenting cells (APCs) (Fig. 1). For instance, macrophages as APCs differentiate in tissue from circulating monocytes. They can phagocytize, engulf and kill microorganisms by secreting digesting enzymes. Macrophages can release cytokines to recruit cells of both the adaptive and innate immune system and, thus, induce and maintain pathological processes such as inflammation (Winnall et al., 2011; Bhushan & Meinhardt, 2017). As part of immune responses against pathogens, macrophages act via their phagocytic capacity and production of pro-inflammatory molecules including cytokines. Similarly, DCs 'professionally' process and present antigens derived from engulfed pathogens on their surface via HLA molecules that can be recognized by naïve T cells (Janeway, 2001). Subsequently, adaptive immune reactions are induced that link responses of the innate and adaptive immune systems (Heuzé et al., 2013). Moreover, both macrophages and dendritic cells are involved in maintaining physiological tissue homeostasis (Davies et al., 2013; Wynn et al., 2013; Bhushan & Meinhardt, 2017).

In the light of the plasticity of their functions, the focus of this thesis is set on the role of macrophages and DCs in the human testis under physiological and pathological conditions, i.e. testis cancer development.

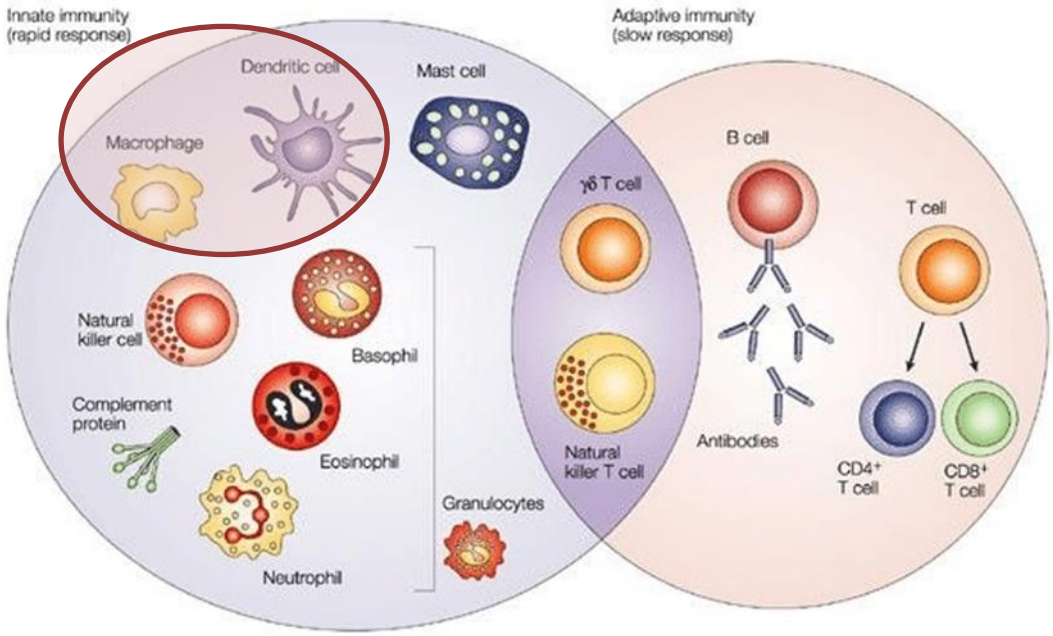

Fig. 1: Components of the innate and adaptive immune system. The mature immune system is divided into innate and adaptive immune responses. The innate immune system is comprised of mast cells, macrophages, dendritic cells, natural killer cells (NK cells) and granulocytes (basophils, eosinophils and neutrophils), whereas cells of the adaptive immune system are B cells and T cells; NK cells and γδT cells are defined as cells of both the innate and adaptive immune systems. Immune cells that are research subject in this thesis are highlighted by a red circle. Modified from Dranoff, 2004.

1.2 The testis under physiological conditions

1.2.1 The immune privilege of the testis

The mammalian testis has been identified as an immune privileged organ enabling normal germ cell development (Meinhardt and Hedger, 2011). Immune privilege is defined as a special immune environment with the capacity to suppress the rejection of foreign tissue grafts (Fijak et al., 2010; Meinhardt & Hedger, 2011; Fijak et al., 2017). Taking the key function of the immune system to recognize and respond to xeno-, allo- and autoantigens as well as the expression of autoantigens by meiotic and post-meiotic 96+germ cells into consideration, the testicular immunosuppressive

environment is essential to ensure normal germ cell development (Meinhardt and Hedger, 2011; Fijak et al., 2017).

Local immunoregulation in the testis is established through two key features, illustrated in Figure 2 and Figure 3. First, the meiotic and post-meiotic germ cells that first emerge with the onset of puberty are sequestered from direct contact with immune cells (Fig. 2). The testis is comprised of two distinct cellular compartments: the interstitial space, where steroidogenic Leydig cells, vasculature, lymphatics and immune cells are located, and the seminiferous tubules, where spermatogenesis occurs as spermatogonia develop into spermatozoa embedded in the epithelium formed by Sertoli cells (Fig. 2) (Zhao et al., 2014). Second, the secretion and expression of immunoregulatory molecules including cytokines, hormones and other signaling ligands collectively determines the local immune milieu. Somatic cells such as Leydig cells and Sertoli cells contribute to forming an immunosuppressive environment by expression of molecules including activin A, testosterone, programmed death ligand-1 (PDL-1), growth arrest-specific 6 (Gas6), protein S (ProS) and transforming growth factor β (TGF-β) (Fig. 3) (Zhao et al., 2014). In addition, immune cells, particularly macrophages, are central to preservation of the testicular immunosuppressive milieu. These typically display an immunosuppressive, M2 phenotype and produce anti-inflammatory cytokines, such as IL-10 and TGF-β (Zhao et al., 2014; Bhushan and Meinhardt, 2017; see Chapter 2& 3). Spermatogenic cells can also contribute to the immune suppressive environment by the expression of FasL which can bind the Fas-receptor on T-lymphocytes to induce apoptosis in these cells and thus prevent a strong immune reaction against germ cells (Zhao et al., 2014). Thus, germ cell development is supported by the actions of immune cells in a healthy testis due to these immunosuppressive mechanisms.

In contrast, breakdown of the (local) tolerance towards germ cells results in vigorous autoimmune reactions (autoimmune orchitis) mediated by cells of the adaptive immune system (Fijak et al., 2018). Clinical conditions such as infectious orchitis demonstrate that the testicular immune privilege does not preclude innate and specific immune responses causing inflammation and subsequent infertility (Fijak et al., 2018). Moreover, testicular cancer is associated with impairment of the physiological immune environment as reflected by influx of non-resident immune cells and altered local cytokine and chemokine expression (Klein et al., 2016; Loveland et al., 2017).

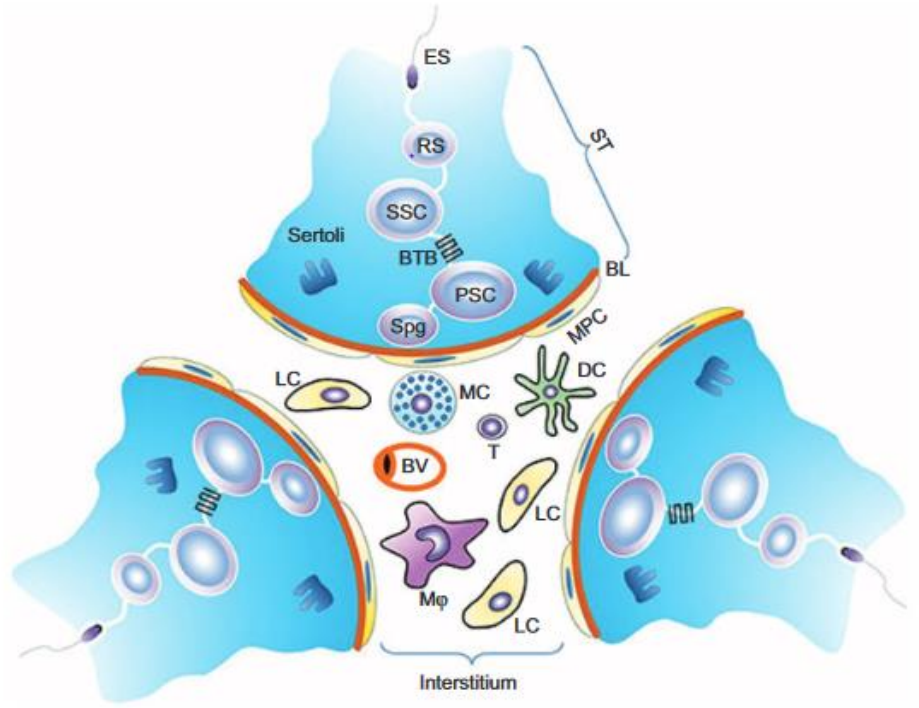

Fig. 2: Schematic of the testis. The testis is compartmentalised into the seminiferous tubules with the germinal epithelium (ST) and the interstitial compartment. This compartmental division is required to allow germ cell development and avoid autoimmune attack against germ cell-specific autoantigens that are first expressed at the onset of puberty. In the seminiferous epithelium, germ cell development takes place, with spermatogonia, spermatocytes, round and elongated spermatids enclosed by Sertoli cells which are the key structural element of the adult seminiferous tubule. Adjacent Sertoli cells are connected by tight junctions which form the blood-testis barrier (BTB) that functionally divides the seminiferous epithelium into the basal and adluminal compartments. The BTB sequesters autoantigens of maturing germ cells from immune cells. In addition to the immune suppressive cytokine milieu, the immune privileged state is preserved by this complementary mechanism. BL, basal lamina; BTB, blood testis barrier; ES, elongated spermatid; MPC, myoid peritubular cell; PSC, primary spermatocyte; RS, round spermatid; SPG, spermatogonia; SSC, secondary spermatocyte; ST, seminiferous tubule. From Zhao et al., 2014.

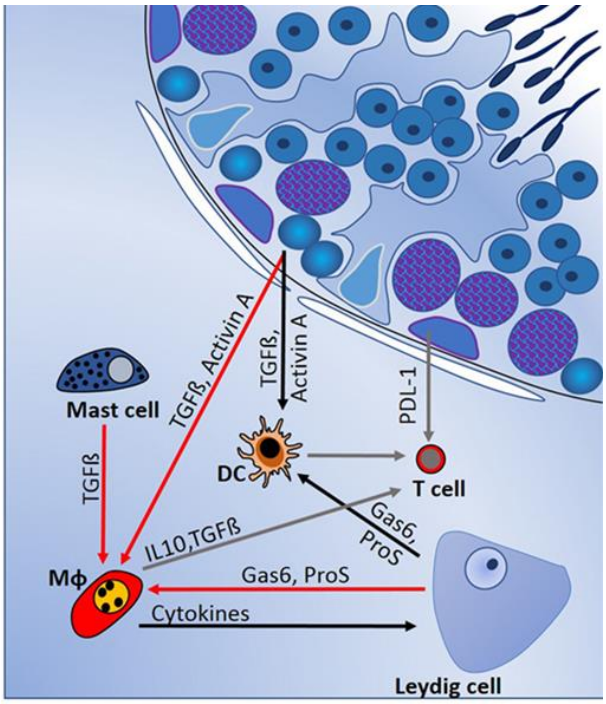

Fig. 3: Regulation of immune responses in the testis is mediated by a combination of structural and cellular-derived factors. Production of cytokines and other immuno-regulatory molecules by interacting cell types (mast cells, dendritic cells (DC), T cells, macrophages (Mφ), and Leydig cells) in the testicular interstitial space creates a complex immuno-regulatory environment, as outlined in the text. From Loveland et al., 2017.

1.2.2 Contribution of testicular macrophages and other immune cells to the immune privilege of the testis

The human testis contains a wide variety of immune cells that bear cell-specific markers, namely mast cells (tryptase), macrophages (CD68, CD163, CD206), T-lymphocytes (CD3, CD4, CD8, Foxp3), and dendritic cells (CD11c) (Frungieri et al, 2002, Hvarness, 2013, Klein et al., 2016; additional data presented in Chapter 2). Within the myeloid lineage, DCs and macrophages can be distinguished by the expression of specific surface markers. In the human testis, phenotypically different macrophage populations with distinct marker subsets have been identified: macrophages which express CD68 (lysosomal glycoprotein) or CD163 (cell surface glycoprotein member of the scavenger receptor cysteine-rich superfamily) and CD206 (mannose receptor, c-type lectin) (Frungieri et al, 2002; Klein et al., 2016; Zheng et al., 2016; see Chapter 2).

Macrophages can be classified into either M1, as classically-activated macrophages (pro-inflammatory properties) or M2, as alternatively activated macrophages (anti-

inflammatory properties). The differentiation into one or the other phenotype depends entirely on various signals (Sica and Mantovani, 2012; Martinez and Gordon, 2014).
In contrast to knowledge of macrophage biology in rodents, the mechanisms that underpin functional polarization into M1 and M2 macrophages in the human testis have yet to be elucidated. Unfortunately, the identification of macrophage subsets is challenging, since the presence of various macrophage markers (CD45, CD11c, CD68, CD163, CD206), cytokines (TNF-a, IL-12, IL-10, TGF-β) and chemokine receptors (e.g. CCR2) can overlap with their expression in other immune cell types. As a result, more than one marker should be used for an assured identification of macrophage and DCs subsets.
DeFalco et al. analysed macrophage populations in adult mice and revealed two different macrophage populations, interstitial-localized (CSF1R+, MHCII-) and peritubular-localized (CSF1R-, MHCII+) macrophages which are distinguished by the presence or absence of MHCII and the level of the receptor for cytokine stimulating factor, CSF, using both immunofluorescence and flow cytometry (DeFalco et al., 2015). Since acute depletion of CX3CR1+ macrophages in the adult testis led to reduction in the proliferation and differentiation of spermatogonia, DeFalco hypothesized that the peritubular macrophages serve a specific role in maintenance of spermatogonial stem cells due to their localisation in close proximity and their synthesis of CSF. Subsequent work using a CX3CR1 transgenic mouse model that expresses a green fluorescence protein reporter construct confirmed these observations, providing additional evidence to classify the interstitial MCSFR+/MHCII− macrophages as immune suppressive cells that express immunosuppressive genes, respectively, and peritubular M-CSFRlo/MHCII+ expressing alternative M2-type activation genes (Mossadegh-Keller et al., 2017). These outcomes indicate that peritubular macrophages are able to present antigens, in contrast to the interstitial macrophages which do not express MHCII molecules required for antigen presentation. Therefore, interstitial macrophages might be immunosuppressive and lack the capacity to activate other immune cells, such as T-cells which belong to the adaptive immune system. Such dual roles for testicular macrophages remain to be elucidated in the human.
In addition to macrophages, CD11c+ DCs are present in the human testis (Klein et al., 2016; Zheng et al., 2016; data presented in Chapter 2). Additionally, Zheng et al. showed the presence of cells with different DC markers, such as CCR6, DC-SIGN, CD1a+/CD207+ and CD123+/BDCA-2+ (CD303), sparsely distributed within the in-

terstitial compartment of the normal human testis (Zheng et al., 2016). However, the functions of DCs in the human testis under physiological conditions are not yet understood (Klein et al., 2016; Zhao et al., 2014). Existing data indicate that these DCs are immature, based on detection of specific, single markers such as CCR6, DC-SIGN, CD1a (Zheng et al., 2016). These findings are in agreement with observations in rats, where testicular DCs are not able to activate lymphocytes under normal conditions (Guazzone et al., 2011). Nevertheless, in man, the numbers of DCs and T-lymphocytes are very low in comparison to rat or mice testes (Pöllänen, 1993; Rival et al., 2006, Pérez et al., 2013; Klein et al., 2016; Zheng et al., 2016). This suggests that some functionalities of testicular immune cells vary between species.

1.2.3 The immunosuppressive role of cytokines and chemokines in the testis

Cytokines exert control of immune cell functions, driving either immune-stimulatory or immune-suppressive reactions. Control of cytokine synthesis and activity is necessary, otherwise the immune system would produce an uncontrolled pro-inflammatory response, especially after an inflammatory insult. To regulate inflammation, cytokines and chemokines in the local environment can control macrophage phenotypes by differentiating them into pro-inflammatory (M1) or anti-inflammatory (M2) phenotypes (Sica and Mantovani, 2012). For instance, formation of M1 cells is typically promoted by pro-inflammatory interferon-γ, TNF-α and LPS, whereas M2 differentiation can be driven by IL-4 and IL-13. Additional factors are involved in the prevention and modulation of DC subsets and M2 formation, including vascular endothelial growth factor (VEGF), macrophage colony-stimulating factor (M-CSF), TGF-β, IL-10, IL-6, and prostaglandin E2 (PGE2) (Sica and Mantovani, 2012; Genin et al., 2015; Heusinkveld et al., 2011a); Gottfried et al., 2008). The adult mammalian testis has an immune-suppressive environment partly build by the presence of anti-inflammatory cytokines such as IL-10, TGF-β, and activin A (Zhao et al., 2014). Therefore, these cytokines can influence macrophage and DC polarization, and control their differentiation into different functional phenotypes in the testis to protect germ cells from autoimmune attack.

1.2.4 Complexity of signaling pathways: TGF-β and IL-10 influence pro-inflammatory cytokine expression

Testicular expression of the cytokines TGF-β and IL-10 is important to maintain the immunosuppressive environment. Both cytokines are known as negative regulators of pro-inflammatory cytokine synthesis, restricting production of key molecules such as IL-1, IL-2, IL-6, IL-12, IFN-γ, TNF-α, as well as MHCII molecules (Fig. 4, A/B) (Gratchev, 2017; de Waal Malefyt et al., 1993; Fiorentino et al., 1991; Steensberg et al., 2003; Couper et al., 2008), and thus they are generally known to have the capacity to resolve pro-inflammatory cytokine reactions (Yoshimura et al., 2003). TGF-β and IL-10 have been detected in the human testis as well as in testicular germ cell neoplasia, as described later in this thesis (Chapter 2). TGF-β has been shown to be associated with disease progression in lung and pancreatic cancer (reviewed by Miyazono et al., 2018). The capability of macrophage subsets to contribute to testicular germ cell tumour progression via their expression of TGF-β will be analysed in Chapter 3 and Chapter 4.

The transforming growth factor beta (TGF-β) superfamily of ligands consists of structurally related dimeric signalling molecules that exhibit the characteristic feature of signalling via transmembrane receptors that have intracellular serine/threonine kinase activity. There are three TGF-β isoforms: TGF-β1, -2, and -3, each with a homodimer of a distinct gene product (Lui et al., 2003). These proteins, produced by multiple cell types, are secreted by circulating monocytes and tissue macrophages (Assoian et al., 1987; Grotendorst et al., 1989). In the testis, TGF-β1 is produced by Sertoli cells, peritubular cells and immune cells (e.g. mast cells and resident macrophages) (Skinner and Moses, 1989; Pöllänen et al., 1988; Dobashi et al., 2002; Zhao et al., 2014). The TGF-β monomers feature 3 intermolecular disulphide bonds and dimerise through a separate single intermolecular disulphide bond. Monomers are synthesized with a 5’ pre-region that is cleaved following entry into the endoplasmic reticulum. The pro-region, which is directly attached to the mature ligand is cleaved after dimerization but remains associated with the TGF-β signalling protein. This ‘latency-associated peptide’ (also known as LAP) blocks interaction between TGF-βs and the receptors; these ligands are activated by environmental changes such as pH shifts that cause the LAP to dissociate (Harrison et al., 2011). After secretion, TGF-βs can bind to first a Type II receptor subunit, TβRII, and then to a Type 1 receptor moiety, TβRI (ALK5), ultimately forming a hetero-tetrameric receptor complex for ca-

nonical signalling (Sanz-Rodrigues et al., 2004; Chen et al., 2008; Gratchev, 2008; Loveland and Hedger, 2015). The binding of a TGF-β molecule enables the constitutively active type II receptors to recruit and phosphorylate type I receptors. Inside the plasma membrane, SMAD anchor for receptor activation (SARA) mediates presentation of the signal transducers Smad2 and/or Smad3 to the type I receptor kinase. The phosphorylation of Smads leads to a conformation change that causes dissociation of the type I receptor and SARA. Phosphorylated Smad2 and Smad3 form dimers (either homo- and hetero-dimers, depending on cellular context and signal input) that oligomerize with the co-Smad, Smad4. The trimeric complex translocates into the nucleus to activate various target genes through binding to co-factors that determine which signalling outcomes are effected (Hill, 2016).

TGF-β is widely regarded as a therapeutic target to inhibit inflammation (reviewed in Walton et al., 2017). It has also been reported to block the synthesis of pro-inflammatory target genes in macrophages (Fig. 4, A) (Gratchev, 2017). Additionally, in human kidney, TGF-βs can inhibit RANTES expression, which is necessary for expression of pro-inflammatory cytokines such as TNF-α (Dai et al., 2011). Other studies have reported that inhibition of pro-inflammatory cytokines such as IL-1, IL-2, IFN-γ and a reduction of MHCII molecules are mediated by TGF-βs (Ding et al., 1990; Dubois et al., 1990; Dong et al. 2001; Romieu-Mourez et al., 2007). A recent study provided evidence that, in human M2 macrophages with high levels of TGF-βRII, TGF-β can also activate the non-canonical Smad signaling pathway by activating Smad1/5, rather than Smad 2/3 (Gratchev, 2017). It is interesting to speculate that, during the progressive development of testicular neoplasia, an inhibition of Smad signaling pathways could affect anti-inflammatory cytokine expression, which in turn may increase local production of pro-inflammatory cytokines. Dias et al. (2009) have reported the upregulation of inhibitory Smads, as well as the activin A inhibitory inhibin and betaglycan molecules, within seminomas in a subset of patients, providing a rationale for further studies to test this hypothesis (Dias et al., 2009).

IL-10 is an anti-inflammatory cytokine, which has also been called “cytokine synthesis inhibitory factor” (CSIF), as it can influence immune cells (T-cells, macrophages) and alter cytokine expression. For example, IL-10 can be expressed by M2 macrophages and inhibit the production of the pro-inflammatory cytokines IL-1α/β, IL-6, IL-8, and

TNF-α (Fig. 4, B) (de Waal Malefyt et al., 1993; Fiorentino et al., 1991; Steensberg et al., 2003).

To effect signalling, IL-10 can bind to the extracellular domains of IL10R1, which dimerizes with IL10R2. In human T-cells and monocytes, cell surface binding of IL10 leads to recruitment of the cytoplasmic proteins, JAK1 and TYK2, which phosphorylate and thereby activate STAT1α and STAT3 (Finbloom and Winestock, 1995). STAT3 forms a homodimer that translocates into the nucleus to mediate transcriptional regulation of IL-10-responsive genes by high-affinity binding of the activated STAT to target genomic sequences.

The signalling pathway of IL-10 and other cytokines can vary between different immune cell subtypes, due to formation of STAT homo- and heterodimers; this is considered as an important mechanism for providing cell- and context-specificity for gene induction (Finbloom and Winstock, 1995; Zhang et al., 1995; Ma et al., 2015). Interestingly, STAT3 is also important in mice for activation of pro-inflammatory IL-6 signalling. STAT3 can induce the expression of SOCS3 that regulates various cytokine signaling pathways including that of IL-6 (O'shea and Murray, 2008). For both cytokines, STAT3 is required (Yasukawa et al., 2003). However, the IL-10 inhibitory effect of IL-6 has to be elucidated. SOCS3 feedback in mouse eye macrophages has also been shown to be permissive for IL10/STAT3 signalling that promotes alternative macrophage activation (M2) (Nakamura et al., 2015). A definite role for these factors in the immune-suppressive environment of the adult mammalian testis remains to be elucidated.

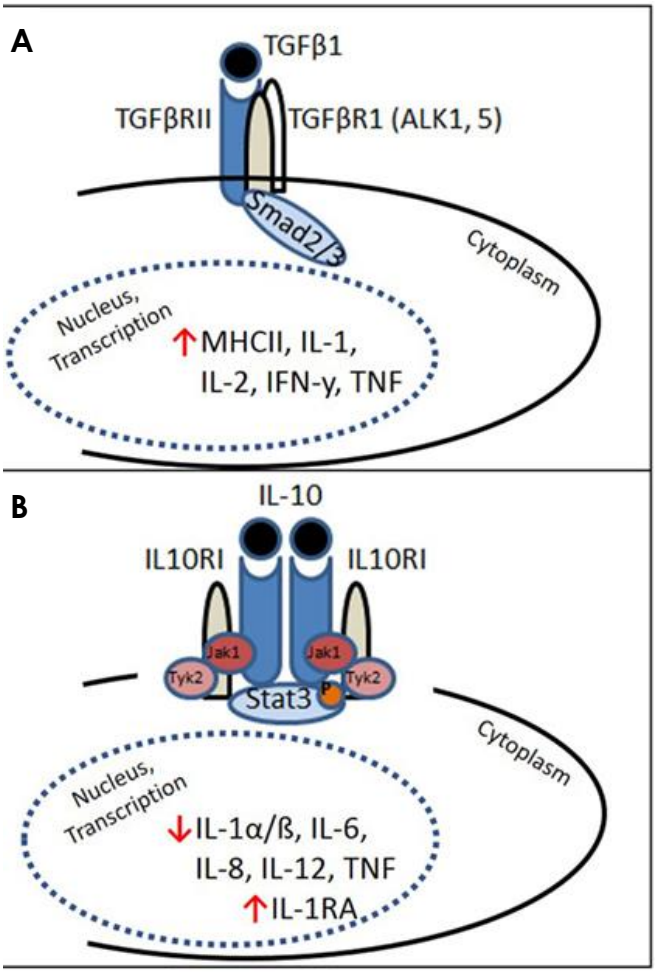

Fig. 4: Signaling pathways of TGF-β and IL-10. (A) TGF-β-signaling *via* Smads 2 and 3 suppresses pro-inflammatory cytokine production and reduces cell-mediated immunity. (B) IL10 actions, mediated *via* JAK–STAT signaling, inhibit pro-inflammatory cytokines and induce anti-inflammatory responses (e.g., IL1RA production). From Loveland et al., 2017.

1.2.5 Functional macrophage polarization by cytokines, chemokines and hormones

The testis as an immune-privileged organ has a specific immune-suppressive milieu partly provided by the local synthesis of anti-inflammatory cytokines including IL-10, TGF-β and activin A. These cytokines have the capacity to influence macrophage and DC differentiation into different functional phenotypes, depending on the local environment formed by characteristic cytokine profiles (Sica and Mantovani, 2012). Formation of cells with the M1 phenotype is enhanced by the actions of interferon-γ, TNF-α and LPS, each of which is considered to be pro-inflammatory. The emergence of the immune-suppressive M2 macrophage phenotype is driven by the actions of IL-4 and IL-13. Additionally, the formation and modulation of DC subsets and M2 mac-

rophages can be influenced by VEGF, macrophage colony-stimulating factor (M-CSF), TGF-β, IL-10, IL-6, and PGE2 (Sica and Mantovani, 2012; Genin et al., 2015; Heusinkveld et al., 2011a; Gottfried et al., 2008). Within the murine testis, it appears that in addition to IL-10 and TGF-β, immune complexes and glucocorticoids play a role in M2 polarization (Bhushan and Meinhardt, 2017). Macrophage treatment with glucocorticoids can lead to upregulation of CD163 (an M2 marker) (Schaer et al., 2002). It was also reported that human macrophages upregulate the TGF-βRII following glucocorticoid stimulation, leading to an activation of TGF-β-specific gene expression in response to TGF-β1 (Gratchev et al., 2005; Gratchev et al., 2008). This phenomenon has been proposed to be of relevance for patients undergoing treatment for atherosclerotic lesions and may have important implications for understanding tissue-dependent features of macrophage polarization.

1.3. Testicular germ cell tumours

1.3.1 Classification and epidemiology

Testicular cancer can be classified according to histopathological features into germ cell tumours derived from non-invasive germ cell neoplasia (GCNIS) and those unrelated to GCNIS (>95%) versus non-germ cell tumours (<5%) (Fig. 5) (Raijpert-De Meyts et al., 2016; Moch et al., 2016). Among GCNIS-derived testicular germ cell tumours (TGCT), approx. 60% of cases are morphologically homogeneous seminomas.

TGCT are the most common cancer type in young men in the range of 19-43 years of age (Richiardi et al., 2004; Chia et al., 2010; Jørgensen et al., 2014). In non-seminomatous TGCT, the peak incidence is at 25 years, compared to 35 years in seminoma (Raijpert-De Meyts et al., 2016). The incidence of TGCT diagnosis is increasing worldwide, particularly in regions located in North America, Europe and Oceania. Denmark and Norway have the highest incidences, with rates above 10 cases per 100,000 inhabitants (World Standard Population) (Huyghe et al., 2003; Richiardi et al., 2004; Chia et al., 2010; Myrup et al., 2010).

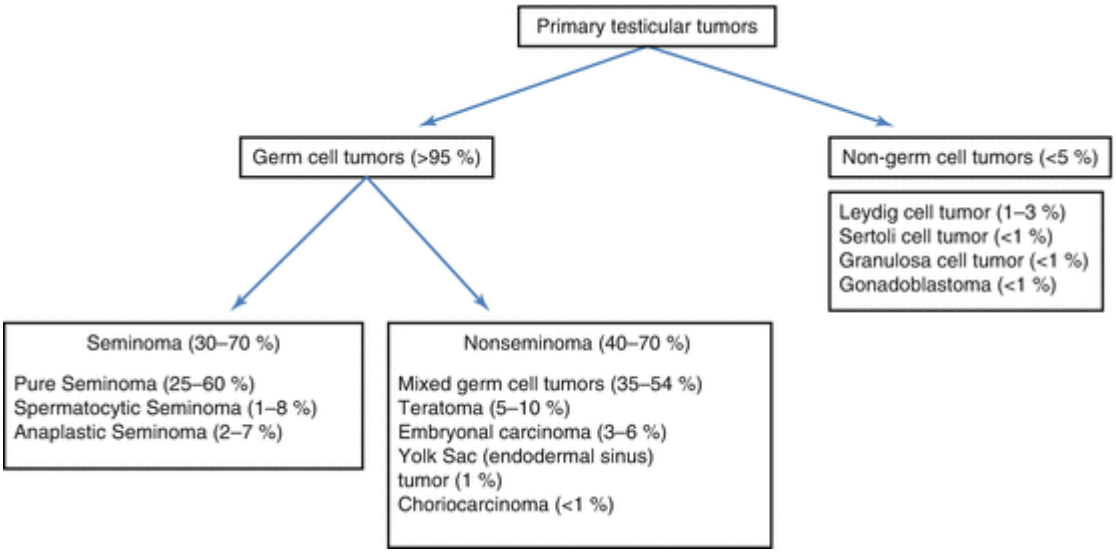

Fig. 5: Classification of testicular tumours. From McGinley and Rampersaud, 2014.

1.3.2 Pathogenesis

TGCTs develop from a precursor, germ cell neoplasia in situ (GCNIS) cell (Berney et al., 2016). Although there is no direct observation of its onset, GCNIS is understood to arise from primordial germ cells or gonocytes that fail to differentiate properly during fetal life, based on their expression of molecular markers characteristic for these cells, and on their highly similar morphology (Rajpert-De Meyts, 2006; illustrated in Fig. 6). As consequence of either intrinsic or environmental factors that prevent normal differentiation, these pre-GCNIS cells remain as developmentally arrested germ cells through childhood. The aetiology of this disease and the relative contribution of genetic and environmental factors to GCNIS formation and disease progression is not fully established, and both are likely to contribute (Myrup et al., 2010). Associations with cryptorchidism, hypospadias, and impaired spermatogenesis, both at the individual and population level, have led to the postulation of a testicular dysgenesis syndrome, which probably originates in utero (Skakkebaek et al., 2001; Raijpert-De Meyts et al., 2016). Furthermore, a family history of testicular cancer has to be considered as significant risk factor (Hemminki and Li, 2004). Although the cure rate is reported as 90-95% (Mortensen et al., 2014), the co-morbidities associated with this condition, and the frequency of relapse remain as clinical challenges (Daugaard et al., 2016).

During puberty, the normal alteration of hormones and behaviour of testicular somatic cells is considered to be responsible for the increased proliferation rate of GCNIS and

their transformation into a neoplastic cell with the capacity for unchecked proliferation and invasion (Rajpert-De Meyts, 2006; Rajpert-De Meyts et al., 2016). TGCT are manifested in young men as one of two predominant subtypes, seminomas, which are homogeneous and appear similar to gonocytes, or as non-seminomas, in which heterogeneous tissue types differentiate from the neoplastic precursors (Fig. 6). Other rare germ cell tumour subtypes, classified as pediatric and spermatocytic seminomas are not discussed further here, as their origins and biology is different (reviewed in Boublikova et al., 2014).

It has been predicted that approximately 70% of patients who have GCNIS will develop homogeneous seminoma and/or heterogeneous non-seminoma during a period of 7 years (Giwercman and Skakkebaek, 1993; Rajpert-De Meyts et al., 2016). However, it is not well understood why GCNIS develops into either seminoma or non-seminoma. Genetic changes such as chromosome 12p abnormalities, including the presence of an isochromosome of 12p and chromosome 12p overrepresentation, have been implicated by experimental evidence, as have SNPs in several genes encoding proteins central to germline differentiation (Pyle and Nathanson, 2016). Additional studies of the genome revealed undermethylation of 5-methyl cytosine in both GCNIS and seminoma specimens. Interestingly, in non-seminomas which typically contain a mixture of differentiated tissue types, only a small number of imprinted genes and LINE1 are demethylated (Rajpert-De Meyts et al., 2016; Kawakami et al., 2006; Smiraglia et al., 2002; Netto et al., 2008; Almstrup et al. 2010; Wermann et al. 2010; Ushida et al., 2012). These features highlight the complexity of these germline cells and have led investigators to anticipate that a sequence of unique events may determine how TGCTs arise and develop that is distinct for each individual. Whether the immune cell milieu contributes to these outcomes is an area of high interest and of relevance to TGCT as well as other solid tumours.

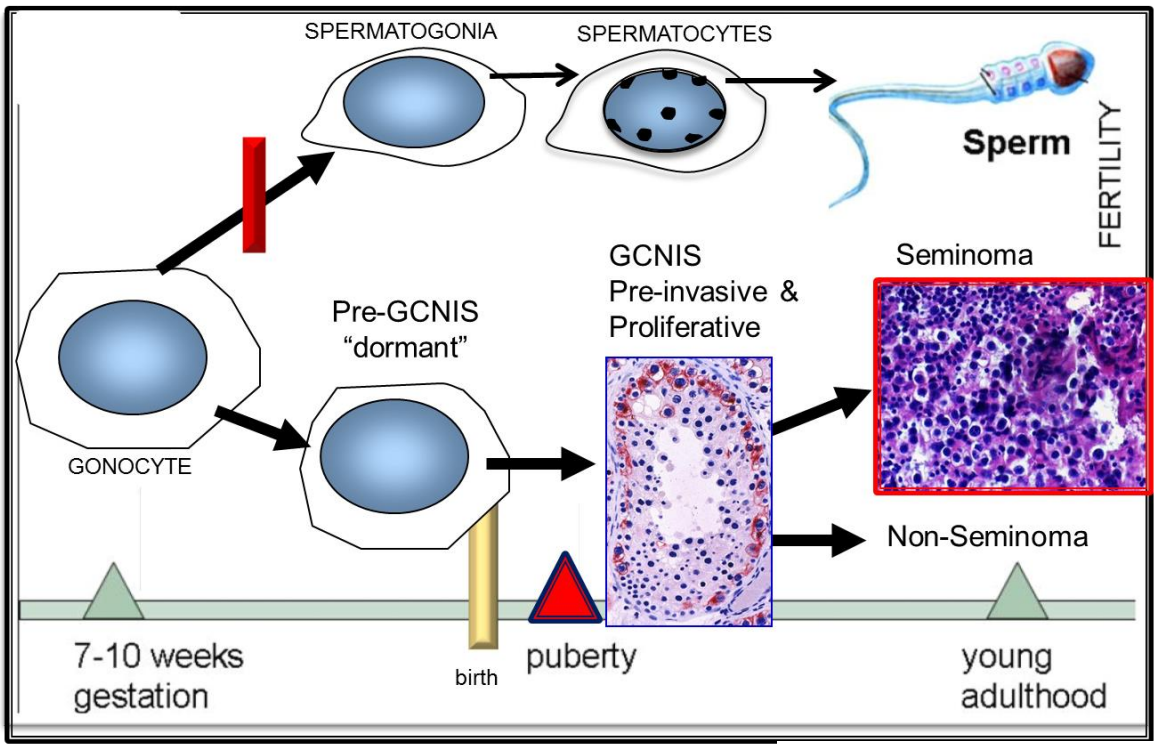

Fig. 6: Development of testicular germ cell tumours (TGCTs). Gonocytes that fail to differentiate properly but survive past birth can develop into the precursor germ cell neoplasia in situ (GCNIS) cells, most probably following more than one developmental insult that converts a non-neoplastic, dormant pre-GCNIS cell into a more proliferative GCNIS. During puberty, an alteration of the somatic environment, including those in response to hormones, may be permissive for increased proliferation of GCNIS and allow certain cells to transform into homogenous seminoma or heterogeneous non-seminoma that will be diagnosed as forming TGCTs. Adapted from K. L. Loveland.

1.3.3 Immune cells associated with testicular cancer

The testicular neoplasia subtypes GCNIS and seminomas frequently contain immune cell infiltrations (Bell et al., 1987; Nakanoma et al., 1992; Wei et al., 1992; Bols et al., 2000). Recent studies have shown that several different immune cell types can be present simultaneously in the testicular germ cell tumour environment. This includes T-cells (CD3), B-cells (CD20) and various antigen-presenting macrophage and DC subsets (Klein et al., 2016; Zheng et al., 2016). Zheng et al. identified two distinct macrophage subtypes, CD68+/CD163- and CD163+/CD68-, in seminoma specimens (Zheng et al., 2016), however these were not further characterised, nor was the relationship between different immune cell types thoroughly explored. Zheng et al. identified CD11c+cell aggregates around seminoma tumour cell clusters and postulated that these cells are CD11c+mDCs that could recruit CD68+ macrophages (Zheng et

al., 2016). However, CD11c is also expressed by M1 macrophages (Hume, 2008), thus additional analysis to resolve this is required, and respective new results are described in this thesis (Chapter 2).

Among DC subsets, myeloid DCs, can exhibit stimulatory functions, whereas plasmacytoid DCs are reportedly involved in immune suppression and tolerance (Ma et al., 2013). Both types are characterised as immune-suppressive DC (Ma et al., 2013; Tran Janco et al., 2015). In general, different DC subsets are involved in tumour progression and anti-tumour immunity, and their functions appear to be complex and potentially context-dependent (Ma et al., 2013). Typical markers for human pDCs are CD123, CD303 (also known as BDCA-2) and CD304 (BDCA-4), whereas mDCs are stratified into two subclasses depending on their surface antigen profiles; mDC1 express CD1c and CD11c, and mDC2 have CD11c and CD141 (Tran Janco et al., 2015). Zheng et al. identified different markers for mDCs in the testis, such as CD11c and DC-SIGN (Zheng et al., 2016). Additionally, other DC subsets such as CD1a+/CD207+ and pDCs (CD123+/CD303+ (BDCA-2+) were detected within seminoma specimens (Zheng et al., 2016); a third pDC marker, CD304 (BDCA-4) was not included in that study.

The importance of providing a clear documentation of antigen-presenting cell subtypes is demonstrated from investigations of other cancer types, such as breast cancer and melanoma, in which various DC subsets (CD11c, CD141 (BDCA-3) and CD11c, CD1c (BDCA-1)) are present (Broz and Krummel, 2015). Of significance, tumours which contain CD141+DC cells show a better clinical outcome (Broz et al., 2014; Sluijter et al., 2015; Broz and Krummel, 2015). The recruitment of DCs is most likely the consequence of local chemokine secretion, since the receptor for CCL20, CCR6, is expressed on the myeloid DCs present in these tumours. Further investigation in these tumour subtypes as well as in TGCTs is warranted to specifically identify the cytokine and chemokine receptors which are expressed by DCs. However, it must be recognized that a detailed analysis of DC populations that includes determination of how their functional polarization is associated with cancer is challenging, due to their diversity. Developments including the application of single cell RNA-sequencing of patient-derived samples obtained following surgery should aid clarification of the frequency and function of different immune cell subtypes.

1.3.4 Function of tumour-associated macrophages and dendritic cells

In their role as antigen presenting cells, DCs and macrophages can provide crucial information about the physiological state of the individual to the immune system. Mature DCs and M1 macrophages are known to be potent killers of tumour cells (Mantovani et al., 2002; Koh and DiPietro, 2011; Mills et al., 2000). Tumour cells have the capability to alter their microenvironment and, thus, influence adjacent macrophage and DC phenotypes (Sica et al., 2002). Tumour infiltrating dendritic cells (TIDC) in breast cancer and tumour associated macrophages (TAM) are mostly immune-suppressive and known to indicate a poor patient prognosis (Mantovani et al., 2002; Tran Janco et al., 2015). In this respect, TAMs are relatively well characterized in cancers other than TGCT. For instance, TAMs are functionally similar to M2 macrophages, which can express CD163 and CD206, and they can modulate their immune-suppressive properties by producing higher level of anti-inflammatory cytokines (Sica et al., 2008 a); Yang and Zhang, 2017). In contrast, significant diagnostic challenges posed by DC diversity are clinically important to resolve in cases of cancer, because the presence of TIDCs can indicate a poor or good prognosis that depends on the cancer type (Tran Janco et al., 2015). TIDCs can exhibit low costimulatory molecules and subsequently low antigen cross-presentation capacity and high expression of regulatory molecules and receptors, which are associated with immunosuppression (Harimoto et al., 2013; Krempski et al., 2011; Tran Janco et al., 2015)

Another important aspect of DC contributions to cancer development is their maturation stage. Immature DCs are immune-suppressive, and in certain cancer types it has been shown that a high density of immature DCs correlated with a poor outcome and a low survival rate in animal models (Van Beek et al., 2014). Interestingly, in many cancer types such as breast cancer, neck and head cancer, and melanoma, pDCs display an immature DC phenotype which tends to be tolerogenic with low production of IFNγ (Tran Janco et al., 2015). pDC can express Indoleamine-pyrrole 2,3-dioxygenase (IDO) that induces Treg expansion or produce inducible T-cell co-stimulator ligand (ICOSL), that can control Treg expansion and be permissive for breast cancer progression via Treg-related IL-10 (Redpath et al., 2013; Veglia and Gabrilovich, 2017). Importantly, in the testis, tumour associated mDC (CD11c+DC-SIGN+CCR6+HLA-DR-CD83-) are postulated to comprise immature DC subsets

(Zheng et al., 2016). These findings indicate that mDC in the testis and pDC in other cancer types are immature and may exert immune-suppressive effects.

Zheng et al. have shown that mDC express CCR6, which can bind CCL20 when expressed by immature DCs (Schutyser et al., 2003). It has been reported that eosinophils, dendritic cells and macrophages, including TAMs, can also express CCL20 (Caux et al., 2002; Mantovani et al., 2002). Furthermore, the recruitment and phenotype of DCs seems to be completely individual, when different tumour growth stages are compared (Krempski et al., 2011; Scarlet et al., 2012). However, this has to be further investigated in TGCT by the identification of the full suite of cytokine and chemokine receptors which can be expressed by DC subsets.

1.3.5 Contribution of tumour cells to macrophage and DC polarization

As described above, chemokines and cytokines play an important role in macrophage and DC recruitment and polarization in various types of cancers (Section 1.3.5). In recent years it has been recognized that tumour cells are a key contributor to the tumour cell immune microenvironment, through the secretion of macrophage recruitment and polarization factors. The functional polarization of macrophages into an immunosuppressive phenotype may occur in response to IL-6 and CCL-2 secreted by tumour cells (Conti and Rolens, 2004; Roca et al., 2009; Sierra-Filardi et al., 2014).

Interestingly, both IL-6 and CCL-2 are highly expressed in the testicular cancer microenvironment where macrophages (CD68, CD163) and DC subsets such as CD11c+mDCs are detectable, providing evidence that neoplastic germ cells directly drive macrophage and DC functionality (Klein et al., 2016; Zheng et al., 2016). However, the cellular origin of IL-6, CCL-2 and other key factors, as well as the responsive cell types remains to be determined and will be described later in this thesis (Chapters 2, 3 and 4).

Another potential polarization factor is CCL5, which can also be expressed by cancer cells and might be associated with testicular neoplasia (Azenshtein et al., 2002; Soria and Ben-Baruch, 2008; Klein et al., 2016). In other cancer types, CCL5 is known as a monocyte/macrophage activation and recruitment factor for immature DC (Scarpino et al., 2000; Locati, 2002). CCL17 and CCL22 can be expressed by tumour cells (Mantovani et al., 1992) and can affect T-cell polarization. The detection of chemo-

kines CCL2, CCL18, CCL17 in different tumours has been linked to the functional polarization or presence of immune-suppressive M2 macrophages (Roca et al., 2009; Kim et al., 2009; Erler et al., 2009; Mantovani et al., 2008). The production and localization of these chemokines in testicular neoplasia may be important to both the innate and adaptive immune responses at different phases of TGCT development. CCL17 was recently described as being highly upregulated in Sertoli cells surrounding GCNIS but not in later stages, as well as present in a subset of cells within the interstitium with morphological characteristics of immune cells (Szarek et al., 2018). The functional impact of this chemokine on tumour cells or somatic cells present in testicular neoplasia remains unknown.

Tumour cells have the capability to elude strong immune reactions by expression of cytokines that drive macrophage and DC polarization and subsequently inhibit the function of these antigen-presenting cells (Gabrilovich, 2004). Interestingly, in carcinoma of the cervix, tumour-derived IL-6 and PGE2 can drive M2 macrophage polarization (Heusinkveld et al., 2011a/b), demonstrating the potential of tumour cells to drive macrophage polarization by their production of cytokines and chemokines. However, much remains to be learned about the cytokine and chemokine profiles associated with recruitment and polarization of macrophage and DC subsets in the human testis, reflecting their putative pathological roles in testicular neoplasia. These topics are addressed by the experiments presented in this thesis.

1.3.6 Immune checkpoints

Innate and adaptive immune responses play important roles in controlling and suppressing tumour cell growth (Schreiber et al., 2011). For instance, APCs belonging to the innate arm of the immune system can recognise and present antigens to T cells, thereby activating the adaptive immune system (Janeway, 2001). This can enable an effective immune reaction to be mounted against cancer cells that will restrict tumour growth or progression. However, synergistic immune reactions must be orchestrated by immune cells that can be influenced by so called immunologic regulators. Several negative immunologic regulators, e.g. TIM-3/Galectin-9, PD-1/PD-L1, can suppress effective immune reactions to subsequently enhance tumour growth (Fig. 7).

One of the best understood pathways is that used by cytotoxic T lymphocyte-associated antigen 4 (CTLA-4) and the programmed cell death protein 1 (PD-1/PD-L1). A blockade of CTLA-4 by antibodies leads to strong immune responses against tumour cells (Leach et al., 1996; van Elsas et al., 1999). However, PD-1 is expressed by activated T-cells and can bind to the ligands PD-L1 and PD-L2. Interestingly, these ligands are negative regulators of T-cell activation and are expressed by both, APCs and tumour cells, with the functional outcome being repression of T-cell effector functions (Postow et al., 2015) (Fig. 7). In TGCTs, particularly seminoma, PD-L1 was identified as present in approximately 73% of cases (n=208) but absent from the pre-invasive GCNIS (Fankhauser et al., 2015). Seminomas are mostly associated with an increase in macrophage and DC subsets which could correlate with this reported detection of PD-L1 in most seminoma samples. In mouse models, tumour cells, macrophages and DCs (cells with CD11c, CD11b (CD1c counterpart of mouse CD11b), Gr1 and F4/80) can express PD-L1 (Deng et al., 2014). Additionally, in mice, DCs can also express PD-1 (Lim et al., 2016). This suggests that DCs might interact with tumour cells by binding PD-L1 through PD-1 which means that TCs could suppress DCs in addition to T cells However, in healthy human donors, some DC subsets express PD-L1 (CD141+ mDC and CD123+pDC), while others do not (CD1c+mDC). In contrast, in hepatocellular carcinoma (HCC) patients, all three DC subsets, CD141+ mDC, CD123+pDC and CD1c+mDC, are able to express PD-L1 (Lim et al., 2016).

In mice the expression of PD-L1 by DC can inhibit T cell proliferation and activation through downregulation of NF-kB (Krempski et al., 2011). NF-κB pathway can anergize the immune system and subsequently promote tumour growth (Xia et al., 2014). Lim et al. showed that PD-1 deficient mice (DCs) have increased IL-2 and IFN-γ cytokine expression *in vitro*; this suggested that PD-L1 expressed by DCs is responsible for the immune-suppression of T-cells by decreasing IL-2 and IFN-γ cytokine expression and antigen-specific CD8+ proliferation *in vivo*. Additionally, in a hepatocellular carcinoma (HCC) patient, Lim et al. have shown that PD-1 can be expressed by CD11c+cells (Lim et al., 2016). Therefore, treatment with anti-PD-1 antibodies could have an effect on circulating DC, an outcome that has yet to be directly documented. However, revealing DC and macrophage subsets which express high levels of PD-L1 and/or PD-1 and are associated with testicular cancer could be a helpful avenue for

development of evidence-based therapies that capitalize on new knowledge about immune checkpoints to reinforce anti-tumour immunity.

Furthermore, the immune checkpoint TIM-3 is also known as regulator of immune reactions and is expressed by macrophages and dendritic cells as well as Galectin-9 (Das et al., 2017). A binding of TIM-3 to Galectin-9 leads to a suppression of the innate immune system (Das et al., 2017).

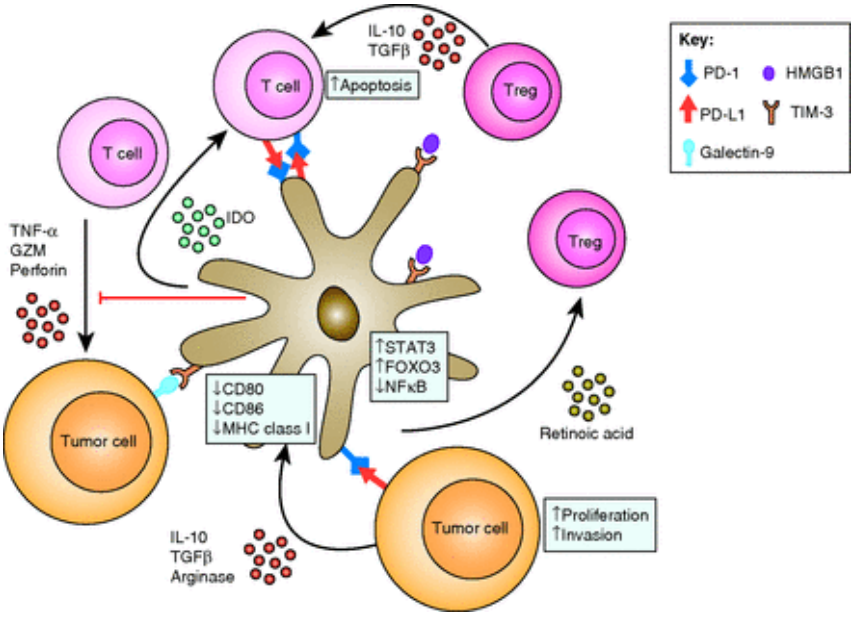

Fig. 7: Immune checkpoints and the immune-suppressive role of TIDCs. DCs can migrate to the tumour environment and upregulate the expression of molecules such as T cell Ig and mucin domain 3 (TIM-3), programmed cell death protein (PD-1) and programmed death-ligand 1 (PD-L1) that are known as immune checkpoints. TIDCs can interact with T cells by binding of PD-1 and PD-L1 which leads to an immune-suppression of T cells. TIDCs activate the production of retinoic acid that induces Treg differentiation. Additionally, TIDCs upregulate the expression of TIM-3 by tumour-induced IL-10, TGF-b1, VEGF-A, IDO. A binding of TIM-3 and High mobility group box 1 protein (HMGB1) leads to an immunosuppressive or non-immunogenic phenotype. From Tran Janco et al., 2015.

CONCLUSION

Macrophages and DCs display phenotypic plasticity that exhibit completely different functions. Macrophages can be involved in tissue remodelling, cell homeostasis and play an important role in the testis to maintain an immunosuppressive milieu that protects germ cells from autoimmune attack. In contrast, macrophages and DCs can also be involved in tumour progression and tumour destruction. TGCTs are most frequently associated with immune cell infiltrations that include macrophages and DCs. Thus, we characterised macrophages and DC subsets that are associated with pathological alterations such as testicular neoplasia (Chapter 2). Additionally, we investigated how tumour cells modulate immune cell responses (addressed in Chapters 3 and 4). In conclusion, it is important to understand how immune cells, which serve an immune-protective role in the healthy testis, may contribute to the emergence or progression of TGCTs using strategies that reflect their diversity and functional flexibility.

Chapter 2

Detailed analysis of immune cells in the human testis in normal physiological and pathological conditions, with a focus on macrophage and dendritic cell subsets

CHAPTER 2: Detailed analysis of immune cells in the human testis under physiological and pathological conditions, with a focus on macrophage and dendritic cell subsets

2. INTRODUCTION

This study was conducted to analyse immune cells that are specifically associated with TGCTs, with a focus on antigen-presenting-cells (APCs) such as macrophages and dendritic cells. Macrophage and dendritic cell subsets show different phenotypic characteristics and can change their functional state depending on the environment (Stout et al., 2005). Tumour cells can alter the local microenvironment by their production of cytokines and chemokines, thus affecting the function of APCs (Schraml and Reis e Sousa, 2015); subsequent functional polarization of APCs into immune-suppressive phenotypes under the influence of tumour cell products is therefore possible (Mantovani et al., 2002).

In this study, an identification of macrophage and DC subsets associated with testicular neoplasia (GCNIS and seminoma), in comparison with those present in clinical specimens with normal spermatogenesis was conducted. The tumour-immune-cell environment was evaluated to assess potential factors such as chemokines and cytokines that may recruit and promote differentiation of macrophages and DCs under pathological conditions. In addition, we examined chemokine receptor expression in macrophages to confirm that these cells are potential targets of the previously detected chemokines. We also characterized M1 and M2 macrophage cytokine expression profiles, revealing pro-inflammatory (M1: IL-12, TNF-a) and anti-inflammatory (M2: IL-10, TGF-b) cytokines, underpinning the concept that there is a dual function of immune cells, such as macrophages, in the testis.

This is the first comprehensive study to reveal a functional polarization and recruitment of macrophage and dendritic cell subsets associated with neoplasia (GCNIS and seminoma) caused by the alteration of the cytokine and chemokine milieu. Outcomes from this study contribute to understanding the pathological development of GCNIS into seminoma by revealing the characteristics of immune cell subsets and how they contribute and respond to the specific microenvironment of neoplasia in the human testis.

2.1 MATERIAL AND METHODS

2.1.1 Patients

Testicular tissue was obtained from men, who underwent testicular biopsies during andrological work-up for infertility (Bergmann and Kliesch, 2010; Marconi et al., 2012), during vasectomy or vasectomy reversal, or during surgery for testicular cancer. Specimens were collected at the Department of Urology, Pediatric Urology and Andrology at Giessen University Hospital and at the Department of Clinical Andrology, Center for Reproductive Medicine and Andrology at the University of Münster. All patients had given their written informed consent to use archived tissue specimens for research purposes (approved by the ethics committee of the Medical Faculty of the Justus Liebig University Giessen; Ref. No. 100/07; 26/11; 156/16).

2.1.1.1 Routine Histology

Testicular tissue specimens were immediately fixed by immersion in Bouin's solution overnight and embedded in paraffin for further histological and immunohistochemical analyses. Depending on the material (e.g. sample size) available, a fraction was also snap-frozen using liquid nitrogen and cryopreserved for RNA extraction, cDNA synthesis, and RT-qPCR. For histological evaluation, 5µm thick sections were prepared and stained with hematoxylin and eosin (HE) according to standard protocols. Afterwards, the HE-stained tissue sections were analysed to assess spermatogenic status and histopathological alteration, including a score count evaluation of spermatogenesis according to Bergmann & Kliesch (2010). Score counts (SC) can range from 10 to 0, which reflects the frequency of tubules containing elongated spermatids, with an SC 10 corresponding to elongated spermatids being present in every tubular cross-section and SC 0 corresponding to the complete absence of elongated spermatids. Subsequently, pathological conditions such as germ cell neoplasia in situ (GCNIS) and homogeneous seminoma specimens were identified. Testicular tissue specimens were grouped as follows: Group 1: normal spermatogenesis (nsp) without immune cell (lymphocytic) infiltrates (n=12; median age: 32 years, range 18-46 years; range of score count 9–10, median 10). Group 2: GCNIS associated with inflammatory infiltrates (n=17; median age: 32 years, range 28–45 years). Group 3: manifest seminoma associated with immune cell infiltration (n=17; median age: 34 years, range 21–61 years).

2.1.2 Immunohistochemistry

Bouin's fixed, paraffin-embedded tissue samples from human testis were evaluated by immunohistochemistry (IHC) and immunofluorescence (IF) (see Tab. 2.1.2.1, list of antibodies). Markers used were (1) for M1 macrophages: CD11, CD68; (2) for M2: CD163, CD206; (3) for mDC1: CD1c, CD11c; (4) for mDC2: CD11c, CD141; (5) for pDC: CD123, CD303, CD304; (6) for T cells: CD4, CD8; (7) for B cells: CD19. Antibodies recognising IL-6 (cytokine), Rab7 (phagocytosis marker), and CCR1, CCR2, CCR3, CCR4, CCR5 and CCR8 (chemokine receptors) were also used.

IHC staining was performed using 5 µm sections of Bouin'sfixed and paraffin-embedded samples. Every section was deparaffinised in Xylol (2x 10 min.) and rehydrated using an ethanol gradient (100%, 96%, 80%, 70%, ddH2O, 5 min each). Afterwards, heat-mediated antigen retrieval by Tris-EDTA treatment or Citrate-treatment was conducted using a microwave oven (15 min, 460 Watt)(see Appendix). Wash steps were performed after each antibody incubation using wash buffer containing 0.1%Tris-EDTA, TritonX100 in ddH2O. Endogenous peroxidase activity in tissue sections was blocked by exposure to 3% (v/v) H_2O_2 at room temperature (RT) for 30 min. After washing, a blocking solution (5% BSA in wash buffer) was applied for 30 min at RT, then tissue sections were treated with the primary antibody (Tab. 2.1.2.1, antibodies and dilution) overnight at 4°C in a humid chamber. sections were washed, incubated with secondary antibodies (Tab. 2.1.2.2) at room temperature for 1 h, then washed and exposed to peroxidase-conjugated streptavidin (Vectastain Elite ABC Kit; Vectorlabs, Burlingame, CA, USA) for 30 min at RT. Visualization was performed by using 3-Amino-9-Ethylcarbazole (AEC) (Biologo, Kronshagen, Germany) or 3,3′-Diaminobenzidine (DAB) (Biologo, Kronshagen, Germany) solution, depending on the antibody sensitivity. Nuclear counterstaining employed hematoxylin (Carl Roth GmbH & Co. KG, Karlsruhe, Germany). Afterwards slides were treated with Kaiser's glycerin gelatine (Merck, Darmstadt, Germany). For negative controls, treatment with primary antibodies was omitted. The visual evaluation was made with an upright microscope (Leica DM750 with Leica ICC50 HD, Solms, Germany).

Tab. 2.1.2.1 List of primary antibodies

Primary antibody	**Manufacturer**	**Dilution**
monoclonal mouse anti-human **CD11c** antibody	Novocastra, Germany, NCL-L-CD11c-563	1:100
monoclonal rabbit anti-human **CD11c** antibody 10 µl at 0.103 mg/ml	Abcam ab52632	1:100
monoclonal mouse anti-human **CD68** antibody	DAKO, Denmark MO876	1:100
rabbit polyclonal anti-human **CD163** 0.6mg/ml	DB biotech, Slovakia DB045-0.5	1:100
monoclonal mouse anti-human **CD206** 200µg/ml	Santa cruz sc-376108	1:100
monoclonal mouse anti-human **CD123** 0.5mg/ml	BD pharmingen 555642	1:100
anti-human **CD141**	Sigma ALDRICH HPA002982	1:50
rabbit anti-human **CD303** (ANTI-CLE4C) 0.5mg/ml	Sigma ALDRICH HPA029432	1:20
rabbit anti-human **CD304** (ANTI-NRP1) 0.2mg/ml	Sigma ALDRICH HPA030278	1:20
monoclonal rabbit anti-human **CD4**, Clone OKT4 25µg	Abcam ab133616	1:250
monoclonal mouse anti-human **CD8** 0.5mg/ml	Ebioscience Cat:14-0008-80 Clone lc1	1:250
monoclonal mouse anti human **CD19** 0.5mg/ml	Ebioscience Cat:14-0190-80 Clone lc1	1:500
monoclonal mouse anti-human **IL-6** 500µg	invitrogen AHC0762	1:100
monoclonal mouse anti-**Rab7** 2.1 mg/ml	Abcam ab50533	1:100
rabbit anti-human **CCR1** 0.5mg/ml	Novus NB100-56334ss	1:20
rabbit anti-human **CCR2** 1mg/ml	Novus NBP1-48337ss	1:50
rabbit anti-human **CCR3** 1mg/ml	Novus NBP1-77065	1:100
goat anti-human **CCR4** 1mg/ml	Novus NB100-717	1:50
monoclonal mouse anti-human **CCR5** 25ug	R&D MAB181	1:50
goat anti-human **CCR8** 1 mg/ml	Novus NB100-710	1:50

Tab. 2.1.2.2 List of secondary antibodies

Secondary antibody	**Manufacturer**	**Dilution**
Biotinylated rabbit anti-goat E0466	Dako, Glostrup, Denmark	1:200
Biotinylated goat anti-rabbit E0432	Dako, Glostrup, Denmark	1:100
Biotinylated goat anti-mouse E0433	Dako, Glostrup, Denmark	1:100

2.1.3 Semi-quantitative analysis of infiltrating immune cells

The ratio of M1 to M2 macrophage numbers was analyzed and quantified by visual inspection of slides from every patient group which had been stained with M1- and M2-specific markers (IHC). Patient samples from every group were separately analyzed for each marker and scored as follows: 0, no cells with signal detected; 1, individual cells detected; 2, multiple cells detected, scattered distribution; 3, moderate frequency of cells detected, sparse infiltrate; 4, high frequency of cells with positive staining, dense infiltrate. Data are expressed as mean ± SD by GraphPad (Prism 5). Statistical significance was evaluated using One Way Anova followed by Tukey post-test. A p-value less than 0.05 indicated a statistical significance.

2.1.4 Immunofluorescence

IF staining was performed as described above (Section 2.1.2), up through the incubation with primary antibodies. Subsequently, slides were washed 3x 5 min on a shaker, and the secondary antibodies diluted in washing buffer added for IF double staining (detection of two marker for one section) and incubated for 1 h at RT (Tab. 2.1.3.1). Afterwards, sections were incubated with 4′,6-diamidino-2-phenylindole (DAPI, 0.2 µg/ml, diluted in washing buffer) (Merck, Darmstadt, Germany) for 10 min, washed and mounted using Fluoromount™ Aqueous Mounting Medium (Merck, Darmstadt, Germany). The visual evaluation was conducted by means of a fluorescence microscope (Olympus, Center Valley, PA, USA).

Tab. 2.1.3.1 List of secondary antibodies (IF)

Secondary antibody	**Manufacturer**	**Dilution**
Alexa 488 donkey anti-rabbit	Thermo Fisher R37118	1:100
FITC goat anti-mouse	Sigma ALDRICH F0257-1ML	1:100
Cy3 donkey anti-		1:200
Alexa donkey 594 anti-rabbit	Thermo Fisher R37119	1:100

2.1.5 RNA extraction, cDNA synthesis, RT-PCR and quantitative real-time PCR

Snap-frozen testicular biopsies were cryopreserved until RNA extraction and used for cytokine and chemokine expression profiling. The same patient groups as for IHC/IF experiments (nsp n=4, GCNIS n=6, seminoma=10) were used. For CCL15 analysis, six additional nsp samples were used to subsequently confirm the presence of CCL15 in the testis under normal conditions (nsp=10, GCNIS=4, seminoma=6). Total RNA was extracted using TRizol® (Sigma Aldich, St. Louis, MO, USA) according to the manufacturer`s protocol. cDNA was synthesized using MultiScribe® Reverse Transcriptase (50 U/µl, Applied Biosystems, Waltham, MA, USA). For RT-PCR, specific primers were designed to analyze cytokines/chemokines, chemokine receptors,

prostaglandin synthase E2 and distinct immune checkpoint molecules (Tab. 2.1.5.1, primer list). Five µl of cDNA plus 20 µl master mix according to Tab. 2.1.5.2 were prepared and PCR run was performed (Appendix, Chapter 2). PCR products were visualized using a 1.5% agarose gel (Appendix, Chapter 2) for 75 min at 130 V.

2.1.5.1 Tab. of designed primer

Target	**Accession number**	**Used as:**	**Forward primer, 5'- 3'**	**Reverse primer, 5'- 3'**
GAPDH	NM_002046.6	Housekeeper	TGACAACAGCCTCAAGATC	TCCTTCCACGATACCAAAG
Bactin	NM_001101.4	Housekeeper	TTCCTTCCTGGGCATGGAGT	TACAGGTCTTTGCGGATGTC
IL-6	NM_000600.4	Potential macrophage polarization factor	TACCCCCAGGAGAAGATTCC	AGATGCCGTCGAGGATGTAC
PTGES 2	NM_004878.4	Potential macrophage polarization factor	GGACGGAGGAGATGAAGTG	GCGGACAATGTAGTCAAAGG
TIM-3	AB924452.1	Immune checkpoint	CCTATCTGCCCTGCTTCTAC	TCACATCCCTTTCATCAGTC
Galectin-9	NM_009587.2	Immune checkpoint	TCAATGGGACCGTTCTCAG	TTGAAGTGGAAGGCAATGTC
CCR1	NM_001295.2	chemokine receptor	AAAGCCCCAGAAACAAAGAC	TTGCATCCCCATAGTCAAAC
CCR2	NM_001123041.2	chemokine receptor	GACCCACAAGATAAAGAAGC	TTGAGGTCTCCAGAATAGG
CCR3	NM_001837.3	chemokine receptor	GTGGTGGTGGTGATGATCC	ATGCCCCCTGACATAGTGG
CCR4	NM_005508.4	chemokine receptor	CTGCTCTTCGTGTTTTCCC	AAAGCCCACCAAGTACATCC
CCR5	NM_000579.3	chemokine receptor	TAGTGGGATGAGCAGAGAAC	GGCGAAAAGAATCAGAGAAC
CCR8	NM_005201.3	chemokine receptor	GTTTGGGACTGTAATGTGC	TGATCGTCCTCACCTTTAG

Tab. 2.1.5.2 Master mix for RT-PCR

Reagents	**Per attempt**
$MgCl_2$ 25 mM	1 µl
PCR buffer 10x	2 µl
RNAse free H_2O	15.37 µl
dNTPs 10 mmol	0.5 µl
Primer rev. 10 pmol/ µl	0,5 µl
Primer for. 10 pmol/ µl	0,5 µl
Gold Amplitag 5U/ ml	0,13 µl
Total	20 µl

For quantitative analysis of mRNA expression, real-time PCR amplification was performed using specific Taqman Gene Expression Assays (Tab. 2.1.5.3) (LifeTechnologies, Carlsbad, CA, USA). For each specimen, triplicate determinations were performed using 2 µl cDNA (diluted 1:20 in RNAse free H_2O) plus 5 µl TaqMan® Gene Expression Master Mix (LifeTechnologies), 0.5 µl TaqMan® Gene Expression Assay (Tab. 2.1.5.3, specific Taqman Probe) and 2.5 µl RNAse free H_2O (per well). qRT-PCR was performed on a CFX96 RealTime cycler (Bio-Rad, Munich, Germany). Relative gene expression was calculated using CFX Manager Software 3.0 (Bio-Rad). For statistical analysis, a one-way-ANOVA test was performed followed by a Tukey's Multiple Comparison Test (GraphPad, Prism 5.01). Relative gene expression was calculated using the ΔΔCT method. Data were expressed as fold-change, normalized to *ACTB* as well as calibrated to nsp.

2.1.5.3 Table of TaqMan probes

Target	Product No.
Human ACTB	Hs01060665_g1
Human GAPDH	Hs02758991_g1
Human IL-1b	Hs01555410_m1
Human IL-12a	Hs01073447_m1
Human TNFα	Hs00174128_m1
Human IL-6	Hs00174131_m1
Human IL-10	Hs00961622_m1
Human TGFβ1	Hs00998133_m1
Human CCL2	Hs00234140_m1
Human CCL5	Hs00982282_m1

2.1.6 Protein isolation, SDS-PAGE and western blot

2.1.6.1 Protein isolation from cryopreserved testis tissue

Snap-frozen biopsies were washed twice with PBS, before 1 ml lysis buffer (APL buffer, Qiagen) was added and specimens were incubated for 5 min at RT. Afterwards, the tissue was homogenized by a Homogenizer (IKA® T-10 basic Ultra Turrax Homogenizer IKA® Werke GmbH & CO. KG, Staufen, Germany) for 6x 30 sec., then protein was extracted by using AllPrep® RNA/ Protein Kit (Qiagen) according to the manufacturer's protocol. Protein concentration was measured using a Bicinchoninic Acid Protein Assay Kit (Sigma Aldrich) according to the manufacturer's protocol. The absorbance of the solution was measured with a photometer at a wavelength of 562 nm.

2.1.6.2 Protein isolation from paraffin-embedded testis tissue

Paraffin-embedded tissue was cut and 4 sections (with a thickness of 10 µm) were collected into an Eppendorf tube. Afterwards, protein isolation was performed using Qproteome FFPE Tissue Kit (Qiagen, Hilden, Germany) according to the manufacturer's protocol. The protein concentration was measured as described above (2.1.6.1).

2.1.6.3 Gel electrophoresis

For the gel electrophoresis, 11.7 µl of the sample (total concentration between 30 and 40ng/ml, diluted in RNase free water) plus 4.5 µl NuPAGE® sample buffer and 1.8 µl NuPAGE® Reducing agent were suspended and incubated for 10 min at 72°C. In the meantime, a NuPage® Novex 4–12% Bis–Tris gels (Invitrogen) was prepared

in the gel apparatus (BioRad) filled with diluted 3-(N-morpholino)propanesulfonic acid (MOPS) buffer (50 ml *NuPAGE*® MOPS Running Buffer 10x and 950 ml ddH2O) then samples were loaded into the wells, alongside a molecular size ladder (Page Ruler™Plus, Thermo Scientific). The electrophoresis was initially run at 50V (collecting phase). After 15 min, electrophoresis speed was increased by running the gel at 200V for an additional 45 min (separation phase).

2.1.6.4 Protein transfer

The apparatus for protein transfer was prepared and filled with transfer buffer (50 ml NuPAGE® transfer buffer, 1 ml NuPAGE® antioxidant, 200 ml Methanol, 749 ml ddH2O). Polyvinylidene difluoride (PVDF) membrane (Thermo Fisher) was activated for 2 min by soaking in methanol; sponges and whatman filter (BioRad) were incubated in transfer buffer. Protein transfer was performed at 30 V for 1h 15 min.
After the successful protein transfer, non-specific binding sites were blocked using blocking buffer (1.5 g BSA, 1.5 g milk powder in 30 ml PBS) for 30 min on a shaker at RT. In the meantime, primary antibodies against Rab7 (dilution 1:2000), p65 (dilution 1:500), and β-Actin (dilution 1:5000) were incubated overnight at 4°C. Antibody dilution was performed using washing buffer containing 1% BSA, 0.1% Tween in PBS. On the next day, primary antibodies were discarded and PVDF-membranes were washed 3 x times with washing buffer. Afterwards, unspecific binding sites were blocked with goat or mouse serum (5% of the serum, diluted in washing buffer) for 15 min at RT. The solution was discarded, replaced with secondary antibody (PO-anti mouse, 1:5000; PO-anti rabbit, 1:5000) diluted in washing buffer and incubated for 1 h at RT. After the incubation, the membrane was washed 2 x times using PBS/ 0.1% Triton and finally washed with PBS. Antibody staining was visualized by using Luminata (Immobilon Forte Western HRP substrate, Merck). Luminata was incubated for 1 min and developted by x-ray film (Amersham Hyperfilm ECL, GE Healthcare) and x-ray cassette (Henry Schein). Development solution (TETENAL) was added until the protein bands were visible. Afterwards, the visible protein bands were fixed with fixation solution (TETENAL). The development was stopped with 3% acetic acid.

Tab. 2.1.6.5.2 List of primary antibodies (WB)

Primary antibody	**Manufacturer**	**Dilution**
monoclonal mouse anti-human Rab7 2.1 mg/ml	Abcam ab50533	1:2000
Monoclonal rabbit anti-human p65 (NF-κB subunit) 1 mg/ml	Sigma Aldrich SAB5600083-100UL	1:500

Tab. 2.1.6.5.2 List of secondary antibodies (WB)

Secondary antibody	**Manufacturer**	**Dilution**
Biotinylated goat anti-rabbit E0432	Dako, Glostrup, Denmark	1:100
Biotinylated goat anti-mouse E0433	Dako, Glostrup, Denmark	1:100

2.1.7 Analysis of immune cells in testes of Gilz KO and WT mice

2.1.7.1 Histology

The following protocol was adapted from Sivanjah Indumathy, Monash University, Clayton, Australia. The testis tissue was collected and fixed in PBS with 4% paraformaldehyde (PFA) for 5 hours. Afterwards, the testis tissue was placed in 15% sucrose solution diluted in PBS and incubated overnight at 4°C. On the next day, sucrose solution was discarded, replaced with 30% sucrose diluted in PBS and incubated overnight at 4°C. Testis tissue was washed 3x in PBS for 5 min and dried using tissue paper. Then the testis tissue was transferred in a plastic mold and slowly filled with Tissue-Tek OCT and put on dry ice. The testis tissue was stored in -80°C until slides were cut. Upon use, the tissue was cut in 5 µm-10 µm thick sections using a sliding microtome (Leica SM2000 R, Solms, Germany) and transferred to microscope slides. Afterwards, the slides were stored at -20°C until needed.

2.1.7.2 Flow cytometry

The mechanical dissociation of the testes was conducted immediately after the dissection. The tubules were gently separated and transferred in a 15 ml Falcon tube containing DMEM. The tubes were inverted twice and after 15 min, supernatant was transferred into a fresh Falcon tube and centrifuged at 1000rcf. Then the supernatant was discarded and the cell pellet resuspended in 1 ml FACS buffer. The cells were counted, splitted into Eppendorf tubes and stained (see antibody list 2.1.7.2 and 2.1.7.3). For flow cytometric analysis, ten thousand events were acquired for each sample using the BD LSR Fortessa x20 flow cytometer (BD Bioscience, San Jose, USA). Data were analysed using FlowJO Version 10 (Tree Star, Ashland, USA) in the following manner.

Table 2.1.7.2: List of direct conjugated antibodies (Myeloid panel)

Immune cell type	Antibody	Dilution	Fluorophore
All immune cells	CD45 (BD)	1:100	Pe-Cy7
Macrophages (pan)	F4/80 (Affymetrix)	1:100	APC
DC	CD11c (Biolegend)	1:100	Pacific blue
M1	MHCII (Biolegend)	1:100	BV710
M2	CD206 (Biolegend)	1:100	BV610
Macrophages (pan)	CD11b (Biolegend)	1:100	FITC

Table 2.1.7.3: List of direct conjugated antibodies (Lymphoid panel)

Immune cell type	Antibody	Dilution	Fluorophore
All immune cells	CD45 (BD)	1:100	Pe-Cy7
T cells	CD3 complex (Biolegend)	1:100	AF647
NK cells	NK1.1 (Biolegend)	1:100	BV421

2.2 RESULTS

2.2.1 Human testis: Assessment of immune cells under physiological and pathologic conditions

2.2.1.1 Anti-inflammatory M2 macrophages detectable in the normal testis whereas pro-inflammatory M1 macrophages were absent

Testicular biopsies with normal spermatogenesis (range of spermatogenesis score counts 7-10) contained cells bearing macrophage specific markers such as CD68 (monocytes, macrophages), CD163 and CD206 (M2 macrophages). In contrast, CD11c+ cells (macrophages and DC) were hardly present under normal conditions (single cells in three of twelve patient samples) (Fig. 2.2.1.1/ 2.2.1.3). Other dendritic cell markers such as CD123, CD141, CD303, CD304 as well as a B-cell marker (CD19) were not detectable in the non-inflamed tissue (Fig. 2.2.1.1). However, positive for CD4 and CD8 on single cells (T-cells) could be identified. All detectable immune cells were scattered and located in the interstitial compartment.

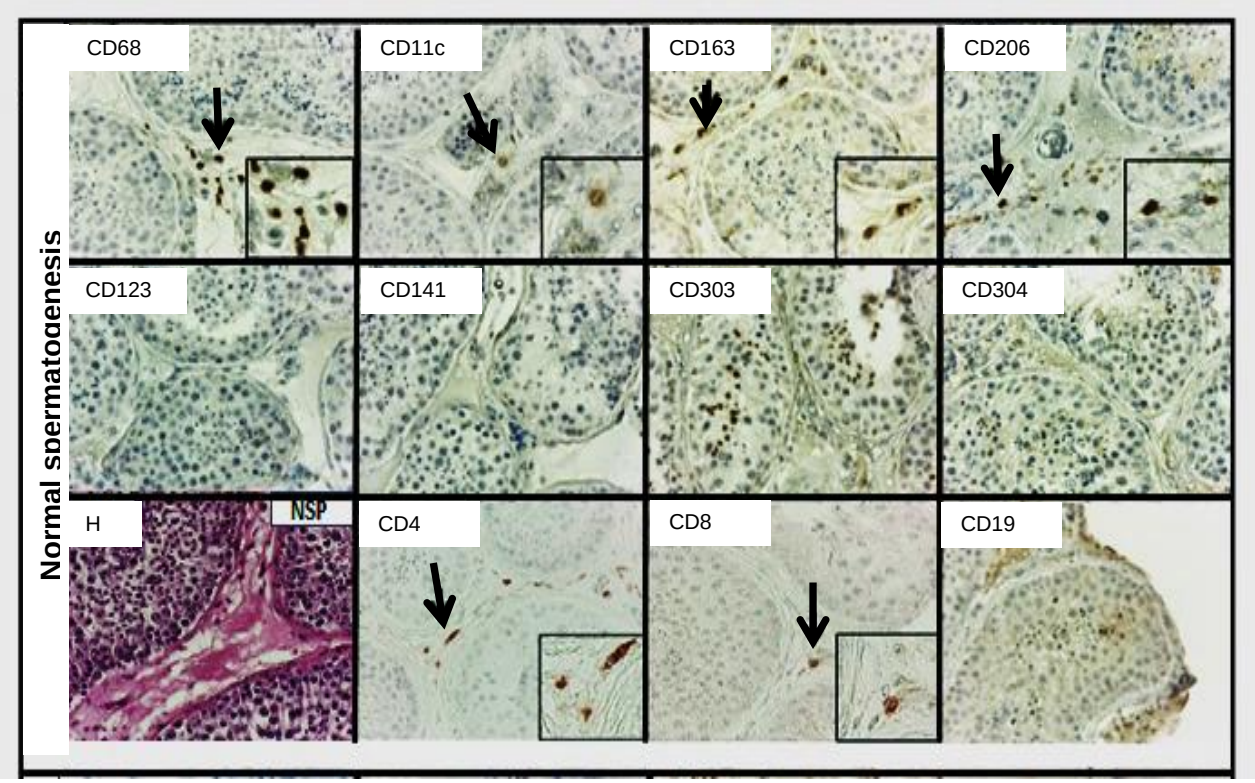

Fig. 2.2.1.1: Analysis of immune cell populations in non-inflamed human testis tissue showing normal spermatogenesis (see hematoxylin-staining, nsp = normal spermatogenesis) by immunohistochemistry (IHC, 40x). Exemplary hematoxylin staining showed the testis histology under normal conditions. For a detailed immune cell analysis, different CD markers were used such as: CD68 (macrophages and monocytes), CD11c (dendritic cells and macrophages), CD163, CD206 (M2 macrophages), CD123, CD141, CD303 and CD304 (dendritic cells), CD4 and CD8 (T-cells) as well as CD19 (B-cells). Nsp samples contained cells of the innate immune system such as CD68+cells, M2 macrophages (CD163+ and CD206+) and sparse CD11c+ cells as well as few cells of the adaptive immune system, e.g. T-cells (CD4+, CD8+). Dendritic cell marker such as CD123+, CD141+, CD303+, CD304+ and B-cells (CD19) were not detectable. All detectable immune cells were highlighted using black arrows and shown with a higher magnification (see insets). H= hematoxylin.

2.2.1.2 IHC analysis revealed increased immune cell populations associated with testicular germ cell neoplasia

In contrast to the normal human testis, neoplasia (e.g. GCNIS and seminoma) is associated with increased numbers of infiltrating immune cells, showing a maximum in seminoma (Fig. 2.2.1.2, hematoxylin-staining, white arrows). The presence of different macrophage and dendritic cell markers such as CD68 (monocytes, macrophages), CD11c (macrophages and DC), CD163 and CD206 (M2 macrophages) and CD11c, CD123, CD141, CD303, CD304 (DC) were revealed. Additionally, sections of all GCNIS and seminoma tissue specimens contained cells of the adaptive immune system such as T-cells (CD4, CD8) and B-cells (CD19)(Fig. 2.2.1.2, A/B).

The main focus of this study was the detection of macrophage and dendritic cell markers by IHC. In GCNIS samples, CD68+ and CD11c+ cells were detectable and localized in the interstitial compartment as well as within seminiferous tubules (Fig. 2.2.1.2, A). Particularly, the detection of CD68+ and CD11c+ cells revealed a co-localization of these markers in close proximity to GCNIS cells (Fig. 2.2.1.2, A). In seminoma samples, CD68+ and CD11c+ cells were found around and within tumour cell clusters (Fig. 2.2.1.2, B). Furthermore, of M2-specific markers such as CD163 and CD206 could be identified in samples of all three patient groups (nsp, GCNIS, seminoma). Additionally, the following markers were used for the identification of DCs: CD11c, CD123, CD141, CD303, CD304. Of note, all markers were detectable in neoplasia samples. However, in GCNIS only single cells exhibiting dendritic cell markers were detectable, whereas in seminoma samples these markers were frequently present (Fig. 2.2.1.2, A/B). To sum up, in human testicular neoplasia (GCNIS/ seminoma), a detection of increased macrophage and dendritic cell markers such as, CD163, CD206 (M2), CD68 (monocytes, macrophages), CD11c (DC, macrophages) and CD123, CD141, CD303, CD304 (DC) was observed (Fig. 2.2.1.2, A/ B).

A semi-quantitative scoring analysis revealed a significant increase of M2 macrophage marker (CD163) associated with testicular neoplasia compared to the normal testis (Fig. 2.2.1.2/ 2.2.1.3.1). Additionally, GCNIS and seminoma samples showed a significant increase of other macrophage markers such as CD68 and CD11c (Fig. 2.2.1.3.1, A).

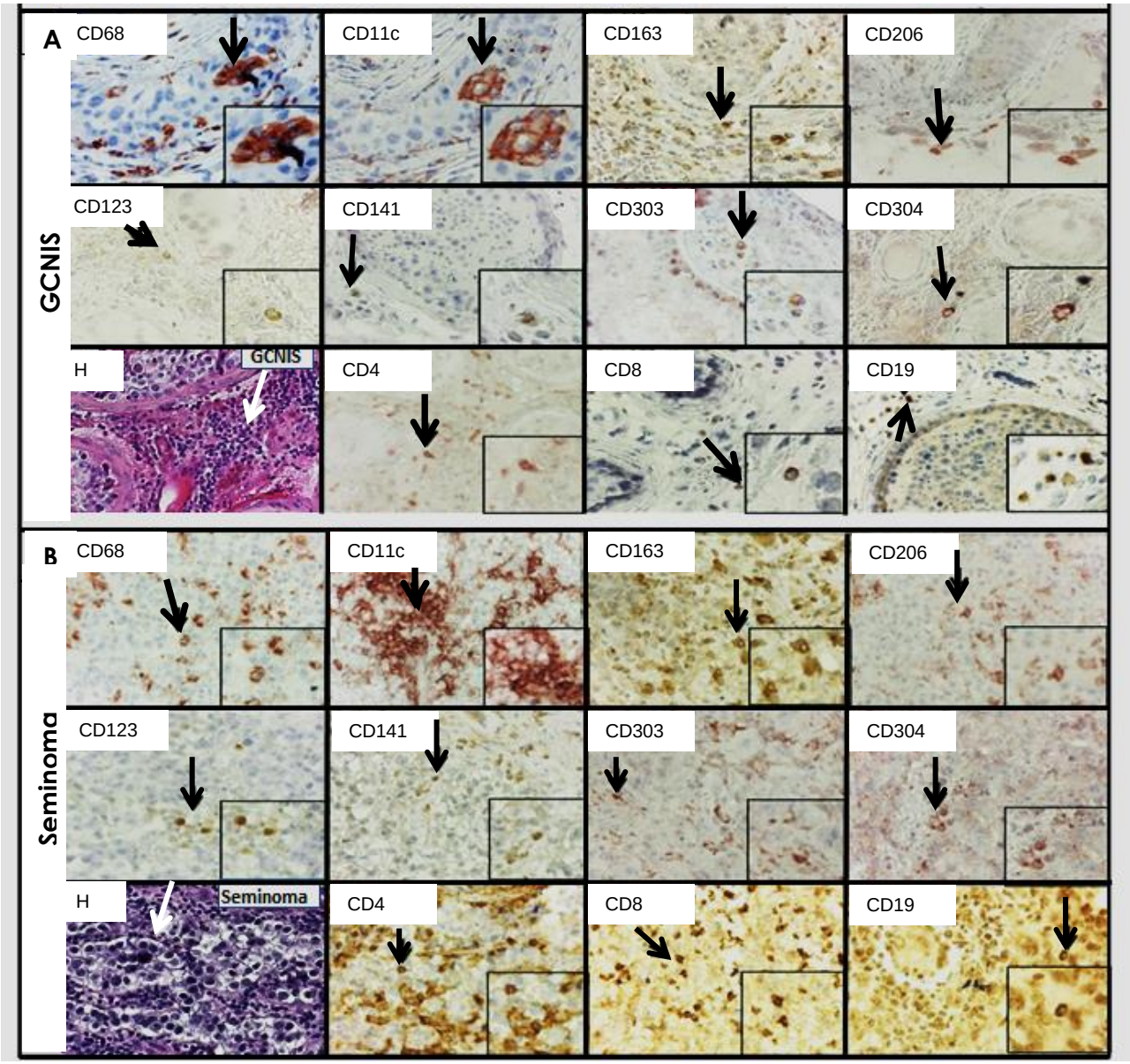

Fig. 2.2.1.2: Analysis of inflammatory immune cell infiltrates associated with testicular neoplasia (GCNIS, seminoma) by IHC (40x). Samples of two different patient groups were analysed: germ cell neoplasia in situ (GCNIS) (B) and seminoma (C). Exemplary hematoxylin-staining revealed mainly focal infiltrates in GCNIS, compared to a disseminated pattern in seminoma samples (20x). For IHC staining, different CD markers were used such as: CD68 (macrophages and monocytes), CD11c (dendritic cells and macrophages), CD163 and CD206 (M2 macrophages), CD123, CD141, CD303 and CD304 (dendritic cells), as well as T- and B-cell cells (CD4+, CD8+, CD19). IHC staining of GCNIS specimens revealed increased numbers of CD11c+ and CD68+ cells, which were detectable within the seminiferous epithelium around GCNIS cells and in the interstitial compartment. Additionally, single cells exhibiting dendritic cell markers such as CD123+, CD141+, CD303+, CD304+ were detectable (B). Seminoma samples showed a further increase of all immune cell types mentioned above (C). Respective immune cells were highlighted by black arrows and were shown with a higher magnification (see insets). H= hematoxylin.

2.2.1.3 Identification of DC and macrophage subsets associated with testicular germ cell neoplasia by immunofluorescence (IF) double-staining

In non-inflamed testis tissue, we detected M2 specific markers such as CD163 and CD206 as well as CD68 (monocyte and macrophage marker) in the interstitial compartment (IHC, Fig. 2.2.1.2, B). An IF double staining was conducted to confirm the presence of M2 macrophages (CD163+/CD206+) in normal testis (nsp) as well as neoplasia specimens (GCNIS, seminoma) (Fig. 2.2.1.2, B). An identification of M2 macrophages (CD163+/CD206+) was possible in all three patient groups (nsp, GCNIS, seminoma).

Particularly, CD68+ and CD11c+ cells were co-localized in the neoplasia specimen as shown by IHC (Fig. 2.2.1.2, B) supported by a double-detection of CD68+/CD11c+ cells (M1 macrophages) (Fig. 2.2.1.3.1, B). Of note, CD68+/CD11c+ cells were not detectable in nsp

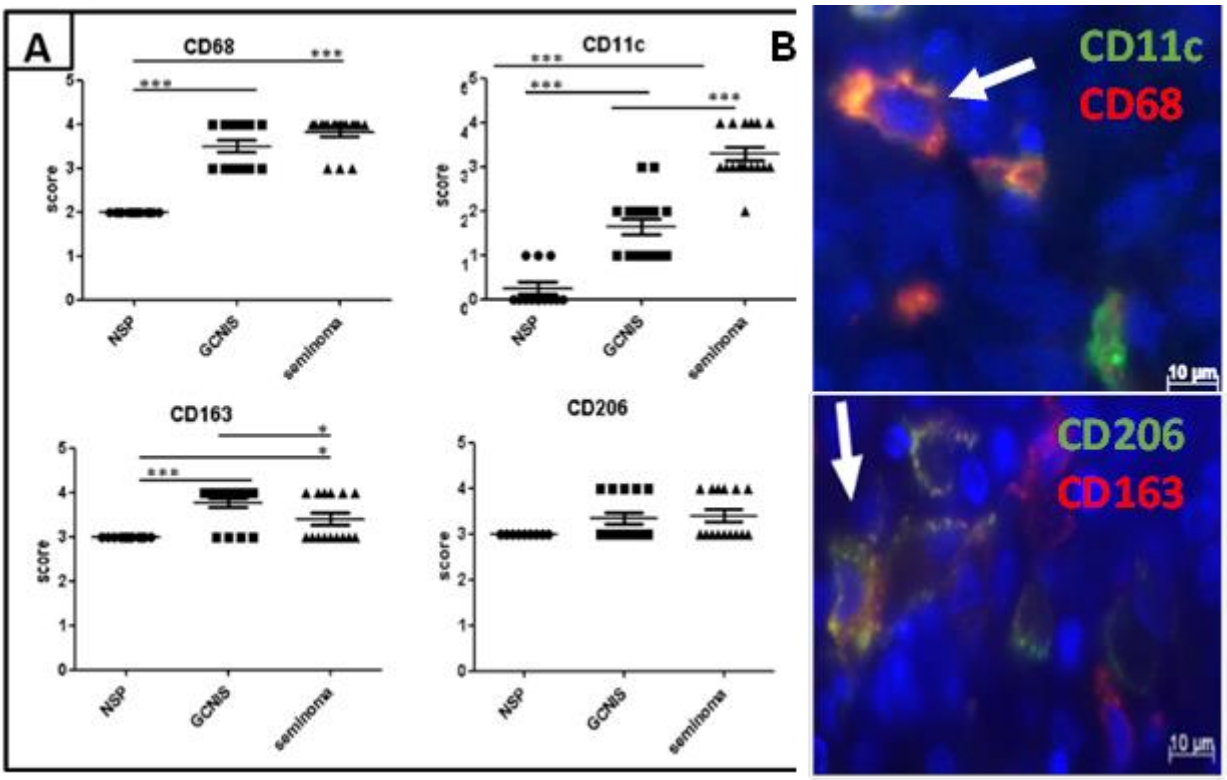

Fig. 2.2.1.3.1: Identification of markers compatible with M1 and M2 macrophage subsets (nsp, GCNIS, seminoma). (A) Semi-quantitative scoring of immunohistochemical data revealed M1 and M2 macrophage-specific markers which were identified as M1 and M2 macrophages associated with testicular neoplasia by (B) IF double staining. (nsp n= 12, GCNIS n=17 and seminoma n=17; score of 0=not detected, 1=single cells, 2=scattered, 3= sparse, 4=dense). Conducting IF double-staining confirmed the presence of M1 (CD11c+ (green)/ CD68+(red), merged: orange) and M2 (CD163+(red)/CD68+(green) in seminoma sample, merged: orange (white arrow). Significance tested by one-way ANOVA (*P<0.05,**P<0.01,*P<0.001).

Furthermore, besides M1 macrophages, two different immune cell phenotypes were observed using CD68 and CD11c markers: CD68+/CD11c- (macrophages) and CD68-/CD11c+ (DC). As CD11c is also a specific marker of different dendritic cell subsets, an analysis of additional DC markers such as CD1c, CD11c, CD123, CD141, CD303, CD304 was conducted by IHC and IF (for IHC, refer to Fig. 2.2.1.2 B and C). A detailed analysis by IF revealed the presence of three different DC subsets: mDC1 (CD1c+/CD11c+), mDC2 (CD11c+/CD141+) and pDC (CD123+/CD303+/CD304+) (Fig. 2.2.1.3.2).

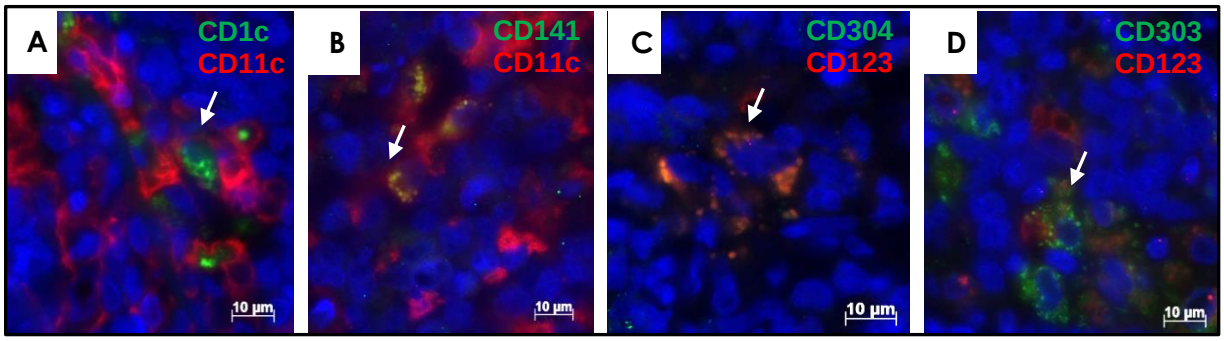

Fig. 2.2.1.3.2: Different dendritic cell subsets detectable in seminoma specimen using IF double-staining. Observation of CD1c+ and CD11c+ (mDC1) (A), CD11c+/CD141+ cells (mDC2) (B) and CD123+/ CD303+ (C), CD123+/CD304+ (D) (pDC). merge: orange.

2.2.2 Potential function of immune cells in the human testis

2.2.2.1 M2 macrophages as contributors of the immune suppressive milieu in the testis

The testis is known as an immune-privileged organ where germ cells are protected from autoimmune attack. Immune suppressive Treg cells, mast cells and macrophages can contribute to this immune suppressive environment by cytokine expression. For instance, in the non-inflamed testis, immune cells compatible with the phenotype of M2 macrophages (CD163+/CD206+) were frequently found and the respective cytokine expression profile revealed immune suppressive properties relating to this phenotype, reflected by the presence of IL-10 and TGF-β (Fig. 2.2.2.1). In contrast, immune cells compatible with the phenotype of pro-inflammatory M1 macrophages (CD11c+/ CD68+) could not be identified under normal conditions, whereas CD68+ (monocytes and macrophages) cells and single CD11c+ (macrophages and DC) cells were detectable (Fig. 2.2.1.2/ Fig. 2.2.1.3, A). In line with these IHC-based findings, transcript levels of M1-related cytokines such as TNFα and IL-12b were low compared to TGF-β or neoplasia samples (Fig. 2.2.2.1; 2.2.2.2).

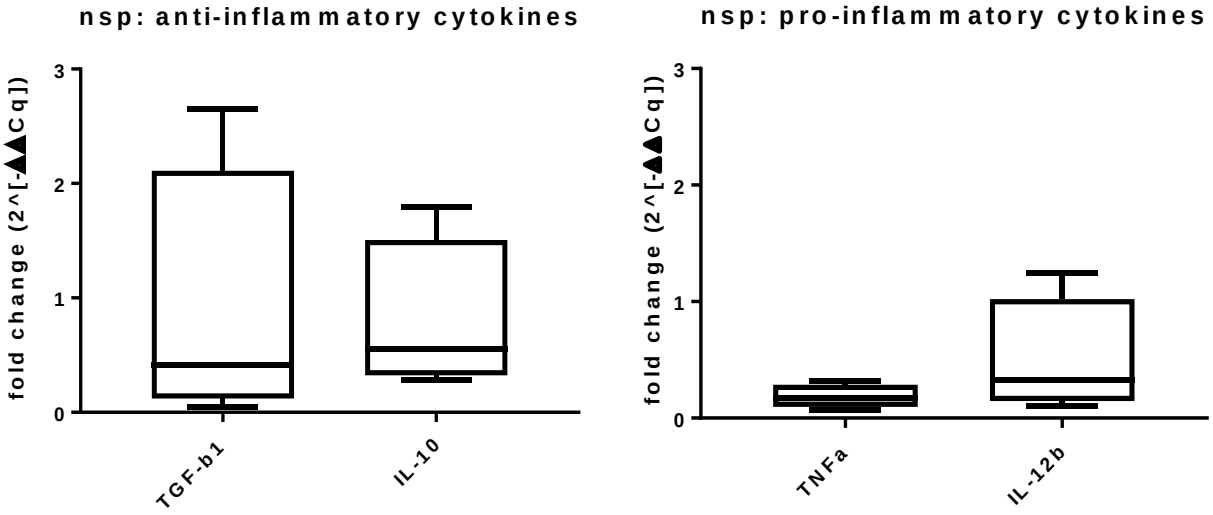

Fig. 2.2.2.1: Analysis of M1 (pro-inflammatory: TNFα and IL-12b) and M2 (anti-inflammatory: TGF-β1 and IL-10) related cytokine transcript levels in normal testes (nsp; n=4). Anti-inflammatory cytokines such as TGF-β1 and IL-10 were detectable whereas pro-inflammatory cytokines were hardly expressed. Relative gene expression normalised to β-actin and human placenta.

2.2.2.2 M1 and M2 macrophages balance pro- and anti-inflammatory cytokine milieu in testicular germ cell neoplasia

Expression M1-related pro-inflammatory cytokines such as TNFα and IL-12b was detected in GCNIS and seminoma specimens (Fig. 2.2.2.2, A). In comparison to the normal testis, transcript levels of these cytokines were significantly increased in neoplasia samples. An analysis of M2-related cytokines such as IL-10 and TGF-β1 determined a significant difference between normal testis and GCNIS (IL-10 and TGF-β1), and also between GCNIS and seminoma specimens (Fig. 2.2.2.2, B). To sum up, the detection of M1 and M2 macrophages was associated with a milieu comprising both, pro- and anti-inflammatory cytokines at the transcript level (Fig. 2.2.2.2, A and B).

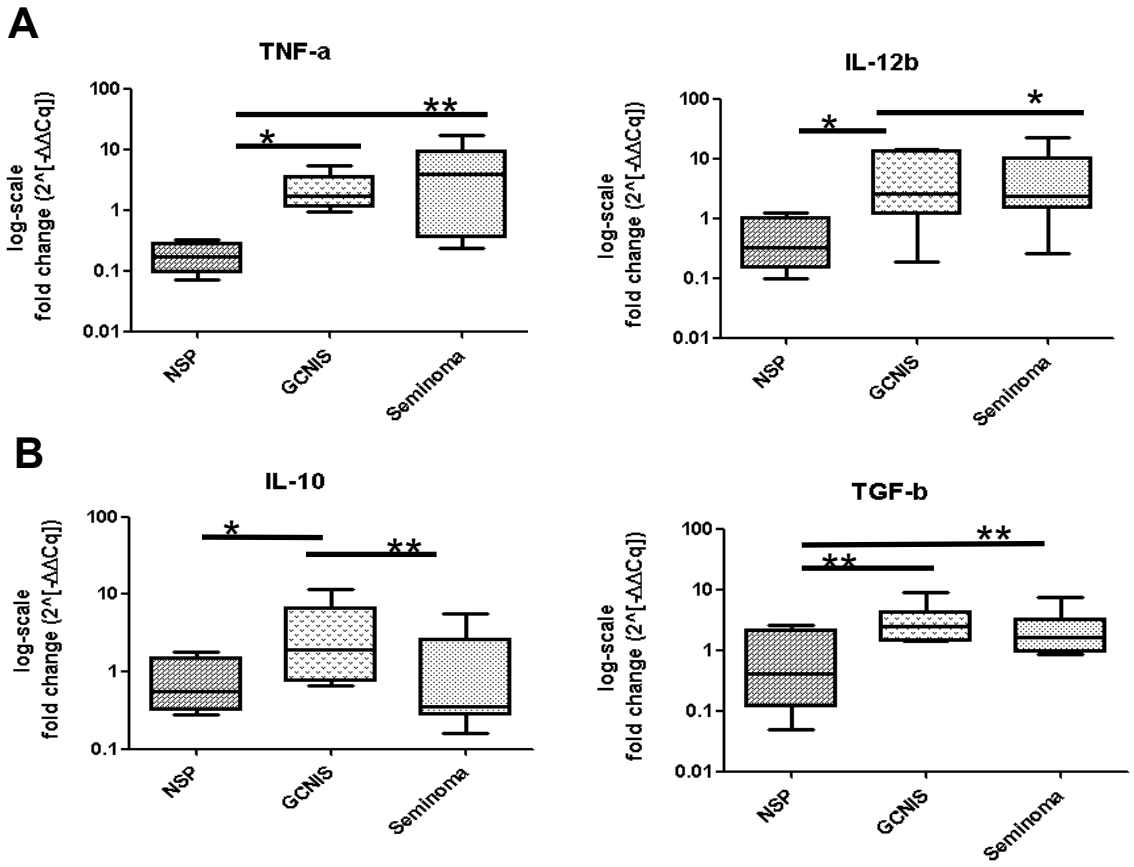

Fig. 2.2.2.2: Comparative analysis of human testis samples (nsp, GCNIS, seminoma) to reveal (A) M1 (pro-inflammatory) and (B) M2 (anti-inflammatory) related cytokine expression. Transcript levels of M1 and M2 related cytokines showed a significant increase of both pro- and anti-inflammatory molecules in testicular neoplasia (nsp n=4, GCNIS n=6, seminoma=10). Relative gene expression normalised to β-actin and human placenta. Significance tested by one-way ANOVA (*P<0.05,**P<0.01).

2.2.2.3 M1 macrophages: Indication of phagocytosis and antigen presenting capabilities

M1 macrophages are also capable to eliminate pathogens by phagocytosis. Therefore, Rab7 (phagocytosis marker for late stage phagosome maturation) was used to study this potential function of M1 macrophages in the human testis. Both, Rab7+/CD11c+ and Rab7+/CD68+ cells could be identified by means of IF in seminoma. Interestingly, not all CD11c+ and CD68+ cells expressed Rab7 (Fig. 2.2.2.3.1, A). Additionally, a western blot was conducted to compare all three categories of testis specimens. A detection of Rab7 (23kDa) was possible in normal testis, GCNIS and seminoma, but in the GCNIS specimen expression was lower (preliminary data) (Fig. 2.2.2.3.1, B). Additionally, a comparison between cryo-preserved tissue and

paraffin-embedded tissue was conducted using the same patient sample (Fig. 2.2.2.3.1, B, seminoma, lane 3 (cryo) vs. lane 4 (paraffin)). A band compatible with Rab7 was detected in both samples, however the band obtained from the paraffin-embedded material was not exactly at 23kDa.

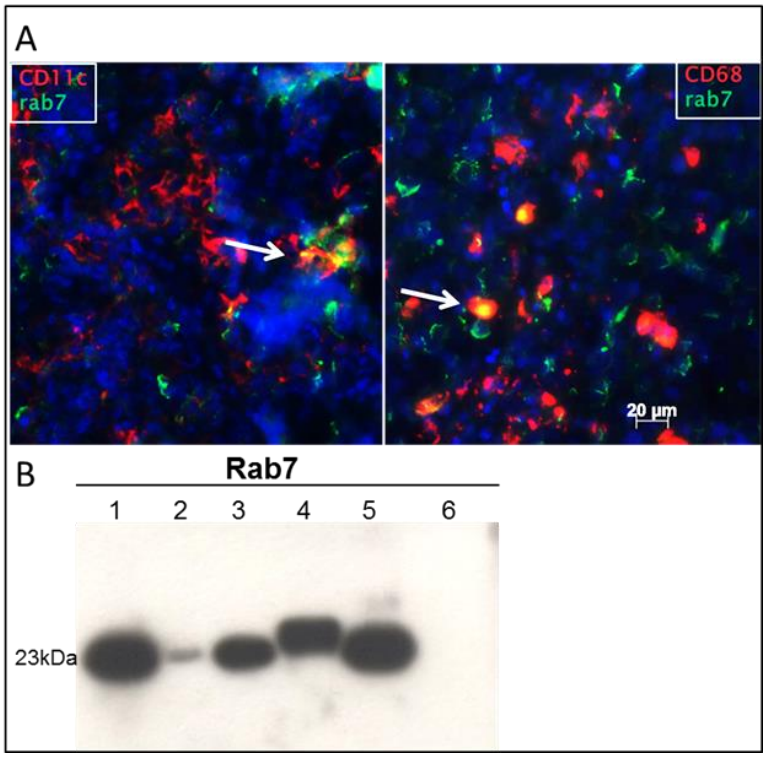

Fig. 2.2.2.3.1: Protein expression analysis of Rab7 (phagocytosis marker for late stage phagosome maturation) using M1 macrophage markers (CD11c and CD68) by (A) IF (seminoma) and (B) western blot (nsp, GCNIS, seminoma). (A) Rab7+/CD11c+ and Rab7+/CD68+ cells were detected in a seminoma sample. IF double detection is shown by white arrows (merge: orange). (B) Rab7 was detected by western blot in all three patient groups. For western blot analysis, cryopreserved tissue was used for protein isolation (1, 2, 3, 5) and compared with a protein extract obtained from paraffin embedded tissue (4). 1= NSP, 2= GCNIS, 3= seminoma, 4= seminoma, 5= positive control (human placenta), 6= negative control.

After the phagocytosis of pathogens, antigen presenting cells (macrophages and DC) can present antigens to T-cells. A detection of CD11c, CD68 (M1 marker) and CD4+T-cells revealed the same alignment pattern in seminoma samples (IHC, Fig. 2.2.1.2). Thus, an IF double-staining of CD4+ cells and CD68+ or CD11c+ macrophages revealed that both cell types in close contact (IF, Fig. 2.2.2.3.2, B). However, the antigen presenting ability of macrophage and DC subsets to T-cells remains to be elucidated. For further functional analysis, APC functional marker should be considered.

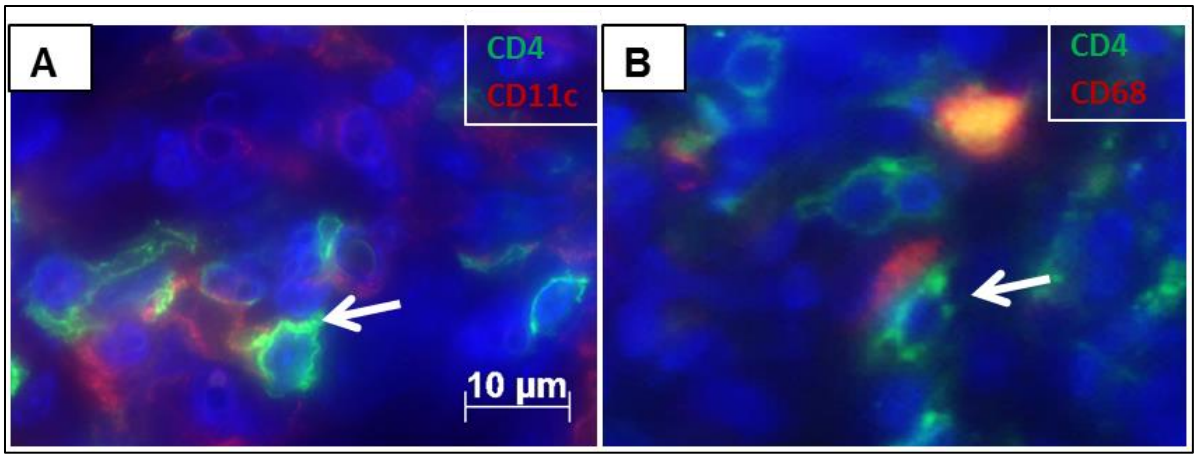

Fig. 2.2.2.3.2: Indication of antigen presentation by detection of CD68+ or CD11c+ cells (M1 macrophages) and CD4+ cells (T cells) by IF. A CD4+ cells are in close contact to CD11c+ cells (A) and CD68+ cells (B), highlighted by white arrow. A and B shows the same magnification.

2.2.3 Recruitment of immune cells by chemokine signalling in the human testis

2.2.3.1 Possible recruitment of CD68+ macrophage precursors by CCL15

Chemokine expression is associated with inflammation to recruit circulating immune cells into the inflamed tissue. Additionally, chemokines are partly responsible for a functional polarization of immune cells, especially macrophages. In contrast to non-immune privileged organs, CD68+ macrophages as well as resident M2 macrophages (CD163+/CD206+) were present in the testis under physiological conditions. . Therefore, an identification of chemokines and specific chemokine receptors was conducted to understand the recruitment and functional polarization of CD68+ and M2 macrophages in the normal human testis. Chemokines typically required for macrophage recruitment such as CCL2, CCL5, CCL17, CCL18, and CCL22 were not expressed in the non-inflamed human testis (see 2.2.3.2.1). Interestingly, CCL15 (mRNA transcript level) was detectable in samples exhibiting nsp, whereas in neoplasia CCL15 was downregulated (Fig. 2.2.3.1.1, A). CCL15-specific receptors (mRNA transcript level) such as CCR1 and CCR3 were detectable in all three categories of testis tissue specimens, indicating that corresponding immune cells could be present (Fig. 2.2.3.1.1, B). Furthermore, CD68+ macrophages were identified as possible targets of CCL15 due to the double-staining of CCR1 by IF (Fig. 2.2.3.1.1, C). A detection of CD68+ and CCR3+ cells was also possible.

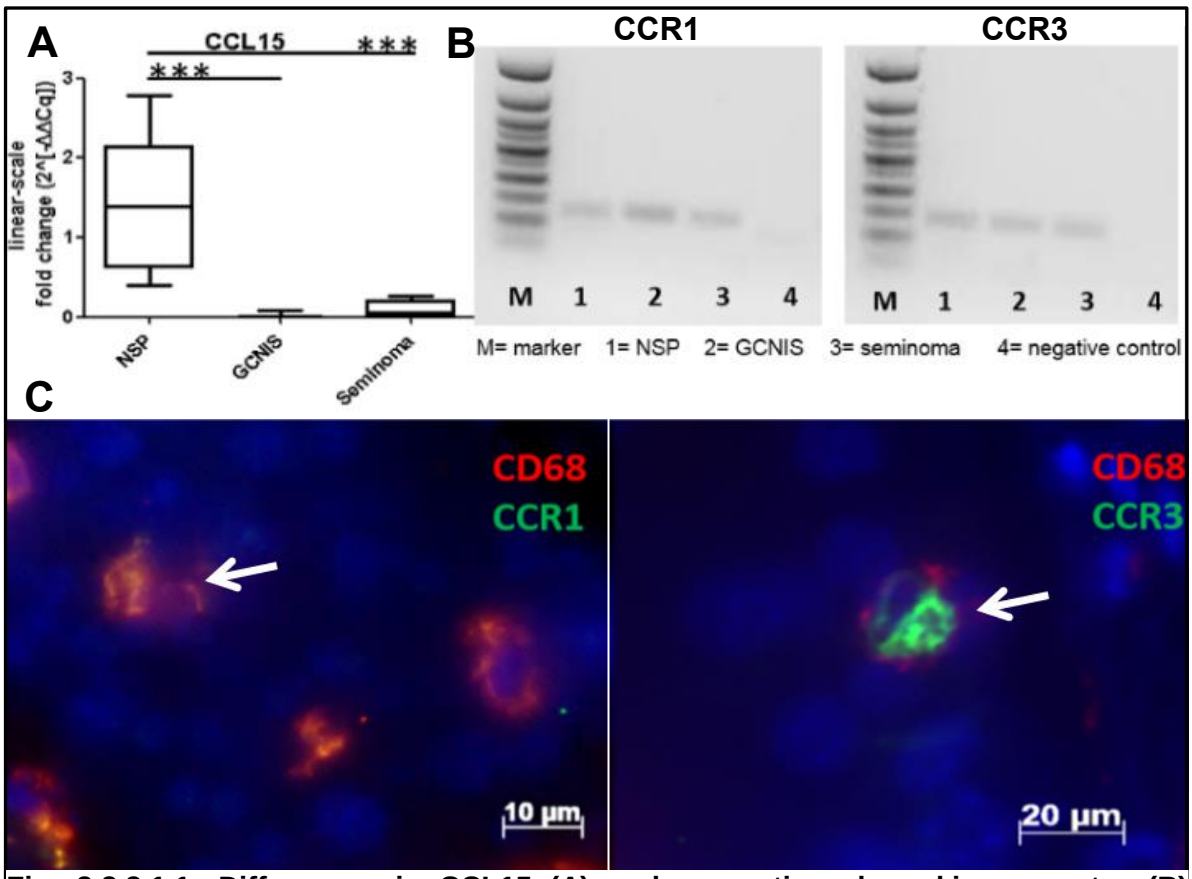

Fig. 2.2.3.1.1: Differences in CCL15 (A) and respective chemokine receptor (B) expression in human testis samples (nsp, GCNIS, seminoma). A) CCL15 mRNA expression was almost absent in neoplasia whereas CCL15 was highly expressed in nsp (relative gene expression normalised to β-actin and NSP; nsp n=4, GCNIS n=6, seminoma=10; significance tested by one-way ANOVA (***P<0.001). B) Transcripts of CCL15-corresponding receptors CCR1 and CCR3 were detectable in all patient groups (PCR). C) Identification of CD68+ cells in nsp, co-staining for CCR1 and CCR3 (white arrows).

2.2.3.2 Chemokine and chemokine receptor expression analysis in testicular germ cell neoplasia

Testicular cancer (GCNIS, seminoma) is associated with infilration of different immune cell populations (see Fig. 2.2.1.2). An identification of chemokines that might be responsible for newly detected macrophages and DCs as non-resident immune cell populations) associated with testicular germ cell neoplasia was conducted. Therefore, a detailed analysis of chemokine (CCL2, CCL5, CCL15, CCL17, CCL18, CCL22) as well as chemokine receptor (CCR1, 2, 3, 4, 5, 8) expression profiles was conducted to reveal significant alterations associated with neoplasia compared to the non-inflamed, normal testis (nsp). In testis samples revealing germ cell neoplasia (GCNIS, seminoma), significantly increased transcript levels of CCL2 ($p<0.05$), CCL5

(p<0.001), CCL18 (p<0.05) and CCL22 (p<0.05) were detected in comparison to nsp. Chemokines such as CCL15 and CCL17 were either not detectable or not significantly increased in neoplasia. The CCR mRNA expression profile determined the presence of all six corresponding receptors binding the chemokines investigated, namely CCR1, CCR2, CCR3, CCR4, CCR5 and CCR8 in all three categories of human testis specimens (Fig. 2.2.3.2.1).

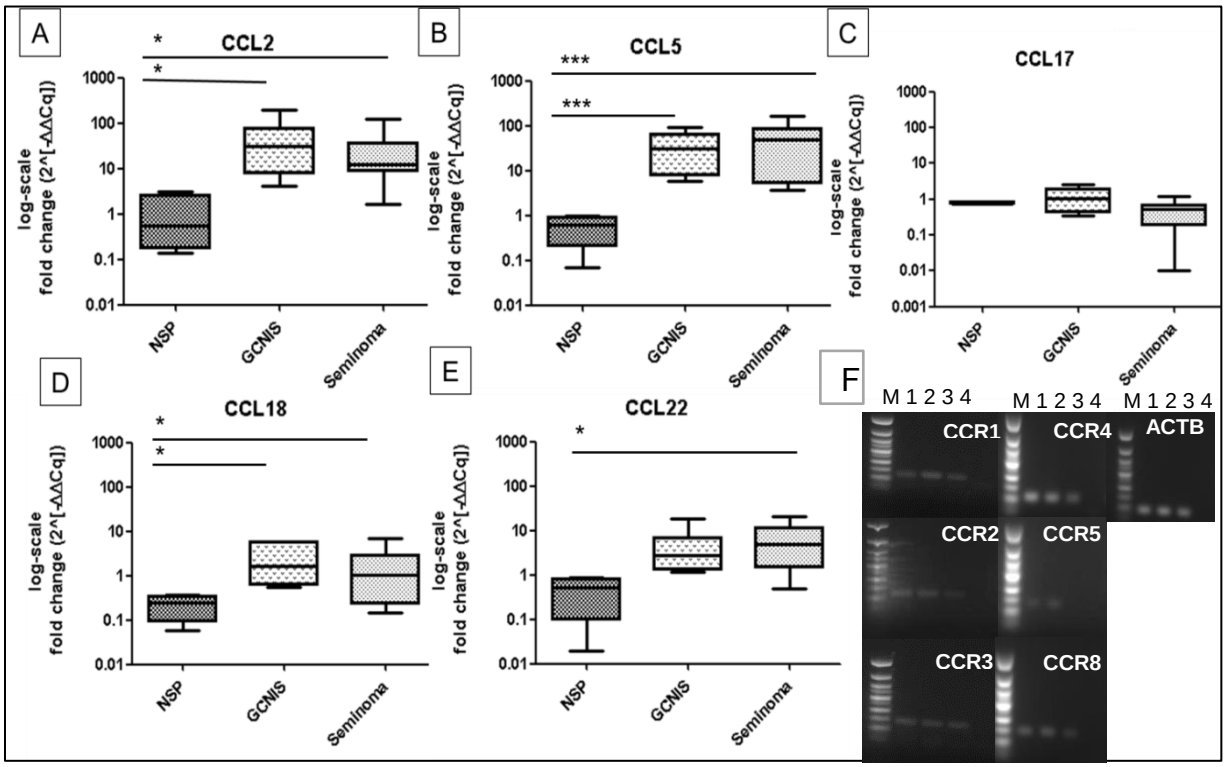

Fig. 2.2.3.2.1: Difference in chemokine and chemokine receptor expression profiles in normal human testis (nsp, n=4) compared to germ cell neoplasia (GCNIS, n=6; seminoma, n = 10). Transcript levels of chemokines CCL2, CCL5, CCL18 and CCL22 were significantly increased in neoplasia samples (CCL22: not significant in GCNIS) (A-E; qRT-PCR; relative gene expression was normalized to ACTB as well as NSP; significance tested by one-way ANOVA (*P < 0.05, **P < 0.01, ***P < 0.001). Detection of corresponding chemokine receptors was possible in all three patient groups (F; RT-PCR; M= marker, 1= NSP, 2= GCNIS, 3= seminoma, 4= negative control).

2.2.4 Tumour-/immune cell interaction and functional polarization of macrophages

2.2.4.1 Potential macrophage polarization factors

Local environmental changes caused by cytokines and chemokines associated with testicular cancer can influence functional polarization of macrophages since macrophages can switch their phenotype due to a stimulus. Therefore, potential macrophage polarization factors such as prostaglandin, TGF-β1, IL-10, and IL-6 can help to elucidate their role in the human testis. Therefore, a detailed analysis was conducted to reveal the presence of these factors in different testis specimens (normal testis, GCNIS and seminoma). As previously mentioned, M2 macrophages were detectable in non-inflamed, normal testis tissue, where also prostaglandin E synthase2 (PTGES2) and IL-10 were expressed (Fig. 2.2.4.1.1/ Fig. 2.2.2.2). Additionally, in GCNIS and seminoma specimens, mRNA expression of PTGES2, IL-10 as well as IL-6 was shown (Fig. 2.2.4.1.1). Interestingly, it could be observed that M2 macrophages express IL-6, whereas in nsp, M2 macrophages were not able to express IL-6 (Fig. 2.2.4.1.2). Additionally, a detection of PTGES2 (mRNA) was possible in both tumour cell clusters as well as immune cell infiltrates obtained from seminoma samples (Fig. 2.2.4.1.1).

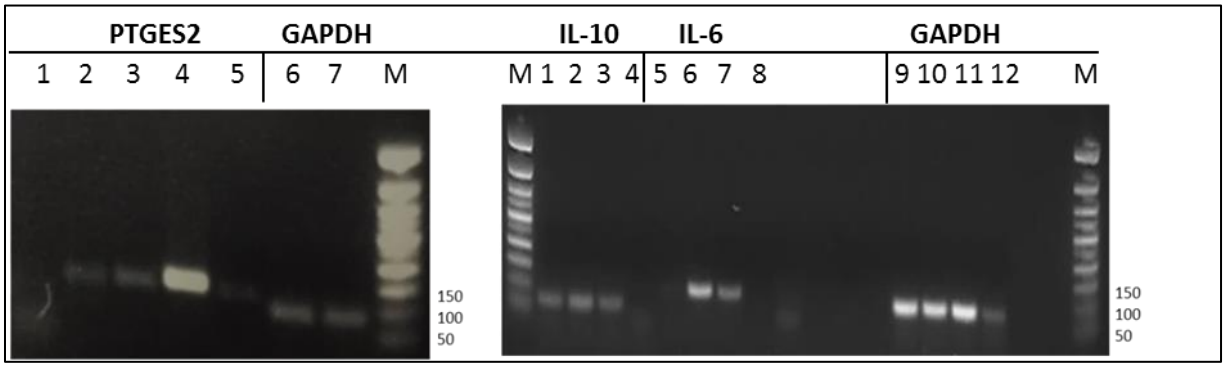

Fig. 2.2.4.1.1: Analysis of potential macrophage polarization factors IL-10, IL-6 and PTGES2 in human testis by RT-PCR. Prostaglandin E synthase (PTGES2) was expressed in nsp as well as tumour cluster and immune cell infiltrates dissected from seminoma (laser-assisted picking). IL-10 was expressed in all three categories of specimens (nsp, GCNIS, seminoma) whereas IL-6 was only detectable in GCNIS and seminoma specimens. Human placenta was used as a positive control. M= marker, PTGES2: 1= negative control, 2= tumour cluster , 3= immune cell infiltrate, 4= positive control, 5= normal spermatogenesis, GAPDH: 6= tumour cluster, 7= immune cell infiltrate, IL-10: 1= normal spermatogenesis, 2= GCNIS, 3= seminoma, 4= negative control, IL-6: 5= normal spermatogenesis, 6= GCNIS, 7= seminoma, 8= negative control, GAPDH: 9= normal spermatogenesis, 10= GCNIS, 11= seminoma, 12= positive control.

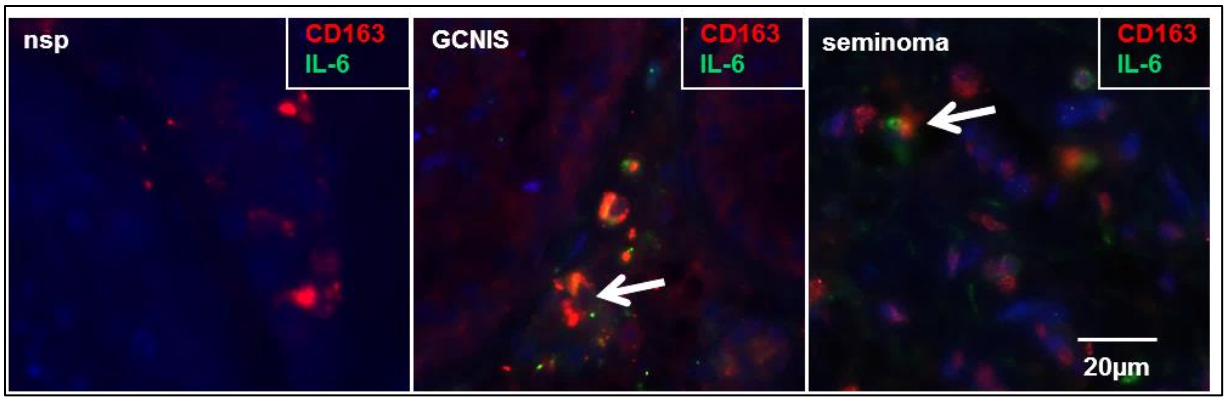

Fig. 2.2.4.1.2: IL-6 expression by CD163+ macrophages (M2) in normal human testis (nsp), GCNIS and seminoma. Co-localization of M2-related marker (CD163, red) and IL-6 (green) in germ cell neoplasia but not in nsp. IL6+/CD163+cells were highlighted by white arrow, merged=orange).

Additionally, an analysis regarding specific prostaglandin receptors was conducted to confirm the presence of target cells in specimens from all three patient groups selecting prostaglandin E receptors EP1, EP2, EP3 and EP4 (Fig. 2.2.4.1.3). In all three categories of specimens (nsp, GCNIS and seminoma) mRNA expression of EP2, EP3 and EP4 was detectable (Fig. 2.2.4.1.3). However, the role of prostaglandin as a macrophage polarization factor has to be further investigated.

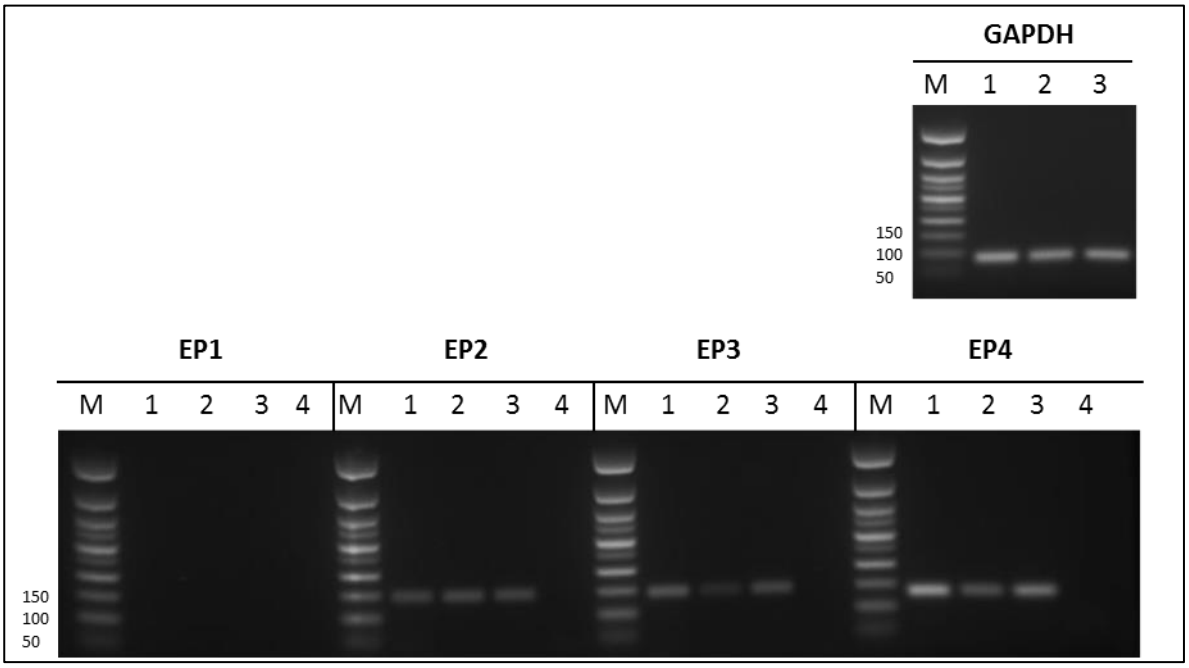

Fig. 2.2.4.1.3: Analysis of specific prostaglandin E receptors (EP1, EP2, EP3, EP4) in human testis by RT-PCR. EP2, EP3 and EP4 was expressed in all three categories of specimens (nsp, GCNIS, seminoma), whereas EP1 was not detectable. GAPDH was used as housekeeper. M= marker, 1= NSP, 2= GCNIS, 3= seminoma, 4= negative control.

2.2.4.2 Identification of potential prognostic testicular cancer marker: Signalling pathways (p65, NF-κB) and immune checkpoints T-cell immunoglobulin mucin-3 (TIM-3) and Galectin-9 associated with testicular cancer

An analysis of immune checkpoint TIM-3/Galectin-9 and NF-kappa-B p65 subunit was performed in normal testis tissue as well as specimens with germ cell neoplasia. A detection of p65 (protein) was possible in GCNIS and seminoma samples, whereas p65 was not expressed in nsp (Fig. 2.2.4.2.1). Additionally, an analysis of TIM-3/Gal-9 known as immune checkpoints was conducted revealing TIM-3 and Galectin-9 expression in nsp and neoplasia specimens (GCNIS and seminoma) (Fig. 2.2.4.2.2).

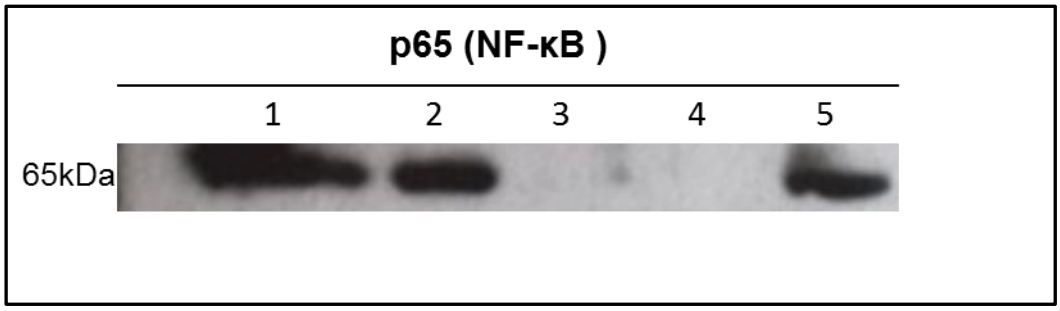

Fig. 2.2.4.2.1: Protein expression of p65 (NF-κB pathway) in normal human testis as well as germ cell neoplasia by western blot. p65 was detectable in GCNIS and seminoma specimens but not in nsp. 1= GCNIS, 2= seminoma, 3=nsp, 4= negative control, 5= positive control (human placenta).

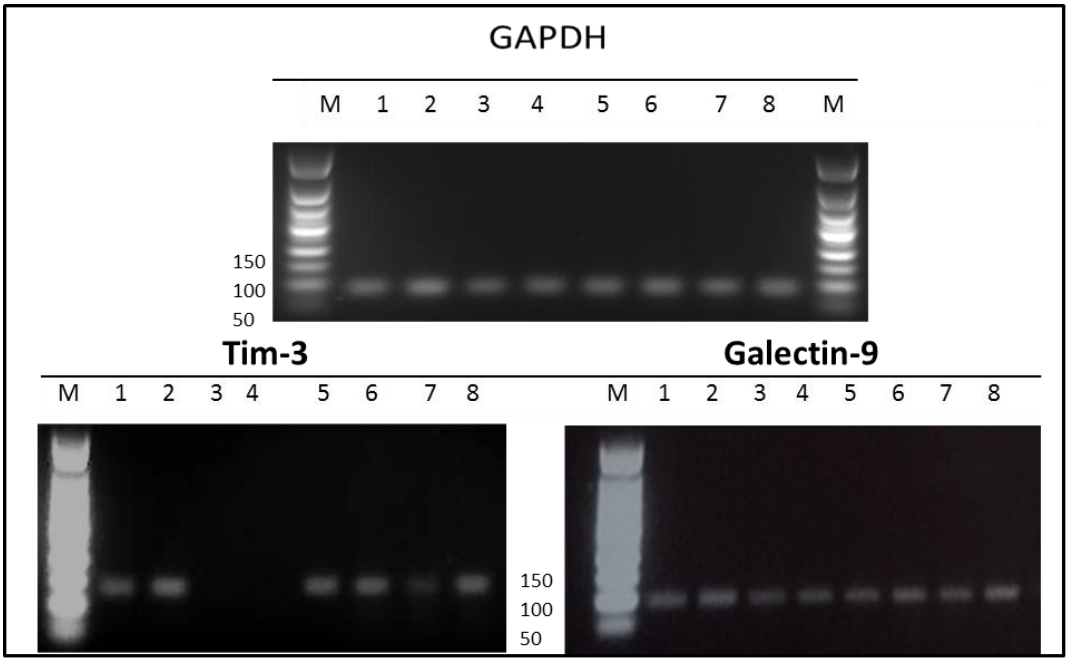

Fig. 2.2.4.2.2: Analysis of immune checkpoint T-cell immunoglobulin mucin-3 (Tim-3)/ Gal-9 expression in normal human testis as well as germ cell neoplasia by RT-PCR. Tim-3 and Galectin-9 were detectable in all nsp (n=2) and seminoma specimens (n=3), whereas in GCNIS (n=3) only one of three samples was positive. M= marker, 1= NSP1, 2= NSP2, 3= GCNIS1, 4= GCNIS2, 5=GCNIS3, 6=seminoma1, 7=seminoma2, 8=seminoma).

2.2.4.3 Impacted spermatogenesis in glucocorticoid-induced leucine zipper protein (GILZ) KO mice influenced testicular immune cell populations

This preliminary study was conducted to elucidate the influence of Glucocorticoid-Induced Leucine Zipper (GILZ) on immune cell populations in the testis. Thus, the effect of Gilz on spermatogenesis was examined by histological evaluation, whereas flow cytometry was performed to study the effect on immune cell populations in Gilz knock-out (KO) mice versus wildtype (WT) animals.

Gilz KO mice showed a reduced testis weight in comparison to the WT (Fig. 2.2.4.3.1, A, B). Additionally, a histological analysis (HE-staining) of Gilz KO mouse testis (week 8-12) revealed that the seminiferous epithelium was strongly affected. Furthermore, the cells in the seminiferous epithelium (SE) were visually identified as tubules with complete loss of germ cells (Fig. 2.2.4.3.1, C, D).

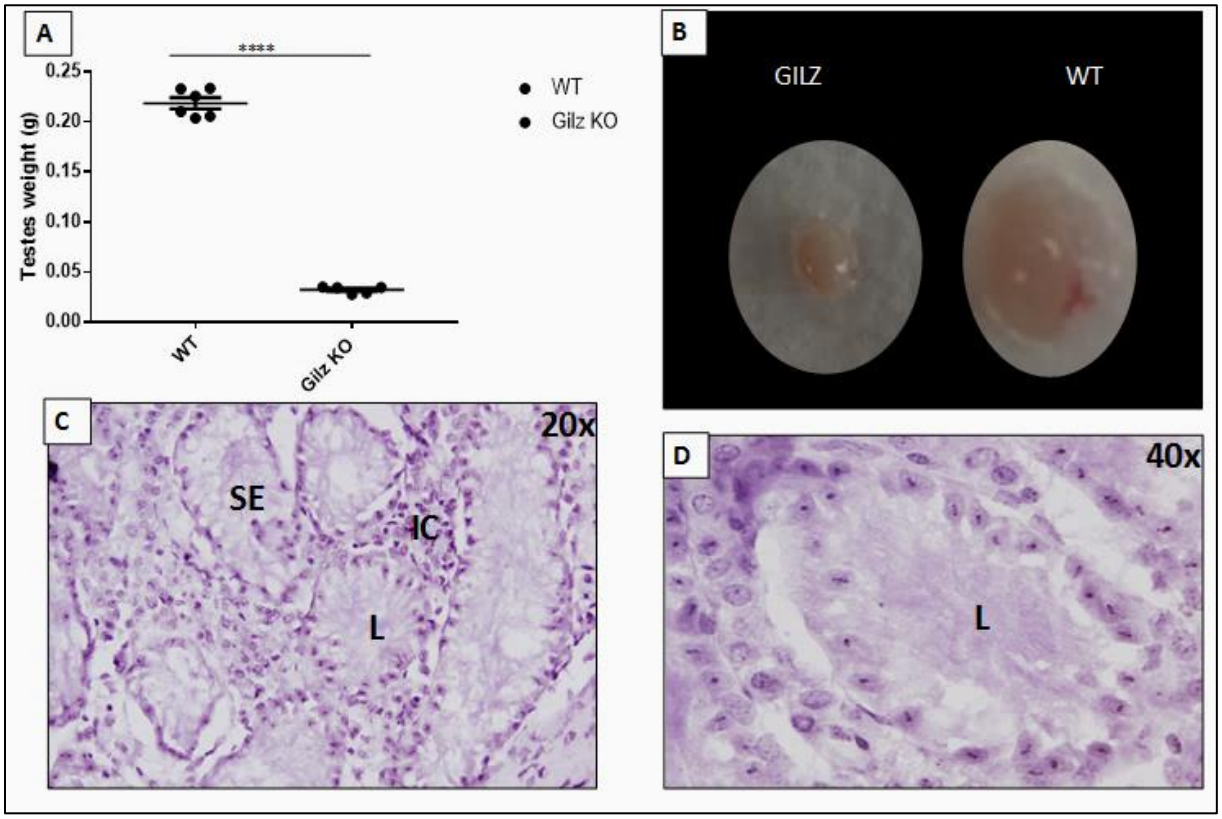

Fig. 2.2.4.3.1: Analysis of testes weight and testis histology in Gilz KO mice (8-12 weeks). After dissection, testes of WT and Gilz KO mice were measured (A, B). Gilz KO mice testis showed a significantly reduced weight compared to Gilz WT mice (WT n=6, Gilz KO n=5). Afterwards, the testes were prepared for cryo-cutting. 5µm slides were cut and stained with Hematoxylin for histological analysis (C, D). WT: n=6; Gilz KO: n=5. Abbreviations: L=lumen, SE=seminiferous epithelium, IC=interstitial compartment. Significance tested by one-way ANOVA (*P < 0.05, **P < 0.01, ***P < 0.001).

Additionally, we analysed immune cells populations in this mouse model by flow.Gilz KO vs. WT immune cell populations were compared to reveal a potential role of Gilz on immune cell populations and factors which were expressed during the spermatogenesis and were absent in the Gilz KO due to the impaired spermatogenesis. Immune suppressive M2 macrophages were frequently found in the WT testis, whereas Gilz KO testis contained less M2 macrophages (CD206+ cells: 25.4%) than the WT (CD206+ cells: 58.9%) (Tab. 2.2.4.3.1). Moreover, a reduction of the macrophage population expressing F4/80+ (pan-macrophage marker) was associated with Gilz KO (F4/80+ cells: 14.9% in Gilz KO vs. 57.5% in WT mice). Similar effects were seen with CD11c+ cells (DC, NK, macrophages) (CD11c: 34.6% in Gilz KO vs. 55.1% in WT mice) (Tab. 2.2.1.4). A detection of CD11b and MHCII positive cells showed no difference in Gilz KO (CD11b: 75.2%; MHCII: 18.9%) and WT testes (CD11b: 77.8%; MHCII: 17.4%) (Tab. 2.2.4.3.1). Our preliminary data showed also a difference in lymphoid immune cell populations compared between Gilz KO and WT animals (Tab. 2.2.1.4.2). T-cells such as CD3+ and NK1.1+ cell numbers were increased in the Gilz KO in comparison to the WT (CD3: 33.8% (Gilz KO) vs. 18.3% (WT); NK1.1:19.2% (Gilz KO) vs. 9.73% (WT) (Tab. 2.2.4.3.2). This suggests a strong effect of GILZ on immune cell populations and subsequently the immune privileged testis.

Tab. 2.2.4.3.1: Preliminary analysis of myeloid immune cells (ICs) using a testes pool of two animals. Immune cell populations were shown in percentages of all gated CD45+ immune cells.

Marker	% WT	% GILZ	Immune cells
CD45+	3.85	10.2	all immune cells
CD11b	77.8	75.2	granulocytes, monocytes/macrophages, dendritic cells, NK cells, and subsets of T and B cells
F4/80	57.5	14.9	pan-macrophages
CD11c	55.1	34.6	dendritic cells, NK, macrophages?
MHCII	17.4	18.9	M1
CD206	58.9	25.4	M2

Tab. 2.2.4.3.2: Preliminary analysis of lymphoid immune cells using a testes pool of two animals. Immune cell populations were shown in percentages of all gated CD45+ immune cells.

Marker	% WT	% GILZ	Immune cells
CD45+	11.7	23.6	all immune cells
CD3+	18.3	33.8	T cells
NK1.1	9.73	19.2	NK cells

2.3 DISCUSSION

In the present study, an analysis of immune cells in the normal human testis (nsp) in comparison to testicular germ cell neoplasia, i.e. GCNIS and seminoma, was performed using IHC and IF.

Additionally, an analysis of immune cells in mice testis in comparison to pathological altered tissue caused by the absence of Gilz was conducted. For instance, it has been shown that macrophages influence spermatogenesis (DeFalco et al., 2015). But can an impacted spermatogenesis also influence immune cell populations? Thus, the effect of Gilz on spermatogenesis was examined by histological evaluation and clearly revealed a pathological alteration due to an impacted spermatogenesis. Furthermore, the absence of Gilz using Gilz KO mice revealed an affected immune cell homeostasis since M2 macrophages were decreased whereas NK and T cells were increased compared to the WT.

In the human, immune cells under physiological conditions are mainly, resident macrophages (CD68+, CD163+) and mast cells, accompanied by few T-cells (CD3+) (Tung and Teuscher, 1995; Hvarness et al., 2013; Klein et al., 2016; Frungieri et al., 2002; Winnal et al., 2011; Pérez et al., 2013; Fijak et al., 2018). Additionally, in this study, individual CD4+ and CD8+ T-cells are detectable in the normal, non-inflamed testis. It is known that CD4 is also expressed by Treg cells (CD4+/FoxP3+), which are considered to be important players maintaining the immune suppressive milieu in the testis (Jacobo et al., 2009; Bonelli *et* al., 2009). Further cell types, especially M2 macrophages, with immunosuppressive functions have been described in studies of mouse testis (Bhushan & Meinhardt, 2017).

The data shown here indicate, that M2 (CD163+/CD206+) macrophages are present in the human testis under physiological conditions. Both immune cell types, Treg and M2 macrophages, are immunosuppressive which explains the detection of anti-inflammatory cytokines (IL-10, TGF-β) in nsp. Further immunosuppressive regulation mechanisms to be considered in the testis are immune checkpoints such as TIM-3 and its ligand Galctin-9 (Loveland et al., 2017), which otherwise have been associated with autoimmunity and chronic viral infections (Sabatos et al., 2003; Golden-Mason et al., 2009). TIM-3 can regulate effector pathways and act as a negative regulator of T cell activation and can be expressed by T cells as well as macrophages and dendritic cells (DC) (Ocaña-Guzman et al., 2016). Interestingly, a detection of TIM-3 and Galectin-9 is possible in human testis specimens with nsp as well as germ

cell neoplasia. This result suggests that TIM-3/ Galectin-9 could play an important role to regulate T cell activation in the immunosuppressive testis as well as in testicular cancer.

In nsp, besides M2 (CD163+ and CD206+) macrophages, CD68+/CD11c- macrophages and sparse CD11c+ DCs were detectable.

However, the investigations of testicular germ cell neoplasia revealed a switch of immune cell populations associated with a pro-inflammatory cytokine milieu. For instance, in neoplasia there were considerable numbers of CD11c+ and CD68+cells detectable (Klein et al., 2016). Interestingly, in this study a co-localization of CD11c+ and CD68+ cells was possible. Zheng et al. showed the presence of aggregate unit forming myeloid CD11c+ DC and suggested a recruiting function of CD68+ macrophages due to their co-localization in seminoma (Zheng et al., 2016). Hume showed that CD11c can also be expressed by macrophages (Hume, 2008). Therefore, an IF double-staining was conducted and revealed CD68+/CD11c+ cells. These CD68+/CD11c+ cells can be classified as M1 macrophages since recent studies observed M1 phenotypes that express CD11c+/CD68+ in different human tissues associated with inflammation (Vianello et al., 2016; Li et al., 2017). The appearance of this M1 phenotype in the diseased human testis indicates a functional polarization of macrophages associated with testicular cancer. This suggests that CD68+/CD11c- macrophages detected in nsp can differentiate into either M1 (CD68+/CD11c+) or M2 (CD163+/CD206+). For instance, CD68+/CD11c- macrophages might be driven by an altered cytokine and chemokine milieu associated with germ cell neoplasia. Previous results postulate that Th1 immune responses are important to drive the M1 polarization. Klein et al showed a significant increase of IFN-γ as a cytokine of Th1-immune responses in testis cancer (Klein et al., 2016). Interestingly, IFN-γ and TNF-α have a strong impact on M1 polarization (Genin et al., 2015). Transcripts of both cytokines were detectable in testis tissue specimens with neoplasia in conjunction with M1 macrophages. Accordingly, there is suggestive evidence that increased numbers of macrophages of the M1 (CD11c+/CD68+) phenotype associated with neoplasia correlate with high expression of pro-inflammatory cytokine such as TNF-α and IL-12.

Interestingly, not all CD11c+ cells express CD68. Therefore, further immune cell types that can express CD11c such as DCs were analyzed. Different DC subsets such as mDC1 (CD1c+/CD11c+), mDC2 (CD141+/CD11c+) and pDC

(CD123+/CD303+/CD304+) could be identified in the human testis, i.e. under pathological conditions. Interestingly, a co-localization of CD4+ cells and CD68+ or CD11c+ cells could be observed by means of IF, suggesting that CD68+ and CD11+ cells are able to present antigens to CD4+ T cells. This could explain the increased detection of CD19+ B cells in neoplasia samples (Klein et al., 2016), which require activation by T cells. Besides antigen presentation, different DC subsets may have an influence on macrophage differentiation. Zheng et al. showed that CD11c+/DC-SIGN+/CCR6+ DC can express IL-4 which is besides IL-10, IL-13, PGE_2 one of the cytokines leading to an M2 polarization (Zheng et al., 2016; Chen and Smyth, 2011; Genin et al., 2015; Martinez et al., 2009; Schraufstatter et al., 2012). However, the polarization and functional role of pDC and mDC in testicular germ cell neoplasia as well as other testicular pathologies is still largely unclear and needs to be further examined.

Furthermore, a detection of M2 macrophages as well as M2-related anti-inflammatory cytokines (IL-10 and TGF-β) is possible in nsp as well as in GCNIS and seminoma specimens, with a significantly higher expression in neoplasia compared to nsp (e.g. CD163, IL-10 and TGF-β). Notably, both M2-related cytokines have been associated with cancer progression and surveillance in different cancer types (Sica et al., 2006; Derynck et al., 2001). Interestingly, IL-10 was significantly higher expressed in GCNIS specimens ($p<0.01$). GCNIS is the precursor of (homogenous) seminoma development in approx. 60% of affected patients (Rajpert-De Meyts et al., 2016). Therefore, it could be postulated that the secretion of IL-10 and other cytokines maintains an immune suppressive milieu and favours seminoma formation and progression by avoiding an effective anti-tumour (tumoricidal) immune response. However, testicular cancer is associated with the presence of both, M1 and M2 macrophages, as well as a pro- and anti-inflammatory cytokines. Thus, previous results indicating a balanced action of pro-inflammatory M1 and anti-inflammatory M2 macrophages associated with testicular cancer.

The investigation of functional macrophage polarization could be helpful to better understand the control of cancer progression by a specific immune environment. Subsequently, potential macrophage polarization factors such as IL-10, PTGES2, TGF-β1 and IL-6 were revealed in line with earlier results indicating a pivotal role of IL-6 in the development of testicular germ cell neoplasia (Klein et al., 2016). An identification of IL-6 expressed by M2 macrophages in the neoplasia specimen but not in nsp un-

derpinning previously hypothesis from Klein et al. (Klein et al., 2016). Additionally, mRNA level have confirmed that IL-6 is only associated with GCNIS and seminoma, but not in testicular inflammation due to other pathologies (Klein et al., 2016). Weagel et al. showed that macrophage polarization is a spectrum which depends on many different factors (Weagel et al., 2015). For instance, M2 macrophages can be classified into M2a, M2b, M2c and M2d. Among these, M2b macrophages can express IL-6 (Weagel et al., 2015). Moreover, Chanmee et al. and Lu et al. have shown that M2c macrophages positive for CD163 and CD206 can express high amounts of TGF-β1 and IL-10 (Chanmee et al., 2014; Lu et al., 2013). This M2c macrophage phenotype shares characteristics of M2 macrophages that were detectable in testis specimens with nsp and neoplasia. However, it could be that other macrophage subclass subsets are associated with neoplasia since some M2 macrophages can express IL-6. This suggests that some M2 subclass macrophages drive the functional polarization of macrophages. Besides M2 macrophages, cancer cells themself might secrete immune suppressive factors and, thus, control macrophage polarization. For instance, it has been shown that cervical carcinoma-derived IL-6 and PGE2 have an influence on M2 polarization (Heusinkveld et al., 2011b).

Additionally, to understand the recruitment and differentiation of macrophages in the human testis, the presence of chemokines which are known as chemoattractants were investigated. Interestingly, a detection of the chemokine CCL15 was possible in nsp. This observation suggests that this chemokine might be important for the migration of CD68+ macrophages. This indicates that blood circulating CD68+ monocytes are precursors of macrophages recruited to the testis that can subsequently differentiate into both M1 and M2 phenotypes, depending on the environment. This hypothesis is supported by the expression of CCL15-related receptors such as CCR1 and CCR3 by CD68+ cells in normal testis tissue (nsp). Additionally, Wang et al. have shown that CD68+ macrophages are believed to originate from circulatory monocytes/macrophages (Wang et al., 1994). This suggests that monocyte derived cell type can be recruited by CCL15 In the healthy testis, mediators such as IL-10, TGF-β, prostaglandin and glucocorticoids play a role in macrophage polarization and might drive CD68+ cells into an immune-suppressive M2 phenotype (Martinez et al., 2009; Wang et al., 2017).

In contrast, there is a downregulation of CCL15 in testicular germ cell neoplasia and an upregulation of different other chemokines. Comprehensive analysis of the chem-

okine gene expression profiles using qRT-PCR could reflect the interaction of different immune cells and the recruitment of macrophages and DC associated with testicular germ cell neoplasia. Especially chemokines are important for the migration and differentiation of monocytes/ macrophages in a tissue-dependent manner (Sica et al., 2006). Interestingly, increased transcript levels of chemokines such as CCL2, CCL5, CCL18, and CCL22 were detectable in samples with neoplasia compared to nsp. These results are in line with reports concerning other cancer entities. Recent studies have shown an upregulation of CCL2 in primary prostate and invasive breast cancer associated with a recruitment of M2 macrophages (Fang et al., 2016; Mizutani et al., 2009; Ueno et al., 2000). Fang et al. showed that an *in vivo* gene silencing leads to a tumour growth inhibition and reduced M2 recruitment in breast cancer (Fang et al., 2016). Therefore, we speculated that CCL2 is one of the important M2 attractants. Furthermore, CCL18 expression levels have been shown to influence disease outcomes in cancer patients, especially in cutaneous lymphoma and breast cancer (Miyagaki et al., 2013; Narita et al., 2011). Interestingly, CCL18 in colorectal cancer has the opposite effect, with high levels correlated with better survival (Yuan et al., 2013). In contrast, Schraufstatter et al. have shown that CCL18 leads to a maturation of cultured monocytes to macrophages in the M2 spectrum (Schraufstatter et al., 2012). Additionally, CCL18 increased the expression of other chemokines such as CCL2 and CCL22 and cytokines such as IL-10 which are also detectable in human neoplasia (Schraufstatter et al., 2012). Concerning the human testis, expression of IL-10 was significantly increased in GCNIS in comparison to nsp, where CCL18 transcript levels were virtually not detectable. However, it has been shown that CCL18 and CCL22 can be expressed by M2 macrophages (Mantovani et al., 2002). Thus, it has to be considered that signals other than CCL18 and CCL22 support M2 macrophage polarization in the human testis under physiological conditions. On the other hand, recent studies revealed further evidences that chemokines such as CCL2, CCL18, and CCL17 can be expressed by different tumours (Roca et al., 2009; Kim et al., 2009; Erler et al., 2009; Mantovani, 2008). It can be assumed that tumour cells strongly influence immune cells polarization to drive them into immune-suppressive phenotypes, however a complete suppression of immune responses does obviously not occur.

CONCLUSION

Human testicular germ cell neoplasia is commonly associated with infiltrating immune cells. Besides few T-lymphocytes, antigen-presenting-cells (APC) such as CD68+ and sparse CD11c+ cells were detected in normal testis (nsp). Both of these markers, CD11c (integrin glycoprotein) and CD68 (glycoprotein), are typically expressed by macrophages, whereas CD11c can also be expressed by DCs. Macrophage and DC subsets have different phenotypic characteristics. Both immune cell types can change their functional state depending on the environment. Especially M1 (classically activated) and M2 (alternatively activated) macrophages are known for their different function in cancer development. Previous studies have shown that the critical immune suppressive M2 phenotype can be driven by tumour derived and T cell (Th1 or Th2) derived cytokines. Therefore, a detailed analysis of different macrophage (M1 and M2) and DC subsets which are might be driven by cytokines and chemokines associated with testicular germ cell neoplasia was conducted. In neoplasia specimens a detection of macrophage subtypes such as M1 (CD68+/CD11c+, pro-inflammatory properties), M2 (CD163+/CD206+, anti-inflammatory, pro tumorigenic), DCs such as pDC, mDC1 and mDC2 (plasmocytoid: CD123+/CD303+/CD304+; myeloid: CD1c+/CD11c+ and CD11c+/CD141+) is possible. In contrast, in specimens of normal, non-inflamed testes (nsp) CD68+/CD11c- macrophages, single CD11c+cells and M2 macrophages which seem to be important for maintaining the immune privilege were detectable. This suggested a recruitment and a functional polarization of macrophages from CD68+ cells (nsp) into M1 (CD68+/CD11c+) or M2 (CD163+/CD206) under pathological conditions of neoplasia (GCNIS and seminoma) (Fig. 2.3.1/2.3.2). Furthermore, M1 related pro-inflammatory cytokines such as TNF-α, IL12 and M2 related cytokines such as IL-10 and TGF-β were detectable in all neoplasia samples. Additionally, potential factors (chemokines) for the recruitment and polarization of immune cells are revealed. Interestingly, an upregulation of chemokines such as CCL2, 5, 18, 22 which are possibly responsible for monocyte/ macrophage recruitment and/ or differentiation is detectable in testicular germ cell neoplasia. Furthermore, in neoplasia samples a downregulation of CCL15 is observable. In the normal testis, CCL15 is detectable and might be important to recruit CD68+ cells which express the chemokine specific receptors, CCR1 and CCR3. Those macrophages could then differentiate into another phenotype depending on the local en-

vironment. Moreover, testicular cancer is associated with M2 polarization factors such as TGF-β1, IL-6 and PTGES2 (Fig. 2.3.2). Accordingly, elevated numbers of M2 macrophages as well as increased expression of M2 related anti-inflammatory cytokines was observed in neoplasia compared to nsp. However, besides M2 polarization factors we detected TNF-α as M1 polarization factor as well as an increased frequency of M1 macrophages. We assumed that there might be a balance between tumour suppressive M1 macrophages and tumour progressive M2 macrophages in testicular cancer which can be easily influenced by cytokine and chemokine expression. This depends on the tumour environment that is influenced by different immune cell types and tumour growth and other immune cell interactions e.g. Th1 and Th2. However, tumour cells drive the M2 differentiation (Fig. 2.3.2). Subsequently, M2 macrophages are the dominating immune cell population that support tumour grow. Therefore, as clinical outcome an inhibition of typical M2 polarization factors should be considered rather than an inhibition of recruitment factors (chemokines) since this would also influence the recruitment of M1 macrophages. A decrease of immunosuppressive M2 macrophages in this tumour environment would probably reinforce immune reactions against cancer by pro-inflammatory M1 macrophages.

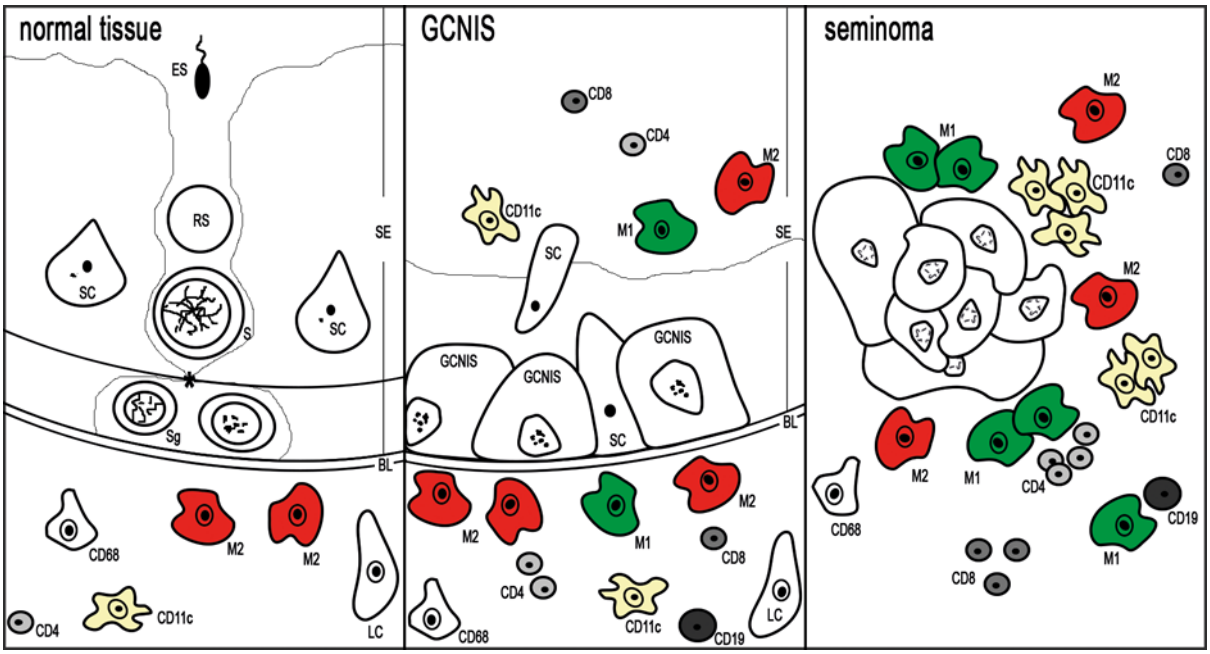

Fig. 2.3.1: Summary of immune cell types detected in GCNIS and seminoma in comparison to normal testis tissue (nsp). Testes with nsp contain only M2 macrophages, mast cells (not shown), CD68+ macrophages, single CD4+ T cells and single CD11c+ cells. In GCNIS, M2 (CD163+/CD206) macrophages and also M1 (CD68+/CD11c) macrophages were detectable. Additionally, T cells such as CD4+ and CD8+, B cells (CD19) and CD11c dendritic cells were found. Interestingly, M1 macrophages and DCs form cell aggregations around the tumor cells. Immune cells: T-lymphocytes: CD4+, CD8+, B-lymphocytes: CD19+, macrophages: CD163+, CD206+ (M2), CD68+, CD11c (M1), CD68+, dendritic cells/ macrophages: CD11c+, Somatic cells: Sertoli cells (SC), Leydig cells (LC), spermatogonia (Sg), spermatocytes(S), round spermatid (RS), elongated spermatid (ES). Basal lamina (BL), seminiferous epithelium (SE), blood testis barrier (*).

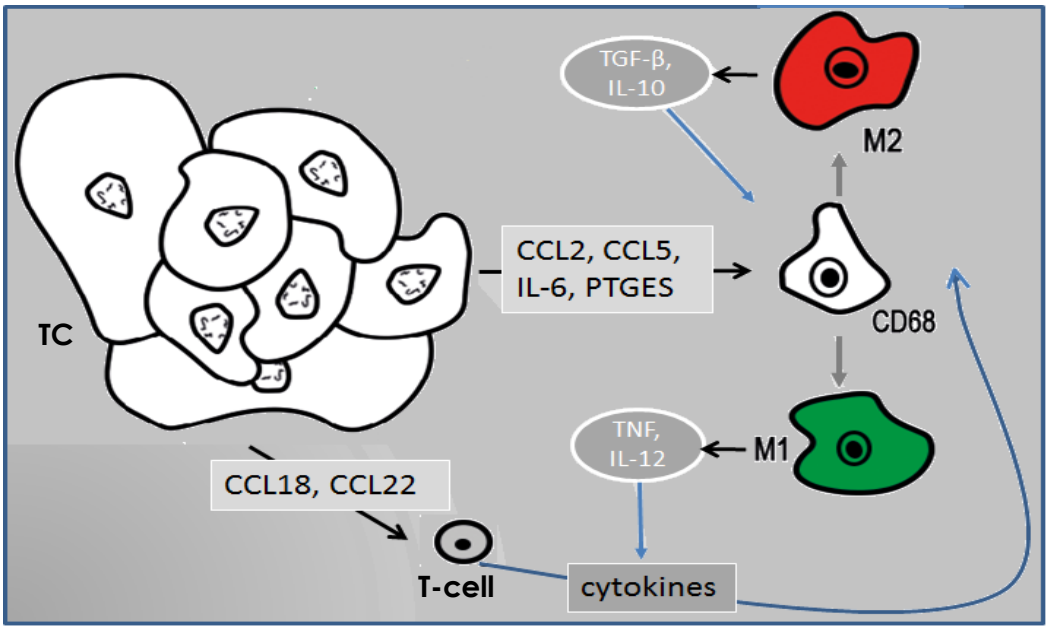

Fig. 2.3.2: Functional macrophage polarization in the tumour environment: Monocytes and macrophages can become either M1 or M2 macrophages depending on the stimuli present in their microenvironment. Both pro-inflammatory M1 (producing TNF and IL-12) and anti-inflammatory M2 (producing TGF-β and IL-10) macrophage subsets are present in testicular germ cell neoplasia (GCNIS, seminoma). Note that tumour cells can secrete macrophage recruitment and polarization factors such as chemokines, cytokines and PTGES. T-cells can influence the microenvironment by expression of different cytokines and influence macrophage polarization as well.
TC=tumour cell, M1=M1 macrophages, M2=M2 macrophages. PTGES=prostaglandine E synthase. Black arrows indicate cytokine or chemokine expression by cell types; blue arrows indicate the influence on cell differentiation or cytokine expression; grey arrows show differentiation of macrophages.

CHAPTER 3

Assessment of mono-cultured tumour and immune cells of relevance to testicular neoplasia: the TCam-2 seminoma and THP-1 macrophage cell lines

CHAPTER 3: Assessment of mono-cultured tumour and immune cells of relevance to testicular neoplasia: the TCam-2 seminoma and THP-1 macrophage cell lines

3 INTRODUCTION

In the healthy human testis with complete spermatogenesis, both CD68+macrophages and M2 macrophages were detected, whereas a new macrophage subtype, corresponding to the M1 macrophage phenotype, was identified in specimens with neoplasia. We hypothesized that a functional polarization of macrophages had arisen due to the environmental change associated with the emergence of neoplastic testicular germ cells. Thus, we proposed that in addition to the contribution of hormonal changes of puberty altering the testicular milieu, an important environmental shift is driven locally by cytokines and chemokines which can influence immune cell recruitment and polarization. To understand this mechanism, our working group previously established a tumour/ immune cell co-culture model using seminoma cells and peripheral blood mononuclear cells (PBMCs) that included an analysis of all immune cell types (Klein et al., 2017). The present study builds on this cell-culture model to examine in more detail how macrophages and seminoma cells contribute to the testicular tumour microenvironment (see chapter 4), by constructing a cell culture model using a human monocytic leukemia cell line (THP-1) and a human seminoma cell line (TCam-2), which are characterised in this chapter.

THP-1 cells are a well-established human macrophages model, in which the progenitor THP-1 cells (monocyte-derived) can be differentiated into M0, M1 and M2 macrophage subsets using protocols that involve progressive exposure to specific factors (Park et al., 2007; Lund et al., 2016; Genin et al., 2015). The evaluation of polarization outcomes has relied on a cohort of RNA and protein markers.

TCam- 2 cells were originally derived from a human seminoma (Mizuno et al., 1993). It is the only robust model of human testicular germ tumour cells, retaining features of seminoma cells which are shared with human gonocytes evidenced by the expression of pluripotency markers e.g. OCT3/4, NANOG and LIN28 (deJong et al., 2008; Eckert et al., 2008). As shown by deJong et al., TCam-2 cells are the first well-characterized seminoma-derived cell line, that features characteristic foetal germ cell responses to TGF-beta ligands and retinoic acid (de Jong et al., 2008; Young et al., 2011).

With the objectives of revealing what cytokines and chemokines present in testicular germ cell tumours are potential macrophage polarization factors, and subsequently to understand their impact on the functional polarization of macrophages, THP-1 cells were first differentiated into M0, M1 and M2 macrophages using an established protocol, and afterwards validated by measuring both RNA and protein changes by qRT-PCR, flow cytometry and a multiplex cytokine and chemokine analysis. The expression of receptors determined to be present in macrophages within TGCTs was evaluated, and the influence on macrophage phenotype of signalling moieties present in tumours or associated with these specific receptors was measured. The potential for TCam-2 cells to synthesize factors that may recruit and alter macrophage function was also examined by qRT-PCR (recruitment factors e.g CCL2 and CCL5) a multiplex cytokine and chemokine analysis.

3.1 MATERIAL AND METHODS

3.1.1 Cell cultures

3.1.1.1 TCam-2 (human seminoma cell line)

TCam-2 cells (human seminoma derived cell line) (Mizuno et al., 1993; deJong et al., 2008) originally obtained from Prof Kitizawa, Japan) were cultivated in a T75-flask containing 1640RPMI (Gibco, Paisley, UK) with 1% Pen/Strep (Gibco, Paisley, UK) and 10% fetal calf serum (FCS; Quantum Scientific, Minto, Australia) at 37°C and 5% CO_2 until the cells were approximately 90% confluent. The medium was replaced every 2 days. For the cell transfer, the cells were washed with 1 ml PBS and 1 ml 0.1% trypsin/ versene solution (TV) (Gibco, Paisley, UK) added with the flask left for at least 2 min in the incubator. The cell detachment was visualized using an inverted brightfield microscope (Primo Vert, Zeiss). After successful detachment, the cell suspension containing 0.1% TV was transferred in a 15 ml Falcon tube and centrifuged at 239rcf, RT for 2 min. Afterwards, the supernatant was discard and 2 ml of RPMI1640 (1% Pen/Strep and 5% or 3% FCS) was added, the cells were resuspended, counted and seeded at a density of $1x10^5$ cells per well in a 6 well plate (Falcon®, Corning Life Science, Tewksbury, USA). After the experimental incubation, TCam-2 cells were collected for mRNA analyses into Trizol (see sections 3.1.3 and 3.1.4) or were snap frozen immediately on dry ice and stored at 80°C for subsequent protein analyses (sections 3.1.5 and 3.1.6).

3.1.1.2 THP-1 (human monocytic leukemia cell line)

THP-1 cells (human monocytic leukemia cell line; provided by Dr. Ashley Mansell, Hudson Institute of Medical Research, Clayton, Australia) were cultivated as a non-adherent cell line in T75-flask containing 1640RPMI with 1% Pen/Strep (Gibco) and 10% FCS at 37°C and 5% CO_2 until confluent. Media was changed every 2-3 days, with the cell suspension transferred into a 15 ml Falcon tube for centrifugation at 239rcf, RT for 2 min. The cell pellet was resuspended in 2 ml of RPMI1640 (1% Pen/Strep and 10% FCS) and seeded for experiments at $1x10^5$ cells per well in 6 well plates. To induce differentiation (see reagents, Tab. 3.1.1), cells were first treated with phorbol 12-myristate 13-acetate (PMA, 20 ng/ml, Biolegend) for 24 h (Fig. 3.1.2), then the newly adherent and differentiated M0 macrophages were treated with either Lipopolysaccharide (LPS, 10 pg/ml) and IFN-γ (20 ng/ml, Biolegend) for M1 differen-

tiation, or with IL-4 (20 ng/ml, Biolegend) and IL-13 (20 ng/ml, Biolegend) for M2 differentiation, for a further 43 h incubation (Fig. 3.1.2). After this incubation, the cells were designated for further treatments with cytokines, chemokines and TGF-β signaling pathway inhibitor (e.g. IL-10, activin A, Transforming growth factor beta-1 (TGF-β1), CCL2, CCL5, CCL15 (see Tab. 3.1.1) and/ or RNA extraction and subsequent cDNA synthesis (PCR)(see 3.1.3/ 3.1.4), protein isolation (SDS-PAGE, western blot) (see 3.1.5), multiplex (see 3.1.6) or the cells fixed for Flow cytometric analysis (see 3.1.7).

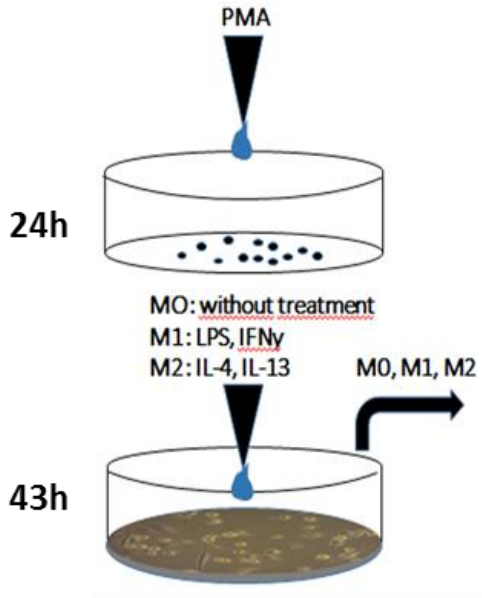

- Cytokine and chemokine treatment
- RNA extraction, cDNA synthesis (qRT-PCR)
- Protein isolation (SDS-PAGE, western blot)
- Supernatant collection (multiplex)
- Cell fixation (Flow)

Fig. 3.1.1.2: Schematic of the in-vitro THP-1 setup for macrophage differentiation. Human monocyte-derived THP-1 cells were treated with PMA and incubated for 24 h. Afterwards, the differentiated THP-1 cells (now activated M0 macrophages) were treated with either LPS (10 pg/ml) or IFN-γ (20 ng/ml) to differentiate them into M1 macrophages or with IL-4 (20 ng/ml) and IL-13 (20 ng/ml) to differentiate into M2 macrophages. After the differentiation, cells were collected for the following procedures and analyses: RNA extraction, cDNA synthesis (qRT-PCR), protein isolation (SDS-PAGE, western blot), supernatant collection (multiplex) and cell fixation (Flow).

3.1.1 Table of. Reagents for THP-1 treatment

Protein name	Manufacturer	Cat. No.
Phorbol 12-myristate 13-acetate (PMA)	Biolegend	423301
Lipopolysaccharide (LPS)	Sigma	8630
Recombinant Human IFN-γ (carrier-free)	Biolegend	570202
Recombinant Human IL-13 (carrier-free)	Biolegend	571102
Recombinant Human IL-4 (Animal-Free)	Biolegend	714904
Recombinant Human CCL15 (MIP-1δ) (carrier-free)	Biolegend	587402
Recombinant Human CCL5 (RANTES) (Animal-Free)	Biolegend	717004
Recombinant Human CCL2 (MCP-1) (Animal-Free)	Biolegend	716504
IL-10	Biolegend	715602
Transforming growth factor beta 1 (TGF-β1)	Cell Signaling	8915LC
Activin A	Abcam	ab50051
SB431542	Cell Signaling	14775

3.1.2 Cell migration

Previously differentiated THP-1 cells (M0, M1, M2) were cultivated in 6 well plates until confluent. Cells were treated with CCL15 (20 ng/ml), CCL2 (20 ng/ml) or CCL5 (20 ng/ml), and a cell-free gap created from one side of the culture well to the other with a pipette tip. For orientation and subsequent measurement of gap closure, lines were drawn along the edges of the initial gap, and the extent of gap closure was measured from photographs taken at different time points using ImageJ, an image processing program for scientific analysis (t= 0 h, 24 h, 48 h, 72 h)(Fig. 3.1.2). The area that was measured at each time point was compared to the starting gap size. The percentage of gap closure is presented relative to t= 0 h.

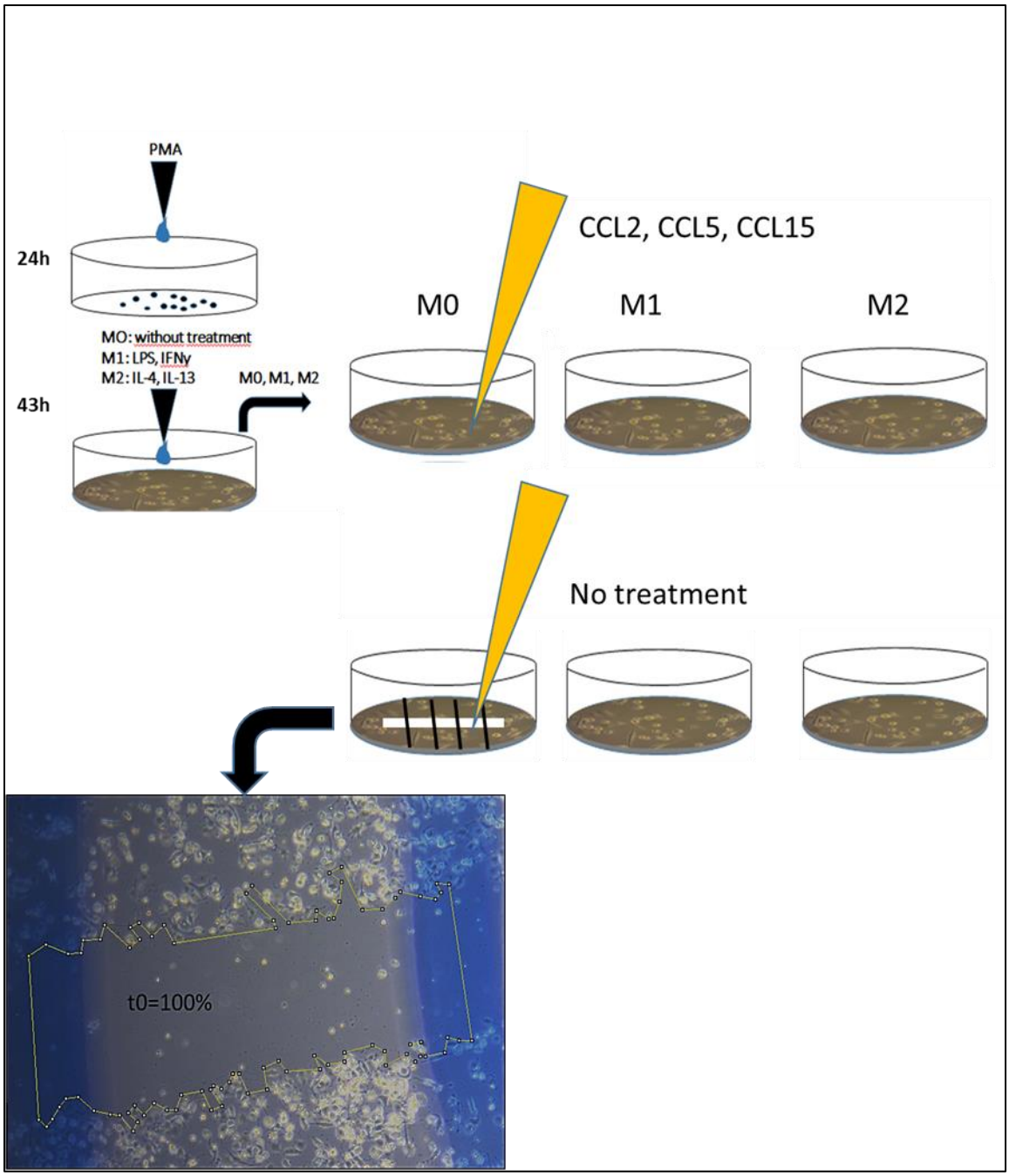

Fig. 3.1.2: Schematic of migration assay also called wound healing assay using differentiated THP-1 cells (M0, M1, M2). THP-1 cells were treated with cytokines and LPS, and then differentiated into M0, M1 and M2 macrophages. Afterwards the cells were cultivated in 6 well plates until confluent (90%). Then M0, M1 and M2 macrophages were treated with different chemokines such as CCL2 (20 ng/ml), CCL5 (20 ng/ml) and CCL15 (20 ng/ml)(n=3). Next a gap was scratched in each well by using a pipette tip. For orientation, lines were drawn directly on the well, and the extent of gap closure was measured at different time points using ImageJ (t= 0 h, 24h, 48h, 72h). The area that was measured at t= 24 h, 48 h, 72 h and compared with t=0 h set to 100%, thus the percentage of gap closure is shown as a percentage relative to t= 0 h.

3.1.3 Reverse transcriptase PCR (with RNA isolation)

For extraction of total RNA, cells were washed with PBS then 1 ml TRIZOL was added to each well and the plate incubated on a shaker for 10 min at RT. Afterwards, a cell scraper (BD Falcon, Bedford, USA) was used to remove all attached cells, with differentiated THP-1 cells being extremely tightly attached. The TRIZOL cell suspension was collected and frozen at -80° or processed immediately. Then 150 µl Chloroform was added, mixed (by shaking) and incubated for 5 min at RT. The solution was centrifuged at 4°, 10621 rcf for 15 min. Afterwards the aqueous phase was transferred into a new tube and precipitated with 500 µl 2-Propanolol, washed 2x with cold 70% Ethanol afterwards the pellet was air dried and resuspenden with 21 µl RNAfree water.

The DNase I kit (Ambion, LifeTechnologies) was used according to the manufacturer's protocol (see Apendix). RNA was quantified using Nanodrop photometer (NP80, Implen). Synthesis of cDNA was performed using 500 ng DNA-free total RNA, 1 µl SuperScript® III reverse transcriptase (200 U/µl, LifeTechnologies, Grand Island, NY, USA), 4 µl 5x First Strand buffer (LifeTechnologies, Grand Island, NY, USA), 1 µl random hexamer primers (50 µM, Promega, Applied Biosystems), 1µl DTT (0.1M, Invitrogen), 1 µl dNTP mix (10 mM, Sigma-Aldrich, Castle Hill, Australia) and 1 µl Molecular Water (Carl Roth GmbH & Co. KG, Karlsruhe, Germany), per sample, according to the enzyme manufacturer's protocol. Negative control samples lacked SuperScript® III (enzyme volume replaced with molecular water). The cDNA synthesis program was conducted as in Tab. 3.1.3.

Table 3.1.3: RT program for cDNA synthesis

65°C	25°C	50°C	70°C	4°C
5 min	10 min.	1 h.	15 min.	hold

3.1.4 Quantitative RT-PCR

Quantitative real-time PCR was conducted for analyses of CD markers in macrophages and cytokine and chemokine mRNA transcript levels in M0, M1, M2 and TCam-2 cells. For the measurement of pro-inflammatory cytokines, such as IL1b, IL-12, TNFa, and anti-inflammatory cytokines, such as IL-10, TGF-β1, as well as pleiotropic IL-6 and chemokines including CCL2 and CCL5, Taqman probes (Thermo Fisher Scientific) were used (see Tab. 3.1.4.1) in a Taqman Assay, according to the

manufacturer's protocol. The samples were prepared using 8 µl TaqMan® Gene Expression Assay and 2 µl sample (diluted 1:20 in Molecular water) (see Appendix, Chapter 3).

For the analysis of CD markers to identify macrophage subsets, Oct3/4 to identify TCam-2 cells, Inhba (activin A, pleitropic cytokine), and chemokine receptors such as CCR1, CCR2, CCR3, CCR4 and CCR5, primers were designed using Oligo Explorer, Version 1.1.2 (see primer details, Tab. 3.1.4.2). The analysis was conducted using SybrGreen, according to the manufacturer's protocol. The samples were prepared using 2 µl sample, 2 µl Molecular Water, 0.5 µl primer (10 pm, each forward and reverse) and 5 µl SYBRGreen (Thermo Fisher Scientific) and analysed by Applied Biosystem 7900HT Fast Real-Time PCR machine. Each reaction was performed in technical triplicates which were averaged and calculated using SDS v2.4 (Applied Biosystems). For statistical analysis, a One Way ANOVA was performed followed by a Tukey *post hoc* test (GraphPad7.01). Data are shown as fold-change normalized to ACTB; term human placenta RNA (supplied by Ursula Manuelpillai) was used as a positive control.

3.1.4.1 Table of TaqMan probes

Target	**Product No.**
Human ACTB	Hs01060665_g1
Human GAPDH	Hs02758991_g1
Human IL-1b	Hs01555410_m1
Human IL-12a	Hs01073447_m1
Human TNFα	Hs00174128_m1
Human IL-6	Hs00174131_m1
Human IL-10	Hs00961622_m1
Human TGFβ1	Hs00998133_m1
Human CCL2	Hs00234140_m1
Human CCL5	Hs00982282_m1

3.1.4.2 Table of designed primers

Target	Accession number	Utility	Forward primer, 5'-3'	Reverse primer, 5'- 3'
GAPDH	NM_001256799.2	House-keeper	AA-GCCTGCCGGTGACTAAC	CGCCCAATACGACCAAATC
Bactin	NM_001101.4	House-keeper	GCATGGGTCAGAAGGATTC	ACGCAGCTCATT-GTAGAAGG
CD11c	NM_001286375.1	M1	AGACAGGAGCAG-GACATTG	GAACTGCATCAGGGAAAAC
CD68	BT009923.1	M1	GCTGGCTGTGCTTTTCTCG	TCCTGTGGCTGGTTGTTCC
CD163	DQ058615.1	M2	CTGTTTTGTCACCAG-TTCTC	CTCCAGCCATTATTACACAC
CD206	NM_002438.3	M2	GGACTGGGTTGC-TATCACTC	AACCCGATCCCTTGTAGAG
CCR1	NM_001295.2	chemokine receptor	AAA-GCCCCAGAAACAAAGAC	TTGCATCCCCATAGTCAAAC
CCR2	NM_001123041.2	chemokine receptor	GACCCACAAGATAAA-GAAGC	TTGAGGTCTCCAGAATAGG
CCR3	NM_001837.3	chemokine receptor	GTGGTGGTGGTGATGATCC	ATGCCCCCTGACATAGTGG
CCR4	NM_005508.4	chemokine receptor	CTGCTCTTCGTGTTTTCCC	AAAGCCCAC-CAAGTACATCC
CCR5	NM_000579.3	chemokine receptor	TAGTGGGATGAGCAGA-GAAC	GGCGAAAAGAATCAGA-GAAC
Inhba	NM_002192.3	Activin A	TCGGAGATCATCAC-GTTTGC	GGGACTTTTAGGAA-GAGCCAGAC

3.1.5 Western blot

3.1.5.1 Protein Isolation

As described above, the media of the cultivated and differentiated M1 (THP-1) cells was collected by aspiration and frozen for further analyses by Multiplex, while the cells were washed with ice-cold PBS then 200 µl ice-cold cell lysate solution (10x Lysis buffer (Cell Signaling, #9803) diluted 1:10 in distilled water containing phosphatase (Cell Signalling, #5870S) and protease inhibitor (Cell Signalling, #5871S) diluted 1:100 to prevent proteolytic degradation was added to each well. After 5 min on ice, cells were collected from individual wells using a cell scraper, then transferred to an Eppendorf tube, kept on ice for 20 min and vortexed every 5 min. Afterwards, the tubes were centrifuged at 10621rcf for 10 min. The supernatant was collected for protein concentration measurement against a standard of bovine serum albumin, and frozen at -80°C or directly used for SDS-PAGE. For SDS-PAGE, 30 µg of protein per lane was used.

3.1.5.2 SDS-PAGE

The 10-12% running gel was cast 2 h before the protein transfer was conducted to allow an appropriate polymerization of the gel (see Appendix, Chapter 3). The samples were prepared by adding 2x SDS sample buffer (see appendix) plus β-mercaptoethanol then mixed. The samples were boiled for 5 mins at 95°C for protein denaturation. Then 3 µl of a pre-stained protein molecular size ladder (*PageRuler* Prestained Protein Ladder, Fisher Scientific) was used and 10 µl in each gel, and each sample was loaded into a well. The gel was run at 30 mA until the loading dye entered the separating gel, and the voltage was increased to 50mA for at least 1 h until the loading dye reached the bottom of the gel.

3.1.5.3 Protein transfer

While the SDS-gel was running, transfer buffer (see appendix, Chapter 3), Whatman paper (BioRad, Hercules, California, USA) and membrane were prepared as follows. Four pieces of blotting paper were cut to a size slightly smaller than the gel and incubated in transfer buffer along with 4x sponges. Then the PVDF-membrane (Millipore Immobilon P Transfer Membrane IPVH 00010 PVDF 0.45 µm pore size) was carefully cut to the gel size, incubated in methanol for 30 sec then incubated in transfer buffer. Next the gel and PVDF membrane were incubated in transfer buffer. Then the gel and PVDF membrane were prepared for the protein transfer (see chapter 2, Fig. 2.1.6.4, transfer assembly). Protein transfer proceeded with the transfer cassette immersed in transfer buffer at 100 Volts for 2 h at RT.

3.1.5.4 Protein detection

After transfer, the PVDF membrane was carefully separated from the gel and washed twice with TBST (0.05% Tween in Tris-buffered saline TBS) for at least 5 min. All incubations and washes were performed at RT. The membrane was blocked with 3-5% BSA/TBST for 1 h on a rocking plate, then the primary antibody (diluted in blocking buffer, 1:800) was added and incubated with rocking for an additional hour. The membrane was next washed three times using TBST buffer for 5-10 min. The secondary antibody (diluted in 3-5% BSA/TBST, 1:5000) was added and incubated for 1 h with rocking, then the membrane was washed two times for 8 min using TBST. For

the chemiluminescent reaction, 400 µl of lumi-light western blotting substrate 1 and 2 (Roche, Germany, Mannheim) were mixed, added and incubated for 2 min. Visualization of antibody binding to target proteins was conducted using BIORAD Chemi Doc™ MP.

3.1.5.4.1 Table of primary antibodies

Primary Antibody	Manufacturer	Dilution	Cat. No.
pSmad2- 255	Cell Signaling	1:800	pS5255
pSmad3-423/425	Cell Signaling	1:800	9513S
Smad3	Cell Signaling	1:800	9520S
a-tubulin	Sigma-Aldrich	1:3000	T5168

3.1.5.4.2 Table of secondary antibodies

Secondary Antibody	Manufacturer	Dilution	Cat. No.
Anti-Rabbit IgG Peroxidase	Sigma-Aldrich	1:5000	A9169
Anti-Mouse IgG Peroxidase	Sigma-Aldrich	1:5000	A9044

3.1.6 Multiplex Cytokine /Chemokine analysis

The medium from cultivated and differentiated THP-1 (M0, M1, M2) cells was collected for multiplex analysis. For cytokine and chemokine analysis, two separate Luminex Multiplex Kits (Merck Millipore, Australia) were used (see Appendix, kits). Magnetic beads were used to isolate the reaction products for measurement in cell supernatants, that is more efficient and sensitive for analysis of small samples than traditional ELISA kits. The supernatants of cultivated cells exposed to factors to induce THP-1 cell differentiation into M0, M1 and M2 cells, or without exposure (e.g. TCam-2 cells) that were used for this analysis were centrifuged at 239rcf for 2 min to exclude remaining cells, then collected in Eppendorf tubes for storage at -80°C or else immediately proceeded. Analysis was conducted using a Corning™ 96-Well Filter Plate Fluid Guard (Fisher Scientific), and samples were prepared according to the kit manufacturer`s protocol. The MULTIPLEX analysis (see Appendix) of each sample

(using triplicates) was conducted and the results visualized using Bioplex 200 (Bio-rad).

3.1.7 Flow

3.1.7.1 Cell collection and fixation

For analysis of cell surface markers by Flow cytometry, cultivated cells exposed to factors to induce THP-1 cell differentiation were grown to near confluency. After removal of the supernatant (used for cytokine and chemokine analysis, described in 3.1.6), 1 ml of 0.1% TV was added in each well for at least 3 min at 37°C in 5% CO_2. Then each cell suspension was transferred into a Falcon tube and centrifuged at 239rcf for 2 min, RT. The supernatant was removed, the cell pellet washed in 1 ml PBS and centrifuged again for 2 min. For fixation, the supernatant was discarded and 1 ml of 4% PFA (in Millipore water) was added and incubated for 15-20 min at RT. The tubes were centrifuged at 239rcf for 2 min at 4°C. The supernatant was discarded and replaced with 1% BSA/PBS. The cells were washed in BSA/PBS twice then stored for less than 10 days at 4^{o}C for analysis.

3.1.7.2 Staining of fixed cells

The fixed cells were pelleted at 956rcf for 2 min at 4°C; all cell centrifugations were conducted using these conditions unless otherwise noted. The 1% BSA/PBS solution was discarded and 100 µl Perm/Wash (1x saponin-based permeabilisation reagent, ThermoFisher) containing 5% serum (species of origin varied depending on the primary antibody) was added and incubated for at least 10 min. Cells were pelleted by centrifugation, the supernatant removed, and cells were resuspended in Perm/Wash containing the primary antibody (Oct3/4, 1:100) and incubated for 1 h at RT. In the meantime, directly conjugated antibodies were prepared at appropriate dilutions in Perm/Wash (see 3.1.7.2.3). After blocking, cells were spun at 239rcf for 2 min at 4°C and the diluted direct conjugated antibody solution (see Tab. 3.1.7.2.3) was added and incubated for a 45 min in the dark. Next, the cells were pelleted at 239rcf. The supernatant was discarded and the diluted secondary antibody (Donkey anti-goat AF488, 1:300) was added and incubation for 45 min, at RT. Afterwards, 100 µl Perm/Wash was added to each tube and spun down at 239rcf. The supernatant was discarded and the cells were resuspended in Perm/Wash. This step was repeated

twice. The cells were finally resuspended in 150 µl Perm/Wash and stored for up to 6 days at 4°C, until the flow analysis was conducted.

3.1.7.2.1 Table of antibody used for TCam-2 detection (indirect staining)

Antibody	Manufacturer	Dilution	Cat. No.
Oct3/4 (primary antibody)	Santa Cruz	1:100	sc-8629
Donkey anti-goat AF488 (secondary antibody)	Invitrogen	1:300	A11055

3.1.7.2.3 List of direct conjugated antibodies (received from Dr B. Loveland, Burnet Institute, Melbourne, Australia)

Direct conjugated Antibodies	Manufacturer	Dilution	Cat. No.
CD14 PE	BD Biosciences	1:100	347497
CD11c APCH7	Biolegend	1:20	337218
CD68 FITC	Biolegend	1:20	333806
CD163 PE	Biolegend	1:20	333606
CD206 APC	Biolegend	1:20	321110

3.1.7.3 Setting of the Flow cytometer and gating strategy

Ten thousand events were acquired for each sample using the BD LSR Fortessa x20 (BD Bioscience, San Jose, USA). Data were analysed using FlowJO Version 10 (Tree Star, Ashland, USA) in the following manner. The first step was the selection of cells according to their physical properties; both debris and clumped cells were identified based on their position in the plot and subsequently excluded using Forward scatter (FSC) and Side scatter (SSC) setting made using the unstained control vs the stained control. Each antibody was detected using a different voltage setting that depended on the cells being examined and the fluorophore (see list of voltage settings).

3.1.7.3 Table: Voltage of each channel used for Flow analysis

Antibody	**Voltage**
Oct3/4 (A488)	B530: 550; SSC: 300; FSC: 640
CD11c (APCH7)	R780: 780; SSC: 300; FSC: 620
CD14 (PE)	RY586: 580; SSC: 300; FSC: 620
CD68 (FITC)	B530: 550; SSC: 280; FSC: 620
CD163 (PE)	Y586: 570; SSC: 300; FSC: 640
CD206 (APC)	R670: 700 SSC: 300; FSC: 640

3.2 RESULTS

3.2.1 Differentiation of THP-1 cells into M0, M1 and M2 macrophages after cytokine and LPS treatment

For *in vitro* experiments to examine the functional polarization of macrophages associated with testicular cancer (Chapter 2) we used M0, M1 and M2 macrophages obtained by differentiation of THP-1 cells, a monocyte-derived cell line. To polarize the undifferentiated and non-adherent THP-1 cells, a treatment with PMA was first conducted to activate them (black arrow). After every treatment, cells were observed using an inverted brightfield microscope. After this treatment, the previously round and non-adherent THP-1 cells became adherent and differentiated into a fibroblast-like M0 phenotype (Fig. 3.2.1.1, A/3.2.1.1, B, black arrow). Subsequent treatments with different cytokines and with LPS allowed M0 cell differentiation into M1 (LPS and IFNγ) or M2 (IL-4 and IL-13) macrophages. The M1 and M2 cells were more firmly attached and more fibroblast-like in appearance (Fig. 3.2.1.1, C, black arrow).

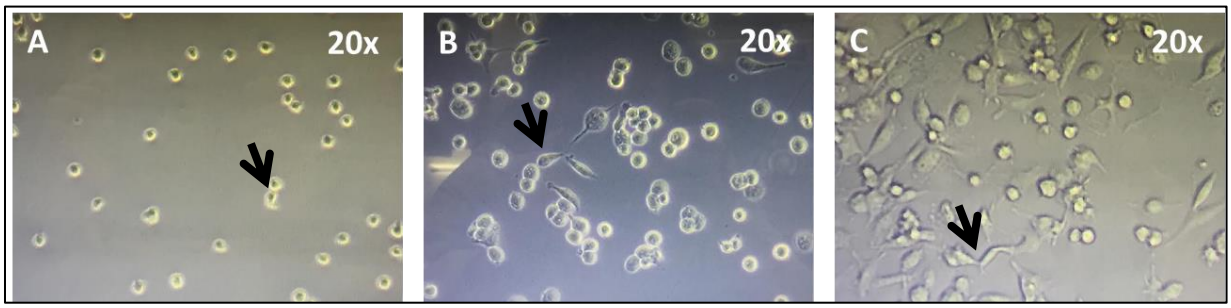

Fig. 3.2.1.1: Analysis of differentiated human monocyte-derived THP-1 cells (M0, M1 and M2 macrophages) by PMA, LPS and cytokine treatment. After the PMA treatment, the round non-adherent THP-1 cells (A) differentiate into adherent, fibroblast-like M0 macrophages (B, black arrow). After M0 macrophages were treated with cytokines (e.g. IFNγ, LPS or IL-4, IL-13) to differentiate them into M1 or M2 macrophages, respectively, the M1 and M2 macrophages were more firmly attached to the wells and had a and more fibroblast-like appearance (C, black arrow).

An analysis measuring typical macrophage markers was conducted by qRT-PCR and Flow after the differentiation steps using PMA, cytokines and LPS. M1-specific markers are CD68 and CD11c, whereas M2 macrophages express CD163 and CD206.
The determination of those markers at the transcript level revealed the success of the differentiation, since M1 macrophages expressed higher levels of CD68 and CD11c transcripts, but lower levels of the M2-specific markers, CD163 and CD206 than M2 macrophages (Fig. 3.2.1.2, A). In contrast, THP-1 cells which were treated to differentiate into M2 macrophages had a higher level of M2-specific marker transcripts than did M1 macrophages (Fig. 3.2.1.2, A). M0 macrophages expressed significantly lower levels of CD68 and CD11c (M1 markers) than did M1 macrophages, and had significantly lower levels of CD163 and CD206 (M2 markers) than M2 macrophages. To sum up, macrophages were successful differentiated.

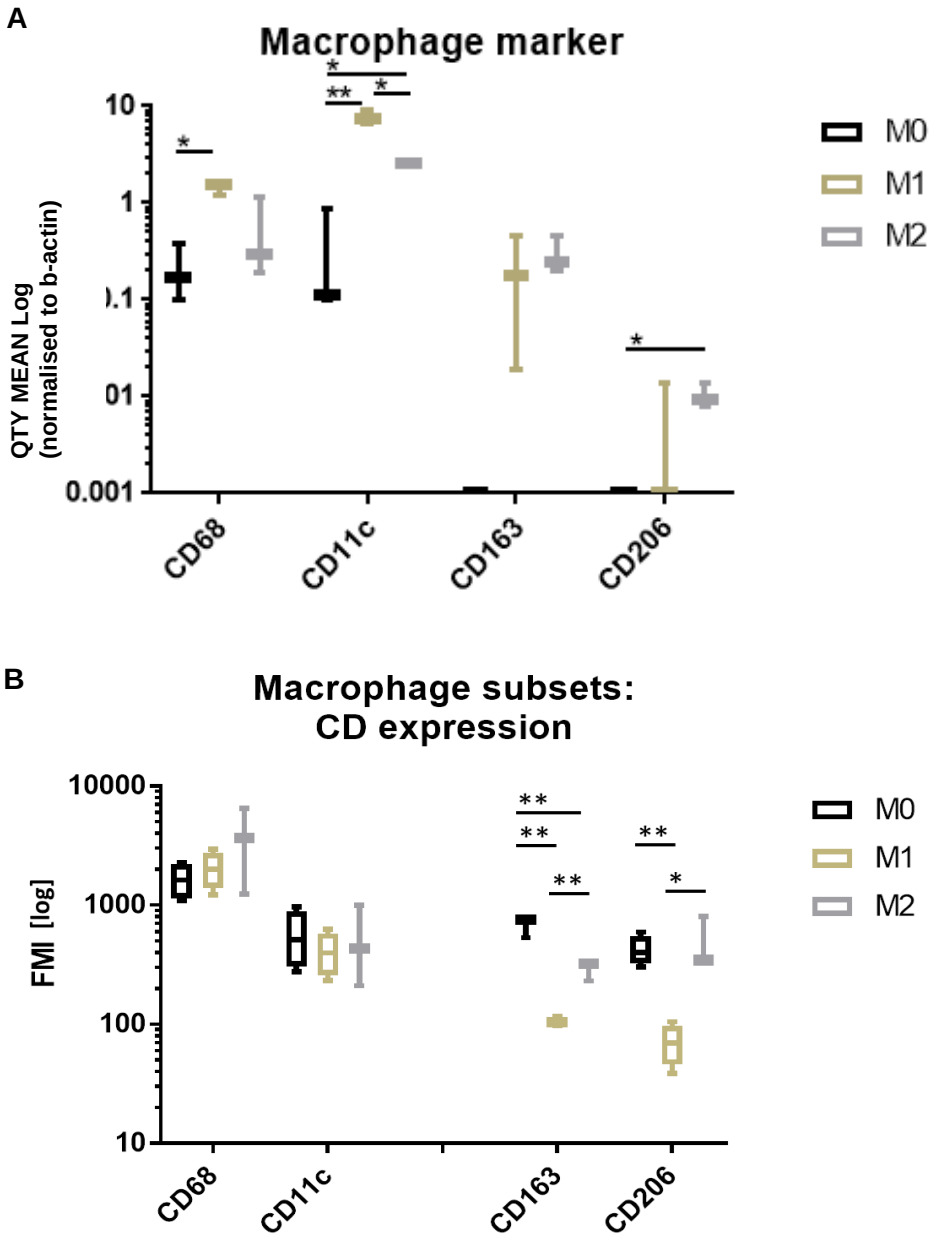

Fig. 3.2.1.2: CD expression analysis of M0, M1 and M2 macrophages (differentiated THP-1 cells) by qRT-PCR and Flow analyses (FMI=Fluorescence Mean Intensity). THP-1 cells treated with PMA (M0), then with either LPS and IFNγ (M1) or IL-4 and IL-13 (M2) were examined for expression of macrophage subtype-specific markers. The levels of M1 markers, CD11c and CD68, and M2 markers, CD163 and CD206 were examined in each cell population by qRT-PCR (the value for each sample was normalised to b-actin) (A) and Flow (B) (n=3). Transcript levels of M1-specific markers were highest in M1 macrophages, M2-specific marker transcripts were highest in M2 macrophages, and M0 macrophage transcript levels were closer to those in M1 cells (A). Flow analysis revealed that M0 macrophages expressed both M1- and M2-specific protein markers (B). M1 macrophages expressed high amounts of CD68 and CD11c, while M2 macrophages expressed high amounts of M2 (significantly higher than M2 marker expression by M1 macrophages) (B). Significance tested by one-way ANOVA (*P < 0.05, **P < 0.01).

3.2.2 Functional characterization of THP-1 derived M0, M1 and M2 macrophages through analysis of cytokine expression and wound healing activity

Macrophages of distinct phenotypes have different functions relating to pro-inflammatory (in M1 macrophages) or anti-inflammatory and wound-healing actions (M2 macrophages). Following differentiation of THP-1 cells by PMA, LPS and cytokine treatments into M0, M1 and M2 macrophage subtypes, their individual capacities for typical macrophage functions was evaluated by examining their cytokine expression profiles and migratory properties (functionally relevant to wound healing), using qRT-PCR, multiplex chemokine and cytokine assays (derivative of ELISA) and/or a 'scratch' wound healing assay. The mRNA cytokine profiles revealed that M0 macrophages expressed transcripts encoding pro-inflammatory cytokines, including IL-12a and TNF-α, as well as the anti-inflammatory cytokines TGF-β1 and Inhba (dimerizes to form activin A; pleitropic cytokine) (Fig. 3.2.2.1). The 'pro-inflammatory' M1 macrophages contained relatively higher transcript levels for pro-inflammatory cytokines such as IL-12a, TNF-α, IL-6, in addition to Inhba and TGF-β1. M2 macrophages expressed transcripts encoding anti-inflammatory cytokines e.g. IL-10, TGF-β1, Inhba and IL-6 (also pleiotropic) (Fig. 3.2.2.1).

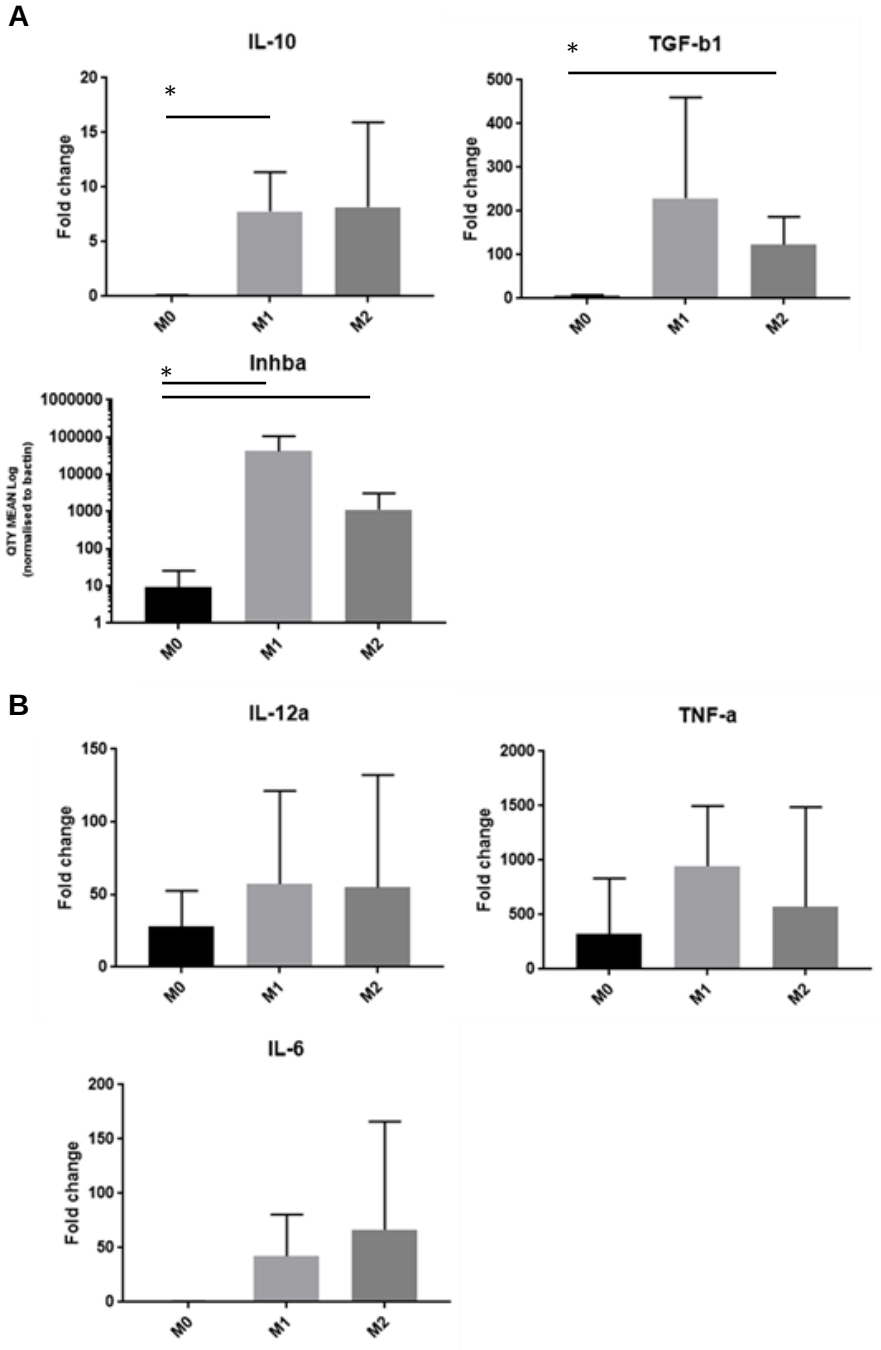

Fig. 3.2.2.1: mRNA transcript profiles demonstrating relative pro-/ and anti-inflammatory cytokine expression by M0, M1 and M2 macrophages (differentiated THP-1) (n=3)**.** M2 macrophages expressed relatively higher levels of transcripts encoding IL-6, Inhba, IL-10 and TGF-β1 (anti-inflammatory cytokines, A) whereas M1 macrophages expressed pro-inflammatory cytokines such as IL-12a, TNF-α and the pleiotropic cytokine IL-6 (B). M0 macrophages showed transcript level of TGF-β (anti-inflammatory cytokine (A)) and pro-inflammatory cytokine (B) such as IL-12. Cytokines such as IL-6, IL-10, TGF-β1, IL-12a and TNF-α are relative to b-actin and human placenta (Taqman probes) whereas Inhba is relative to b-actin (individual primer design). Significance tested by one-way ANOVA (*P < 0.05).

The cytokine protein profile in the M0 macrophage supernatant exhibited lower amounts of IL-10, TGF-β1, IL-12 and TNF-α relative to that from M1 and M2 macrophages; secretion of IL-6 from M0 cells was barely detected (Fig. 3.2.2.2). M1 macrophages are known to express pro-inflammatory cytokines including IL-6, IL-12 and TNF-α (Martinez and Gordon, 2014). After differentiation of THP-1 cells into the M1 subtype, specific pro-inflammatory cytokines were secreted (Fig. 3.2.2.2, B). Additionally, production of IL-6, IL-12 and TNF-α was higher in the supernatant of M1 macrophages in comparison to M0 and M2 (Fig. 3.2.2.2, B). In contrast, higher levels of specific anti-inflammatory M2 related cytokines such as IL-10 and TGF-β1 were produced by M2 macrophages (Fig. 3.2.2.2, A). Collectively, these results highlight and confirm the expected functional differences between the M0, M1 and M2 macrophages generated from THP-1 cells (Genin et al., 2015).

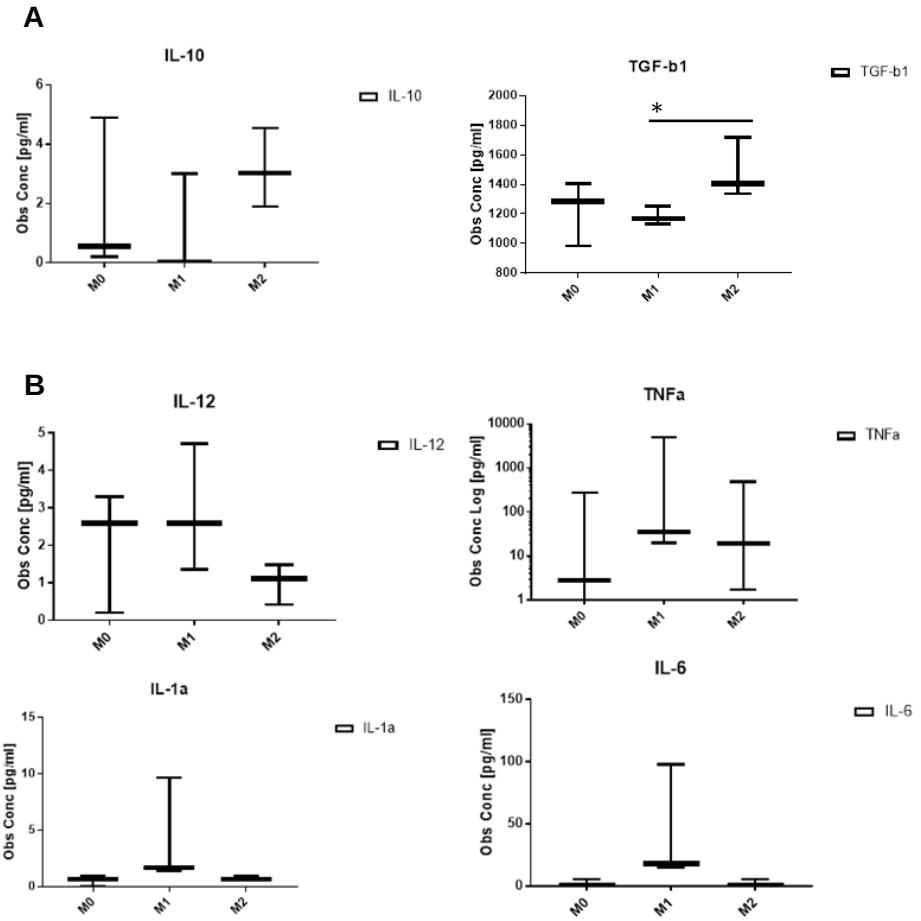

Fig. 3.2.2.2: Pro-/and anti-inflammatory cytokine profile of M0, M1 and M2 macrophages (differentiated THP-1) by multiplex chemokine and cytokine assay (n=3). M2 macrophages expressed **anti-inflammatory cytokines (A)** such as IL-10 and TGF-β1 whereas M1 macrophages expressed **pro-inflammatory cytokines (B)** such as IL-12, TNFα, IL-1a and the pleiotropic cytokine IL-6. M0 macrophages secreted besides anti-inflammatory cytokines (A) also pro-inflammatory cytokines (B) such as IL-12 and TNFα. Significance tested by one-way ANOVA (*P < 0.05).

An additional analysis of the potential wound healing activity of individual macrophage subsets was conducted using a cell 'scratch' assay (method described in Section 3.1.2). This is based on knowledge that M2 macrophages have additional properties such as contributing to angiogenesis and wound healing (Genin et al., 2015; Hagemann et al, 2009), activities that require these cells to migrate. A 'wound' was simulated in a plate of confluent cells by scratching a gap across the bottom of the well using M0, M1 and M2 macrophages (differentiated THP-1). After 24h the gap was slightly closed by M1 (1.98%) and M2 (3.56%) cells. After 48 h, there was an increase in the gap closure by M0 (6.33%) and M1 (3.39%) cells but a decrease by M2 (1.72%). Interestingly, after 72 h, M2 macrophages showed the greatest extent of gap closure (13.94%) in comparison to M0 (6.92%) and M1 (6.3%) cells (Fig. 3.2.2.3).

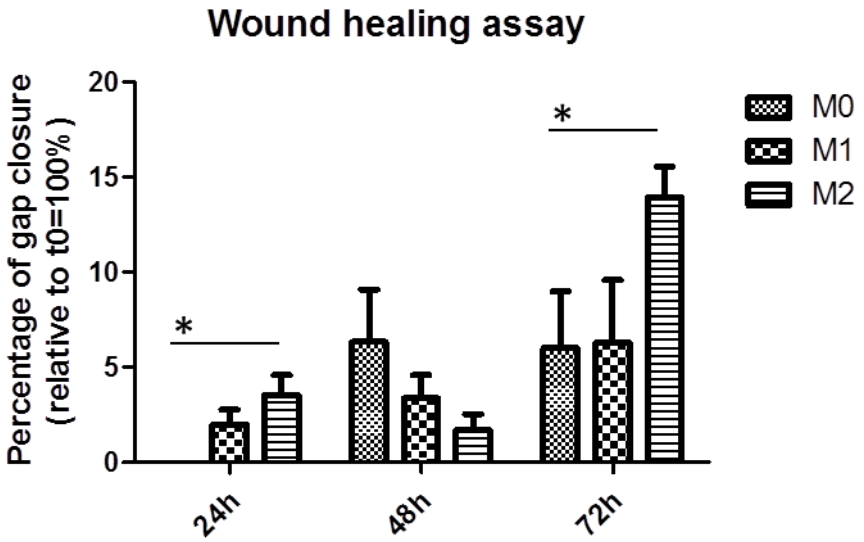

Fig. 3.2.2.3: A scratch assay measuring relative migration activity was conducted to reveal the potential wound healing activity of each macrophage subset (M0, M1 and M2). Individual macrophage subtypes were cultivated in a 6 well plate to 90 % confluence. A gap was created across the well with a pipet tip, and the extent of gap closure was measured daily (at t= 24 h, 48 h, 72 h) (n=3). After 24 h, M2 macrophages showed the strongest gap closure (3.56%) compared to M0 (0%) and M1 (1.98%) macrophages. M2 macrophages showed the strongest gap closure effect after 72 h (13.94%) whereas M0 and M1 macrophages reached a percentage of approximately 7%. Significance tested by one-way ANOVA (*$P < 0.05$).

3.2.3 Chemokine and chemokine receptor expression by THP-1 derived M0, M1 and M2 macrophages

Examination of testicular neoplasia samples revealed the presence of the chemokines CCL2 and CCL5 (see Chapter 2), which were previously identified as macrophage recruitment and polarization factors in other cancer types e.g breast cancer (CCL2, CCL5) and primary prostate cancer (CCL2) (Fang et al., 2016; Mizutani et al., 2009; Ueno et al., 2000; Soria and Ben-Baruch, 2008). Interestingly, both tumour cells and macrophages can express these chemokines. Thus, we analysed the potential for THP-1-derived macrophage subsets to produce both chemokines (CCL2, CCL5) and their specific chemokine receptor subunits (CCR1, CCR2, CCR3, CCR5), to determine if these macrophages could be the cellular targets of these particular chemokines.

Both CCL2 and CCL5 mRNA transcripts were detected at relatively low levels in M0 macrophages, and proteins encoded by both were detected in the multiplex analysis (Fig. 3.2.3.1, A/ B). M1 and M2 macrophages contained high levels of CCL2 and CCL5 transcripts relative to M0 cells, whereas the CCL2 protein level in M1 cells was significantly higher compared to M0 and M2 macrophages but CCL5 protein levels were not different between these cell types (Fig. 3.2.3.1, A).

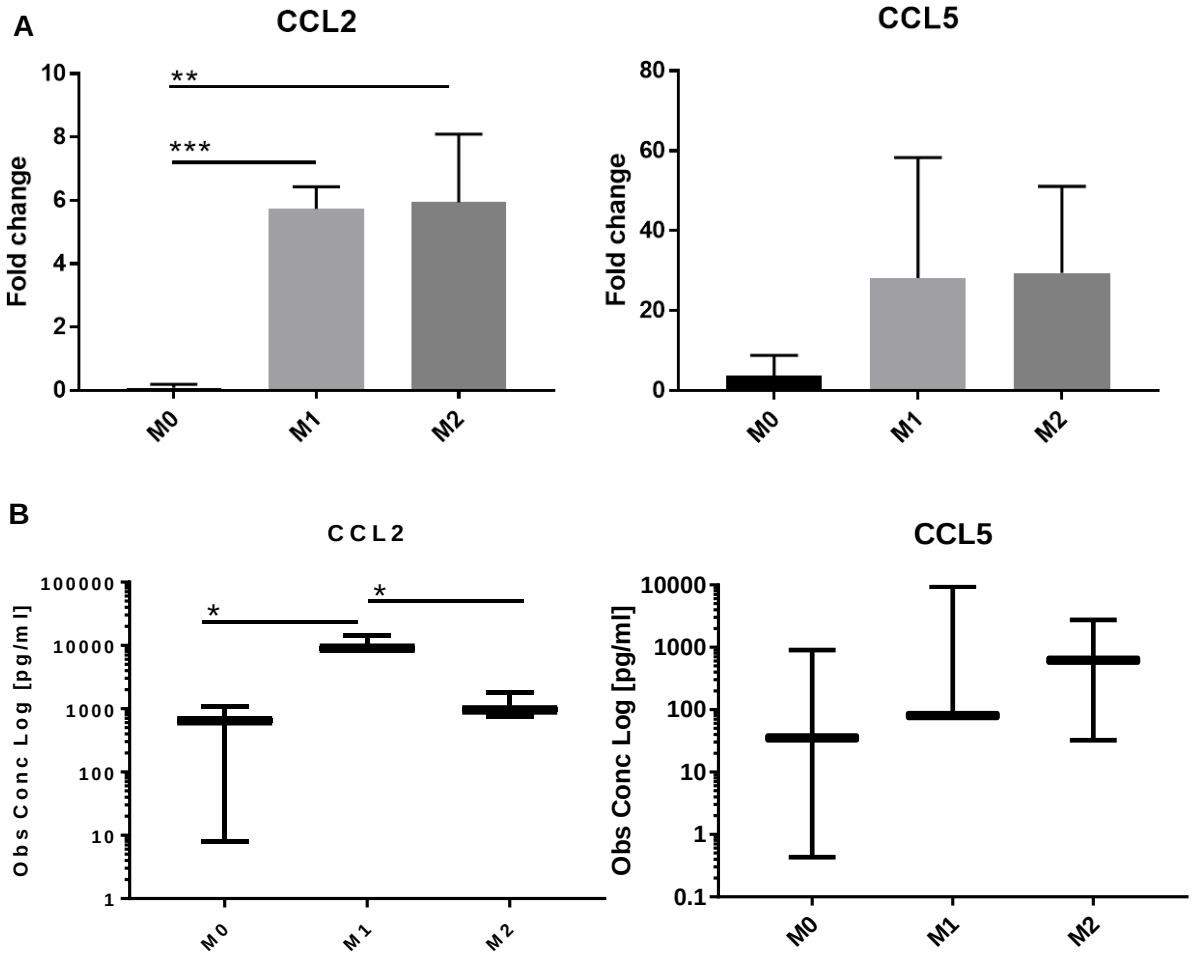

Fig. 3.2.3.1: Chemokine transcript and protein expression profiles of M0, M1 and M2 macrophages determined using qRT-PCR and Multiplex (n=3). Relative gene expression was normalised to ACTB and human placenta, with M0 cells containing relatively lower transcript levels than M1 and M2 subtypes. (A). M1 macrophages produced a significantly higher amount of CCL2 protein compared with M0 and M2 macrophages. Significance tested by one-way ANOVA (*P < 0.05, **P < 0.01, ***P < 0.001).

As previously mentioned, macrophages are targets of chemokines which can be expressed by tumour cells (Roca et al., 2009; Kim et al., 2009; Erler et al., 2009; Mantovani, 2008). The present study was conducted to assess which macrophage subsets might be targets for these locally-produced chemokines by examining chemokine receptor mRNA levels. M0 macrophages contained *CCR1* and *CCR2* transcripts, whereas other chemokine receptors, *CCR3* and *CCR5* were not detected (Fig. 3.2.3.2). Similar to M0 macrophages, M2 and M1 macrophages also contained *CCR1*, whereas the *CCR2* transcript was barely detected in M1 cells and undetectable in M2 cells (Fig. 3.2.3.2). Additionally, both M1 and M2 macrophages expressed

CCR3 and *CCR5* (Fig. 3.2.3.2), however the levels of both were higher in M1 macrophages (Fig. 3.2.3.2).

These outcomes have implications for the potential responsiveness of these cells to locally produced factors and highlight functional differences between these macrophage subtypes, as summarized here and presented in Tab. 3.2.3. M0 macrophages have the potential to bind CCL5 and CCL15 via CCR1 and to bind CCL2 through CCR2. In addition to the potential to bind CCL5 and CCL15 via CCR1 contrast, M1 and M2 macrophages may also bind these ligands through CCR3 and CCR5 (CCL5) receptors. Thus, in summary, these results indicate that M0 and M1 macrophages can bind CCL2, CCL5 and CCL15, whereas M2 can bind CCL5 and CCL15 (see Tab. 3.2.3).

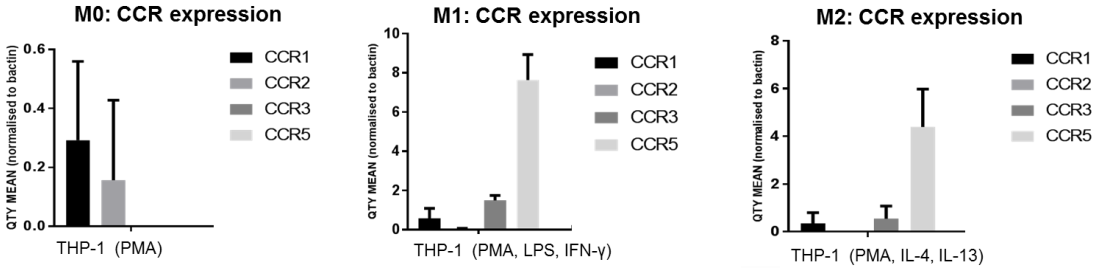

Fig. 3.2.3.2: Chemokine receptor transcripts measured in M0, M1 and M2 macrophages (differentiated from THP-1 cells) using qRT-PCR (n=3). M0 macrophages had detectable levels of *CCR1* and *CCR2* but not CCR3 or CCR transcripts, whereas M1 and M2 expressed *CCR1*, *CCR3* and *CCR5*, and M1 cells had a barely detectable level of the *CCR2* transcript. Relative gene expression was normalised to *ACTB* in each sample and human placenta which served as the positive control.

Table 3.2.3: Summary of chemokine receptor transcripts detected in individual expression macrophage subsets. Receptor name in bold; ligands for each receptor listed below; tick = detected; n. d. = not detected)

	M0	**M1**	**M2**
CCR1 ***CCL5, CCL15***	✓	✓	✓
CCR2 ***CCL2***	✓	✓	n.d.
CCR3 ***CCL5, CCL15***	n.d.	✓	✓
CCR5 ***CCL5***	n.d.	✓	✓

3.2.4 M0, M1 or M2 macrophage (THP-1 derived) treatment with cytokines and chemokines

Data presented in Chapter 2 identified that different macrophage subsets are detectable in neoplasia specimens when compared to healthy adult testis tissue with normal spermatogenesis. This indicates that a functionally distinct macrophage polarization state is associated with testicular neoplasia, and led us to the identification of potential macrophage polarization factors associated with testicular neoplasia. Experiments were undertaken to determine the influence of these cytokines, such as IL-10, activin A, and chemokines, such as CCL2, CCL5 and CCL15, on individual macrophage subsets, with the objective of determining how they might change the synthesis of subtype-specific markers and cytokines.

Under normal culture conditions, M0 macrophages contain transcripts encoding both pro-inflammatory cytokines such as IL-1b, IL-12a and anti-inflammatory cytokine TGF-β. After exposure to either IL-10 (20 ng/ml) or activin A (25 ng/ml), only the IL12-a mRNA was decreased following exposure to IL-10; no other significant changes were detected (Fig. 3.2.4.1).

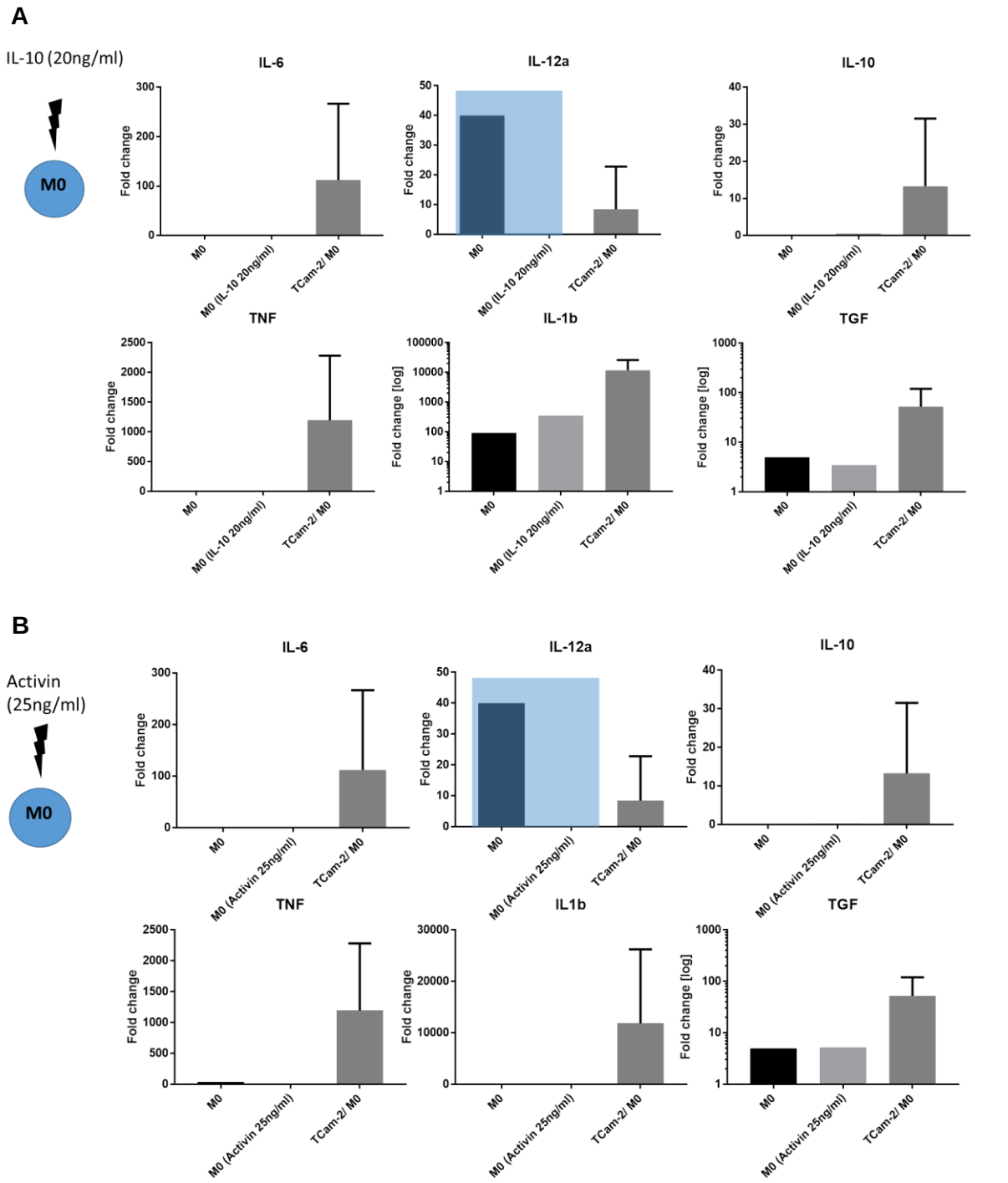

Fig. 3.2.4.1: Effect of IL-10 (20 ng/ml)(A) or activin A (25 ng/ml) (B) treated M0 macrophages (differentiated THP-1) by analysing mRNA transcript profile of pro-/ and anti-inflammatory cytokine expression. M0 macrophages (without IL-10 or activin A treatment) expressed transcript level of pro-/ and anti-inflammatory cytokines such as IL-12a, IL1b and TGF-β1. M0 macrophages that were treated with IL-10 and activin A showed an increased IL-12 transcript level whereas the levels of other cytokines did not change. Monoculture: n=1 (preliminary data); co-culture: n=3).

M0 macrophages showed expression level of CCL5 and a hardly expression of CCL2. After a treatment with IL-10 (20ng/ml, A) or activin A (25ng/ml, B) M0 macrophages showed an increase of CCL-2 and CCL-5 expression (mRNA transcript levels) (Fig. 3.2.4.2, A/ B).

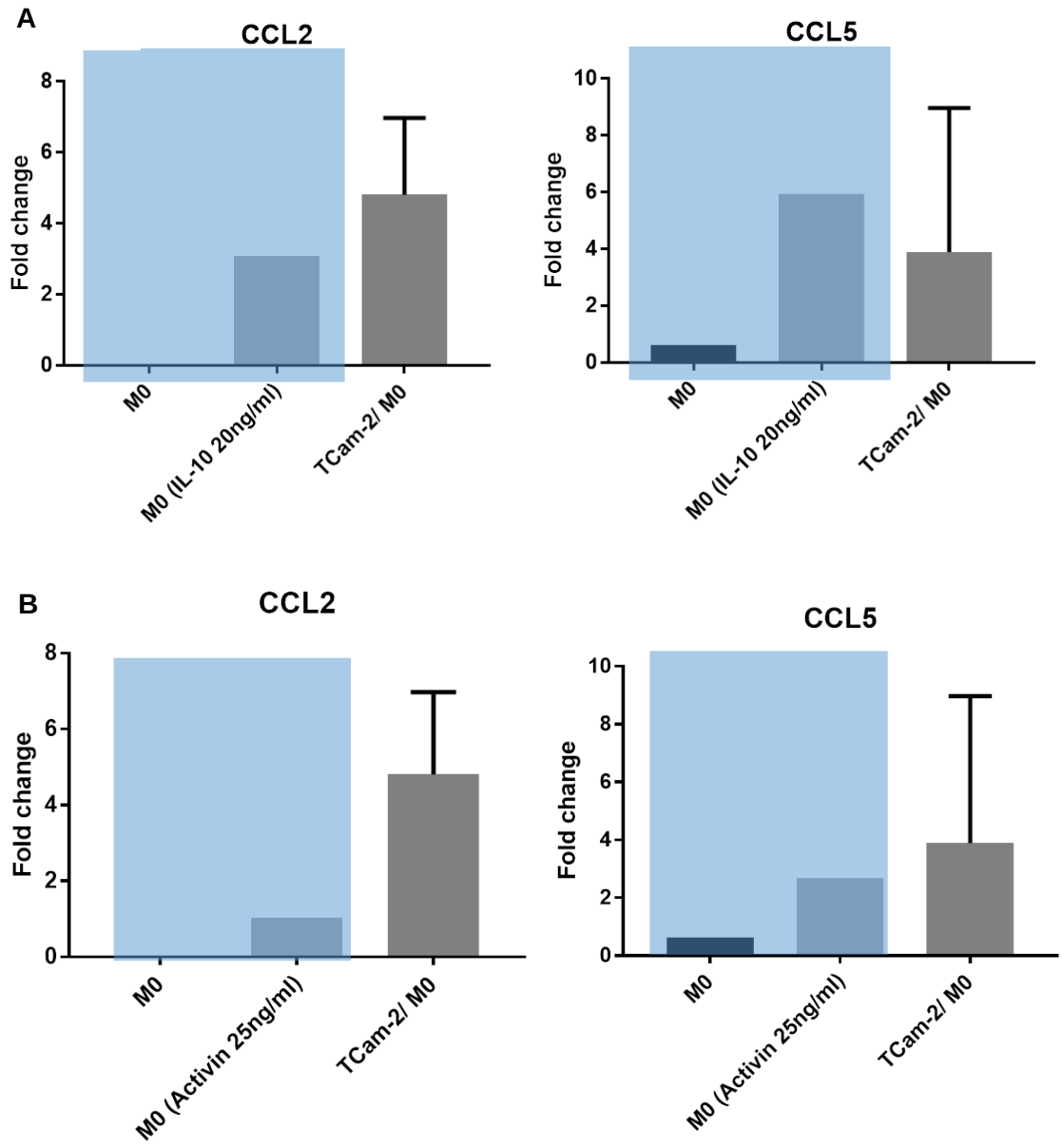

Fig. 3.2.4.2: Effect of IL-10 (20ng/ml) (A) or activin A (25ng/ml) (B) treated M0 macrophages (differentiated THP-1) by analysing mRNA transcript level of chemokine expression. M0 macrophages without IL-10 (A) and activin A (B) treatment expressed no transcript level of CCL2 whereas CCL5 was hardly detectable. M0 macrophages that were treated with IL-10 showed an increased transcript level of CCL2 and CCL5 (A) as well as activin A treated M0 macrophages (B). Monoculture: n=1 (preliminary data); co-culture: n=3).

After exposure to either CCL15 (20 ng/ml) or activin A (25 ng/ml), M1 specific CD11c and M2 specific CD206 marker (transcript level) were decreased whereas activin A treated M0 macrophages showed additional a significantly reduction of CD68. Transcript level of M2 specific CD163 was not detectable in both groups.

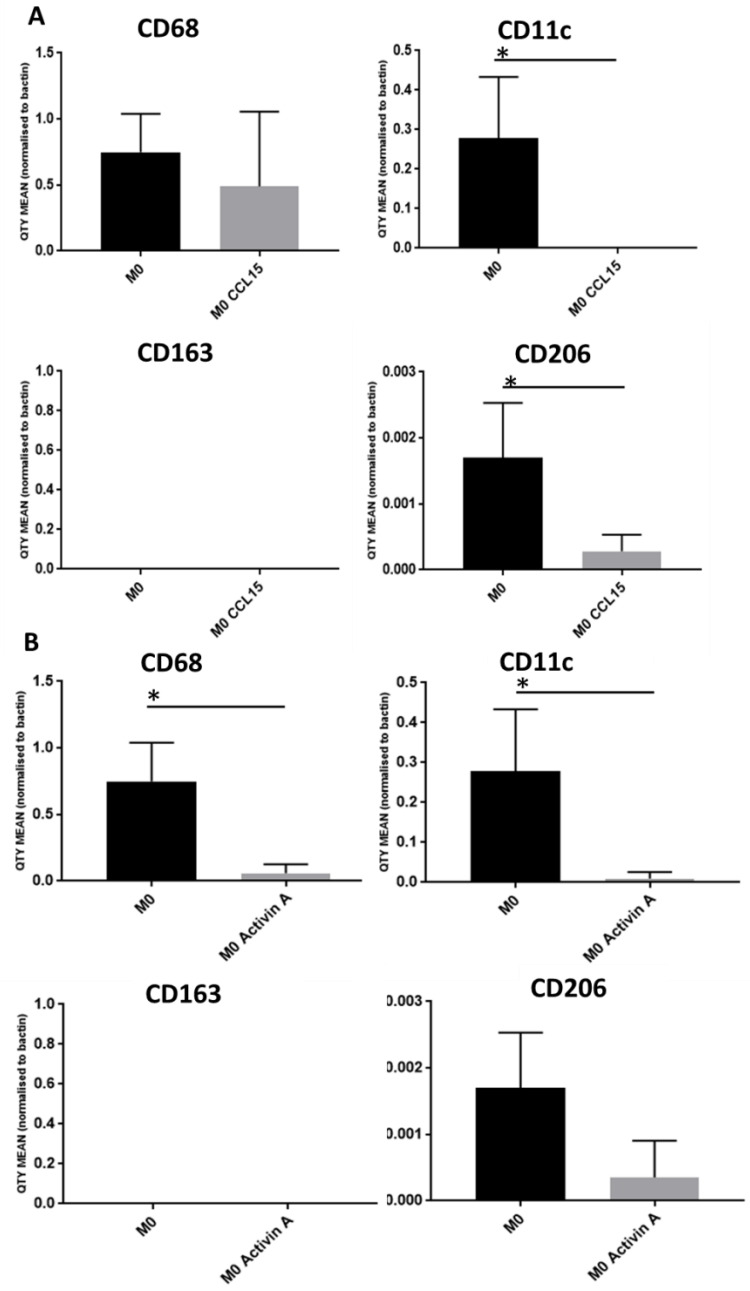

Fig. 3.2.4.3: Effect of CCL15 (20ng/ml) (A) or activin A (25ng/ml) (B) treated M0 macrophages (differentiated THP-1) by analysing mRNA transcript level of specific macrophage marker as an indication of macrophage polarization (n=3)**.** M0 macrophages without CCL15 (A) and activin A (B) treatment expressed transcript level of CD68, CD11c and CD206 but no transcript level of CD163. M0 macrophages exposed to CCL15 (A) and activin A (B) showed a reduction of m1 and m2 marker. Significance tested by student t-test (*P < 0.05).

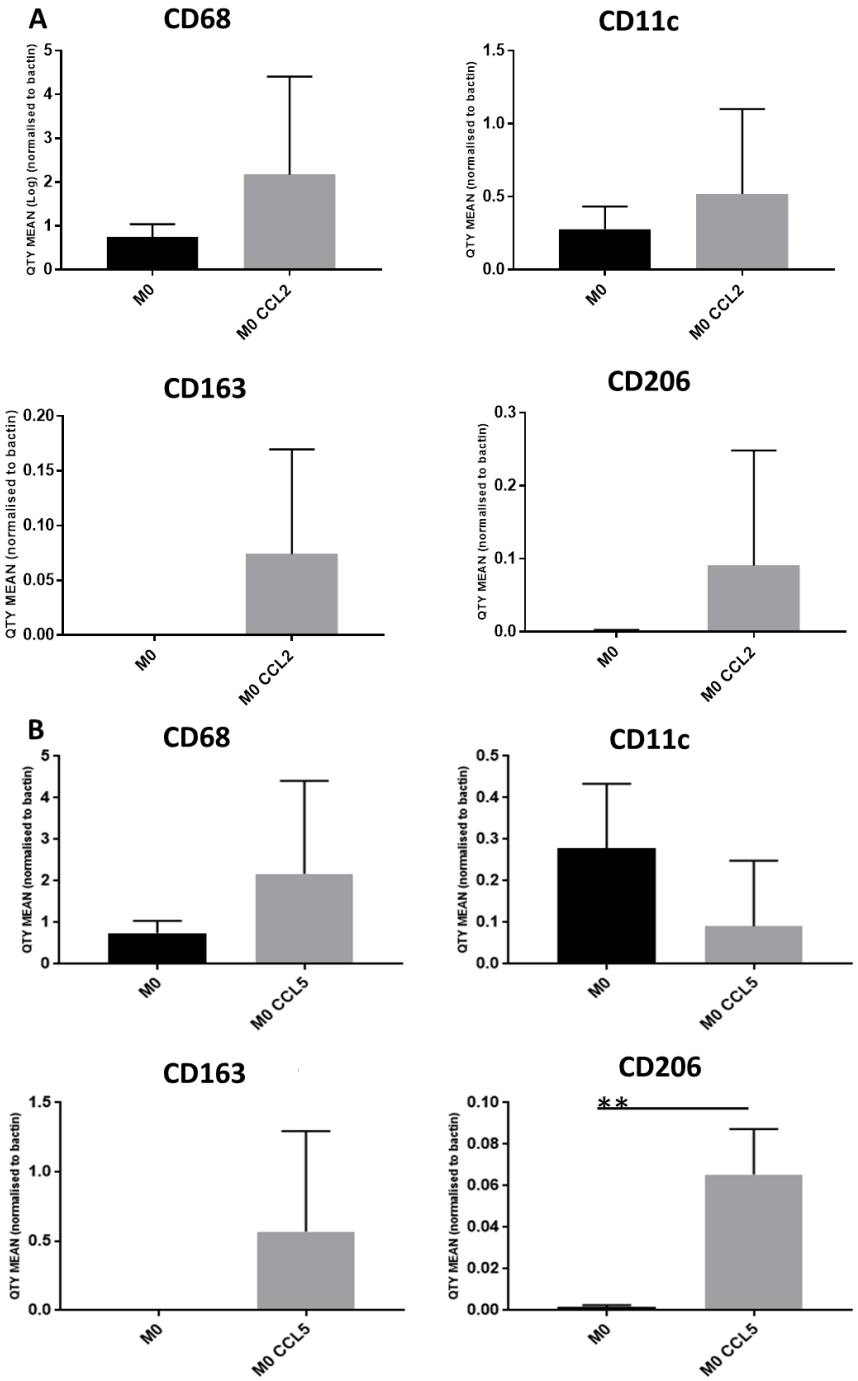

Fig. 3.2.4.4: Effect of CCL2 (20ng/ml) (A) or CCL5 (20ng/ml) (B) treated M0 macrophages (differentiated THP-1) by analysing mRNA transcript level of specific macrophage marker as an indication of macrophage polarization (n=3**).** M0 macrophages without CCL2 (A) and CCL5 (B) treatment expressed transcript level of CD68, CD11c and CD206 but no transcript level of CD163. M0 macrophages exposed to CCL2 (A) and CCL5 (B) showed increased transcript level of m1 and m2 specific marker (excluded CD206 of CCL5 treated M0). Significance tested by student t-test (**P < 0.01).

3.2.5 Inhibition of Smad2/3 signalling pathway of macrophage subsets by SB-431542 and Follistatin (inhibitors)

TGF-β and activin A are known as macrophage polarization factors (Sierra-Filardi et al., 2007; Zhang et al., 2016). Their effect on the polarization of macrophages from M0 and M1 into the M2 subtype was confirmed after treatment with either TGF-β (20 ng/ml) or activin A (25 ng/ml). In addition, inhibitors of activin A and/or TGF-β signalling, SB-431542 (10 µM, can inhibit both ligands) and follistatin (250 ng/ml, specific to activin) were tested for their effect on this transition. Cells were pre-treated with these ligands to increase or with inhibitors to block Smad2/Smad3 activation, which mediate activin A and TGF-β signalling pathway activity and thus enable the M0 and M1 differentiation into M2 macrophages. At first, pathway activation was interrogated using antibodies to detect total Smad3, phosphorylated Smad3 (pSmad3) and pSmad2 after a treatments with either TGF-β or activin A. Next, the impact of pre-treatment with inhibitors SB-431542 and follistatin on the extent of Smad2 and Smad3 phosphorylation arising from TGF-β and activin A treatment was assessed. Treatment of M0 macrophages with TGF-β (20 ng/ml, without inhibitor pre-treatment) activated Smad2 and Smad3, as evidenced by increased signals for the phosphorylated forms of these transcription factors (Fig. 3.2.5.1, B/ C, lane 1). Pre-treatment with SB431542 prior to TGF-β the pSmad2 and pSmad3 band signal was lower compared to that observed in MO cells lacking inhibitor pre-treatment (Fig. 3.2.5.1, B/ C, lane 2 and 3). Additionally, the activin A treated M0 cells showed a strong pSmad2 and pSmad3 protein band (Fig. 3.2.5.1, B/ C, lane 4) while pre-treatment with SB-431542 or follistatin showed a lower Smad2 and pSmad3 signals (Fig. 3.2.5.1, B/ C lane 5 and 6). However, Smad3 was detected in all treated groups whereas the TGF-β1 group showed the strongest protein band (Fig. 3.2.5.1, A, lane 1).

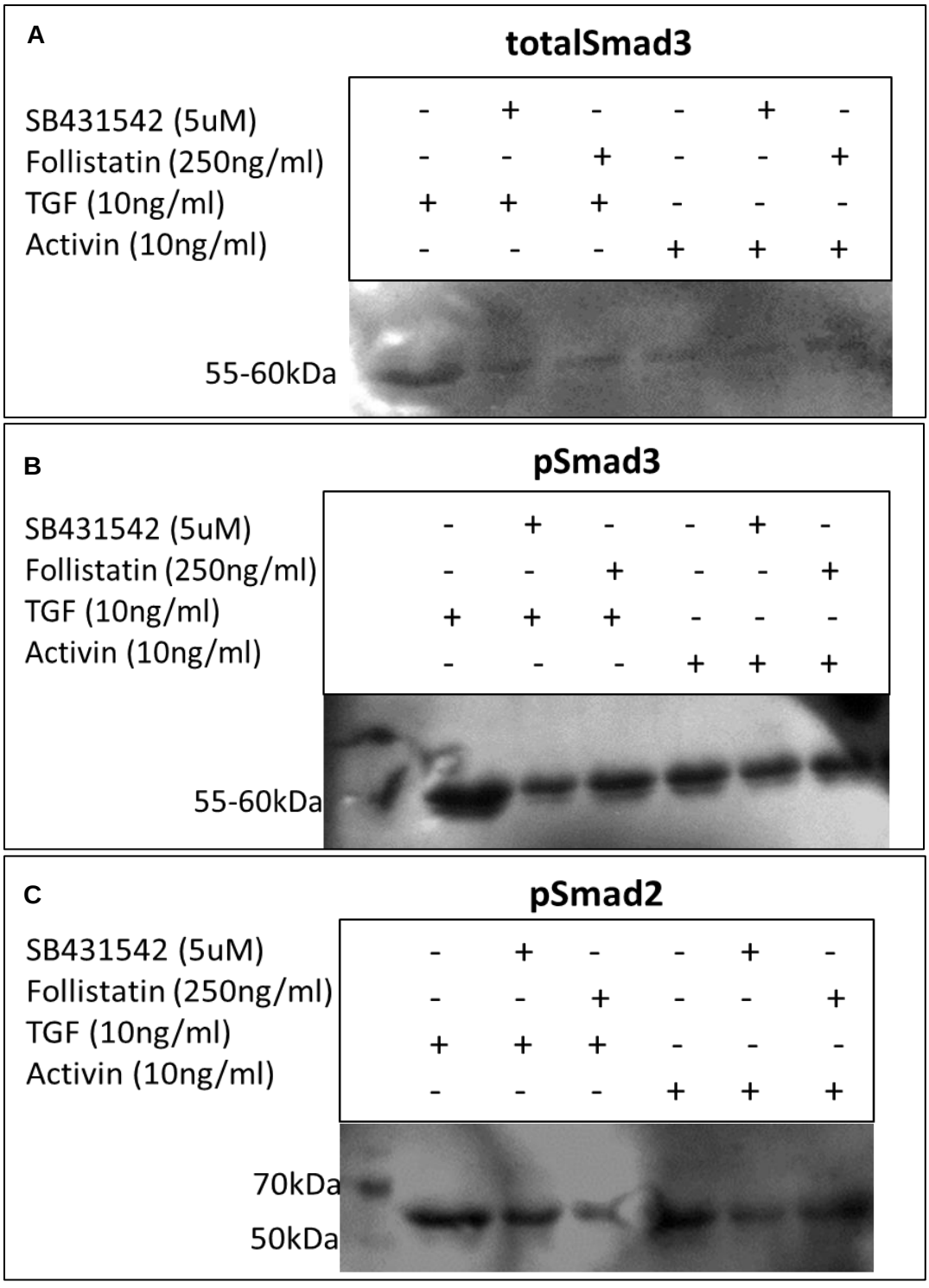

Fig. 3.2.5.1: Inhibition effect of Smad2/3 signaling pathway using TGF-β1 and activin A and SB431542 and Follistatin treated M0 macrophages (THP-1 derived) (preliminary data). M0 macrophages were treated with TGF-β (20ng/ml) or activin A (10ng/ml, without the inhibitor pre-treatment) and a strong detection of pSmad2 and pSmad3 was possible. Whereas, M0 macrophages which were pre-treated with inhibitors (e.g. SB431542 and Follistatin), showed a decrease of the protein bands. All groups showed an expression of Smad3.

3.2.6 Migration assay reveals individual macrophage subsets as targets of specific chemokines

Chemokines are recruitment factors of immune cells. As previously mentioned, we have detected CD68+macrophages and CD163+/CD206+ M2 macrophages in the human testis. Additionally, we revealed the presence of the chemokine CCL15 in the non-inflamed testis. Thus, we assumed that macrophage precursor and M2 macrophages can be recruited to the non-inflamed testis. In contrast, testicular neoplasia was associated with CCL2 and CCL5 (see chapter 2). Interestingly, there was an correlation between the new revealed chemokine milieu and the increased macrophage populations associated with testicular cancer. Therefore, we assumed that CCL2 and CCL5 are recruitment factors of macrophages which can then differentiate into other phenotypes due to the tumour environment. Thus, we conducted a migration assay using M0, M1 and M2 that were treated with CCL15 and M1 and M2 macrophages were treated with CCL2, CCL5 and CCL15 to reveal the chemotaxis effect.

After the CCL15 treatment, M0 macrophages showed a significantly increased migration effect in comparison to the untreated group after 24 h (M0 CCL15: 12.62%, M0: 0%) (Fig. 3.2.6.1, A). After 48 h, CCL15 treated M0 macrophages showed a significantly increased migration effect compared to the untreated group (M0 CCL15: 16.25%, M0: 6.33%) (Fig. 3.2.6.1, A). The strongest effect of the treated group was to see after 72 h (22.8%) that was significantly increased compared to the gap closure of the untreated group which didn’t change after 48 h (6.03%) (Fig. 3.2.6.1, A). In contrast, the treated M1 macrophages showed after 24 h a gap closure of 6.9% whereas the untreated group reached 1.98%. After 48 h, the treated group showed a slight decrease (5.57%) and the untreated group a slight increase (3.39%) of the gap closure (Fig. 3.2.6.1, B). After 72 h the untreated group showed an increase and reached 6.3% gap closure in comparison to t= 24 h (1.98%) and t= 48 h (3.39%) whereas the treated group showed an decrease (0.72%)(Fig. 3.2.6.1, B). The treated M2 macrophages showed a gap closure of about 7.65% after 24 h and 7.93% after 48 h whereas the control group showed less effect (t= 24 h: 3.56%, 48 h=1.71%) (Fig. 3.2.6.1, C). After 72 h either the control group or treated group showed an increase of the gap closure of about 13.94% (control group) and 14.73% (treated group) (Fig. 3.2.6.1, C).

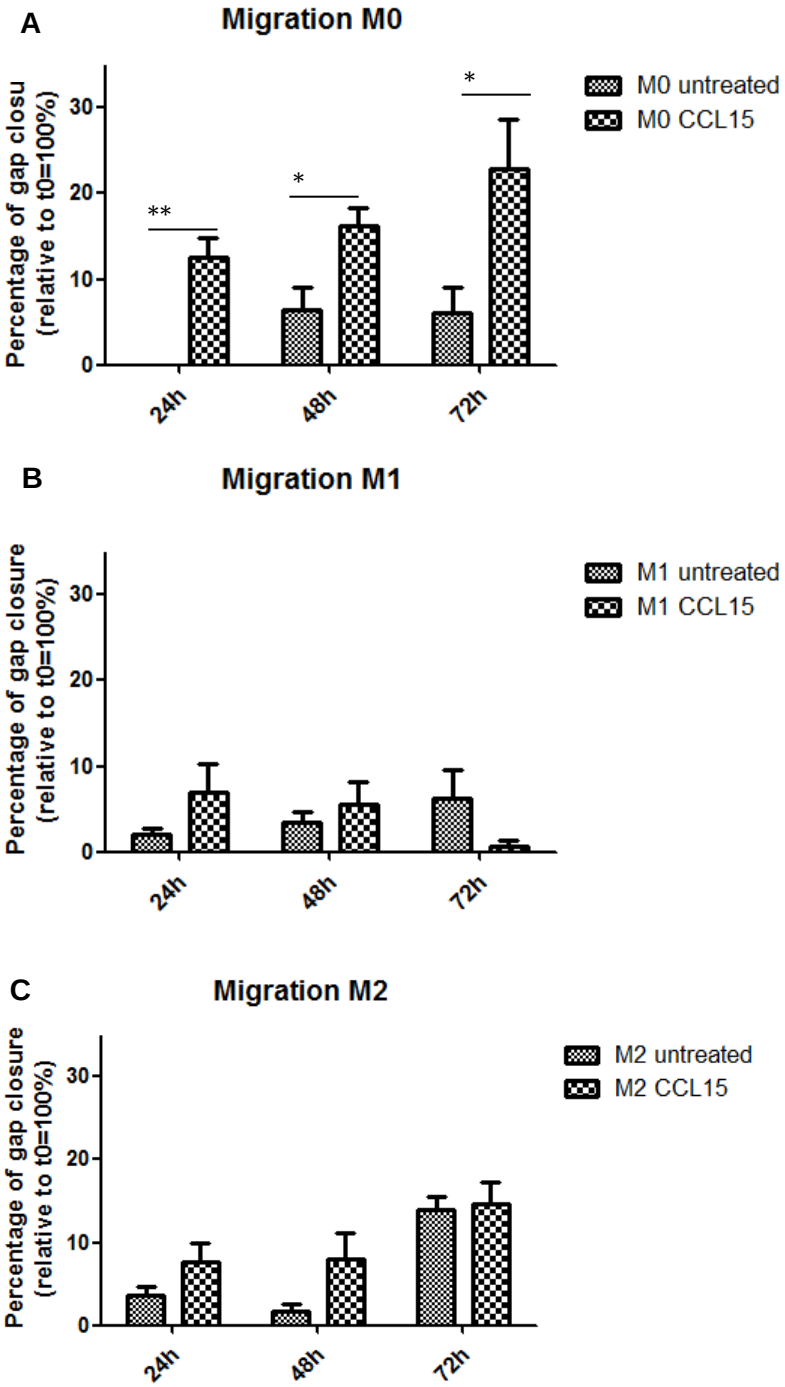

Fig. 3.2.6.1: A Scratch assay was conducted to reveal the recruitment activity of CCL15 using different macrophage subset (M0, M1 and M2). Macrophages were cultivated in a 6 well plate and after reaching a confluence of about 90%, a gap was scratched and the gap closure was measured at different time points (t= 24 h, 48 h, 72 h)(n=3). M0 macrophages treated with CCL15 showed the strongest migration effect in comparison to M1 (B) and M2 (C) macrophages. Comparing CCL15 treated M0 macrophages with the control group revealed a significantly increased gap closure effect (A). M1 macrophages showed the lowest migration effect of gap closure and after 72 h there was a decrease (0.72% gap closure). After 24 h, treated M2 macrophages showed a gap closure of 7.65% whereas the untreated group reached 3.56%. After 72 h both groups showed an increase (CCL15 M2: 14.73%, M2: 13.97%). Significance tested by one-way ANOVA (*P < 0.05, **P < 0.01, ***P < 0.001).

Interestingly, M1 macrophages which are treated with CCL2 showed a stronger migration effect than the group that were treatment with CCL15. After 24 h, the treated M1 macrophages showed a significant gap closure of about 11.92% whereas the untreated group showed a 2.94% gap closure (Fig. 3.2.6.2, A). After 48 h there was a slightly increase of both groups (M1 CCL2: 15.05%, M1: 4.93%) but the strongest effect was to see after 72 h (M1 CCL2: 21.13%, M1: 8.16%) (Fig. 3.2.6.2, A). All in all, M1 macrophages which were treated with CCL2 showed a significant increase of gap closure compared to the control group (A). In contrast, M2 macrophages showed no significant effect of the CCL2 treatment compared to the control group (Fig. 3.2.6.2, B).

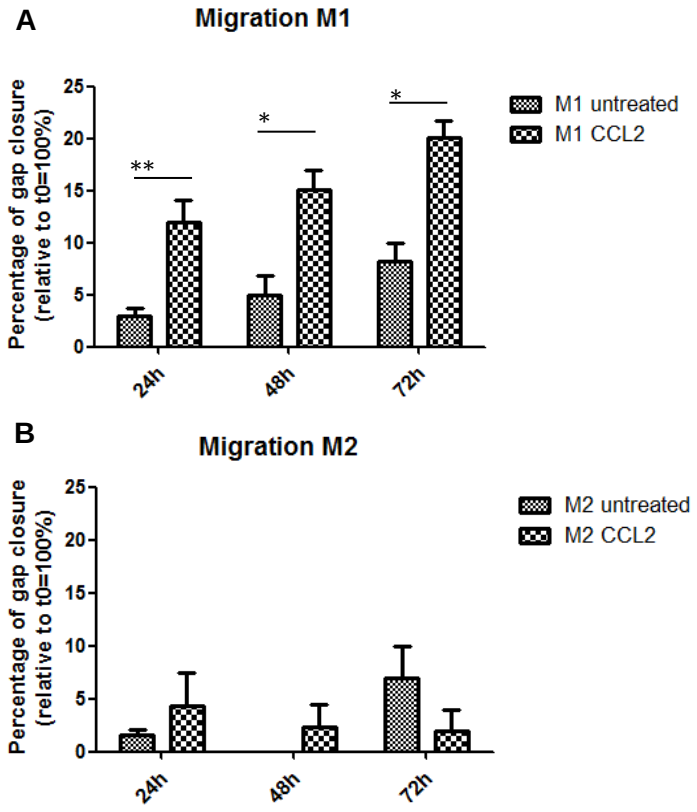

Fig. 3.2.6.2: A Scratch assay was conducted to reveal the recruitment activity of CCL2 using different macrophage subsets (M1 and M2). Macrophages were cultivated in a 6 well plate and after reaching a confluence of about 90%, a gap was scratched and the gap closure was measured at different time points (t= 24 h, 48 h, 72 h)(n=3). The untreated M1 macrophages showed a slight gap closure after 24 h (4%) which reached after 72 h a maximum of about 10% (A). M1 macrophages which were treated with CCL2 showed significant increase of gap closure compared to the control group (A). M2 macrophages showed a slight gap closure without the CCL2 treatment which was increased compared to the treated M2 macrophages (B). Significance tested by one-way ANOVA (*P < 0.05, **P < 0.01, ***P < 0.001).

Additionally, M1 and M2 macrophages were treated with CCL5. Treated and untreated M1 macrophages showed after 48 h a significant difference (M1 CCL5: 15%, M1: 2%) (Fig. 3.2.6.3, A). After 72 h, CCL5 treated M1 macrophages showed a reduction of the gap closure whereas the untreated group reached 4% (Fig. 3.2.6.3, A). CCL5 treated M2 macrophages showed after 24 h a significant increase compared to the control group (M2 CCL5: 13%, M2: 2%) (Fig. 3.2.6.3, B). After 48 h and 72 h, the treated group showed no significant difference compared with the control group (Fig. 3.2.6.3, B).

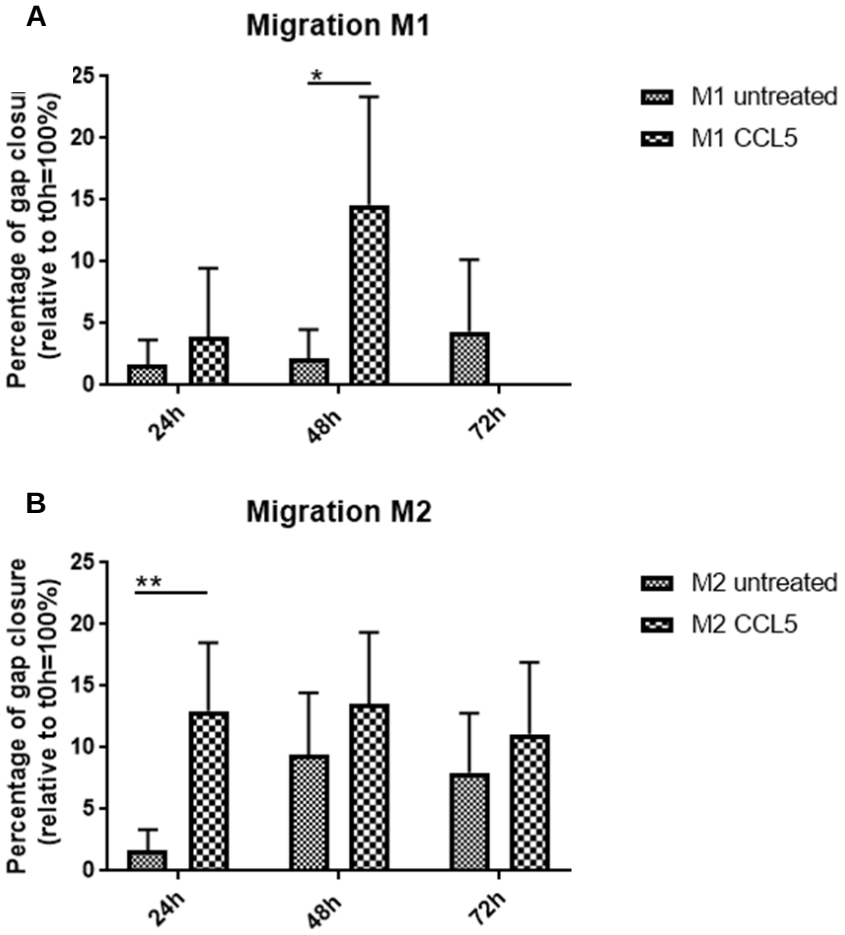

Fig. 3.2.6.3: A Scratch assay was conducted to reveal the recruitment activity of CCL5 using different macrophage subset (M1 and M2). Macrophages were cultivated in a 6 well plate and after reaching a confluence of about 90%, a gap was scratched and the gap closure was measured at different time points (t=24 h, 48 h, 72 h)(n=3). Treated M1 macrophages showed a strong gap closure effect after 48 h (15%) which was significantly increased compared with the untreated control group (2%) (A). After 72 h treated M1 macrophages showed a decreased migration effect. In contrast, M2 macrophages showed strong migration effects (B). After 24 h, CCL5 treated M2 macrophages showed a gap closure of about 13% which was slightly increased after 48 h (14%) whereas the untreated group showed also strong migration effects compared to M1 macrophages (A/ B). Significance tested by one-way ANOVA (*P < 0.05, **P < 0.01, ***P < 0.001).

3.2.7 Cytokine and chemokine expression by TCam-2

It is known that tumour cells itself can express different cytokines and chemokines to recruit and influence immune cell functions. Therefore, we analysed if TCam-2 (monoculture) can express cytokines and chemokines.

We revealed that cultivated TCam-2 can express TGF-β1 (anti-inflammatory cytokines) and IL-6 (pro/-and anti-inflammatory cytokine) that was significantly increased compared to other cytokines (IL-10, IL-1a, IL-12b and TNF-α (Fig. 3.2.7.1).

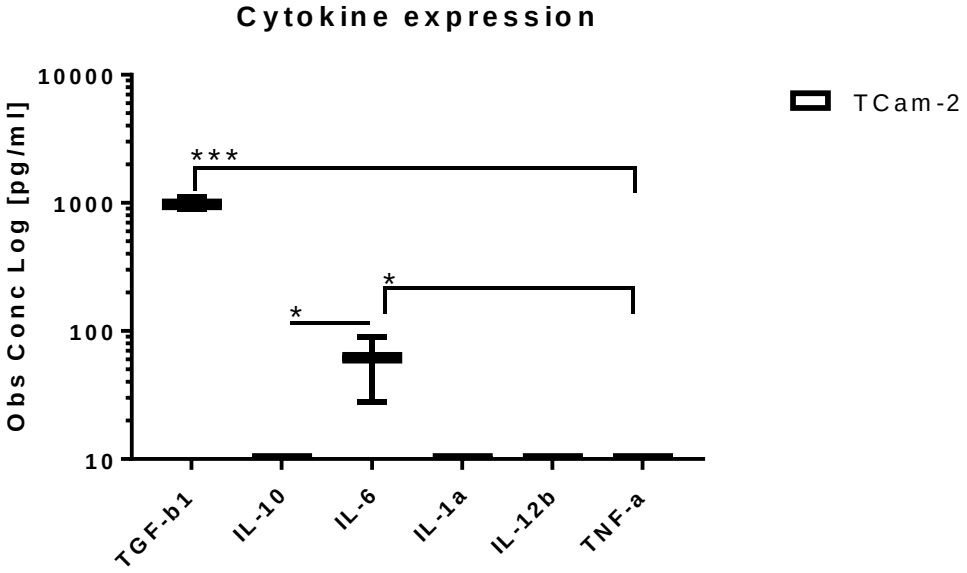

Fig. 3.2.7.1: TCam-2 analysis of anti-/ and pro-inflammatory cytokine expression of by Multiplex (n=3). Cultivated TCam-2 cells expressed the anti-inflammatory cytokine TGF-β1 (anti-inflammatory) and the pleiotropic cytokine IL-6 which were significantly increased compared with other cytokines such as IL-10 and IL-1a, IL-12b, TNF-α (pro-inflammatory). Significance tested by one-way ANOVA (*P < 0.05, **P < 0.01, ***P < 0.001).

Additionally, we analysed the expression of Chemokines such as CCL2 and CCL5 (mRNA and protein). The cultivated TCam-2 cells showed a slight expression of CCL2 whereas CCL5 was not detectable (transcript level) (Fig. 3.2.7.2, A). The protein analysis revealed that CCL2 was secreted whereas CCL5 was hardly expressed (protein level) (Fig. 3.2.7.2, B).

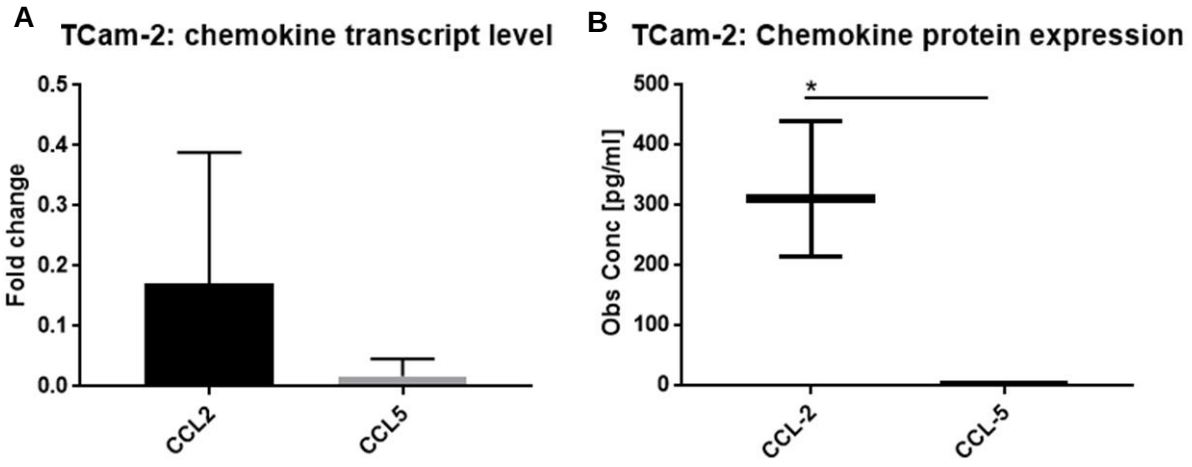

Fig. 3.2.7.2: TCam-2 analysis: Chemokine transcript expression level and protein expression by qRT-PCR (A) and Multiplex (B) (n=3). Cultivated TCam-2 cells showed transcript level of CCL-2 whereas CCL5 was hardly detectable. A protein analysis revealed the expression of CCL2 whereas CCL5 was hardly detectable as well. Relative gene expression was normalised to ACTB and human placenta. Significance tested by one-way ANOVA (*P < 0.05).

3.3 DISCUSSION

Testicular germ cell tumours typically contain a variety of macrophage subtypes in close contact with the neoplastic cells. These macrophage subsets have contrasting properties, both anti- and pro-inflammatory, and are known to exhibit either tumour progressive (M2) or tumour destructive (M1) phenotypes in other neoplastic conditions (Sica et al., 2006; Sica et al., 2008; Allavena et al., 2008; Biswas and Mantovani, 2010). Tumour cells can themselves control the functional polarization of macrophages by producing cytokines and chemokines (Lewis and Pollard, 2006; Duluc et al., 2007; Heusinkveld et al., 2011b). In this thesis, potential macrophage polarization factors have been identified in specimens of human testicular neoplasia (see Chapter 2). Thus, this study was conducted to establish components of a cell culture model that could be used to examine functional interactions between macrophages and TGCTs. The human monocyte-derived THP-1 and the TCam-2 seminoma cell lines were selected as well-established models of each cell type that could be manipulated and used to characterize macrophage-tumour cell interactions. In the present chapter, potential macrophage polarization factors are examined in detail, while in Chapter 4 the TCam-2 and THP-1 cells are used in co-culture to model the testicular tumour environment and observe their interactions.

In the present study, THP-1 cells are characterized regarding the presence of hallmark CD marker proteins and functional properties. A recently established protocol for THP-1 differentiation into specific macrophages subsets (Genin et al., 2016) was used to differentiate THP-1 cells into M0, M1 or M2 macrophages by successive exposure to PMA, cytokines and LPS. In addition to characterization of subtype-specific CD markers, cytokine and chemokine expression and characterization of chemokine receptors were conducted to identify what potential recruitment factors may be influencing the behaviour and/or phenotypes of these cells. Additional experiments treating the differentiated macrophages with cytokines and chemokines found in the testicular tumour environment (Chapter 2) identified potential macrophage polarization factors and examined whether one or more cytokines are necessary or sufficient to drive functional differentiation. To assess whether TCam-2 cells might be to influence macrophage polarization, cytokine and chemokine profiling of this cell line was also conducted.

For an identification of different macrophages subsets following *in vitro* differentiation of the THP-1 cell line, the markers used were those described in human testis clinical

specimens in Chapter 2: M1, CD11 and CD68; M2: CD163 and CD206. CD68+ macrophages were also detected which could not be classified as with M1 or M2 phenotypes.

In the present study, M0 macrophages were shown to contain high transcript and protein levels of CD68. This therefore indicates that M0 cells are a precursor of macrophages which subsequently differentiate into another phenotype, either M1 or M2, depending on the cytokine milieu they encounter after the recruitment. In the healthy testis with normal spermatogenesis, the predominantly anti-inflammatory milieu is predicted to promote the M2 phenotype. Interestingly, the culture of M0 macrophages led to synthesis of both M1 (CD68 and CD11c) and M2 (CD163 and CD206) marker expression in these cells. This can be interpreted as an indication that M0 macrophages become poised to differentiate into either M1 or M2 macrophages, with their subsequent phenotype influenced by cytokine and chemokines. The presence of transcripts and proteins encoding both pro-/and anti-inflammatory cytokines in M0 macrophages was demonstrated, including IL-10, TGF-β1, TNF-α, lL-12, CCL2 and CCL5. It could be that this cytokines and chemokines were secreted by macrophages due to the long incubation time (43 h). However, all detectable cytokines are known as potential M2 macrophage polarization factors such as IL-10, TGF-β1 whereas TNF-α is a potential M1 polarization factor (Urban et al., 1986; Hagemann et al., 2006; Lu et al., 2013; Chanmee et al., 2014; Genin et al., 2015,).

Both, M1 and M2 macrophages expressed specific CD markers, CD68 and CD11c (M1) and CD163 and CD206 (M2) whereas macrophages which were differentiated into M2 showed significantly increased M2 marker expression compared to M1 macrophages. Additionally, both, M1 and M2 macrophages expressed nearly the same transcript level of pro-/and anti-inflammatory cytokines whereas the protein analysis clearly confirmed the anti-inflammatory property of M2 macrophages due to the expression of high amounts of IL-10 and TGF-β as well as the pro-inflammatory property of M1 macrophages by the expression of high amounts of IL-12, IL-6, TNF-α (Biswas and Mantovani, 2010; Blagih and Jones, 2012; Haschemi et al., 2012; Cai et al., 2012). Interestingly, *in vivo* studies of murine macrophages revealed that M2 macrophages can re-polarize into M1 due to the plasticity caused by cytokines expression (Guiducci et al., 2005). Therefore, the plasticity of macrophages could explain the transcript level of pro-/and anti-inflammatory cytokines expressed by M1 and M2 macrophages. Another reason which should be discussed is the transition

ability. Furthermore, M2 macrophages are known for the wound healing property (Martinez et al., 2008). Therefore, an assay was conducted that simulated a wound by scratching a gap at the bottom of a confluent 6 well plate. All three macrophage subsets were analysed and M2 macrophages showed the strongest wound healing effect by measuring the area of the gap at different time points. This property that is M2 specific can be hereby confirmed. All in all, polarized and well characterized THP-1 macrophages are a useful in-vitro model since M1 and M2 specific properties can be confirmed.

Additionally, an analysis regarding chemokine and chemokine receptors expression by M0, M1 and M2 macrophages was conducted. The inflammatory chemokines CCL2, CCL5 and CCL15 and chemokine specific receptors were addressed due to the chemotaxis capability of immune cells especially macrophages and their potential role as macrophage polarization factors. We revealed clearly that M0 macrophages are targets of all chemokines (CCL2, CCL5 and CCL15) due to the specific receptor expression of CCR1 and CCR2 (transcript levels). However, a migration assay was conducted to confirm the macrophage recruitment effect of chemokines (CCL2, CCL5 and CCL15). Interestingly, M0 and M2 macrophages showed a strong migration effect using CCL15 whereas M1 macrophages showed no migration effect after the treatment with CCL15. This result could probably explain why M2 (CD163, CD206) and macrophage precursor (CD68+) which might be similar to M0 macrophages are present in the human testis where a detection of CCL15 was also possible (Fig. 3.3.1).

In contrast, M1 macrophages expressed low transcript level of CCR2. CCR2 can bind CCL2 (Craig and Loberg, 2006) but it is unclear if protein levels are expressed to bind CCL2. We assumed that these chemokine are responsible for the recruitment and/or for the functional polarization of M1 macrophages since CCL2 was constantly present and associated with testicular neoplasia (see Chapter 2). Conducting a migration assay, M1 macrophages showed a strong migration effect by CCL2 treatment that confirmed our hypothesis (Fig. 3.3.2). Interestingly, a chemokine expression analysis revealed an expression of CCL2 by M1 macrophages. This suggested that M1 macrophages can recruit circulating M1 macrophages as well as M0 macrophages since both subsets expressed specific chemokine receptors to bind CCL2. This would confirm the role of macrophages to reinforce immune reaction by a recruitment of circulating immune cells from the peripheral blood to the inflammatory environ-

ment. However, M2 macrophages expressed other chemokine receptor types than M0, which can target CCL5 and CCL15 but no CCL2. A migration assay was conducted in order to confirm these recruitment properties of CCL15 and CCL5. A conformation was possible since the M2 treatment with both cytokines revealed a strong migration effect (Fig. 3.3.1/3.3.2). Additionally, M2 were able to express CCL5 which indicates that M2 macrophages have an influence on the recruitment of themselves. To sum up, macrophages itself express chemokines such as CCL2 (expressed by M1) and CCL5 (expressed by M2) that can confirm the role of macrophages to reinforce immune reaction by the recruitment of immune cells. However, tumour cells in other cancer types can influence macrophage recruitment by even CCL2 as well as CCL5 (Ueno et al., 2000; Mantovani, 2008; Mizutani et al., 2009; Roca et al., 2009; Kim et al., 2009; Erler et al., 2009; Fang et al., 2016). Interestingly, the cultivation of TCam-2 cells showed an expression profile of both chemokines (CCL2 and CCL5) that could suggest that TCam-2 cells as a seminoma cell line can recruit macrophages and control probably macrophage polarization by tumour specific cytokine expression. Further macrophage polarization depends then on the environment which is given.

We tested the polarization capability of these chemokines by treating M0 macrophages with different chemokines and cytokines such as CCL2, CCL5; CCL15 and activin A. As previously mentioned (Chapter 2), M0 macrophages are precursor of M1 and M2 macrophages. Those macrophages are present in the human testis and we hypothesized an recruitment by CCL15 but it was not clear if this chemokine is also responsible for a functional polarization or if the cytokine milieu in the testis drives functional macrophage polarization since M2 macrophages are mainly present. Interestingly, we were able to show an impact of CCL15 treated macrophages on CD marker expression.since M1 specific CD11c was downregulated but also M2 specific CD206. M1 macrophages (CD68+/CD11c+) were not detectable in the human testis that confirmed our *in vitro* results but M2 macrophages (CD163+/CD206+). However, M2 macrophage polarization can be driven by TGF-β (Zhang et al., 2016) that is constantly present in the testis and indicated that CCL15 is not responsible for a functional polarization of M2 macrophages. This suggested that CCL15 is a recruitment factor of macrophages but also a polarization factor. Additionally, CCL2 and CCL5 treated M0 macrophages expressed higher transcript lev-

el of M2 specific marker (CD163, CD206) that suggested besides the recruitment effect of these chemokines also a polarization effect.

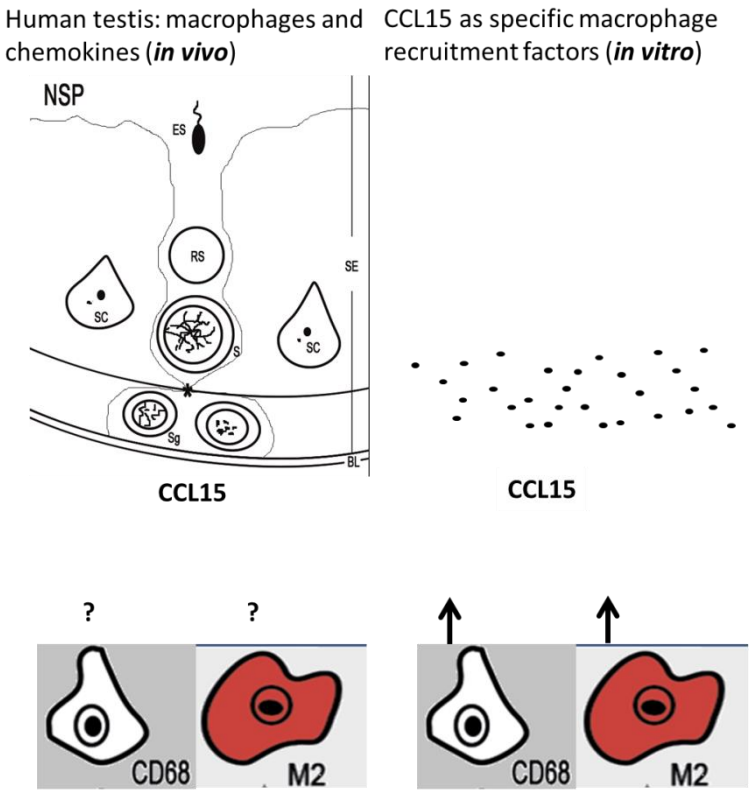

Fig. 3.3.1: Schematic of chemokine and macrophage coherence in the human testis. Besides, CD68+macrophage precursor, anti-inflammatory M2 macrophages are detectable in the human testis. *In vitro* cell culture experiments revealed the chemotactic property of both macrophage subsets that subsequently confirmed those cells as targets of CCL15. IC= immune cells, SC= sertoli cell, RS= round spermatids, ES= elongated spermatids, SG= spermatogonia, BL= blood testis barrier, SE= seminiferous epithelium. As indicated by black arrows, CCL15 can recruit different macrophage subsets.

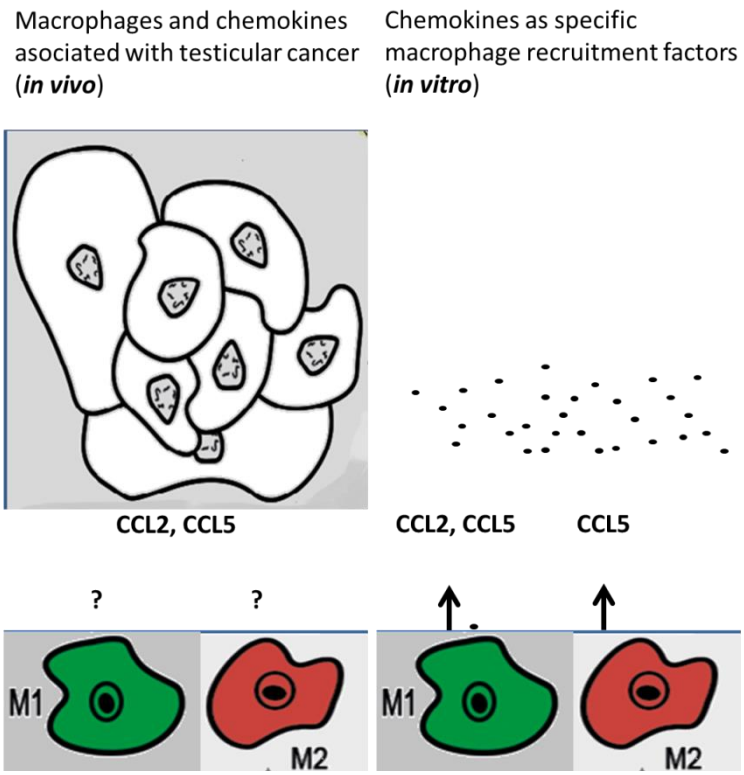

Fig. 3.3.2: Schematic of chemokine and macrophage coherence under pathological conditions e.g. testicular neopasia. Besides M2 macrophages, newly detected pro-inflammatory M1 macrophages are associated with testicular neoplasia. Additionally recruitment factors such as CCL2 and CCL5 were present under this conditions. Specific *in vitro* cell culture experiments revealed that M1 macrophages can be recruited by CCL2 and CCL5 while M2 are attracted to CCL5. As indicated by black arrows, chemokines can recruit different macrophage subsets. IC= immune cells.

CONCLUSION

We differentiated THP-1 cells into different macrophage subsets (M0, M1, M2) by a specific treatment with cytokines and LPS. Subsequently, a confirmation of M1 (pro-inflammatory) and M2 (anti-inflammatory) specific properties was possible. Additionally, a detailed cytokine and chemokine profile of TCam-2 cells was conducted to understand the immune cell recruitment and polarization capability. To sum up, we established and characterized a macrophage and seminoma cell model that can be further used for co-culture analysis (see chapter 4).

CHAPTER 4

The impact of testicular germ cell tumour/ immune cell interactions on the functional polarization of macrophages: Analysis using THP-1 and TCam-2 cells

CHAPTER 4: The impact of testicular germ cell tumour/ immune cell interactions on the functional polarization of macrophages: Analysis using THP-1 and TCam-2 cells

4 INTRODUCTION

As described in Chapter 2, testicular germ cell neoplasia specimens commonly contain different macrophage subsets with distinct properties, such as the tumour-promoting M2 macrophages that produce anti-inflammatory cytokines and the tumoricidal M1 macrophages which synthesize pro-inflammatory cytokines. However in the normal human testis with complete spermatogenesis, M1 macrophages are not detectable. Data presented in Chapter 2 addressed the hypothesis that an altered environment arises with the progression of testicular neoplasia, such that abnormalities in local production of cytokines and chemokines may recruit and polarize macrophages. A detailed analysis of cytokines and chemokines in the testicular tumour environment revealed potential candidates for macrophage recruitment and polarization (discussed in Chapter 2).

As presented in Chapter 3, cell culture models were established to mimic the conditions present in human testicular neoplasia in which germ cell tumours are in direct contact with macrophages. Using the human monocyte-derived THP-1 cell line, differentiation into M0, M1 and M2 macrophages could be driven by treatment of these cells with specific factors. Both M0 and M1 cells could be altered to adopt phenotypes associated with immune-suppressive M2 macrophages. This demonstrates the utility of the THP-1 cells to model the functional plasticity of macrophages in the testis tumour environment.

In addition, the seminoma-derived TCam-2 cell line was shown to synthesize cytokines capable of altering macrophage functions. Data in this chapter presents the results from co-culturing the different THP-1-derived macrophage subsets with TCam-2 cells to simulate and therefore study the immune-/tumour cell interaction. The presence and potential changes in cytokine and chemokine production was measured using qRT-PCR and multiplex protein assays. Additionally, functional macrophage polarization associated with tumour/immune cell interaction was analysed in regards to factors that were secreted in this co-culture. The relevance of Smad signalling pathways to macrophage differentiation and subsequent macrophage polari-

zation was tested using the pathway inhibitor, SB431542, and the outcomes monitored by Flow analysis. This co-culture model was also used to examine the phagocytic capability of each macrophage subset. The results illustrate a functional molecular dialogue between tumour and immune cells that is likely to exist in the adult human testis and change with the progression from GCNIS to neoplasia.

4.1 MATERIAL AND METHODS

4.1.1 Cell co-cultures

TCam-2 cells (a human seminoma derived cell line {Mizuno et al., 1993; deJong et al., 2008}, originally obtained from Prof. Kitizawa, Japan) and THP-1 cells (human monocytic leukemia cell line; provided by Dr. Ashley Mansell, Hudson Institute of Medical Research, Clayton, Australia) were cultivated as described in Chapter 3 (Sections 3.1.1.1 and 3.1.1.2). THP-1 cells were differentiated into M0, M1 and M2 subtypes using phorbol 12-myristate 13-acetate (PMA, 20 ng/ml) for 24 h (Fig. 4.1.1), then either Lipopolysaccharide (LPS, 10 pg/ml) and IFN-γ (20 ng/ml) for M1 differentiation, or with IL-4 (20 ng/ml) and IL-13 (20 ng/ml) for M2 differentiation, for a further 43 h incubation (Fig. 4.1.1).

The cells were counted and each cell type was individually seeded at a density of $1x10^5$ cells per well in a 6 well plate (Falcon®, Corning Life Science, Tewksbury, USA) (Fig. 4.1.1). For IF, glass cover slips were placed into each well before the cells were seeded. THP-1 inhibition of the TGF-β signaling pathway was conducted 1h before TCam-2 cells were added. After the co-culture, cells were designated for RNA extraction and cDNA synthesis (PCR) (see 4.1.2/4.1.3), multiplex (see 4.1.4), IF (see 4.1.5) or fixed for Flow analysis (see 4.1.6).

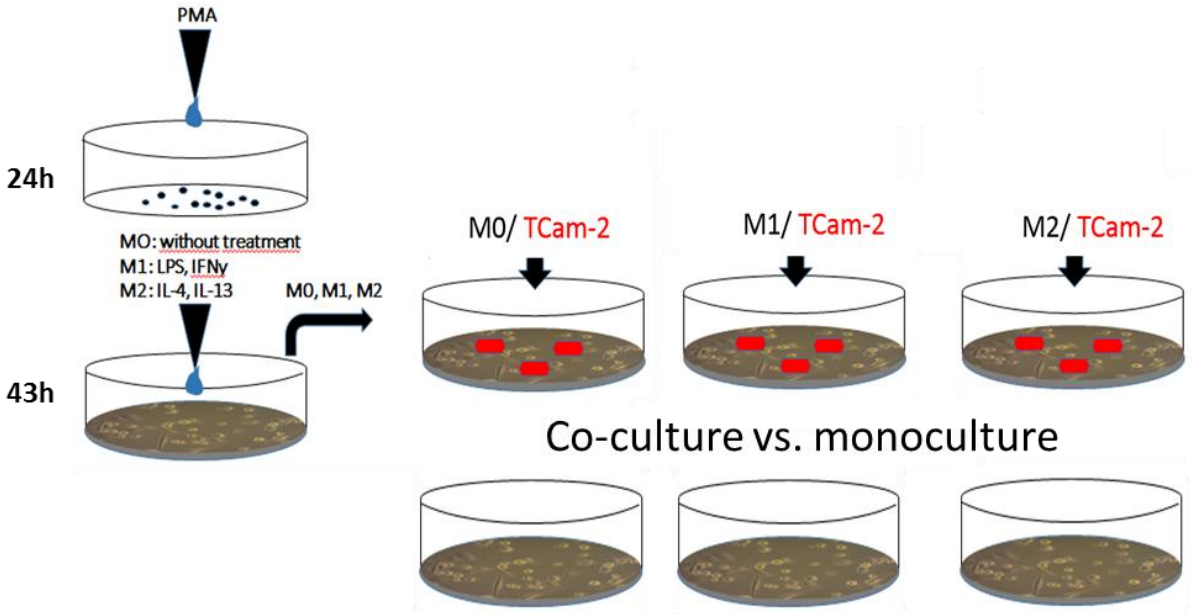

Fig. 4.1.1: Schematic of the *in-vitro* THP-1 setup for macrophage differentiation and following co-culture with TCam-2 cells. Human monocyte-derived THP-1 cells were treated with PMA and incubated for 24 h. Afterwards, the differentiated THP-1 cells (into activated M0 macrophages) were treated with either LPS (10 pg/ml) and IFN-γ (20 ng/ml) for differentiation into M1 macrophages or with IL-4 (20 ng/ml) and IL-13 (20 ng/ml) for differentiation into M2 macrophages. Then TCam-2 and THP-1 cells were co-cultured (at a density of $1x10^5$cells per well of each individual cell type. After co-culture following analyses were conducted: RNA extraction and cDNA synthesis (for transcript analysis by qRT-PCR), supernatant collection (Multiplex for protein measurement) and cell fixation (Flow cytometry for cell-specific marker enumeration).

4.1.2 RNA extraction and reverse transcription

For extraction of total RNA, cells were washed with PBS then 1 ml TRIZOL was added to each well and the plate incubated on a shaker for 10 min at RT. Afterwards, a cell scraper (BD Falcon, Bedford, USA) was used to remove all attached cells, with differentiated THP-1 cells being extremely tightly attached. The TRIZOL cell suspension was collected and frozen at -80° or processed immediately. The DNase I kit (Ambion, LifeTechnologies) was used according to the manufacturer's protocol. RNA was quantified using Nanodrop photometer (NP80, Implen). Synthesis of cDNA was performed using 500 ng DNA-free total RNA, 1 µl SuperScript® III reverse transcriptase (200 U/µl, LifeTechnologies, Grand Island, NY, USA), 4 µl 5x First Strand buffer (LifeTechnologies), 1 µl random hexamer primers (50 µM, Promega or Applied Biosystems), 1 µl DTT (0.1M, Invitrogen), 1 µl dNTP mix (10 mM, Sigma-Aldrich, Castle

Hill, Australia) and 1 µl Molecular Water (Carl Roth GmbH & Co. KG, Karlsruhe, Germany) per sample, according to the enzyme manufacturer's protocol. Negative control samples lacked SuperScript® III (enzyme volume replaced with molecular water). The cDNA synthesis program was conducted as in Chapter 3 (Tab. 3.1.3).

4.1.3 Quantitative RT-PCR

Quantitative real-time PCR was conducted for analyses of CD markers in macrophages, and of cytokine and chemokine transcript levels in M0, M1, M2 and TCam-2 cells. For the measurement of pro-inflammatory cytokines, IL1b, IL-12, TNFa, and anti-inflammatory cytokines, IL-10, TGF-β1, as well as pleiotropic IL-6 and chemokines, CCL2 and CCL5, Taqman probes (Thermo Fisher Scientific) were used (see Tab. 3.1.4.1) in a Taqman Assay, according to the probe manufacturer's protocol. The samples were prepared using 8 µl TaqMan® Gene Expression Assay and 2 µl sample (diluted 1:20 in Molecular Water) (see Appendix, Chapter 3).
For the analysis of CD markers to identify macrophage subsets, Oct3/4 to identify TCam-2 cells, Inhba (activin A, pleitropic cytokine), and chemokine receptors, CCR1, CCR2, CCR3, CCR4 and CCR5, primers were designed using Oligo Explorer, Version 1.1.2 (see primer details, Tab. 3.1.4.2).
The chemokine receptor expression was analysed by using two TCam-2 datasets that were accessed from Geoprofiles series GSE60138. This series included TCam-2 datasets GSM1466229 and GSM1466230, deposited by (Irie et al., 2015). Raw data was collected, and Genebank accession numbers correlated to specific gene names using BioDBnet Db2db software.
The qRT-PCR was conducted using SybrGreen, according to the manufacturer's protocol, as follows. The samples were prepared using 2 µl cDNA sample, 2 µl Molecular Water, 0.5 µl primer (10 pm, each forward and reverse) and 5 µl SYBRGreen (Thermo Fisher Scientific) and analysed by Applied Biosystem 7900HT Fast Real-Time PCR machine. Each reaction was performed in technical triplicates which were averaged and calculated using SDS v2.4 (Applied Biosystems). For statistical analysis, a One Way ANOVA was performed followed by a Tukey *post hoc* test (GraphPad7.01). Data are shown as fold-change normalized to ACTB; term human placenta RNA (supplied by Ursula Manuelpillai) was used as a positive control.

4.1.4 Multiplex Cytokine /Chemokine analysis

The medium from cultivated and differentiated THP-1 cells differentiated into M0, M1, and M2 subtypes was collected for Multiplex analysis. For cytokine and chemokine analysis, two separate Luminex Multiplex Kits (Merck Millipore, Australia) were used (Chapter 3, Table 3.1.6), as this method is more efficient and sensitive for analysis of small samples than traditional ELISA kits. The supernatants of co-cultivated cells were centrifuged at 239rcf for 2 min to exclude remaining cells, then collected into Eppendorf tubes for storage at -80°C or else immediately processed. Samples were prepared according to the kit manufacturer`s protocol using magnetic beads to isolate the reaction products present in cell supernatants for measurement. The MULTIPLEX analysis (see Appendix Chapter 3) of each sample was conducted in triplicates using a Corning™ 96-Well Filter Plate Fluid Guard (Fisher Scientific), and and the results visualized using Bioplex 200 (Biorad).

4.1.5 Immunofluorescence staining

Media was removed from cells grown on coverslips, the cells were washed with PBS then fixed in 4% PFA for 15 min on a platform shaker with gentle rotation. After fixation the cells were washed 3 x 5 mins with PBS, then permeabilised in 1 ml/well 0.1% Triton-X-100/PBS for 10 mins. Primary antibodies (Tab. 4.1.5.1) were diluted in 0.5% BSA/PBS and applied to each coverslip for overnight incubation at 4°C or for 1 h at RT. Coverslips were then washed in 1 ml PBS 4 x 5 min on a rotating platform . Secondary antibodies (Tab. 4.1.5.2) were diluted in 0.5% BSA/PBS, then applied to the coverslips for a 1 h incubation in the dark. Afterwards, cells were washed in 1 ml/well PBS (4 x 5 min) on a rotating platform, incubated for 10 min in DAPI solution (1:10000, diluted in 0.5% BSA/PBS), then washed in 1 ml/well PBS (4 x 5 min). Coverslips were mounted using GVA (Genemed Biotechnologies, South San Francisco, U.S.A.) on Superfrost Plus slides. The slides were stored protected from light at 4°C until analysis was conducted.

Tab.4.1.5.1 Primary Antibodies (IF)

Primary Antibody	Manufacturer	Dilution	Cat.No.
CD45	Dako	1:100	IS75130-2
Oct3/4	Santacruz	1:100	sc-8629

Tab.4.1.5.2 Secondary Antibodies (IF)

Secondary Antibody	Manufacturer	Dilution	Cat.No.
Rabbit anti-mouse A568	Abcam	1:300	483566
Donkey anti-goat AF488	Invitrogen	1:300	A11055

4.1.6 Flow

4.1.6.1 Cell collection and fixation

For flow cytometric analysis of cell surface markers expressed by M0 and M1 macrophages, and of transcription factors expressed by TCam-2 cells, THP-1 cells were first exposed to factors to induce differentiation and grown to near confluency. For co-cultures, each cell type were seeded at a density of $1x10^5$ cells per well (1.6 cm^2) in a 6-well plate (Falcon®, Corning Life Science, Tewksbury, USA), cultured at 37°C in 5% CO_2, and collected at different time points (t= 0 h, 3 h, 6 h, 12 h, 24 h and 48 h). Monocultures were seeded at the same density, and cells collected at 48 h for comparison. After removal of the supernatant for measurements of cytokines and chemokines as described in 4.1.4, 1 ml of 0.1% TV was added in each well for at least 3 min at 37°C in 5% CO_2. Cells were fixed in 1 ml of 4% PFA (in Millipore Water) for 15-20 min at RT. The tubes were centrifuged at 239rcf for 2 min at 4°C, the supernatant was replaced with 1% BSA/PBS, and the process repeated. Cells were stored for less than 10 days in 1% BSA/PBS at 4^oC prior to analysis.

4.1.6.2 Staining of fixed cells

The fixed cells were pelleted at 956rcf for 2 min at 4°C; all cell centrifugations were conducted using these conditions unless otherwise noted. The 1% BSA/PBS solution was discarded and 100 µl BD Perm/Wash™ buffer (containing Fetal Bovine Serum and saponin, ThermoFisher) was added and incubated for at least 10 min at RT. Cells were pelleted by centrifugation, the supernatant removed, and cells were re-suspended in 50 µl Perm/Wash containing the primary antibody (Oct3/4, 1:100) and incubated for 1 h at RT. In the meantime, directly conjugated antibodies were prepared at appropriate dilutions in Perm/Wash (see 3.1.7.2.3). After blocking, cells were spun at 239rcf for 2 min at 4°C and 50 µl of the diluted direct conjugated antibody solution (see Tab. 3.1.7.2.3) was added and incubated for 45 min protected from light. The cells were pelleted at 239rcf, the supernatant discarded and the diluted secondary antibody (Donkey anti-goat AF488, 1:300) added and incubation for 45 min, at RT. Cells were washed twice in Perm/Wash (100 µl in each tube, centrifugation at 239rcf), and the cells were finally resuspended in 150 µl Perm/Wash and stored for up to 6 days at 4°C, until the flow analysis was conducted.

4.1.6.3 Gating strategy

Ten thousand events were acquired for each sample using the BD LSR Fortessa x20 (BD Bioscience, San Jose, USA). Data were analysed using FlowJO Version 10 (Tree Star, Ashland, USA) in the following manner. The first step was the selection of cells according to their physical properties; both debris and clumped cells were identified based on their position in the plot and subsequently excluded using Forward scatter (FSC) and Side scatter (SSC) setting made using the unstained control vs. the stained control. Each antibody was detected using a different voltage setting that depended on the cells being examined and the fluorophore (Chapter 3, Tab. 3.1.7.3).

4.2 RESULTS

4.2.1 Visualisation of TCam-2 and THP-1 interactions in co-culture

Co-culture of TCam-2 and THP-1 cells was used to investigate the nature and specificity of tumour-immune cell interactions, with a focus on cytokine and chemokine expression. TCam-2 and THP-1 derived M0, M1 and M2 macrophages were observed after 24 h co-culture using an inverted brightfield microscope (Fig. 4.2.1). M0 macrophages (Fig. 4.2.1, A) were in close contact with TCam-2 cells, as were M1 (Fig. 4.2.1, B) and M2 (Fig. 4.2.1, C) macrophages.

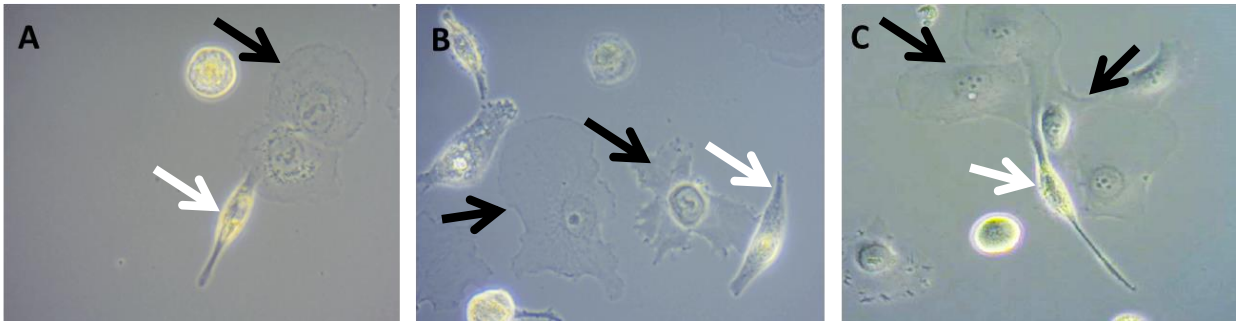

Fig. 4.2.1: Visualisation of tumour-/immune cell interactions using TCam-2 and different THP-1-derived macrophage subsets (M0 (A), M1 (B), M2 (C)) after 24h co-culture. TCam-2 cells, black arrows; macrophage subtypes, white arrows.

4.2.2 Synthesis of immune cell modulators is altered by co-culture

As shown in Chapter 3, cultivated M0 macrophages in monoculture produced detectable levels of the pro-inflammatory transcripts encoding IL-12a and IL-1b, whereas transcripts encoding anti-inflammatory proteins such as TGF-β1 and IL-10 were barely detectable (Fig. 4.2.2.1). Co-cultured M0/TCam-2 cells altered these cytokine transcript profiles. For instance, levels of transcripts encoding the anti-inflammatory cytokines IL-10, TGF-β and Inhba were higher compared the levels detected in monocultures of M0 macrophages and TCam-2 cells (Fig. 4.2.2.1). Pro-inflammatory cytokines such as IL-1b and TNF-α were also highly expressed in this co-culture system, whereas IL-12a was decreased (Fig. 4.2.2.1). Additionally, detection of the transcript encoding the pleiotropic IL-6 was possible in co-cultures of M0 macrophages and TCam-2 cells (Fig. 4.2.2.1). The level of the TGF-β1 protein was also analysed in this

co-culture model. It was detected in after 3 h of M0/TCam-2 co-culture, and the amount of protein detected after 24 h and 48 h was significantly higher than at 3 h of co-culture and in TCam cells grown alone (mono-culture).

Furthermore, mono-cultured M1 macrophages showed transcript level of pro-/ and anti-inflammatory cytokines (e.g. Inhba, IL-10, TGF-β1, Il-12a, TNF-α, Il-1b and IL-6) (Fig. 4.2.2.1/4.2.2.2). A co-culture with M1/TCam-2 leaded to an alteration of pro-inflammatory cytokine transcript level such as a downregulation of IL-12a, TNF-α (excluded IL-1b) and anti-inflammatory cytokine IL-10 whereas TGF-β was increased (Fig. 4.2.2.1). Interestingly, there was a tendency of increased IL-6 cytokine transcript level in this co-culture system (Fig. 4.2.2.1). A detection of TGF-β1 protein level was possible after 3 h M1/TCam-2 co-culture. Additionally, TGF-β1 protein level was analysed using M1/TCam-2 co-culture model. Detection of TGF-β1 protein level was possible after 3 h M1/TCam-2 (Fig.4.2.2.2). After 48 h, the protein expression of TGF-β1 was significantly increased in the M1/TCam-2 co-culture compared to co-cultured M1/Tcam-2 (t= 3 h) and monocultured TCam-2 (Fig.4.2.2.2). However, an analysis of TGF-β1 protein level between both groups, M0/TCam-2 and M1/TCam-2 cells revealed that co-cultured M1/TCam-2 showed a higher expression than M0/Tcam-2 (Fig.4.2.2.2).

M2 macrophages (mono-culture) expressed transcript level of pro-/ and anti-inflammatory cytokines (e.g. Inhba, IL-10, TGF-β1, Il-12a, TNF-α, Il-1b and IL-6) (Fig. 4.2.2.1). However, transcript level of anti-inflammatory cytokines such as IL-10 and TGF-β1 and pro-inflammatory cytokines such as IL-12a and IL-1b as well as the pleiotropic cytokine IL-6 were decreased whereas Inhba and TNF-α were slightly increased in the M2/ TCam-2 co-culture compared with the monoculture (Fig. 4.2.2.1).

In summary, the outcomes of tumour/ immune cell interactions revealed in these co-cultures indicate that synthesis of the immune modulatory factors persists in co-cultures and this cellular crosstalk can influence macrophage function.

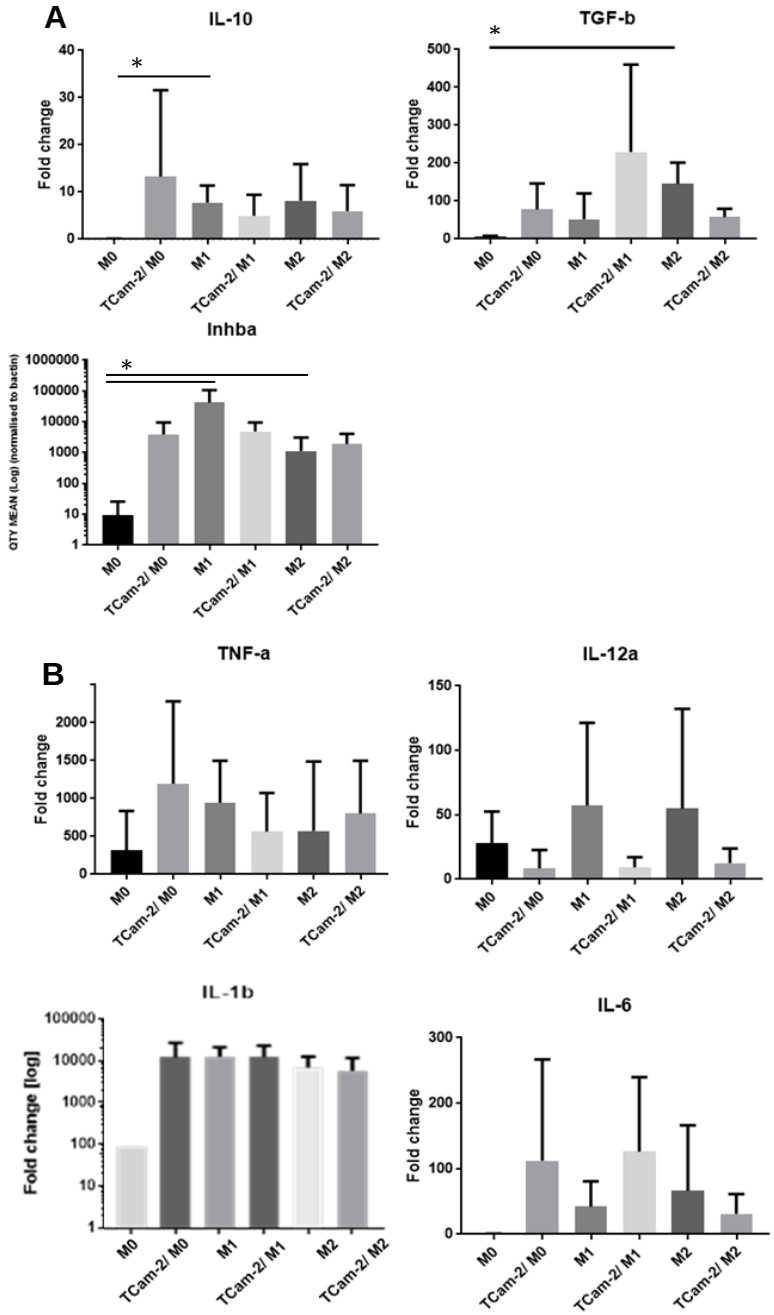

Fig. 4.2.2.1 Tumour/ immune cell interactions affect profiles of transcripts encoding pro- and anti-inflammatory cytokines. Monocultures and co-cultures were conducted with THP-1-derived M0, M1 and M2 macrophages and TCam-2 cells (all n=3, except M0: IL-1b, n=1). Analysis of cytokines with established functions and presence in the testis (A) and cytokines associated with inflammation (B). M0 macrophages showed transcript level of Inhba, TGF-β1 (anti-inflammatory cytokines) and IL-12a and IL-1b (pro-inflammatory cytokines) which were altered after a co-culture with TCam-2 cells. M2 macrophages expressed transcript level of the pleiotropic IL-6 and Inhba, IL-10 and TGF-β1 (anti-inflammatory cytokines) whereas M1 macrophages expressed pro-inflammatory cytokines such as IL-12, TNFα, IL-1a and the pleiotropic cytokine IL-6 which were altered after a co-culture with TCam-2 cells. The fold change value presented for each culture was calculated by delta-delta-Ct method and is relative to b-actin and human placenta (Taqman probes), whereas Inhba is relative to b-actin (individual primer design).

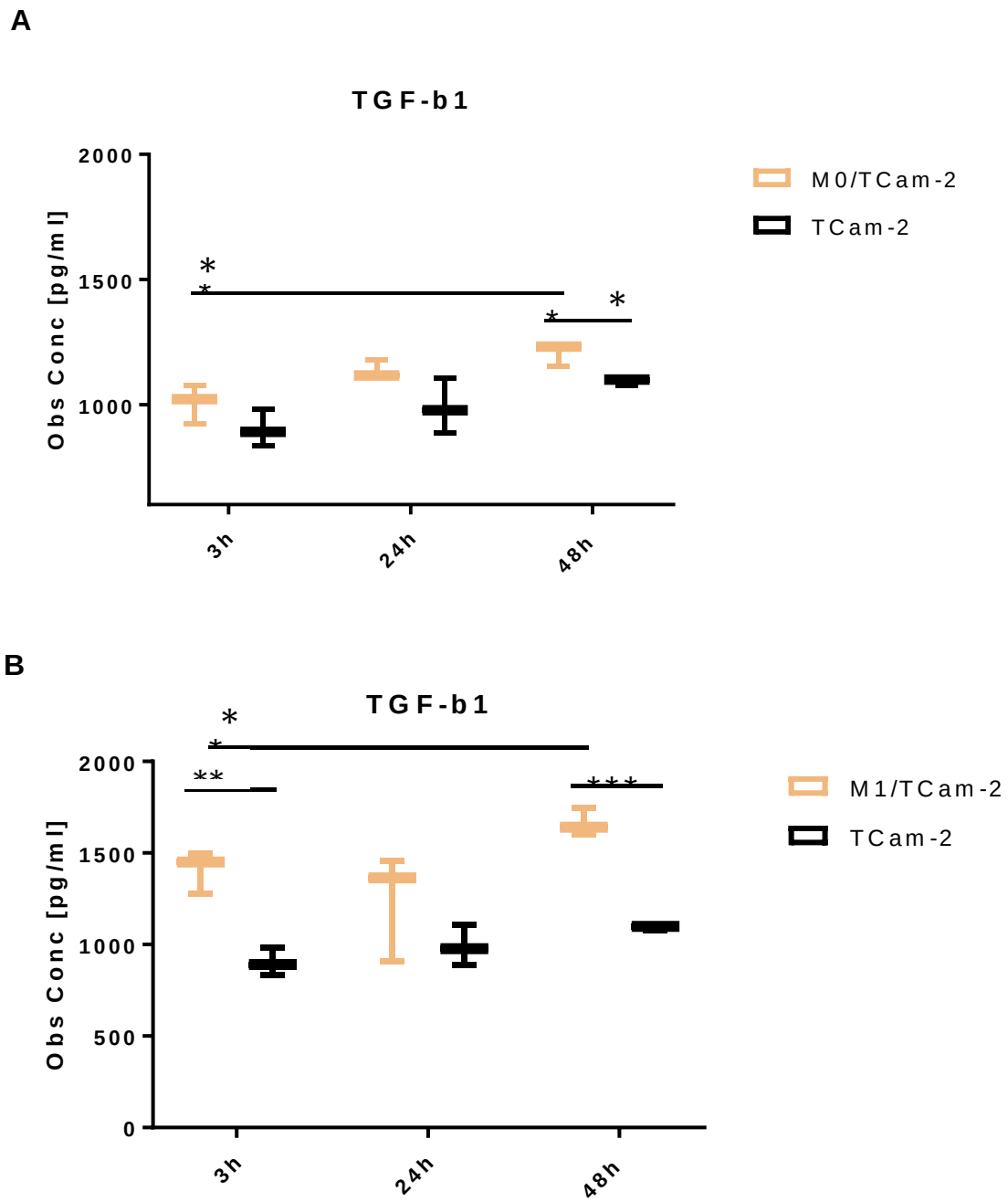

Fig. 4.2.2.2: Analysis of tumour/immune cell interaction effects on TGF-β1 levels in co-cultured M0 (A) or M1 (B) macrophages with TCam-2 cells (n=3)**.** TGF-β1 was measured against a standard provided with the Multiplex Kit. At each time point examined, t= 3, 24, 48 h, TGF-β1 levels were higher in in M0/TCam-2 and M1/TCam-2 co-culture in comparison to the TCam-2 monoculture and co-culture (t= 3 h). Significance tested by student t-test (*P < 0.05, **P < 0.01).

4.2.3 Tumour-immune cell interactions reveal chemokine attractants and M0, M1 and M2 macrophages as target cells (co-culture)

As reviewed in Chapter 2, macrophages are targets of different chemokines which are present under pathological conditions, including testicular neoplasia. Therefore, this co-culture model was used to interrogate the mechanism underpinning recruitment and functional polarization of macrophages. Analysis of two chemokines identified as present in TGCT tumours and their receptors (Chapter 2, Section 2.2.3.2) was undertaken to address the potential recruit and function on immune cells.

The co-cultured TCam-2 cells and THP-1-derived macrophage subsets were observed to be in close contact (Fig 4.2.1). Measurement of chemokine transcript levels revealed the presence of the chemoattractants, CCL2 and CCL5, using this tumour (TCam-2)/ immune cell (M0, M1, M2) co-culture model (Fig. 4.2.3.1). The transcript level of CCL2 was significantly higher in the M0/TCam-2 and M1/TCam-2 co-culture compared to the monocultures. In contrast, M2 cells and co-cultured M2/TCam-2 cells showed no significant difference in CCL2 transcript levels (Fig. 4.2.3.1). Additionally, the CCL5 expression profile was not different between monocultured and co-cultured M0 macrophages, whereas monocultured M1 and M2 macrophages showed a non-significant but clear trend towards higher CCL5 transcript levels, compared to the co-culture with TCam-2. Due to time constraints, a time course was not possible, but the duration of this interaction could be an important feature which determines the outcome of the behaviours of these cells *in vivo* and *in vitro*.

An assessment of chemokine proteins revealed that after only 3 h of co-culture, CCL2 and CCL5 proteins were detectable in M0/TCam-2 and M1/TCam-2 co-culture supernatants (Fig. 4.2.3.2). After 3 h, CCL2 was significantly higher in the M1/TCam-2 co-culture compared to the TCam-2 monoculture (Fig. 4.2.3.2). After 24 h, co-cultured M0/TCam-2 and M1/TCam-2 cells showed an upward trend of CCL2 and CCL5 protein levels that was measured as significantly increased in M0/TCam-2 co-culture compared to monocultured TCam-2 cells (Fig. 4.2.3.2).

In summary, the levels of both CCL2 and CCL5 were measurable after 3 h co-culture and elevated at the 24 h in co-cultures, with CCL2 significantly higher in M1/TCam-2 co-cultures and CCL5 significantly higher in M0/TCam-2 co-cultures.

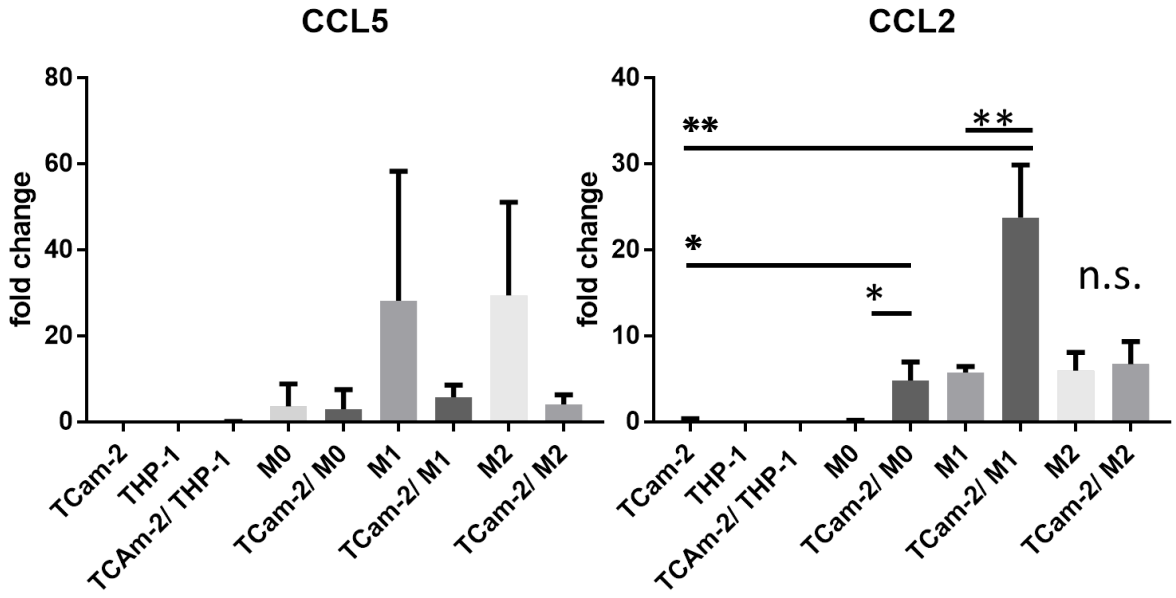

Fig. 4.2.3.1: Chemokine transcript expression profile of co-cultured M0/TCam-2, M1/TCam-2, M2/TCam-2 macrophages compared with monocultured cells by qRT-PCR (n=3). All co-cultured macrophage subtypes contained detectable levels of CCL2 and CCL5 transcripts, whereas only CCL2 was detectable in TCam-2 cells at a low level. Co-cultures of either M0/TCam-2 or M1/TCam-2 exhibited significantly increased *CCL2* compared with the monoculture of these macrophage subtypes. The CCL5 transcript appeared lower (non-significant) in all three co-cultures (M0/TCam-2, M1/TCam-2, M2/TCam-2). The fold change value presented for each culture was calculated by delta-delta-Ct method. Relative gene expression was normalised to ACTB and human placenta. Significance tested by student t-test (n.s. not significant;*P < 0.05, **P < 0.01).

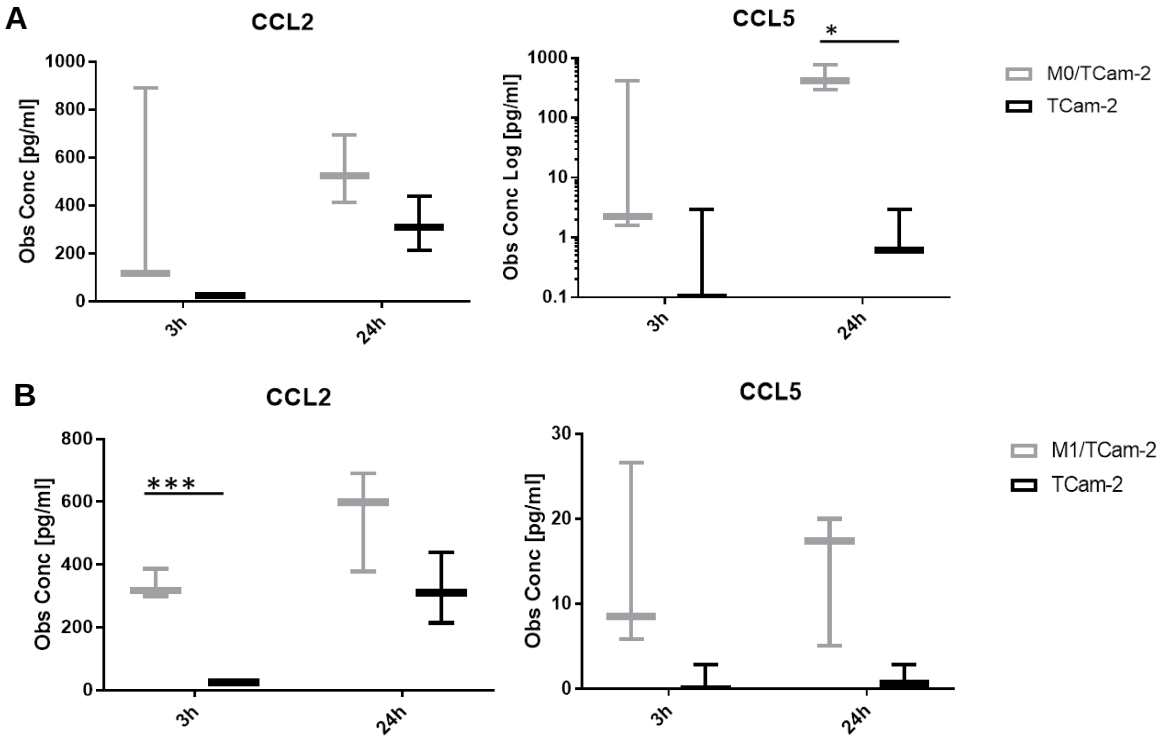

Fig. 4.2.3.2: Chemokine protein levels in TCam-2 cell monoculture supernatants compared to those from co-cultures of M0/TCam-2 (A) or M1/TCam-2 (B). Measurements obtained using the Multiplex assay (n=3). Levels of both CCL2 and CCL5 were measurable after 3 h co-culture and elevated at the 24 h in co-cultures, with CCL2 significantly higher in M1/TCam-2 co-cultures and CCL5 significantly higher in M0/TCam-2 co-cultures. Significance tested by student t-test (*P < 0.05, **P < 0.01, ***P < 0.001).

As previously addressed in Chapter 3, the detection of several chemokine receptor transcripts was possible in monocultured macrophages. A comparative analysis between monocultured and co-cultured macrophages revealed a clear change in chemokine receptor expression, while TCam-2 cells do not express chemokine receptors evidenced by the RNA sequence data from two TCam-2 samples (dataset 1: CCR1: n.d., CCR2: n.d., CCR3: 5, CCR5: n.d.; dataset 2: CCR1: n.d., CCR2: n.d., CCR3: n.d., CCR5: n.d.; n.d.= not detected). Co-cultured M0 macrophages showed a decreased expression of CCR1, whereas CCR2 was not detectable and CCR3 was hardly present (Fig. 4.2.3.3). An analysis of co-cultured M1 and M2 macrophages revealed a decrease of CCR1, CCR3 and CCR5 transcripts compared to monocultures. Interestingly, CCR2 was previously expressed by monocultured M1 but not detectable in the co-culture.

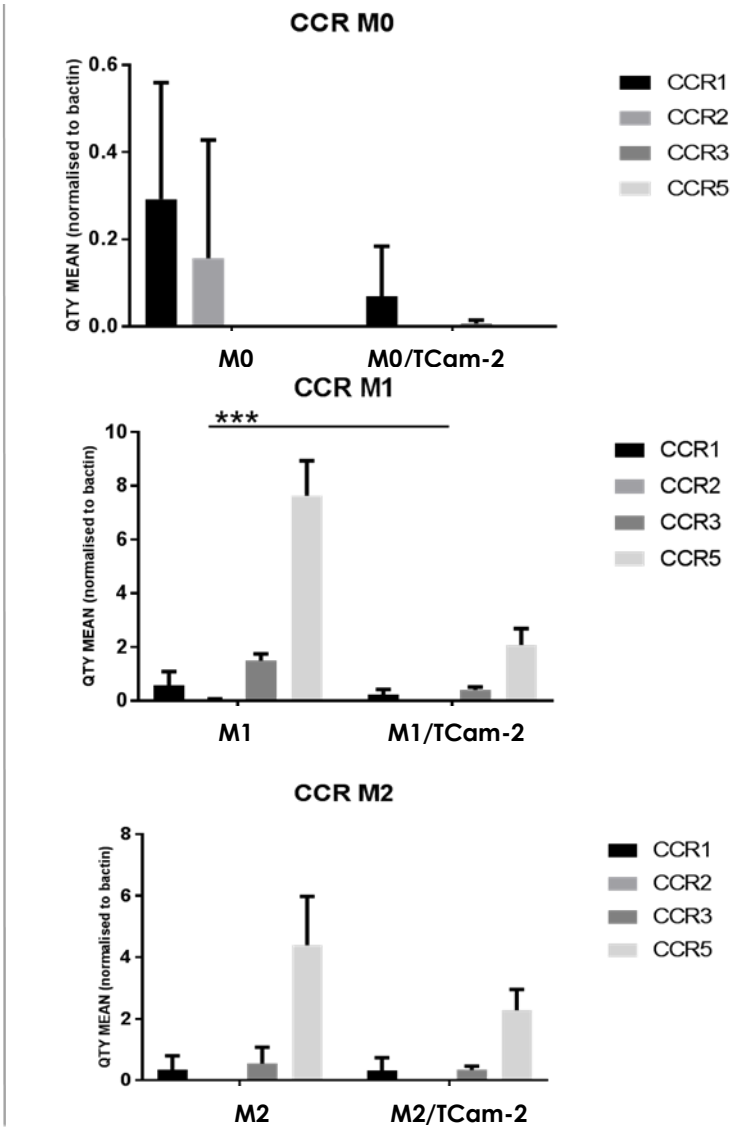

Fig. 4.2.3.3: Comparative analysis of monocultured and co-cultured M0, M1 and M2 (differentiated THP-1) chemokine receptor expression by qRT-PCR (n=3). All receptors such as CCR1, CCR2, CCR3 and CCR5 were higher expressed in the monoculture compared to the co-culture. Relative gene expression was normalised to ACTB. Significance tested by one-way ANOVA (*P < 0.05, **P < 0.01, ***P < 0.001).

4.2.4 TCam-2 cells influence macrophage polarization towards an immunosuppressive M2 phenotype

Using this co-culture model, the impact of the tumour-immune cell interactions on functional macrophage polarization was assessed, with a focus on examining how M0, M1 and M2 specific macrophage marker synthesis was altered. A comparison of

CD expression was conducted in monocultured macrophages vs. co-cultured macrophages using two approaches: qRT-PCR and Flow cytometry.

Co-cultivation of M0 macrophages with TCam-2 cells altered the CD transcript level of M0 macrophages. For instance, compared to monocultured M0 macrophages, co-cultured M0 cells showed a significantly higher level of the M1 marker, CD11c, with CD68 modestly but non-significantly elevated (Fig. 4.2.4.1, A). M2 specific markers CD163 and CD206 were barely detectable in the M0 cells cultured on their own, but co-culture with TCam-2 led significant elevation of the M2 marker, CD163 (Fig. 4.2.4.1, A).

Measurement of M1 and M2 specific markers by Flow cytometry was conducted to assess changes protein levels (Fig. 4.2.4.2, A). Co-culture of M0 cells with TCam-2 cells resulted in significantly higher levels of both M2 markers, CD163 and CD206, at both 24 and 48 hours. M1 markers, CD68 and CD11c were significantly elevated at 48 h in M0/TCam-2 co-cultures.

Additionally, co-cultivation of M1 macrophages and TCam-2 cells altered M1-specific CD transcripts compared to monocultured M1 macrophages. Coculture led to a significant decrease in both CD11c and CD68 (Fig. 4.2.4.1, B). The CD163 transcript could be amplified from monocultured M1 macrophages, while that encoding CD206 was barely detectable; co-culture of the M1 cells with TCam-2 cells did not yield a significant change in either of these (Fig. 4.2.4.1, B). A preliminary assessment (n=1) of protein levels indicated that both M1 (CD68, CD11c) and M2 (CD163, CD206) markers were increased by TCam-2 co-culture (Fig. 4.2.4.3, B).

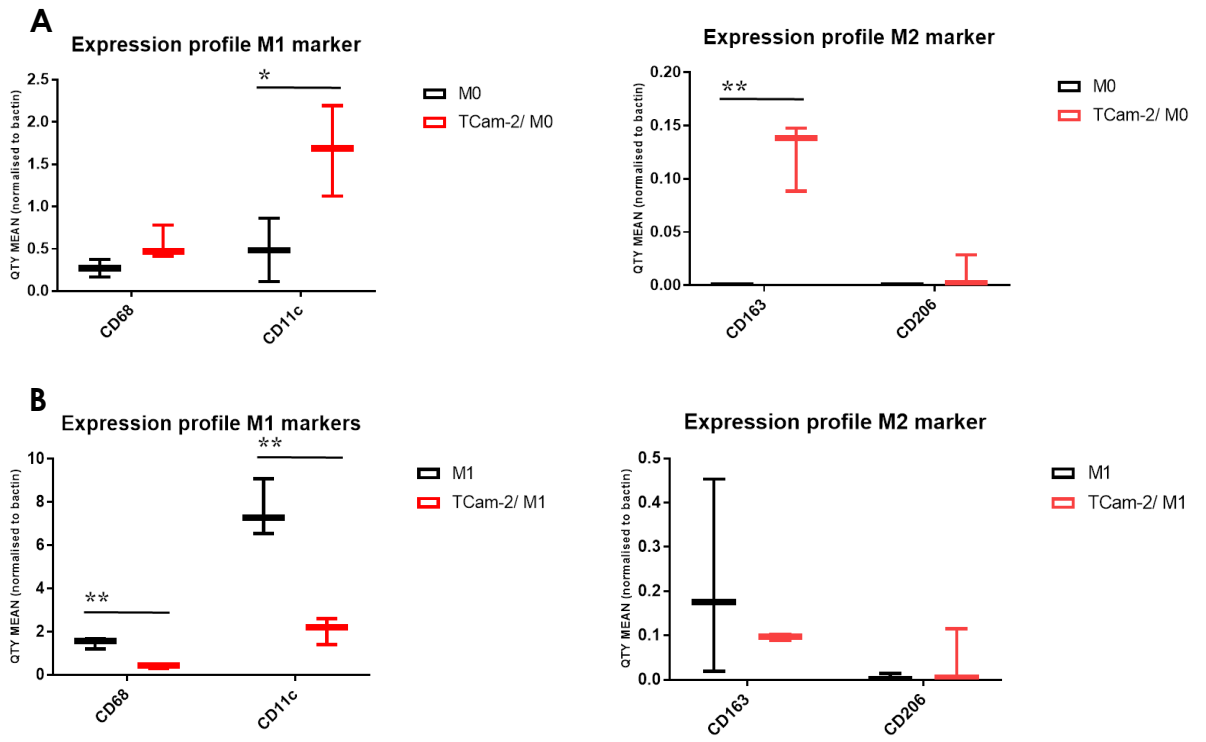

Fig. 4.2.4.1: Transcript expression level (mRNA) of M1 and M2 specific marker by co-cultured M0/TCam-2 (A) and M1/TCam-2 (B) (qRT-PCR, n=3). (A) Co-cultured M0 macrophages showed a significant alteration of M1 (CD11c) and M2 (CD163) specific marker compared with the M0 monoculture. (B) Co-cultured M1 macrophages showed a significantly decreased expression of M1 specific marker (CD11c, CD68). Relative gene expression was normalised to ACTB and human placenta. Significance tested by student t-test (*P < 0.05, **P < 0.01).

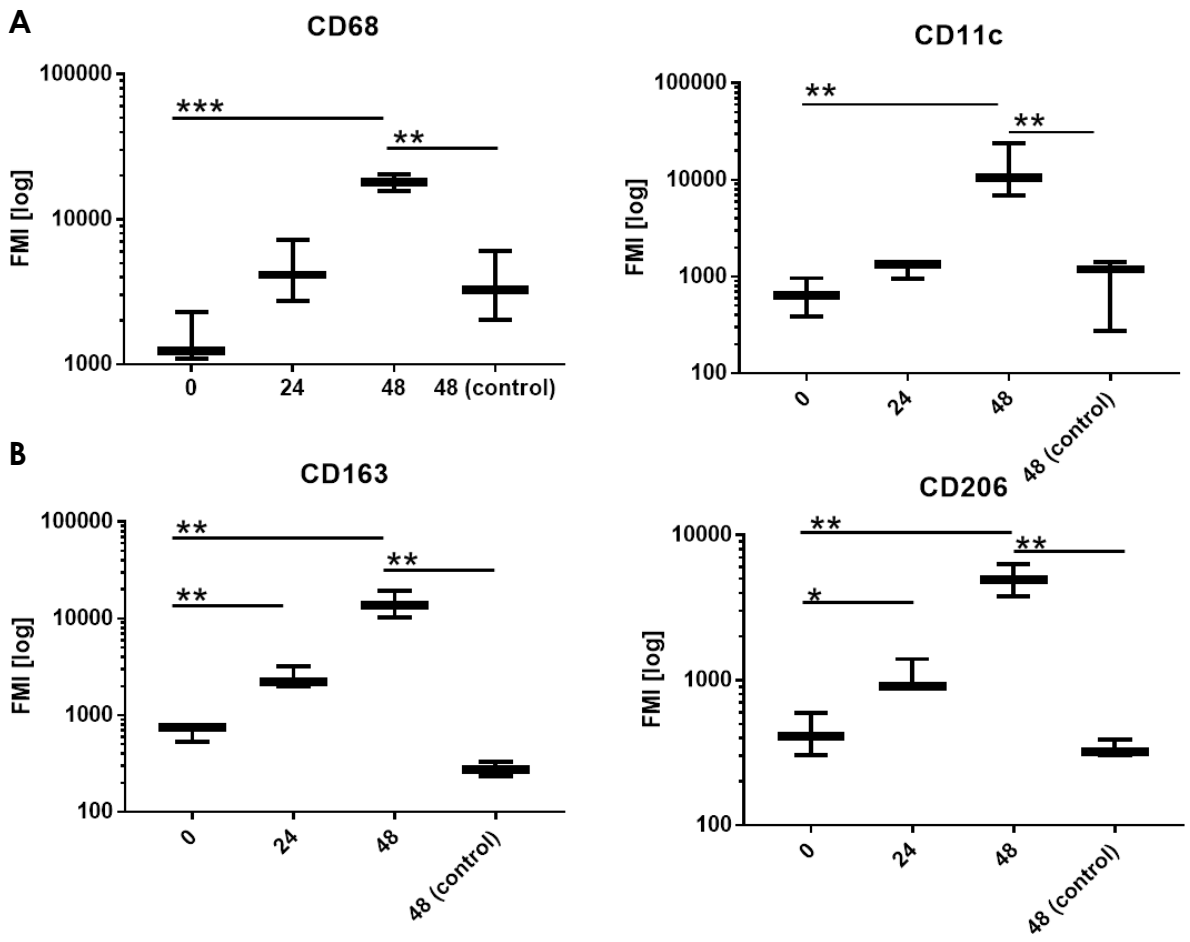

Fig. 4.2.4.2: Levels of M1- (A) and M2- (B) specific markers become elevated by co-culture of M0 macrophages with TCam-2 cells. Co-cultures with M0 macrophages showed significantly higher levels of M1-specific protein markers at 48 h of co-culture (A) and significantly higher levels of M2-specific markers at 24h and 48h of co-culture (B) measured by flow cytometry and shown as fluorescence mean intensity (FMI) (n=3). Significance tested by student t-test (*P < 0.05, **P < 0.01, ***P < 0.001).

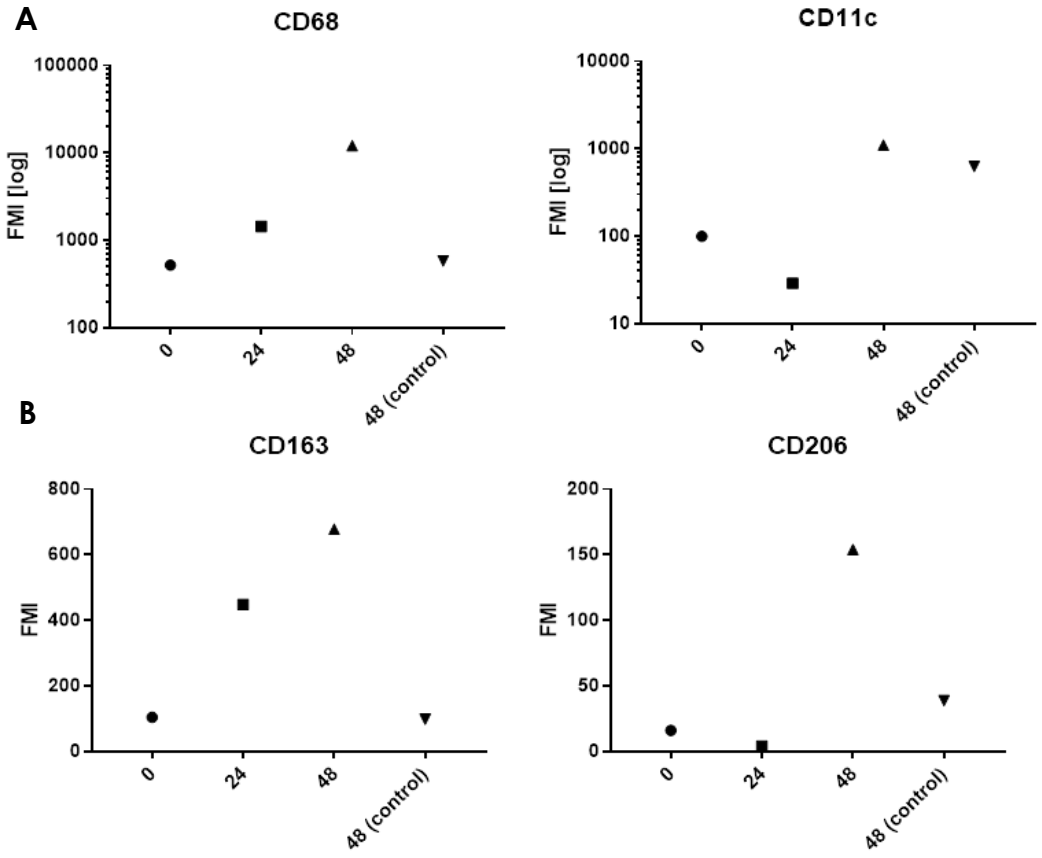

Fig. 4.2.4.3: Levels of M1- (A) and M2- (B) specific markers may be altered following co-culture of M1 macrophages with TCam-2 cell. Markers measured by Flow cytometry (preliminary data, n=1) and shown as fluorescence mean intensity (FMI). Co-cultured M1 macrophages appear to have higher levels of M1 (A) and M2 (B) markers after 48 h.

4.2.5 TGF-β signalling pathway inhibitor (SB-431542) treatment decreases differentiation of immune-suppressive M2 macrophages in M0/TCam-2 and M1/TCam-2 co-cultures.

As previously addressed (see 4.2.4), co-cultured M0/TCam-2 and M1/TCam-2 cells showed increased M2 marker expression compared to monocultured M0 or M1 macrophages. Activin A, IL-10 and TGF-β1 are potential candidates for mediating this increased M2 marker expression since recent studies showed an association of those cytokines and M2 polarization (Mantovani et al., 2002; González-Domínguez et al., 2016). Activin A, IL-10 and TGF-β1 have been previously identified as macrophage polarization factors (Mantovani et al., 2002; Mia et al., 2014; González-

Domínguez et al., 2016). Importantly, transcripts encoding each were detected in the M0/TCam-2 and M1/TCam-2 co-culture (Fig. 4.2.2.1).

Because 48 hours of co-culture with TCam-2 cells of both M0 and M1 macrophages led to significantly increased expression of M2 specific markers (see 4.2.4), these conditions were selected to address the potential that these ligands contribute to the phenotypic change. Therefore, a study was conducted to investigate the effect of blocking TGF-β1 and activin A signaling, by preventing activation of the Smad signalling pathway in conditions that were demonstrated as permissive for macrophage polarization. Before placing M0 and M1 macrophages in co-culture, the pathway inhibitor SB431542 was used to pre-treat them, 1 hour before TCam-2 cell additions. TCam-2 cells were added to pre-treated M0 or M1 macrophages, and the M2 specific markers, CD163 and CD206, measured at 0, 24 and 48 h. After 24 h, pre-treated and co-cultivated M0 macrophages showed a decreased expression of CD163 and a significantly increased expression of CD206 compared to t= 0 h (Fig. 4.2.5, A). Co-cultivated M1/TCam-2 cells showed slightly increased M2 marker levels (Fig. 4.2.5, B). After 48 h, pre-treated and co-cultivated M0 macrophages showed nearly the same level of M2 specific marker as measured t= 0 h, whereas M0/TCam-2 without SB431542 pre-treatment showed significantly increased expression level of CD163 and CD206 (M2 marker) (Fig. 4.2.5, A). Co-cultivated M1 macrophages showed significantly decreased M2 protein level compared to monocultured M1 macrophages (Fig. 4.2.5, B).

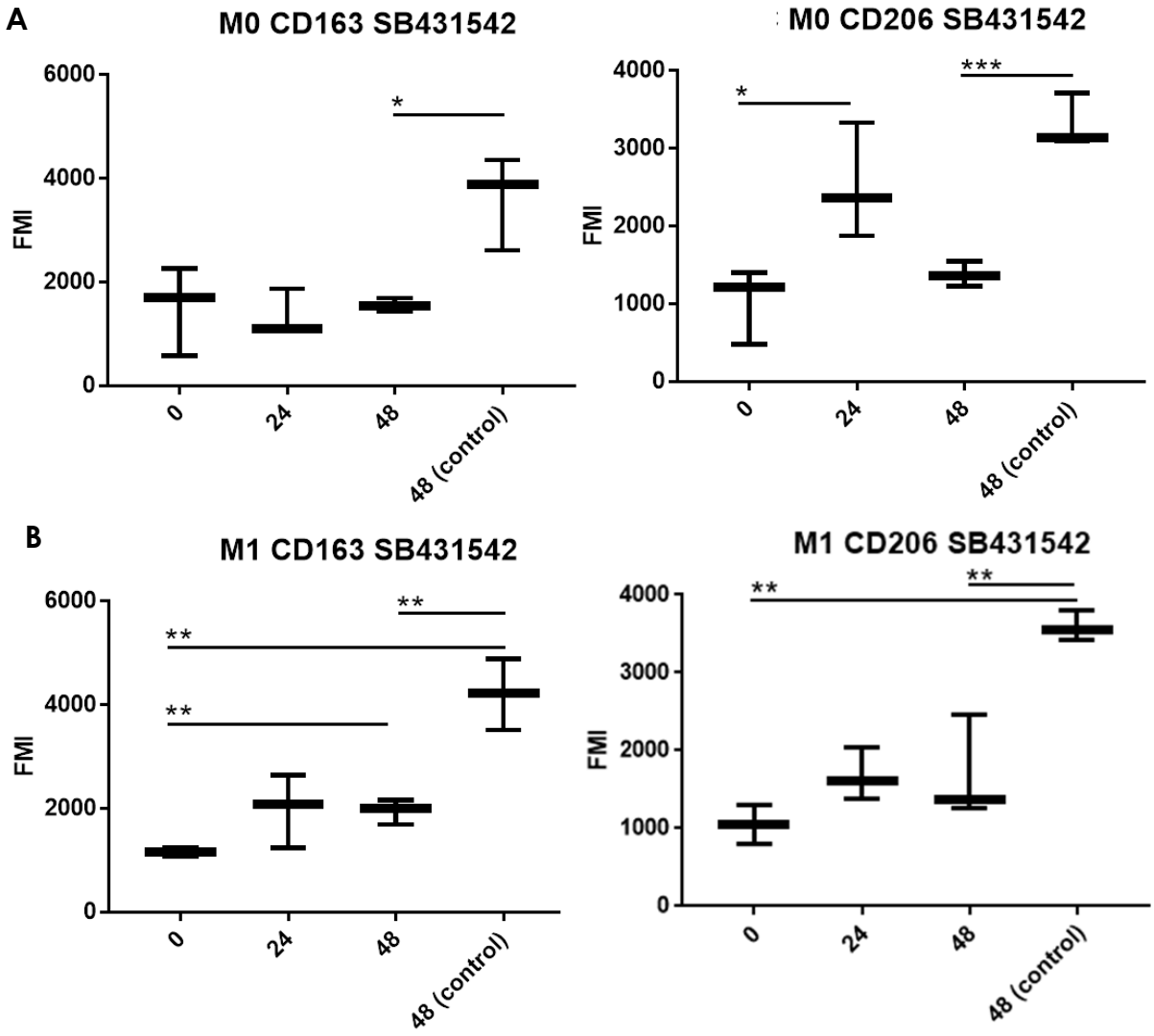

Fig. 4.2.5: M2 (CD163, CD206) specific Protein expression level (FMI) of co-cultured M0/TCam-2 (A) and M1/TCam-2 (B), treated with SB431542 (10 µM) and without SB431542 (control) by Flow (n=3). SB431542 treated M0 and M1 macrophages showed a slightly increase of M2 marker after 24 h and 48 h co-culture. Additionally, co-cultured M0 and M1 macrophages showed significantly increased protein level of M2 specific markers after 48 h compared with the SB431542 treated group. Whereas pre-treated (SB431542) M0/TCam-2 cells showed a reduction of M2 specific marker after 48 h. Significance tested by student t-test (*P < 0.05, **P < 0.01, ***P < 0.001).

4.2.6 Co-cultured M0/TCam-2 and M1/TCam-2 reveal phagocytic activity of THP-1-derived M0 and M1 macrophages

A crucial role of macrophages is their ability to phagocytise pathogens. Several analyses employing flow cytometry and indirect immunofluorescence were conducted to identify the phagocytic activity of M0 and M1 macrophages in relationship to TCam-2 cells. This study was conducted to address phagocytic activity of macrophage subsets on tumour cells and how these macrophage responses are influenced by the presence of tumour cells over time. These outcomes could be helpful to reveal which subset could be exploited for therapeutics by inhibition of tumour derived cytokines that influence macrophage polarization and subsequently phagocytic activity.

4.2.6.1 Flow cytometry used to monitor loss of TCam-2 cells during co-culture with THP-1 derived macrophages

The flow cytometric assay established to examine macrophage phagocytic activity in M0/TCam-2 cells and M1/TCam-2 co-cultures employed CD14 as a marker present on all macrophage subsets (see Appendix, Chapter 4). TCam-2 cells were identified using Oct3/4, which is also known as POU5F1, present in all TCam-2 cells (Young et al., 2011). The disappearance of Oct3/4+ TCam-2 cells during co-culture with M0 or M1 macrophages was presumed to occur via phagocytosis; this was monitored by measuring the percentage of cells present at different time points (t= 3, 24, 48 h) relative to the culture start, with t= 0 h set to 100% (Fig. 4.2.6.1.1). After 3 h, co-cultured M0/TCam-2 showed no significant decrease in Oct3/4+TCam-2 cell numbers (Fig. 4.2.6.1.1). After 24 h, Oct3/4+TCam-2 cells were significantly decreased compared with t= 0 h by approximately 10%. At 48 h of co-culture, the Oct3/4+TCam-2 cell number remained significantly decreased compared to t= 0 h.

The co-cultures of M1 macrophages and TCam-2 cells showed no significant reduction in Oct3/4+TCam-2 cell number at 3 h (Fig. 4.2.6.1.2), however at 24 h the significant decrease in number of Oct3/4+TCam-2 cells was greater than that recorded in the M0/TCam-2 cell cultures, reaching a value approximately 30% lower compared

with t= 0 h. After 48 h, this number also remained significantly lower compared to t= 0 h (Fig. 4.2.6.1.2).

Thus, co-culture of phagocytic M0 or M1 macrophages and TCam-2 cells resulted in a loss of TCam-2 cells. The outcomes at both 24 and 48 hours provide evidence that M1 macrophages have a higher phagocytic activity than M0 macrophages. The trend towards a slight increase in TCam-2 numbers between 24 h and 48 h indicates that the remaining TCam-2 cells remain viable and are likely to be proliferating.

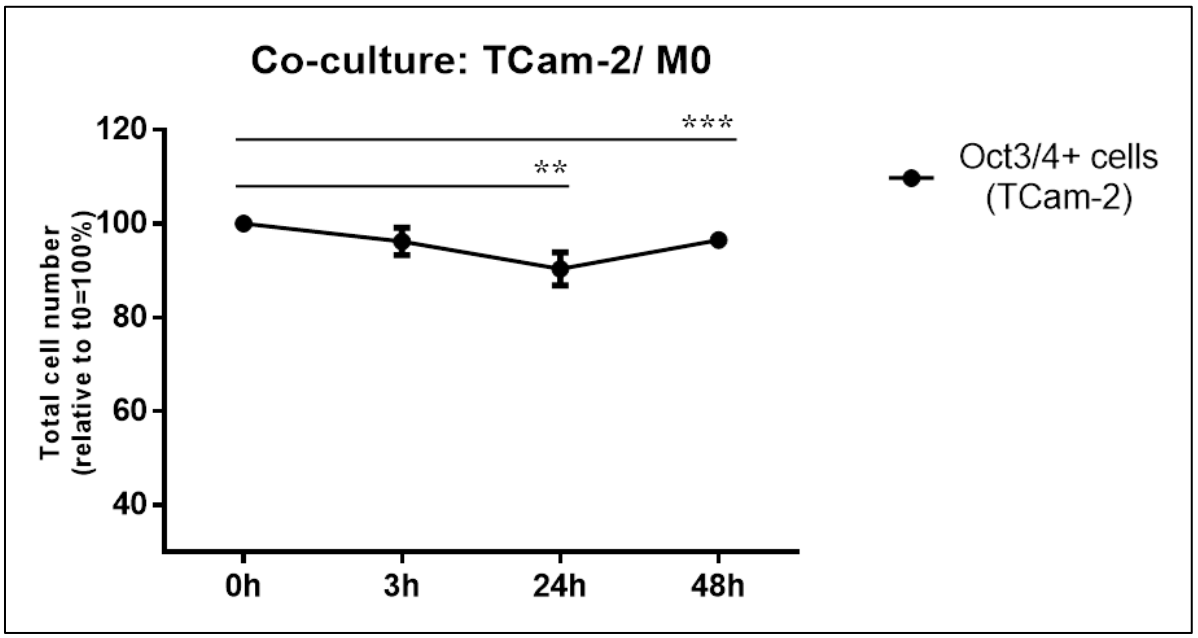

Fig. 4.2.6.1.1: Percentage of Oct3/4+TCam-2 cells measured by flow cytometry in M0/TCam-2 co-cultures (n=3)**.** Co-culture resulted in a significant decrease in Oct3/4+TCam-2 cells at 24 h and 48 h, as an indication of TCam-2 phagocytosis by M0 macrophages. Measured number of Oct3/4+TCam-2 cells at indicated time points is presented as a percentage of the cell number at t0= 100%. Significance tested by one-way ANOVA (**P < 0.01, ***P < 0.001).

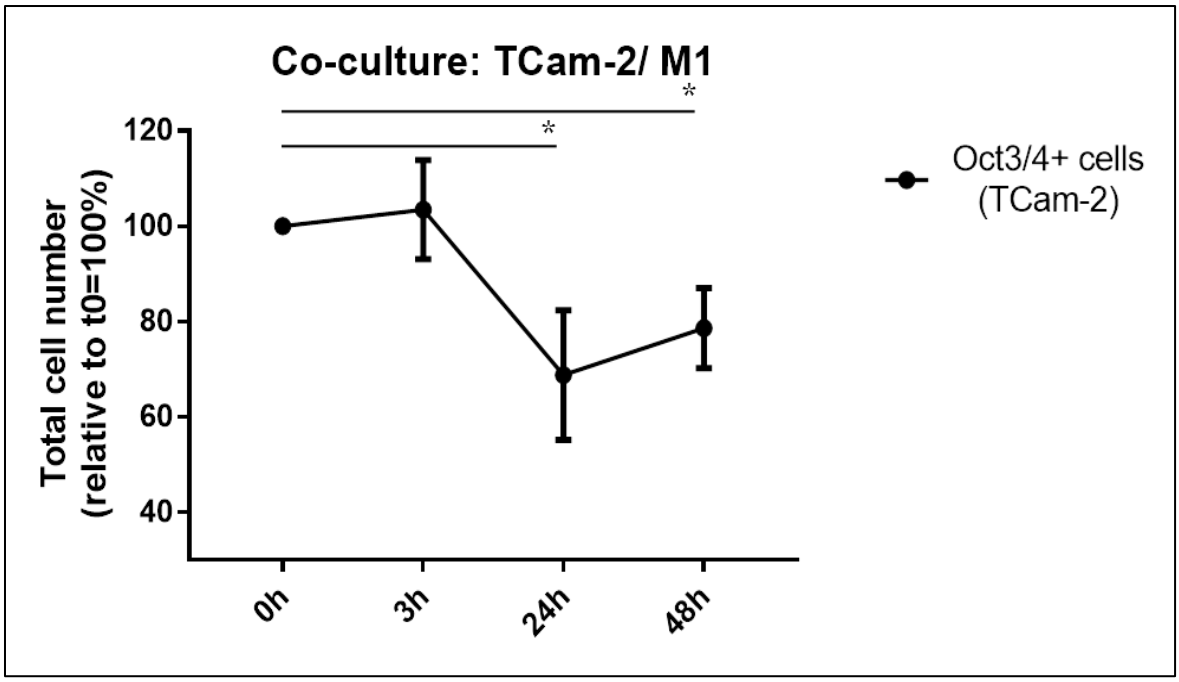

Fig. 4.2.6.1.2: Percentage of Oct3/4+TCam-2 cells measured at different time points in the M1/TCam-2 co-culture as an indication of TCam-2 phagocytosis by M1 macrophages (n=3)**.** Co-cultured M1/TCam-2 revealed a significant decrease of Oct3/4+TCam-2 cells at 24 h and 48 h. Measured number of Oct3/4+TCam-2 cells at indicated time points is presented as a percentage of the cell number at t0= 100%.. Significance tested by one-way ANOVA (*P < 0.05).

4.2.6.2 Flow cytometric tracking of macrophage granularity as an indicator of phagocytic activity

Mutzke et al. showed that the flow cytometric measurement of side scatter in cells can be used as an indicator of macrophage phagocytic activity (Mutzke et al, 2015). In the present study, CD14+M1 macrophages were analysed, as these displayed the greater phagocytic activity towards TCam-2 cells compared to M0 cells (4.2.6.1).

CD14+M1 macrophages were identified with altered granularity at specific time points of the co-culture (t= 3, 6, 12, 24, 48 h). At the beginning of the co-culture, most macrophages had a similar granularity (SSC) (Fig. 4.2.6.2.1, t= 0 h), reflecting the observed uniformity of shape of these cells. At 3 h, the co-cultured CD14+M1 macrophages showed a remarkable shift towards a broad range of granularities and the emergence of cells with a distinctively higher CD14 levels. At 6 h, some CD14+M1 macrophages showed a similar but broad alignment along the x axis which, indicated that all cells have a different granularity (SSC) but the same CD14 expression profile (Y586) (Fig. 4.2.6.2.1). However, some M1 macrophages showed a consistent

alignment along the y axis (Y586) that indicated a variable CD14 expression between individual cells; this distribution pattern was generally the same at 12 h of co-culture. Remarkably at 24 h, CD14+M1 macrophages showed the same profile as observed at t= 3 h (Fig. 4.2.6.2.1), while at 48 h, CD14+M1 macrophages the profile was more similar to that present at t= 6 h. Additional experiments with sampling at t= 3 h, 24 h and, 48 h to capture the time points which showed the greatest alteration of granularity, showed consistent profiles (data not shown). These samples were used for the immunofluorescence experiments reported below.

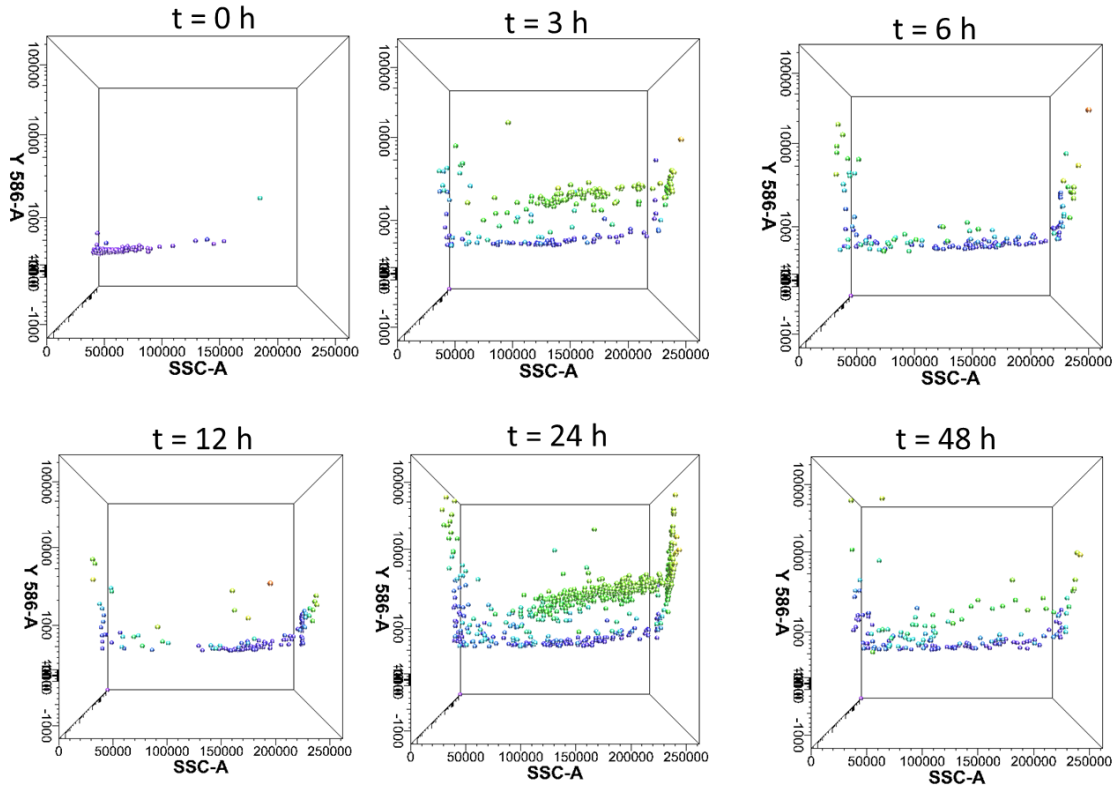

Fig. 4.2.6.2.1: Flow cytometric analysis of CD14 expression (Y586) and granularity (SSC) as an indication of TCam-2 phagocytosis using co-cultured M1/TCam-2. M1/TCam-2 were co-cultured and analysed at different time points (t= 0, 3, 6, 12, 24, 48 h). The M1 population at the beginning of the co-culture (t= 0 h) was relatively consistent in granularity and exhibited no difference regarding CD14 expression. At 3 and 24 h, prominent, different M1 populations could be identified on the basis of CD14 levels and granularity. Different subpopulations are highlighted in distinct colours for ease of visualization. (N.B. Y-axis numbering overlap at '0' value is the result of overlapping of three-dimensional graphs.)

Closer inspection of the 24 h data is shown in Fig. 4.2.6.2.1, the time point at which most distinctive shift was detected in the M1/TCam-2 co-culture. Three macrophage subpopulations with different granularity and CD14 expression were identified, denoted Population 1 (9.9%), Population 2 (58.7%) and Population 3 (15.9%). The remaining 15.54% of cells were scattered and therefore did not identify as a separate group (Fig. 4.2.6.2.2). On the basis of data provided by Mutzke (2015), Populations 2 and 3 are predicted to be engaged in phagocytosis.

This exciting result provided further evidence that THP-1 derived M1 macrophages in co-cultures with TCam-2 cells are actively phagocytic.

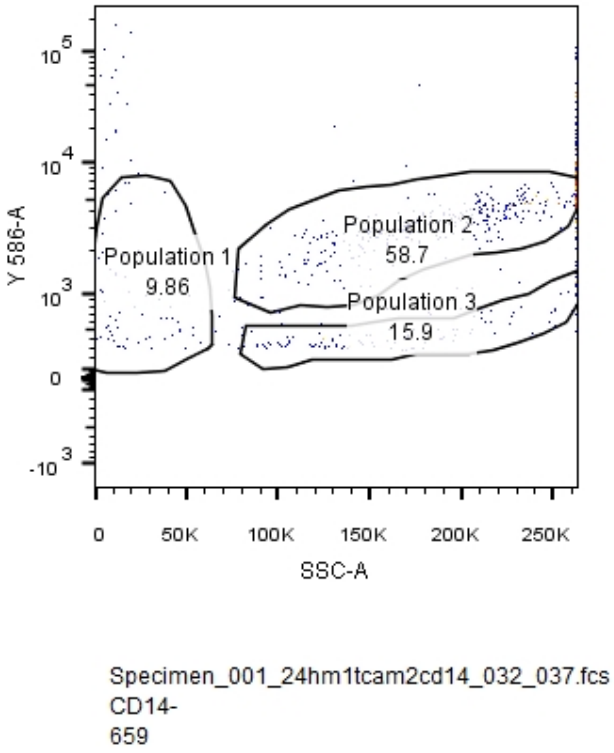

Fig. 4.2.6.2.2: Flow cytometric analysis of CD14 expression (Y586) and granularity (SSC) as an indication of TCam-2 phagocytosis using co-cultured M1/TCam-2. M1/TCam-2 were co-cultured with TCam-2 cells and analysed at 24 h. Three different populations were identified: Population 1 (9.86%) showed the same granularity (SSC), Population 2 (58.7%) showed a shift of the granularity relative to Population 1, and Population 3 (15.9%) showed a granularity shift compared with Population 1 and a different in CD14 expression compared with Population 2. This data is an extraction of the data reported in Fig. 4.2.6.2.1.

4.2.6.3 IF to visualise co-cultures reveals evidence of phagocytosis

An indirect immunofluorescence analysis was conducted to visualize interactions between co-cultured phagocytic macrophages and TCam-2 cells. CD45 was used as a marker for the identification of macrophages of all subsets, and Oct3/4 was the TCam-2 marker. Co-cultured CD45+ M0 macrophages and Oct3/4+TCam-2 cells were in close contact (Fig. 4.2.6.3, A). An observation of the nucleus of TCam-2 cells and macrophages revealed a different nucleus size (DAPI staining). The nucleus of macrophages was smaller than TCam-2 cells. This allowed besides the specific antibody staining an additional identification feature of TCam-2 and macrophages. A detection of CD45+/Oct3/4+ M0 was also possible whereas Oct3/4 was located in the cytoplasm of M0 macrophages (Fig. 4.2.6.3, B). A detection of Oct3/4+TCam-2 cells with a nucleus fragmentation and M0 macrophages (THP-1 derived) with an untypical CD45 expression was possible (Fig. 4.2.6.3, A).

The same experiment was conducted using M1/TCam-2 co-cultured cells. CD45+M1 macrophages showed a fibroblast like structure and were in close contact to Oct3/4+TCam-2 cells (Fig. 4.2.6.2.3, B). In this co-culture model an observation of CD45+/Oct3/4+M1 macrophages were possible as well macrophages with a fragmented nucleus or no nucleus (Fig. 4.2.6.2.3, B).

In summary, phagocytic M0 and M1 macrophages were in close contact to TCam-2 cells whereas some of the macrophages showed a detection of Oct3/4 (TCam-2 marker) that indicates a phagocytic activity and confirmed previous results (4.2.6.1 and 4.2.6.2).

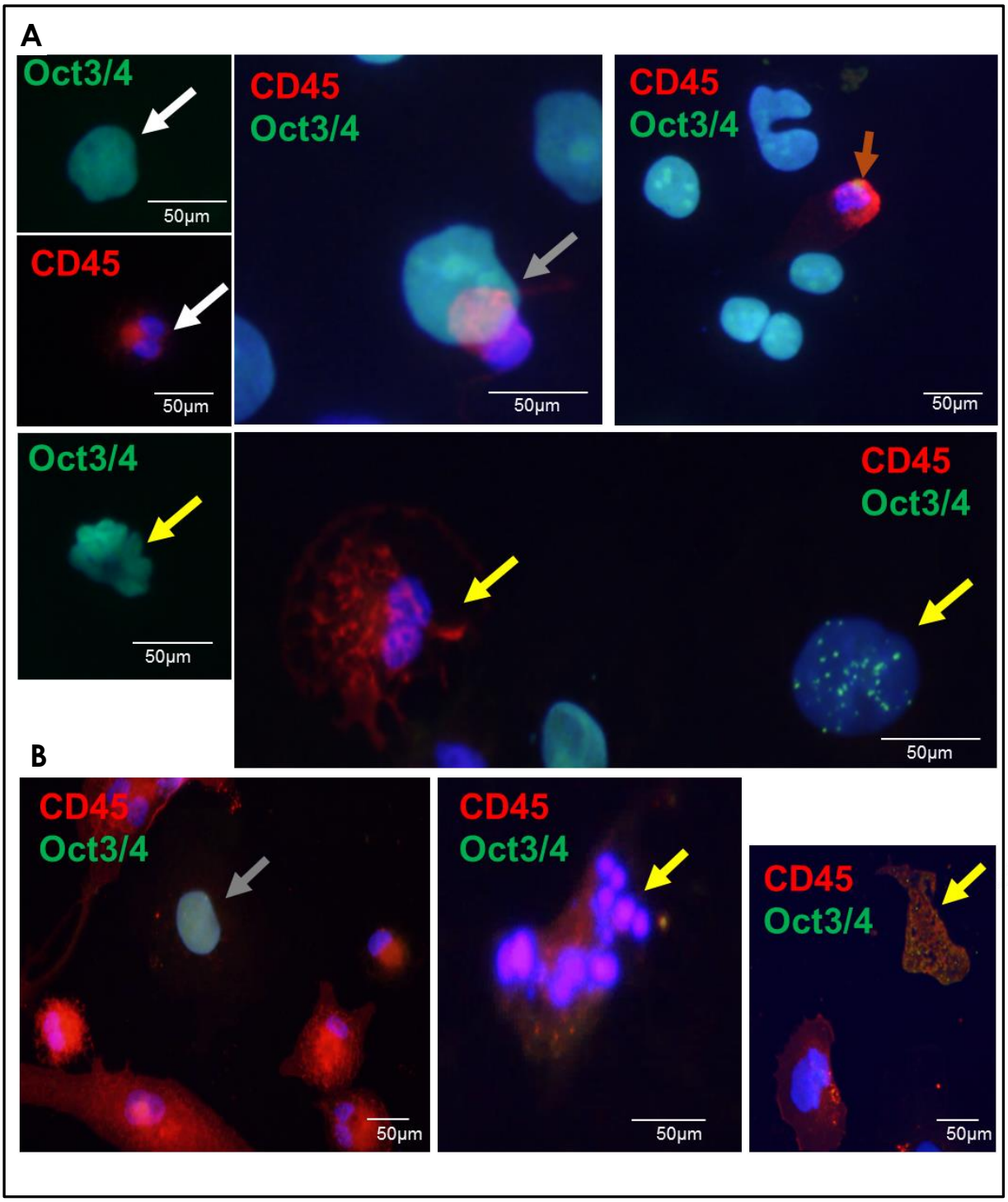

Fig. 4.2.6.2.3: Identification of co-cultured Oct3/4+TCam-2 and CD45+M0 (A) or M1 (B) macrophages after 24 h by IF double-staining (n=3). Oct3/4+TCam cells and CD45+M0 macrophages were identified by IF (A, white arrows). M0 and M1 macrophages were in close contact to TCam-2 cells (A/B, grey arrows). A double-detection of Oct3/4+/CD45+ macrophages was possible and a co-localization of CD45 (red) and Oct3/4 (green) is shown in orange (merged). TCam-2 cells and M0 or M1 macrophages which showed a nucleus fragmentation or which showed an atypical nuclear shape (lack of a nucleus) detection of CD45 or Oct3/4 are highlighted by yellow arrows (A/B).

4.3 DISCUSSION

The widespread occurrence and nature of immune cell infiltrates in GCNIS and seminoma tumours indicates that the tumour microenvironment is permissive for immune cell maintenance. It also suggests that the immune cells may be contributing to tumour survival, perhaps through establishment of a local milieu that supports their proliferation or survival. In this study, a cell co-culture model was established in order to simulate the tumour/macrophage cell interactions observed in testicular germ cell cancers, with the goal of understanding the possible mechanisms behind development and expansion of neoplastic germ cells in adult men. This system employed TCam-2 cells, a human testicular seminoma cell-derived line which exhibits many features of the primitive germ cells from which these tumours are considered to arise (de Jong et al., 2008; Young et al., 2011). The human monocyte cell line, THP-1, was used to generate three different macrophage subtypes following established differentiation protocols to produce cells which were successful differentiated into M0, M1 and M2 macrophages (Genin et al., 2015), as characterised in Chapter 3. The results of this study demonstrate how this approach can contribute to knowledge of the tumour microenvironment, including how these macrophage responses are influenced by the presence of tumour cells.

Co-cultures of TCam-2 cells and differentiated THP-1cells were used to investigate the influence of tumour cells on the functional polarization of macrophages, including through an exploration of the specific cytokine milieu that had been identified in previous literature (Klein et al., 2016) and extended in Chapter 2 of this thesis. In general, cytokines and chemokines can control macrophages phenotypes and can differentiate them into pro-inflammatory (M1) or anti-inflammatory (M2) phenotypes. M1 macrophages can be activated by pro-inflammatory Interferon-γ, TNF-α and LPS, whereas M2 differentiation can be driven by IL-4, IL-13, macrophage colony-stimulating factor (M-CSF), TGF-β, lL-10, IL-6, and PGE2 (Sica and Mantovani, 2012; Genin et al., 2015; Heusinkveld et al. a)/b), 2011; Gottfried et al., 2008). Interestingly, all three co-cultured macrophage subsets showed individual cytokine profiles.

M0 macrophages co-cultured with TCam-2 cells showed an increased anti-inflammatory response based on the production of IL-10, TGF-β1, lnhba, as well as an increased expression of pro-inflammatory cytokines IL-1b, TNF-α and IL-6; ex-

pression of pro-inflammatory IL-12 cytokine was decreased compared to the level detected in M0 monoculture. Enhanced synthesis of anti-inflammatory cytokines such as IL-10 and TGF-β is associated with tumour cell progression and surveillance in several cancer types (Sica et al., 2006; Derynck et al., 2001). Furthermore, in the human testis, factors such as IL-10, TGF-β, prostaglandin and glucocorticoids play a role in M2 polarization and may drive macrophage precursor, M0 macrophages in this co-culture model that might be similar to CD68+macrophages in human testisinto immune-suppressive M2 macrophages (Martinez et al., 2009; Wang et al., 2017, discussed in Chapter 2). Another potential M2 macrophage polarization factor, IL-6, was detected using this co-culture model (Roca et al., 2009). Thus, there are likely to be several components present in the local testicular environment that favour the M2 immuno-suppressive macrophage phenotype which are more highly expressed due to the interactions which occur between seminoma and immune cells.

In addition to the various M2 polarization mediators identified, typical M1 polarization factors were also detected, such as TNF-a (Genin et al., 2015). Additionally, the co-culture of M1 cells with TCam-2 cells led to a decrease in the typical M1-related pro-inflammatory cytokines, IL-12 and TNF-α, with an accompanying increase in transcripts encoding anti-inflammatory IL-6 and TGF-β1 (Zhang et al., 2016). Interestingly, the production of both cytokines by TCam-2 cells (see Chapter 3, Section 3.2.7) further supports the understanding that TCam-2 cells influence the functional polarization of macrophages and drives them into an immunosuppressive phenotype. In the M2/TCam-2 co-culture, levels of the transcripts encoding anti-inflammatory IL-10 and TGF-β1 as well as IL-6 are decreased; the outcome of reduced IL-6 mRNA is different than observed for the other macrophage subsets, and distinguishes this tumour/immune cell interaction.

As previously mentioned, in human testicular germ cell neoplasia specimens exhibiting GCNIS and seminoma, different macrophage subsets were observed in close contact to tumour cells. Using this *in vitro* co-culture model, a direct interaction between TCam-2 cells and cells from each of the differentiated THP-1 derived macrophage subsets was documented. We hypothesized that tumour cells can recruit macrophages through their secretion of different chemokines and subsequently control functional polarization of macrophages by cytokine and chemokine expression. For, instance, it has been shown that tumour cells can express CCL2 and CCL5 chemokine to recruit macrophages to the tumour environment (Weagel et al., 2015). Inter-

estingly, we have detected CCL2 and CCL5 *in vivo* using testicular neoplasia samples and *in vitro* using this co-culture model (Chapter 2, Section 2.2.3.2 and Chapter 4, Section 4.2.3). CCL2 transcript and protein were readily detectable, whereas CCL5 was expressed at a barely detectable level by monocultured TCam-2 cells. This suggests that, besides the seminoma cells themselves, another cell type is responsible for macrophage recruitment *in vivo*. Further analysis revealed that immunosuppressive M2 macrophages can express CCL5; this suggests that, in the tumour environment M2 macrophages, which are also known as tumour associated macrophages (TAM) play an additional role in immune cell recruitment. TAMs have been shown to be similar to M2 macrophages, which can produce high amounts of anti-inflammatory cytokines, such as IL-10 and TGF-β (Sica et al., 2006; Sica et al., 2008). TAM infiltrations indicate a poor prognosis in Hodgkin disease, glioma, cholangiocarcinoma and breast cancer (Steidel et al., 2010; Chen et al., 2011), as these conditions would more likely be permissive for uncontrolled tumour growth.

In multiple tumour types, CCL5 (also known as RANTES) can recruit TAMs, Treg cells and supress the activity of both Th1 cells and cytotoxic T lymphocytes (Cook and Hagemann, 2013; Chang et al., 2012; Schlecker et al., 2012). This suggests that TAMs can recruit macrophages in neoplastic conditions to maintain the immune suppressive milieu and supress the function of other immune cell types to avoid strong immune reactions. Thus, an investigation regarding chemokine receptor expression by macrophage subsets was made to identify which macrophages would likely be targets of specific chemokines found in testicular neoplasia. It is known that CCR1, CCR3 and CCR5 can bind CCL5, whereas CCR2 can bind CCL2. We identified that monocultured M0 and M1 macrophages are both potential targets of CCL2 and CCL5, whereas M2 macrophages are potential targets of CCL5 (Chapter 3; Section 3.2.6).

It was intriguing to note that the transcript level of the specific chemokine receptors CCR1, CCR3 and CCR5 expressed by M0, M1 and M2 macrophages were decreased in the co-culture with TCam-2 cells. The CCR2 transcript which was detected in monocultured M0 and M1 macrophages was not detected in the M0/TCam-2 and M1/TCam-2 co-cultures. This suggested that M0 and M1 macrophages downregulate the expression of CCR2 after binding CCL2 to this receptor. However, co-cultured M0 and M1 macrophages may express an additional CCL2 receptors; the atypical chemokine receptor 2 (ACKR2) is a receptor with CCL2 binding capability

that indicates a role in regulation of inflammation and immune responses (Bonavati et al., 2017). ACKR2 expression is associated with different disease e.g. chronic obstructive pulmonary disease, oral squamous cell carcinomas, colon cancer and breast cancer (Bonavati et al., 2017), but the potential presence and role of ACKR2 expressed by macrophage subsets in this co-culture model, as well as in testicular cancer, remains to be determined.

Additional, it has been shown that co-cultured M0 and M1 altered their phenotype, evidenced by the expression of M2 specific marker (Section 4.2.4). As previously shown M2 macrophages didn't express CCR2 that suggest that after 43 h co-culture an expression of CCR2 was not possible since TCam-2 influenced M0 and M1 macrophage differentiation into an M2 phenotype.

Interestingly, recent studies have shown that an upregulation of CCL2 has also been demonstrated in primary prostate and invasive breast cancer and a positive association with the recruitment of M2 cells has been documented (Fang et al., 2016; Mizutani et al., 2009; Ueno et al., 2000). *In vivo* gene silencing has resulted in tumour growth inhibition and reduced M2 recruitment in a mouse model (Fang et al., 2016).

Roca et al showed that CCL2 influence macrophage polarization into an M2 phenotype (Roca et al., 2009). This suggested that CCL2 is a macrophage recruitment factor as well as a polarization factor. These findings collectively indicate that CCL2 is one of the most important macrophage attractants in many tumour types, including, as shown to be likely here, in testicular neoplasia.

Using this co-culture model, the potential polarization effect of TCam-2 cells on macrophages was also analysed by flow cytometry to measure levels of cell subtype-specific markers. As expected, monocultured M1 macrophages expressed M1-specific markers CD11c and CD68, whereas M2 macrophages had higher levels of M2-specific markers, CD163 and CD206 compared to M1 macrophages. Intriguingly, cultivated M0 macrophages expressed relatively high levels of both M1 and M2 subtype markers, most likely reflecting their identity as a lineage precursor which can differentiate into either M1 or M2 macrophages. Co-culture of each macrophage subset with TCam-2 cells demonstrated specific alterations of CD marker levels, showing that TCam-2 cells can influence macrophage polarization. M0 macrophages exhibited higher transcript and protein levels of immune-suppressive M2-subtype markers when co-cultured, compared to cells cultured on their own. The M0 cell type also dis-

played an M1-specific marker and M1-related pro-inflammatory cytokines, including TNF-α, a known M1 polarization factor. Because both phenotypes were detected in co-cultured M0 cells, we hypothesize that TCam-2 cells can partly influence macrophage polarization into an immunosuppressive phenotype, but other local factors that determine the outcome of this process *in vivo*. Co-cultivated M1 macrophages also showed higher levels of M2 specific marker proteins, CD163 and CD206, when co-cultured with TCam-2 cells, compared to when grown in monoculture.

These findings from flow cytometry analysis indicated that TCam-2 cells influence macrophage polarization through their synthesis of cytokines and chemokines. Using this co-culture model, potential macrophage polarization factors have been identified as IL-10, TGF-β, activin A, IL-6 and CCL2. A preliminary experiment assessed the whether blocking TGF-β1 and activin A actions could alter the the polarization effect of co-culture with TCam-2 cells. Signaling by TGF-β1 and activin A normally occurs via specific cell surface receptor complexes which can be selectively and potently blocked by SB431542 (Inman et al., 2002). Co-culture of M0 or M1 macrophages with TCam-2 cells in the presence of SB431542 prevented the increase in M2 marker expression (CD163, CD206) documented in earlier co-cultures lacking this TGF-β1 and activin A signaling inhibitor. This provides a preliminary indication that either TGF-β1 and/ or activin A are central to the process of macrophage polarization. There is considerable evidence supporting roles for several TGF-β superfamily ligands in the emergence and progression of testicular germ cell neoplasia (reviewed in Loveland and Hedger, 2015). Evidence from murine studies demonstrates that Nodal, BMPs, TGF-β1 and activin A serve many essential roles in normal fetal testis development (Young et al., 2015) during the stages when testicular germ cell tumours are considered to arise from spermatogenic precursor cells, gonocytes that do not develop normally. It will be important to explore if dysregulation of this signalling pathway maintains conditions permissive for inappropriate gonocyte maintenance into adult life by suppressing immune cell responses that would normally remove these cells in infancy.

A crucial function of macrophages is their role as patrolling cells that can recognise and phagocytise pathogens, including tumour cells. M1 macrophages have been previously described as highly phagocytic (Sica and Mantovani, 2012). The potential relevance of this macrophage function to germ cell tumour development was exam-

ined using establishing several approaches. A newly established phagocytosis assay (Mutzke et al., 2015) was conducted to characterise the phagocytosis capability of different THP-1 derived macrophage subsets. Using flow cytometry to measure macrophage granularity changes as alterations in side scatter, the co-culture of both M0 and M1 macrophages with TCam-2 cells provided evidence of dynamic macrophage phagocytic activity. This method was developed using macrophage engulfment of latex beads, resulting an alteration of their granularity (Mutzke et al., 2015). Recent studies have shown that human monocytes can phagocytise 1-3 µm latex beads after only 6-8 min (Gu et al., 2014). We speculate that the phagocytosis of TCam-2 cells that are approximately 40 µm in diameter takes up to 3 h, since Cannon and Swannon showed that latex beads larger than 15 µm in diameter were completely phagocytised by murine bone marrow derived monocytes during an interval of 30 min (Cannon and Swannon, 1992). Interestingly, THP-1 derived macrophages in co-culture with TCam-2 cells displayed a strong granularity shift at 3 h of co-culture, the earliest time point monitored in these experiments. The trend to decreased TCam-2 cell numbers at 3 h co-culture offers further evidence of their phagocytosis by macrophages, but shift number was not significant until the 24 and 48 time points, the next ones measured in these experiments. At 48 h of co-cultivation with TCam-2 cells, the high levels of M2-specific markers on M0 and M1 macrophages indicated they are functionally polarized into an M2 phenotype. This could explain why TCam-2 cell numbers are increased after 48 h compared to at 24 h, since in other cancer types e.g. breast cancer, the immunosuppressive M2 macrophages are more permissive for tumour maintenance and thus play a significant role in tumour progression (Eiro, 2012). This result, which indicates how tumour cells avoid immune reactions by controlling macrophage polarization, would be highly relevant in the *in vivo* circumstances within a testicular germ cell neoplasia, which potentially develops over a period of months or years. The visualization of apparent phagocytosis was enabled through immunofluorescent double-staining, since Oct3/4 was detectable in the cytoplasm of macrophages. Thus, the phagocytic property of M1 macrophages was confirmed using this co-culture model using several different approaches.

CONCLUSION

A tumour/ immune cell co-culture model was established that helped to elucidate a tumour cell-driven mechanism to influence macrophage polarization and avoid immune reactions within testicular germ cell neoplasia. Tumour cells (TCam-2) can express cytokines to maintain a special anti-inflammatory cytokine milieu. Furthermore, they can express chemokines with the capacity to recruit macrophages which can differentiate into immunosuppressive M2 macrophages due to the specific stimulus caused by local production of cytokines and chemokines. Collectively, the evidence provided in this chapter supports the proposal that TCam-2 cells can influence and control macrophage polarization, since all macrophage subtypes expressed M2 specific markers after co-culture with this seminoma cell line. Future work should address the role of specific immune modulators, such as TGF-β and activin A, and the impact and regulation of macrophage phagocytic activity on tumour cell survival and proliferation.

5 FINAL CONCLUSION

This study has shown for the first time that infiltrating DCs and macrophages are highly associated with testicular germ cell cancer, being present in GCNIS and seminoma. The identification that DC and macrophage subtypes with contrasting properties, such as tumoricidal and tumour progressive phenotypes, demonstrates that completely different immune cell activities are active in these tumours. Importantly, this study has provided evidence that seminoma cells have the capacity to control immune cell functional polarization. These findings could help to establish new therapeutics for testicular cancer that target the polarization of immune cells, especially macrophages, by preventing their differentiaton into immunosuppressive phenotypes.
Experiments in this thesis have revealed that macrophages may migrate into the testicular tumour environment by chemotaxis under the influence of the chemoattractant chemokines, CCL2 and CCL5 (Fig. 5.1). Whether seminoma cells or macrophages mediate this recruitment remains to be further explored, and the full range of their impact on immune reactions is yet to be determined. It is expected that M1 macrophages will act to reinforce immune reactions against seminoma cells by their production of pro-inflammatory cytokines that are inevitably associated with neoplasia. In contrast, these findings indicate that both seminoma cells and M2 macrophages can influence macrophage polarization into an immunosuppressive phenotype by secretion of IL-10, TGF-β and IL-6. Outcomes from these experiments showed that, as predicted, suppression of TGF-β signaling pathway activity can inhibit macrophage polarization into immunosupressive M2 macrophages. Collectively, these findings indicate that potential macrophage differentiation inhibitors should be considered, rather than chemotaxis inhibitors, as therapeutics for testicular cancer, since infiltrating immune cells are important for synergistic immune reactions against cancer cells. Learning more about how their functional polarization can be controlled will make this possible.

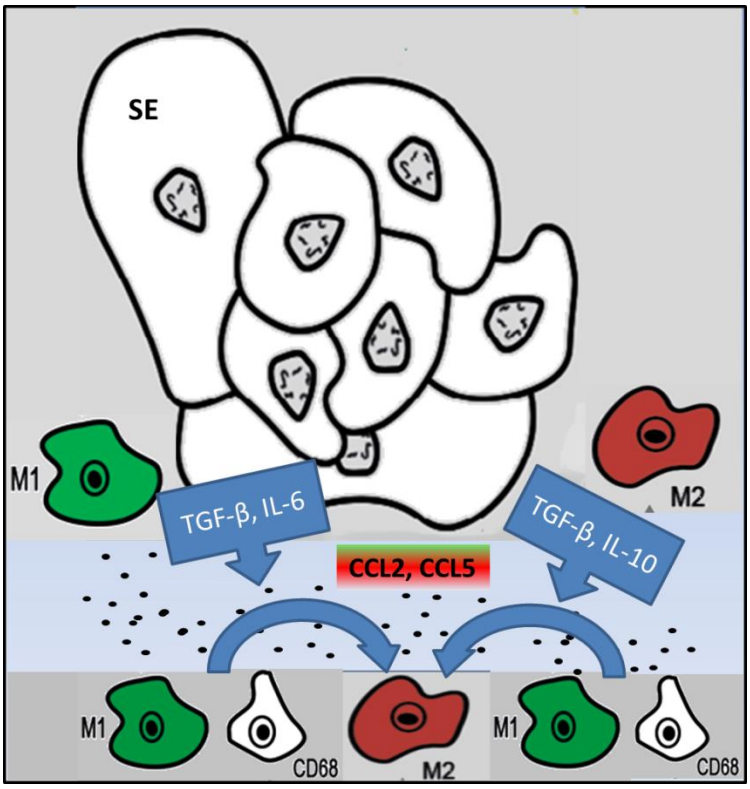

Fig. 5.1: Schematic of key outcomes of macrophage recruitment and polarization associated with testicular cancer. Testicular cancer is associated with CD68+macrophages (probably precursor of M1 and M2), M1 and M2 macrophages. Our findings revealed chemokines (CCL2 and CCL5) which are responsible for macrophage recruitment. Immune modulator such as TGF-β, IL-6 expressed by seminoma cells (SE) as well as IL-10, TGF-β expressed by M2 macrophages can drive previous recruited macrophages into an immunosuppressive M2 phenotype.

6 ABSTRACT

In this study, tissue specimens of normal, non-inflamed human testis with intact spermatogenesis and testicular germ cell neoplasia (GCNIS, seminoma) containing immune cell infiltrations were analysed by immunohistochemistry, immunfluorescence and qRT-PCR to reveal phenotypic and functional differences among the immune cells that are contributing to the respective environment, reflected by cytokine expression profiles. The focus is set on macrophages and dendritic cells.

Using specific macrophage and dendritic cell (DC) markers, different subsets of these immune cell types were identfied in testicular germ cell neoplasia suggesting a functional polarization. Under physiological conditions in the testis, anti-inflammatory M2 macrophages as supported by the presence of TGF-β and IL-10 have been detectable, whereas DCs that express CD11c were rare. In contrast, GCNIS (known as precursor of seminoma) and seminoma was associated with infiltration of different DC subsets, i.e. mDC and pDC. A detailed analysis of macrophages revealed that, pro-inflammatory M1 and anti-inflammatory M2 macrophages are involved in immune cell infiltrates associated with testicular germ cell neoplasia. In line with the detection of M1 macrophages, increased levels of trancripts encoding IL-12 and TNF-α were found in neoplasia. To delinate why both, anti- and pro-inflammatory macrophages could be associated with testicular cancer, chemokines as well as potential macrophage polarization factors were analysed. A detailed chemokine expression profile revealed CCL2, CCL5, CCL18 and CCL22 as well as TGF-β1, TNF-α and IL-6 as potential macrophage polarization factor to be associated with GCNIS and seminoma.

To understand how these factors influence macrophages regarding their migration and differentiation/ polarization, an *in vitro* cell culture model using human monocyte derived THP-1 cells was estabilished. The results obtained indicate that CCL2 and CCL5 recruit macrophages and also influence macrophage polarization. To test whether tumour cells could drive macrophage differentiation, a co-culture model was estabilished using a human seminoma cell line (TCam-2) and THP-1 cells that were differentiated into M0, M1 and M2 macrophages. The co-culture of M0 and M1 macrophages with TCam-2 revealed a functional polarization of the THP-1-derived cells into an immunosuppressive M2 phenotype that may be driven by TGF-β1, IL-6 and CCL2. TGF-β1 signalling pathway inhibitor blocked the polarization towards an im-

munosuppressive M2 phenotype. Furthermore, a functional assessment of THP-1-derived M0 and M1 macrophages was conducted to reveal potential tumoricidial activities. In a phagocytosis assay, M1 macrophages showed high phagocytic activity enabling these cells to reduce TCam-2 cell numbers in the co-culture model. However, TCam-2 cells are likely to escape the tumoricidal activity by driving these macrophages into an immunosuppressive phenotype.

In conclusion, M2 macrophages are the dominating immune cell population that support tumour grow. Therefore, as clinical outcome an inhibition of typical M2 polarization factors should be considered rather than an inhibition of recruitment factors (chemokines) since this would also influence the recruitment of phagocytic, tumour suppressive M1 macrophages. Future work should address the role of specific immune modulators, such as TGF-β and activin A, and the impact and regulation of macrophage phagocytic activity on tumour cell survival and proliferation. Thus, potential macrophage differentiation inhibitors should be considered, as therapeutics to reinforce strong immune reactions against tumour cells.

7 ZUSAMMENFASSUNG

In dieser Studie wurden humane Hodenbiopsien mit normaler Spermatogenese oder Hodenneoplasien (GCNIS, Seminom) mit lymphatischen Infiltraten mittels Immunhistochemie oder Immunfluoreszenz und qRT-PCR analysiert. Funktional unterschiedliche Immunzellen (Makrophagen und dendritische Zellen) wurden durch jeweilige Zytokinexpressionsprofile in den unterschiedlichen Milieus identifiziert.

Unter Verwendung von spezifischen Makrophagen- und dendritischen Zellmarkern wurden verschiedene Immunzellsubtypen mit völlig anderen Funktionen in Neoplasie-Proben identifiziert. In den Hoden unter physiologischen Bedingungen waren entzündungshemmende M2-Makrophagen nachweisbar, die durch das Vorhandensein von spezifischen Marker wie CD163 und CD206 sowie anti-inflammatorischen Zytokinen, TGF-β und IL-10 nachgewiesen wurden. DCs, die CD11c exprimieren, waren kaum detektierbar. Im Gegensatz dazu waren in GCNIS Proben (als Vorstufe von Seminomen bekannt) verschiedene DC Subtypen detektierbar, mDC und pDC. In Seminomen wurden diese Immunzellen mit einer höheren Frequenz nachgewiesen. Eine detaillierte, funktionelle Analyse der DC-Subtypen war jedoch aufgrund ihrer anspruchsvollen Vielfalt in dieser Arbeit nicht möglich und muss weiter analysiert werden. Eine detaillierte Makrophagen-Analyse im Zusammenhang mit Neoplasien ergab, dass proinflammatorische M1 Makrophagen, IL-12 und TNF-α exprimieren und das aber auch antiinflammatorische M2 Makrophagen präsent waren. Eine halbquantitative Bewertung der einzelnen Makrophagen spezifischen Marker ergab, dass eine Balance von beiden, M1 und M2 Makrophagen in Neoplasien vorherrscht. Um zu verstehen, warum entzündungshemmende sowohl als auch proinflammatorische Makrophagen mit Hodenkrebs in Verbindung gebracht werden, analysierten wir Chemokine, die für ihre Funktionen zur Rekrutierung von Immunzellen sowie als potentielle Makrophagen Polarisationsfaktoren bekannt sind. Ein detailliertes Chemokinprofil zeigte, dass die Chemokine CCL2, CCL5, CCL18 und CCL22 nachweisbar waren sowie andere potentielle Makrophagen-Polarisationsfaktoren, TGF-β1, TNF-α und IL-6 mit testikulären Neoplasien (GCNIS und Seminom) assoziiert sind. Um zu verstehen, wie diese Faktoren Makrophagen in Bezug auf ihre Migration und Differenzierung beeinflussen, entwickelten wir ein *In vitro*-Zellkulturmodell mit humanen Monozyten (THP-1-Zellen). Unsere Ergebnisse zeigen, dass CCL2 und CCL5 Makrophagen rekrutieren und auch die Makrophagen polarisation beeinflussen. Um zu

verstehen, warum Tumorzellen eine immunsupressive Makrophagen-Differenzierung begünstigen, wurde ein Co-Kulturmodell unter Verwendung von humanen Seminoma Zellen (TCAM-2) und humanen Monozyten (THP-1-Zellen), die zuvor in M0, M1 und M2 Makrophagen differenziert wurden, entwickelt. Die Co-Kultivierung von M0- und M1-Makrophagen mit TCam-2 offenbarte eine funktionelle Polarisierung dieser Makrophagen zu einem immunsuppressiven M2-Phänotyp, der durch TGF-β1, IL-6 und CCL2 gesteuert werden kann. Jedoch blockierte der TGF-β1-Signalweg-Inhibitor die Polarisation in Richtung eines immunsuppressiven M2 Phänotyp. Zusätzlich wurde eine funktionelle Bewertung von M0 und M1 Makrophagen durchgeführt, um potentielle tumorizide Aktivitäten aufzudecken. Dazu wurde ein Phagozytose-Assay etabliert und zeigte M1-Makrophagen als hoch phagozytische Zellen, die die Anzahl der TCam-2-Zellen in unserem Co-Kultur-Modell reduzieren könnte. Ungünstigerweise treiben TCam-2 diese Makrophagen in einen immunsuppressiven Phänotyp, der das Wachstum von Tumorzellen durch Phagozytose nicht kontrollieren kann.

Zusammenfassend kann gesagt werden, dass M2-Makrophagen die dominierende Immunzellenpopulation, die das Tumorwachstum begünstigen sind. Als klinisches Outcome sollte daher eher eine Inhibition typischer M2-Polarisationsfaktoren als eine Hemmung von Rekrutierungsfaktoren (Chemokinen) in Betracht gezogen werden, da andernfalls auch die Rekrutierung von phagozytischen, tumorsuppressiven M1-Makrophagen beeinflusst werden würde. Zukünftige Arbeiten sollten die Rolle von spezifischen Immunmodulatoren wie TGF-β und activin A sowie den Einfluss und die Regulierung der Phagozytoseaktivität von Makrophagen untersuchen um somit die Proliferation von Tumorzellen zu inhibieren. Daher sollten potentielle Makrophagen-Differenzierungshemmer als Therapeutika zur Verstärkung von Tumor suppressiven Immunreaktionen in Betracht gezogen werden.

8 APPENDICES

Chemicals and reagents

2-Propanolol, ≥99.5%	Carl Roth GmbH & Co. KG, Karlsruhe, Germany
Acetic acid, 99 – 100%	Merck, Darmstadt, Germany
Agarose, peqGOLD Universal agarose	Peqlab Biotechnology GmbH, Erlangen, Germany
3-aminopropyltriethoxysilane (APES)	Merck, Darmstadt, Germany
BSA, Albumin fraction V, ≥98%	Merck, Darmstadt, Germany
Chloroform	Merck, Darmstadt, Germany
3'-Diaminobenzidine (DAB)	Thermo Scientific, Waltham, USA
Diethylpyrocarbonate (DEPC)	Sigma-Aldrich, St. Louis, MO, USA
Disodium phosphate	Carl Roth GmbH & Co. KG, Karlsruhe, Germany
DNA ladder (100bp), peqGOLD	Peqlab Biotechnology GmbH, Erlangen, Germany
EDTA disodium dehydrate	SERVA Electrophoresis GmbH, Heidelberg, Germany
EDTA tetrasodium (EDTA 4Na)	Sigma-Aldrich, St. Louis, MO, USA
Eosin G-solution, 0.5%	Carl Roth GmbH & Co. KG, Karlsruhe, Germany
Ethanol ROTIPURAN®, ≥99.8%	Carl Roth GmbH & Co. KG, Karlsruhe, Germany
Fetal calf serum	Quantum Scientific, Australia
Formalin, 36.5 – 38%	Sigma-Aldrich, St. Louis, MO, USA
GelGreen Nucleid Acid Stain	Biotium, Hayward, CA, USA
GVA	Genemed Biotechnologies, South San Francisco, U.S.A.)
Hydrochloric acid ROTIPURAN®, ≥25%	Carl Roth GmbH & Co. KG, Karlsruhe, Germany
Hydrogen peroxide, 30%	Carl Roth GmbH & Co. KG, Karlsruhe, Germany

Kaiser´s glycerine gelatine	Merck, Darmstadt, Germany
Luminata, Immobilon Forte Western HRP substrate	Merck, Darmstadt, Germany
Magnesium chloride	Carl Roth GmbH & Co. KG, Karlsruhe, Germany
Mayer´s hematoxylin	Carl Roth GmbH & Co. KG, Karlsruhe, Germany
Methanol ≥99 %	Carl Roth GmbH & Co. KG, Karlsruhe, Germany
NuPAGE antioxidant	Invitrogen, Carlsbad, CA
NuPAGE® MOPS Running Buffer	Invitrogen, Carlsbad, CA
NuPAGE® Reducing agent	Invitrogen, Carlsbad, CA
NuPAGE® sample buffer	Invitrogen, Carlsbad, CA
NuPAGE® transfer buffer	Invitrogen, Carlsbad, CA
Page Ruler™Plus	Thermo Scientific, Waltham, USA
1x PBS (Dulbecco´s PBS)	Gibco, Auckland, New Zealand
Picric acid, 98%	Sigma-Aldrich, St. Louis, MO, USA
Potassium chloride	Merck Millipore, Bayswater, VIC, Australia
Potassium dihydrogen phosphate	Merck Millipore, Bayswater, VIC, Australia
RNA-free water	Carl Roth GmbH & Co. KG, Karlsruhe, Germany
Sodium bicarbonate	Sigma-Aldrich, St. Louis, MO, USA
Sodium carbonate	Carl Roth GmbH & Co. KG, Karlsruhe, Germany
Sodium chloride, ≥99.5%	Carl Roth GmbH & Co. KG, Karlsruhe, Germany
Sodium hydroxide pellets	Merck, Darmstadt, Germany
Tetramethylbenzidine	BD Biosciences, San Diego, CA, USA
TrisBASE	Sigma-Aldrich, St. Louis, MO, USA
Tris-Pufferan®, ≥99.9%	Carl Roth GmbH & Co. KG, Karlsruhe, Germany
Triton X-100	Sigma-Aldrich, St. Louis, MO, USA

TRIzol® Reagent Ambion	LifeTechnologies, Carlsbad, CA, USA
Trypsin, 2.5%	Gibco, Auckland, New Zealand
Tween-20	Sigma-Aldrich, St. Louis, MO, USA
Xylene ROTIPURAN®, ≥99.8%	Carl Roth GmbH & Co. KG, Karlsruhe, Germany

Kits

AllPrep® RNA/ Protein Kit	Qiagen, Hilden, Germany
AmpliTaq GOLD DNA polymerase	Applied Biosystems, Foster City, CA, USA
Pierce BCA (Bicinchoninic Acid) Protein Assay Kit	Thermo Scientific, Waltham, USA
BIOPRIME Peroxidase-Substratkit AEC	BIOLOGO Dr. Hartmut Schultheiß e.K., Kronshagen, Germany
Pierce DAB (3'-Diaminobenzidine) Substrate Kit	Thermo Scientific, Waltham, USA
DNase I, recombinant	Roche Diagnostics, Mannheim, Germany
DNA-*free*TM DNA Removal Kit Ambion	LifeTechnologies, Grand Island, NY, USA
Muliplex Human Cytokine/Chemokine Panel I: Detects IL-6, IL-10, TNFα, IL-1a, IL-12 p40, MCP-1 and RANTES	EMD Millipore, Billerica, MA, USA
Multiplex Millipore Multi-species TGFβ1 magnetic panel, 1- plex: Detects TGFβ1	EMD Millipore, Billerica, MA, USA
SuperScript® III Reverse Transcriptase	LifeTechnologies, Grand Island, NY, USA
Qproteome FFPE Tissue Kit	Qiagen, Hilden, Germany
VECTASTAIN Elite ABC Kit	Vectorlabs, Burlingame, CA, USA

Equipment and consumables

7900HT RealTime Cycler	Applied Biosystems, Foster City, USA
BD Polystyrene Filter top (5ml)	Becton Dickinson Labware, Franklin Lakes, NJ, USA
Centrifuge MICRO 120	Hettich Zentrifugen, Tuttlingen, Germany
Centrifuge MIRCO 22R	Hettich Zentrifugen, Tuttlingen, Germany
CFX96TM RealTime Cycler	Bio-Rad, Munich, Germany
CFX Manager Software 2.0	Bio-Rad, Munich, Germany
CO2 incubator	Memmert GmbH & CO. KG, Schwabach, Germany
Corning™ 96-Well Filter Plate Fluid Guard	Thermo Scientific, Waltham, USA
Electronic balance EXPLORER	OHAUS, Nänikon, Switzerland
ELISA microplates (96-well)	Greiner Bio-one, Monroe, NC, USA
Falcon® Tissue culture flasks (T75)	Becton Dickinson Labware, Franklin Lakes, NJ, USA
Falcon® Tissue culture flasks (T25)	Becton Dickinson Labware, Franklin Lakes, NJ, USA
Falcon® Tissue culture plates (6-well)	Becton Dickinson Labware, Franklin Lakes, NJ, USA
Filter tips	Nerbe plus, Winsen/Luhe, Germany
IKA® T-10 basic Ultra Turrax Homogenizer	IKA® Werke GmbH & CO. KG, Staufen Germany
LSRFortessaTM X-20 flow cytometer	BD Biosciences, San Jose, CA, USA
Luminex x-100	http://www.luminexcorp.com
Microplate ELISA reader	Labsystems Multiscan RC, Vantaa, Finland
Microscope Leica DM750	Leica, Solms, Germany
Microwave oven, CB 1273	Bomann, Kempen, Germany
MILLICELL –CM well inserts	Merck Millipore, Bayswater, VIC, Australia
Neubauer counting chamber	Paul Marienfeld GmbH & Co. KG, Lauda, Germany
Olympus Fluorescence Microscope	Olympus America, Center Valley, PA
PCR tubes	Nerbe plus, Winsen/Luhe, Germany
PerfectBlueTM Horizontal Midi Gel Systems	Peqlab Biotechnology GmbH, Erlangen, Germany
PVDF 0.2µm	Thermo Scientific, Waltham, USA
Stericup® Filter units	Merck Millipore, Bayswater, VIC, Australia
SuperFrost glass slides	R. Langenbrink, Emmendingen, Germany
Sliding microtome, Leica SM2000 R	Leica, Solms, Germany
T3 Thermocycler	Biometra GmbH, Göttingen, Germany
TB1 Thermoblock	Biometra GmbH, Göttingen, Germany
Tissue embedder, Leica EG 1150C	Leica, Solms, Germany
Tissue processor Leica TP 1050	Leica, Solms, Germany
Transilluminator UVsolo	Biometra GmbH, Göttingen, Germany

Transilluminator UVIdoc	Biometra GmbH, Göttingen, Germany
Whatman paper	BioRad, Hercules, California

8.1 APPENDIX CHAPTER 2

Buffer

10x TAE buffer, pH 8.0, stock solution
48.4g TrisBASE (Sigma-Aldrich)
3.72g EDTA disodium dihydrate (SERVA)
1l Bidistilled water
Adjust pH with 4M NaOH.

1x TAE buffer, pH 8.0, working solution
100ml TAE stock solution
900ml Bidistilled water

100 ml 1x TAE buffer
Heat buffer contains agarose at 500 Watt in a microwave ofen (Bomann, Kempen, Germany). After agarose is disolved, add:
15 µl GelGreen Nucleid Acid Stain (Biotium, Hayward, CA, USA)

DNA agarose gel electrophoresis
1.5 g peqGOLD Universal Agarose (Peqlab Biotechnology GmbH, Erlangen, Germany)

DEPC H2O

2 ml DEPC

2l Bidistilled water

Mix, let rest for 24h at 37°C, autoclave.

Bouin´s solution

210 ml Picric acid (Sigma-Aldrich)

70 ml 36.5 – 38% Formalin (Sigma-Aldrich)

10 ml Acetic acid (Merck)

Fix testis biopsy samples in Bouin´s solution for 24 h, wash with 70% ethanol and proceed with embedding.

HE staining

Incubate sections for 2x 5 min in xylene, then rehydrate for 5 min in 100%, 96%, 80%, 70%, 60%, 50% ethanol, rinse with distilled water. Incubate 1 min in Mayer´s hematoxylin, wash under tab water for 10min. Incubate in 0.5% eosin for 5 min, wash under tab water. Allow slides to dry and mount slides with Kaisers Glycerine.

PCR program:

Reverse transcriptase (RT) program for DNase treatment

37°C	75°C	4°C
25min	5min	hold

RT program for cDNA synthesis

21°C	42°C	99°C	5°C	4°C
8 min	15 min	5 min	5 min	hold

RT-qPCR program

95°C	95°C	60°C	4°C
10min	15s	1min	hold
	44 cycles		

8.2 APPENDIX CHAPTER 3

Cell lines
TCam-2 cells (human seminoma derived cell line) originally obtained from Prof Kitizawa, Japan.
THP-1 cells (human monocytic leukemia cell line; provided by Dr. Ashley Mansell, Hudson Institute of Medical Research, Clayton, Australia.

Culture media, complete
RPMI1640 Gibco, Auckland, New Zealand
1% penicillin/streptomycin Gibco, Auckland, New Zealand
10% fetal calf serum Quantum Scientific, Australia

10x Versene (EDTA) solution, sterile filtered
8 g NaCl (Roth)
2 g KCl (Merck Millipore)
0.77 g NaOH (Merck)
11.5 g KH2PO4 (Merck Millipore)
2 g EDTA 4Na (Sigma-Aldrich)
1 l Bidistilled water

0.1% trypsin-versene, sterile filtered
10 ml Trypsin, 2.5% (Gibco)
25 ml 10x Versene (EDTA)
215 ml PBS

Tris-buffered saline (TBS), stock solution
60.5 g Tris-Pufferan, ≥99.8% p.a. (Roth)

900 ml Bi-distilled water

Mix until dissolved. Adjust pH to 7.6 using HCl (Roth). Top up with bidstilled water up to 100 ml total volume.

90 g NaCl (Merck

BSA blocking solution
1 g BSA (Roth)

70 ml TBS

10 X Running Buffer (1 litre)
30.3 g Tris base

144 g Glycin

10 g SDS

pH 8.3

1 X Transfer Buffer (1.5 litre)
4.6 g Tris base

21.6 g Glycine

150 ml ethanol

4 X Sample Buffer (25 ml)
6.0 ml 1M Tris HCL pH 6.8

2.5 ml Glycerol (100%)

2 g SDS

12.5 mg Bromophenol blue

5 ml β-mercaptoethanol (14.5M)

Up to 25 ml milliQ water

MasterMix for RT-qPCR, volume/1 reaction
5 µl TaqMan® Gene Expression Master Mix (LifeTechnologies, Carlsbad, CA, USA)

0.5 µl TaqMan® Gene Expression Assay (LifeTechnologies, Carlsbad, CA, USA)

2.5 µl RNA-free water

2 µl cDNA, diluted 1:20

10 µl total volume/1 reaction

Gel for SDS-PAGE

	10%	**12%**
Resolving		
dH_20	**4 ml**	**5.1 ml**
30% Acrylamide	**3.3 ml**	**6.0 ml**
1.5M Tris (pH 8.8)	**2.5 ml**	**3.75 ml**
10% SDS	**100 µl**	**100 µl**
10% Ammonium Persul-fate	**100 µl**	**100 µl**
TEMED	**12 µl**	**12 µl**
Stacking 5%		
dH_20	**3 ml**	**3 ml**
30% Acrylamide	**670 µl**	**670 µl**
0.5M Tris (pH 6.8)	**1.25 ml**	**1.25 ml**
10% SDS	**50 µl**	**50 µl**
10% Ammonium Persul-fate	**50 µl**	**50 µl**
TEMED	**12 µl**	**12 µl**

DNase treatment, volume/1 reaction

1 vol. 10 µg TRIzol® Reagent extracted RNA
0.1 vol. 10x DNase I buffer
1µl rDNase I
Mix gently, incubate at 37°C for 20 min.
Add 1 µl resuspended Inactivation Reagent
Incubate at room temperature for 2 min., flick in between. Centrifuge at 10621 rcf for 1.5 min. Transfer DNase treated RNA into new tube.

8.3 APPENDIX CHAPTER 4

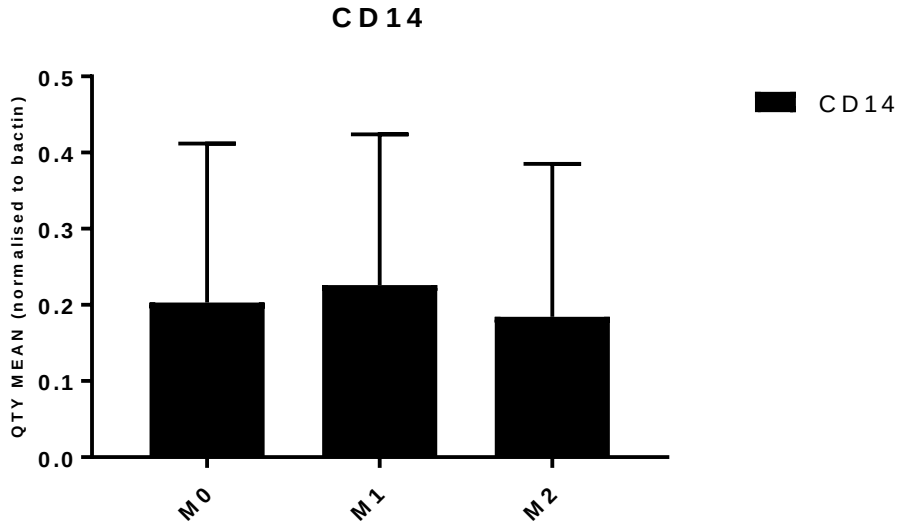

Figure 4: CD14 expression profile of M0, M1 and M2 macrophages (n=3). All three subsets show similar transcripts encoding of CD14.

Reagents

Protein name	Manufacturer	Cat. No.
Phorbol 12-myristate 13-acetate (PMA)	Biolegend	423301
Lipopolysaccharide (LPS)	Sigma	8630
Recombinant Human IFN-γ (carrier-free)	Biolegend	570202
Recombinant Human IL-13 (carrier-free)	Biolegend	571102
Recombinant Human IL-4 (Animal-Free)	Biolegend	714904
Recombinant Human CCL15 (MIP-1δ) (carrier-free)	Biolegend	587402
Recombinant Human CCL5 (RANTES) (Animal-Free)	Biolegend	717004
Recombinant Human CCL2 (MCP-1) (Animal-Free)	Biolegend	716504
IL-10	Biolegend	715602
Transforming growth factor beta 1 (TGF-β1)	Cell Signaling	8915LC
Activin A	Abcam	ab50051
SB431542	Cell Signaling	14775

9 REFERENCES

Allavena, P., Sica, A., Solinas, G., Porta, C., & Mantovani, A. (2008). The inflammatory micro-environment in tumor progression: the role of tumor-associated macrophages. *Critical Reviews in Oncology/Hematology*, *66*(1), 1-9.

Almstrup, K., Nielsen, J. E., Mlynarska, O., Jansen, M. T., Jørgensen, A., Skakkebaek, N. E., & Rajpert-De Meyts, E. (2010). Carcinoma in situ testis displays permissive chromatin modifications similar to immature foetal germ cells. *British Journal of Cancer*, *103*(8), 1269.

Assoian, R.K., Fleurdelys, B.E., Stevenson, H.C., Miller, P.J., Madtes, D.K., Raines, E.W., Ross, R. and Sporn, M.B. (1987). Expression and secretion of type beta transforming growth factor by activated human macrophages. *Proceedings of the National Academy of Sciences*, *84*(17), pp.6020-6024.

Azenshtein, E., Luboshits, G., Shina, S., Neumark, E., Shahbazian, D., Weil, M., Wigler, N., Keydar, I. and Ben-Baruch, A. (2002). The CC chemokine RANTES in breast carcinoma progression: regulation of expression and potential mechanisms of promalignant activity. *Cancer Research*, *62*(4), pp.1093-1102.

Bell DA, Flotte TJ, Bhan AK. Immunohistochemical characterization of seminoma and its inflammatory cell infiltrate. *Hum Pathol* 1987 :**18**; 511 – 520.

Bergmann M, Kliesch S. Testicular biopsy and histology. In Nieschlag E, Behre HM, Nieschlag S (eds) *Andrology*. Male Reproductive Health and Dysfunction. 2010. Springer, Berlin, Heidelberg, pp. 155–167.

Berney, D. M., Looijenga, L. H., Idrees, M., Oosterhuis, J. W., Rajpert-De Meyts, E., Ulbright, T. M., & Skakkebaek, N. E. (2016). Germ cell neoplasia in situ (GCNIS): evolution of the current nomenclature for testicular pre-invasive germ cell malignancy. *Histopathology*, *69*(1), 7-10.

Biswas, S. K., & Mantovani, A. (2010). Macrophage plasticity and interaction with lymphocyte subsets: cancer as a paradigm. *Nature Immunology*, *11*(10), 889.

Blagih, J., & Jones, R. G. (2012). Polarizing macrophages through reprogramming of glucose metabolism. *Cell Metabolism*, *15*(6), 793-795.

Bols B, Jense L, Jense A, Braendstrup O. Immunopathology of in situ seminoma. *Int J Exp Pathol* 2000 :**81**; 211 – 217. doi: 10.1046/j.1365-2613.

Bonavita, O., Mollica Poeta, V., Setten, E., Massara, M., & Bonecchi, R. (2017). ACKR2: An Atypical Chemokine Receptor Regulating Lymphatic Biology. *Frontiers in Immunology*, *7*, 691.

Bonelli M J, Savitskaya A, Steiner C W, Rath E, Smolen J S, Scheinecker C (2009). Phenotypic and functional analysis of CD4+ CD25− Foxp3+ T cells in patients with systemic lupus erythematosus. *J. Immunol*., 182, pp. 1689–1695.

Boublikova, L., Buchler, T., Stary, J., Abrahamova, J., & Trka, J. (2014). Molecular biology of testicular germ cell tumors: unique features awaiting clinical application. *Critical Reviews in Oncology/Hematology*, *89*(3), 366-385.

Broz ML, Binnewies M, Boldajipour B, Nelson AE, Pollack JL, Erle DJ, Barczak A, Rosenblum MD, Daud A, Barber DL (2014). Dissecting the tumor myeloid compartment reveals rare activating antigen-presenting cells critical for T cell immunity. *Cancer Cell* 2014, 26:638-652.

Broz, M. L., & Krummel, M. F. (2015). The emerging understanding of myeloid cells as partners and targets in tumor rejection. *Cancer Immunology Research*, *3*(4), 313-319.

Bryniarski K, Szczepanik M, Maresz K, Ptak M & Ptak W (2004). Subpopulations of mouse testicular macrophages and their immunoregulatory function. *American Journal of Reproductive Immunology* 52 27-35.

Bhushan, S., & Meinhardt, A. (2017). The macrophages in testis function. *Journal of Reproductive Immunology*, 119, 107-112.

Cai, X., Yin, Y., Li, N., Zhu, D., Zhang, J., Zhang, C. Y., & Zen, K. (2012). Re-polarization of tumor-associated macrophages to pro-inflammatory M1 macrophages by microRNA-155. *Journal of Molecular Cell Biology*, *4*(5), 341-343.

Cannon, G. J., & Swanson, J. A. (1992). The macrophage capacity for phagocytosis. *Journal of Cell Science*, *101*(4), 907-913.

Cassetta L, Cassol E, Poli G. Macrophage polarization in health and disease. *ScientificWorldJournal*. 2011;11:2391-402.

Caux, C., Vanbervliet, B., Massacrier, C., Ait-Yahia, S., Vaure, C., Chemin, K., Dieu-Nosjean And, MC., Vicari, A. (2002): Regulation of dendritic cell recruitment by chemokines. *Transplantation.* 2002, 73: 7-11. 10.1097/00007890-200201151-00005.

Chang, L.Y., Lin, Y.C., Mahalingam, J., Huang, C.T., Chen, T.W., Kang, C.W., Peng, H.M., Chu, Y.Y., Chiang, J.M., Dutta, A. and Day, Y.J. (2012). Tumor-derived chemokine CCL5 enhances TGF-β–mediated killing of CD8+ T cells in colon cancer by T-regulatory cells. *Cancer Research*.

Chanmee, T., Ontong, P., Konno, K., & Itano, N. (2014). Tumor-associated macrophages as major players in the tumor microenvironment. *Cancers*, *6*(3), 1670-1690.

Chen, E. P., & Smyth, E. M. (2011). COX-2 and PGE2-dependent immunomodulation in breast cancer. *Prostaglandins & Other Lipid Mediators*, *96*(1-4), 14-20.

Chen, J., Yao, Y., Gong, C., Yu, F., Su, S., Chen, J., Liu, B., Deng, H., Wang, F., Lin, L. and Yao, H., (2011). CCL18 from tumor-associated macrophages promotes breast cancer metastasis via PITPNM3. *Cancer Cell*, *19*(4), pp.541-555.

Chen, Y., Kam, C.S., Liu, F.Q., Liu, Y., Lui, V.C., Lamb, J.R., Tam, P.K. (2008). LPS-inducedup-regulation of TGF-beta receptor 1 is associated with TNF-alpha expressionin human monocyte-derived macrophages. *J. Leukocyte Biol.* 83, 1165–1173.

Chia, V. M., Quraishi, S. M., Devesa, S. S., Purdue, M. P., Cook, M. B., & McGlynn, K. A. (2010). International trends in the incidence of testicular cancer, 1973-2002. *Cancer Epidemiology and Prevention Biomarkers*, *19*(5), 1151-1159.

Conti, I., & Rollins, B. J. (2004). CCL2 (monocyte chemoattractant protein-1) and cancer. In *Seminars in Cancer Biology* (Vol. 14, No. 3, pp. 149-154). Academic Press.

Cook, J., & Hagemann, T. (2013). Tumour-associated macrophages and cancer. *Current Opinion in Pharmacology*, *13*(4), 595-601.

Couper, K. N., Blount, D. G., & Riley, E. M. (2008). IL-10: the master regulator of immunity to infection. *The Journal of Immunology*, 180(9), 5771-5777.

Craig, M. J., & Loberg, R. D. (2006). CCL2 (Monocyte Chemoattractant Protein-1) in cancer bone metastases. *Cancer and Metastasis Reviews*, *25*(4), 611-619.

Da Silva, N., Barton, CR. (2016). Macrophages and dendritic cells in the post-testicular environment. *Cell Tissue Res* 363:97-104.

Dai, C., Wen, X., He, W., & Liu, Y. (2011). Inhibition of proinflammatory RANTES expression by TGF-β1 is mediated by glycogen synthase kinase-3β-dependent β-catenin signaling. *Journal of Biological Chemistry*, *286*(9), 7052-7059.

Das, M., Zhu, C., & Kuchroo, V. K. (2017). Tim-3 and its role in regulating anti-tumor immunity. *Immunological Reviews*, *276*(1), 97-111.

Daugaard, G., Kier, MG., Bandak, M., Mortensen, MS., Larsson, H., Søgaard, M., Toft, BG.,Engvad, B., Agerbæk, M., Holm, NV., Lauritsen, J. (2016).The Danish Testicular Cancer database.*Clin Epidemiol*.8:703-707.

Davies, L. C., Jenkins, S. J., Allen, J. E., & Taylor, P. R. (2013). Tissue-resident macrophages. *Nature Immunology*, *14*(10), 986.

De Jong, J., Stoop, H., Gillis, A.J.M., van Gurp, R.J.H.L.M., van de Geijn, G.J., de Boer, M., Hersmus, R., Saunders, P.T.K., Anderson, R.A., Oosterhuis, J.W. & Looijenga, L.H.J. (2008). Differential expression of SOX17 and SOX2 in germ cells and stem cells has biological and clinical implications. *The Journal of Pathology*, *215*(1), pp.21-30.

De Waal Malefyt, R., Figdor, C.G., Huijbens, R., Mohan-Peterson, S., Bennett, B., Culpepper, J., Dang, W., Zurawski, G. & de Vries, J.E. (1993). Effects of IL-13 on phenotype, cytokine production, and cytotoxic function of human monocytes. Comparison with IL-4 and modulation by IFN-gamma or IL-10. *The Journal of Immunology*, *151*(11), pp.6370-6381.

DeFalco, T., Potter, S. J., Williams, A. V., Waller, B., Kan, M. J., & Capel, B. (2015). Macrophages contribute to the spermatogonial niche in the adult testis. *Cell Reports*, *12*(7), 1107-1119.

Deng, L., Liang, H., Burnette, B., Beckett, M., Darga, T., Weichselbaum, R. R., & Fu, Y. X. (2014). Irradiation and anti–PD-L1 treatment synergistically promote antitumor immunity in mice. *The Journal of Clinical Investigation*, *124*(2), 687-695.

Derynck, R., Akhurst, R.J., & Balmain, A. (2001). TGF-β signaling in tumor suppression and cancer progression. *Nat. Genet*. *29*, 117–129.

Ding, A., Nathan, C. F., Graycar, J., Derynck, R. I. K., Stuehr, D. J., & Srimal, S. (1990). Macrophage deactivating factor and transforming growth factors-beta 1-beta 2 and-beta 3 inhibit induction of macrophage nitrogen oxide synthesis by IFN-gamma. *The Journal of Immunology*, *145*(3), 940-944.

Dias, V.L, Rajpert-deMeyts E., McLachlan, R. & Loveland, K.L. (2009). Analysis of activin/ TGFβ signaling modulators within the normal and dysfunctional adult human testis reveal evidence of altered signaling capacity in a subset of seminomas. *Reproduction 138*:801-11.

Dobashi, M., Fujisawa, M., Yamazaki, T., Okada, H., & Kamidono, S. (2002). Distribution of intracellular and extracellular expression of transforming growth factor-b1 (TGF-b 1) in human testis and their association with spermatogenesis. *Asian J Androl*, *4*, 105-109.

Dong, Y., Tang, L., Letterio, J. J., & Benveniste, E. N. (2001). The Smad3 protein is involved in TGF-β inhibition of class II transactivator and class II MHC expression. *The Journal of Immunology*, *167*(1), 311-319.

Dranoff, G. (2004). Cytokines in cancer pathogenesis and cancer therapy. *Nature Reviews Cancer*, 4(1), 11.

Dubois, C. M., Ruscetti, F. W., Palaszynski, E. W., Falk, L. A., Oppenheim, J. J., & Keller, J. R. (1990). Transforming growth factor beta is a potent inhibitor of interleukin 1 (IL-1) receptor expression: proposed mechanism of inhibition of IL-1 action. *Journal of Experimental Medicine*, *172*(3), 737-744.

Duluc, D., Delneste, Y., Tan, F., Moles, M.P., Grimaud, L., Lenoir, J., Preisser, L., Anegon, I., Catala, L., Ifrah, N. and Descamps, P. (2007). Tumor-associated leukemia inhibitory factor and IL-6 skew monocyte differentiation into tumor-associated macrophage-like cells. *Blood*, *110*(13), pp.4319-4330.

Eckert, D., Biermann, K., Nettersheim, D., Gillis, A.J., Steger, K., Jäck, H.M., Müller, A.M., Looijenga, L.H. and Schorle, H. (2008). Expression of BLIMP1/PRMT5 and concurrent histone H2A/H4 arginine 3 dimethylation in fetal germ cells, CIS/IGCNU and germ cell tumors. *BMC Developmental Biology*, *8*(1), p.106.

Erler, J.T., Bennewith, K.L., Cox, T.R., Lang, G., Bird, D., Koong, A., Le, Q.T. and Giaccia, A.J. (2009). Hypoxia-induced lysyl oxidase is a critical mediator of bone marrow cell recruitment to form the premetastatic niche. *Cancer Cell*, *15*(1), pp.35-44.

Fang, W. B., Yao, M., Brummer, G., Acevedo, D., Alhakamy, N., Berkland, C., & Cheng, N. (2016). Targeted gene silencing of CCL2 inhibits triple negative breast cancer progression by blocking cancer stem cell renewal and M2 macrophage recruitment. *Oncotarget*, *7*(31), 49349.

Fankhauser, C.D., Curioni-Fontecedro, A., Allmann, V., Beyer, J., Tischler, V., Sulser, T., Moch, H. and Bode, P.K. (2015). Frequent PD-L1 expression in testicular germ cell tumors. *British Journal of Cancer*, *113*(3), p.411.

Fijak, M., Bhushan, S., & Meinhardt, A. (2010). Immunoprivileged sites: the testis. *Suppression and Regulation of Immune Responses*. *Humana Press*, Totowa, NJ, 2010. 459-470.

Fijak M., Bhushan S., Meinhardt A. (2017). The Immune Privilege of the Testis. In: Krause W., Naz R. (eds). *Immune Infertility*. Springer, Cham.

Fijak, Monika & Andreas Meinhardt (2006). “The testis in immune privilege”. *Immunological Reviews 213 (2006): 66-81.*

Fijak, M., Pilatz, A., Hedger, M.P., Nicolas, N., Bhushan, S., Michel, V., Tung, K.S., Schuppe, H.C. & Meinhardt, A. (2018). Infectious, inflammatory and ‘autoimmune’male factor infertility: how do rodent models inform clinical practice?. *Human Reproduction Update*. *24*(4), 416-441.

Finbloom, D. S., & Winestock, K. D. (1995). IL-10 induces the tyrosine phosphorylation of tyk2 and Jak1 and the differential assembly of STAT1 alpha and STAT3 complexes in human T cells and monocytes. *The Journal of Immunology*, *155*(3), 1079-1090.

Fiorentino, D. F., Zlotnik, A., Mosmann, T. R., Howard, M., & O'garra, A. (1991). IL-10 inhibits cytokine production by activated macrophages. *The Journal of Immunology*, *147*(11), 3815-3822.

Frungieri, MB., Calandra, RS., Lustig, L., Meineke, V., Köhn, FM., Vogt, HJ., Mayerhofer, A. (2002). Number, distribution patten, and identification of macrophages in the testes of infertile men. *Fertil Steril*;78:298-306.

Gabrilovich, D. (2004). Mechanisms and functional significance of tumour-induced dendritic-cell defects. *Nat Rev Immunol* 2004; 4: 941-952.

Genin, M., Clement, F., Fattaccioli, A., Raes, M., Michiels, C. (2015). M1 and M2 macrophages derived from THP-1 cells differntially modulate the response of cancer cells to etoposide. *BMC Cancer,* 15:577.

Giwercman, A., & Skakkebaek, N. E. (1993). Carcinoma in situ of the testis: biology, screening and management. *European Urology*, *23*, 19-21.

Golden-Mason, L., Palmer, B.E., Kassam, N., Townshend-Bulson, L., Livingston, S., McMahon, B.J., Castelblanco, N., Kuchroo, V., Gretch, D.R. and Rosen, H.R.. (2009). Negative immune regulator Tim-3 is overexpressed on T cells in hepatitis C virus infection and its blockade rescues dysfunctional CD4+ and CD8+ T cells. *Journal of Virology*, *83*(18), pp.9122-9130.

González-Domínguez, É., Domínguez-Soto, Á., Nieto, C., Flores-Sevilla, J.L., Pacheco-Blanco, M., Campos-Peña, V., Meraz-Ríos, M.A., Vega, M.A., Corbí, Á.L. and Sánchez-Torres, C. (2016). Atypical activin A and IL-10 production impairs human CD16+ monocyte differentiation into anti-inflammatory macrophages. *The Journal of Immunology*, p.1501177.

Gottfried, E., Kreutz, M., & Mackensen, A. (2008). Tumor-induced modulation of dendritic cell function. *Cytokine & Growth Factor Reviews*, *19*(1), 65-77.

Gratchev, A., Kzhyshkowska, J., Utikal, J., & S. Goerdt. (2005). Interleukin-4 and dexamethasone counterregulate extracellular matrix remodelling and phagocytosis in type-2 macrophages. Scand. *J. Immunol*. 61: 10–17.

Gratchev, A., Kzhyshkowska, J., Kannookadan, S., Ochsenreiter, M., Popova, A., Yu, X., Mamidi, S., Stonehouse-Usselmann, E., Muller-Molinet,I., Gooi, L., Goerdt, S. (2008). Activation of a TGF-beta-specific multistep gene expression program in mature macrophages requires glucocorticoid-mediated surface expression of TGF-beta receptor II. *J Immunol*. May 15;180(10):6553-65.

Gratchev, A. (2017). TGF-β signalling in tumour associated macrophages. *Immunobiology*, *222*(1), 75-81.

Grivennikov, S. I., Greten, F. R., & Karin, M. (2010). Immunity, inflammation, and cancer. *Cell*, *140*(6), 883-899.

Grotendorst, G. R., Smale, G., & Pencev, D. (1989). Production of transforming growth factor beta by human peripheral blood monocytes and neutrophils. *Journal of Cellular Physiology*, *140*(2), 396-402.

Gu, B. J., Sun, C., Fuller, S., Skarratt, K. K., Petrou, S., & Wiley, J. S. (2014). A quantitative method for measuring innate phagocytosis by human monocytes using real-time flow cytometry. *Cytometry Part A*, *85*(4), 313-321.

Guazzone, V.A., Hollwegs, S., Mardirosian, M., Jacobo, P., Hackstein, H., Wygrecka, M., Schneider, E., Meinhardt, A., Lustig, L. and Fijak, M., 2011. Characterization of dendritic cells in testicular draining lymph nodes in a rat model of experimental autoimmune orchitis. *International Journal of Andrology*, *34*(3), pp.276-289.

Guiducci, C., Vicari, A. P., Sangaletti, S., Trinchieri, G., & Colombo, M. P. (2005). Redirecting in vivo elicited tumor infiltrating macrophages and dendritic cells towards tumor rejection. *Cancer Research*, *65*(8), 3437-3446.

Hagemann, T., Biswas, S. K., Lawrence, T., Sica, A., & Lewis, C. E. (2009). Regulation of macrophage function in tumors: the multifaceted role of NF-κB. *Blood*, *113*(14), 3139-3146.

Hagemann, T., Wilson, J., Burke, F., Kulbe, H., Li, N.F., Plüddemann, A., Charles, K., Gordon, S. and Balkwill, F.R. (2006). Ovarian cancer cells polarize macrophages toward a tumor-associated phenotype. *The Journal of Immunology*, *176*(8), pp.5023-5032.

Haniffa, M., Collin, M., Ginhoux, F. (2013). Identification of human tissue cross-presenting dendritic cells: a new target for cancer vaccines. *Oncoimmunology* 2:e23140.

Harimoto, H., M. Shimizu, Y. Nakagawa, K. Nakatsuka, A. Wakabayashi, C. Sakamoto, & Takahashi, H. (2013). Inactivation of tumor-specific CD8+CTLs by tumor-infiltrating tolerogenic dendritic cells.Immunol. *Cell Biol.*91: 545–555.

Harrison, CA., Al-Musawi, SL., Walton, KL. (2011). Prodomains regulate the synthesis, extracellular localisation and activity of TGF-β superfamily ligands. *Growth Factors.* 2011 Oct;29(5):174-86. doi: 10.3109/08977194.2011.608666.

Haschemi, A., Kosma, P., Gille, L., Evans, C.R., Burant, C.F., Starkl, P., Knapp, B., Haas, R., Schmid, J.A., Jandl, C. and Amir, S. (2012). The sedoheptulose kinase CARKL directs macrophage polarization through control of glucose metabolism. *Cell Metabolism*, *15*(6), pp.813-826.

Hemminki, K., & Li, X. (2004). Familial risk in testicular cancer as a clue to a heritable and environmental aetiology. *British Journal of Cancer*, *90*(9), 1765.

a) Heusinkveld, M., De Vos van Steenwijk, P., Goedemans, R., Ramwadhdoebe, T., Gorter, A., J. P., Welters, M., van Hall, T., van der Burg, S. (2011). M2 Macrophages Induced by Prostaglandin E2 and IL-6 from Cervical Carcinoma Are Switched to Activated M1 Macrophages by CD4+ Th1 Cells. *J Immunol*, 187 (3) 1157-1165; DOI: https://doi.org/10.4049/jimmunol.1100889.

b) Heusinkveld, M., van der Burg, SH. (2011). Identification and manipulation of tumor associated macrophages in human cancers*. Journal of Translational Medicine*.9:216. DOI: 10.1186/1479-5876-9-216.

Heuzé, M.L., Vargas, P., Chabaud, M., Le Berre, M., Liu, Y.-J., Collin, O., Solanes, P., Voituriez, R., Piel, M., Lennon-Duménil, A.-M. (2013). Migration of dendritic cells: physical principles, molecular mechanisms, and functional implications. *Immunol. Rev*.256, 240–254

Hill CS. (2016) Transcriptional Control by the SMADs. *Cold Spring Harb Perspect Biol.*8(10). pii: a022079. doi: 10.1101/cshperspect.a022079.

Hume, D. A. (2008). Macrophages as APC and the dendritic cell myth. *The Journal of Immunology*, *181*(9), 5829-5835.

Huyghe, E., Matsuda, T., & Thonneau, P. (2003). Increasing incidence of testicular cancer worldwide: a review. *The Journal of Urology*, *170*(1), 5-11.

Hvarness, T., Nielsen, JE., Almstrup, K., Skakkebaek, NE., Rajpert-De Meyts, E., Claesson, MH. (2013). Phenotypic characterisation of immune cell infiltrates in testicular germ cell neoplasia. *J Reprod Immunol 2013*;100:135-145.

Irie, N., Weinberger, L., Tang, W.W., Kobayashi, T., Viukov, S., Manor, Y.S., Dietmann, S., Hanna, J.H. and Surani, M.A. (2015). SOX17 is a critical specifier of human primordial germ cell fate. *Cell*, *160*(1), pp.253-268.

Jacobo, P., Guazzone, S., Jarazo-Dietrich, V. A., Theas, M. S., Lustig, L. (2009). Differential changes in $CD4^+$ and $CD8^+$ effector and regulatory T lymphocyte subsets in the testis of rats undergoing autoimmune orchitis. *Journal of Reproductive Immunology,* Volume 81, Issue 1, Pages44–54.

Janeway Jr, C. A. (2001). How the immune system protects the host from infection. *Microbes and Infection*, *3*(13), 1167-1171.

Jørgensen, A., Young, J., Nielsen, J. E., Joensen, U. N., Toft, B. G., Rajpert-De Meyts, E., & Loveland, K. L. (2014). Hanging drop cultures of human testis and testis cancer samples: a model used to investigate activin treatment effects in a preserved niche. *British Journal of Cancer*, *110*(10), 2604.

Kadowaki, N. (2009). The divergence and interplay between pDC and mDC in humans. *Frontiers in Bioscience (Landmark edition)*, *14*, 808-817.

Kawakami, T., Zhang, C., Okada, Y., & Okamoto, K. (2006). Erasure of methylation imprint at the promoter and CTCF-binding site upstream of H19 in human testicular germ cell tumors of adolescents indicate their fetal germ cell origin. *Oncogene*, *25*(23), 3225.

Kim, S., Takahashi, H., Lin, W.W., Descargues, P., Grivennikov, S., Kim, Y., Luo, J.L. & Karin, M. (2009). Carcinoma-produced factors activate myeloid cells through TLR2 to stimulate metastasis. *Nature*, *457*(7225), p.102.

Klein, B., Haggeney, T., Fietz, D., Indumathy, S., Loveland, K.L., Hedger, M., Kliesch, S., Weidner, W., Bergmann, M., Schuppe, H.C. (2016). Specific immune cell and cytokine characteristics of human testicular germ cell neoplasia. *Hum Reprod*, 31 (10): 2192-2202.

Krempski, J., Karyampudi, L., Behrens, MD., Erskine, CL., Hartmann, L., Dong, H., Goode, EL., Kalli, KR., Knutson, KL. (2011). Tumor-infiltrating programmed death receptor-1C dendritic cells mediate immune suppression in ovarian cancer. *J Immunol 2011*; 86:6905-13.

Koh, T. J., & DiPietro, L. A. (2011). Inflammation and wound healing: the role of the macrophage. *Expert Reviews in Molecular Medicine*, 13.

Leach, D. R., Krummel, M. F., & Allison, J. P. (1996). Enhancement of antitumor immunity by CTLA-4 blockade. *Science*, *271*(5256), 1734-1736.

Lee, C.H., Espinosa, I., Vrijaldenhoven, S., Subramanian, S., Montgomery, K.D., Zhu, S., Marinelli, R.J., Peterse, J.L., Poulin, N., Nielsen, T.O. & West, R.B. (2008). Prognostic significance of macrophage infiltration in leiomyosarcomas. *Clinical Cancer Research*, *14*(5), pp.1423-1430.

Lewis, C. E., & Pollard, J. W. (2006). Distinct role of macrophages in different tumor microenvironments. *Cancer Research*, *66*(2), 605-612.

Li, G., Qiao, W., Zhang, W., Li, F., Shi, J., & Dong, N. (2017). The shift of macrophages toward M1 phenotype promotes aortic valvular calcification. *The Journal of Thoracic and Cardiovascular Surgery*, *153*(6), 1318-1327.
Lim, T. S., Chew, V., Sieow, J. L., Goh, S., Yeong, J. P. S., Soon, A. L., & Ricciardi-Castagnoli, P. (2016). PD-1 expression on dendritic cells suppresses CD8+ T cell function and antitumor immunity. *Oncoimmunology*, *5*(3), e1085146.

Locati, M., Deuschle, U., Massardi, M.L., Martinez, F.O., Sironi, M., Sozzani, S., Bartfai, T. & Mantovani, A. (2002). Analysis of the gene expression profile activated by the CC chemokine ligand 5/RANTES and by lipopolysaccharide in human monocytes. *The Journal of Immunology*, *168*(7), pp.3557-3562.

Loveland, K.L., Klein, B., Pueschl, D., Indumathy, S., Bergmann, M., Loveland, B.E., Hedger, M.P. & Schuppe, H.C., 2017. Cytokines in male fertility and reproductive pathologies: immunoregulation and beyond. *Frontiers in Endocrinology*, *8*, p.307.

Loveland, K.L. & Hedger, M.P. (2015). Activins and inhibins in Sertoli cell biology: Implications for testis development and function. In: M. Griswold, ed. *Sertoli Cell Biology*. Elsevier Science (USA). pp 201-221.

Lu, J., Cao, Q., Zheng, D., Sun, Y., Wang, C., Yu, X., Wang, Y., Lee, V.W., Zheng, G., Tan, T.K. & Wang, X. (2013). Discrete functions of M2a and M2c macrophage subsets determine their relative efficacy in treating chronic kidney disease. *Kidney International*, *84*(4), pp.745-755.

Lui, W. Y., Lee, W. M., & Cheng, C. Y. (2003). TGF-βs: their role in testicular function and Sertoli cell tight junction dynamics. *International Journal of Andrology*, *26*(3), 147-160.

Lund, M. E., To, J., O'Brien, B. A., & Donnelly, S. (2016). The choice of phorbol 12-myristate 13-acetate differentiation protocol influences the response of THP-1 macrophages to a pro-inflammatory stimulus. *Journal of Immunological Methods*, *430*, 64-70.

Ma, C., Wang, Y., Dong, L., Li, M., & Cai, W. (2015). Anti-inflammatory effect of resveratrol through the suppression of NF-κB and JAK/STAT signaling pathways. *Acta Biochimica et Biophysica Sinica*, *47*(3), 207-213.

Ma, Y., Shurin, G. V., Peiyuan, Z., & Shurin, M. R. (2013). Dendritic cells in the cancer microenvironment. *Journal of Cancer*, *4*(1), 36.

Mantovani, A., Allavena, P., Sica, A., Balkwill, F. (2008). Cancer-related inflammation.*Nature*.454(7203):436–444.

Mantovani, A., Allavena, P., Sica, A. (2004). Tumour-associated macrophages as a prototypic type II polarised phagocyte population: role in tumour progression. *Eur J Cancer*. 2004;40:1660-7, doi: 10.1016/j.ejca.2004.03.016.

Mantovani, A., Bottazzi, B., Colotta, F., Sozzani, S., & Ruco, L. (1992). The origin and function of tumor-associated macrophages. *Immunology Today*, *13*(7), 265-270.

Mantovani, A., Sozzani, S., Locati, M., Allavena, P., & Sica, A. (2002). Macrophage polarization: tumor-associated macrophages as a paradigm for polarized M2 mononuclear phagocytes. *Trends in Immunology*, *23*(11), 549-555.

Martinez, F. O., Helming, L., & Gordon, S. (2009). Alternative activation of macrophages: an immunologic functional perspective. *Annual Review of Immunology*, 27, 451-483.

Martinez, F.O., Sica, A., Mantovani, A., Locati, M. (2008). Macrophage activation and polarization. *Front Biosci*. 2008;13:453-61, doi: 10.2741/2692.

Martinez, F. O., & Gordon, S. (2014). The M1 and M2 paradigm of macrophage activation: time for reassessment. *F1000Prime Reports*, *6*.

McGinley K.F., Rampersaud E.N. (2014) Testicular Cancer. In: Merseburger A., Kuczyk M., Moul J. (eds) *Urology at a Glance*. pp. 299-303. Springer, Berlin, Heidelberg.

Meinhardt, A., & Hedger, M. P. (2011). Immunological, paracrine and endocrine aspects of testicular immune privilege. *Molecular and Cellular Endocrinology*, 335(1), 60-68.

Mia, S., Warnecke, A., Zhang, X. M., Malmström, V., & Harris, R. A. (2014). An optimized protocol for human M2 macrophages using M-CSF and IL-4/IL-10/TGF-β yields a dominant immunosuppressive phenotype. *Scandinavian Journal of Immunology*, *79*(5), 305-314.

Mildner, A, Jung, S (2014). Development and function of dendritic cell subsets. *Immunity* 40:642-656.

Mills, C. D., Kincaid, K., Alt, J. M., Heilman, M. J., & Hill, A. M. (2000). M-1/M-2 macrophages and the Th1/Th2 paradigm. *The Journal of Immunology*, 164(12), 6166-6173.

Miyagaki, T., Sugaya, M., Suga, H., Ohmatsu, H., Fujita, H., Asano, Y., Tada, Y., Kadono, T. and Sato, S., 2013. Increased CCL18 expression in patients with cutaneous T-cell lymphoma: Association with disease severity and prognosis. *Journal of the European Academy of Dermatology and Venereology*, *27*(1), pp.e60-e67.

Miyazono, K., Katsuno, Y., Koinuma, D., Ehata, S., & Morikawa, M. (2018). Intracellular and extracellular TGF-β signaling in cancer: some recent topics. *Frontiers of Medicine*, 1-25.

Mizuno, Y., Gotoh, A., Kamidono, S., & Kitazawa, S. (1993). Establishment and characterization of a new human testicular germ cell tumor cell line (TCam-2). *Nihon Hinyokika Gakkai zasshi. The Japanese Journal of Urology*, *84*(7), 1211-1218.

Mizutani, K., Sud, S., McGregor, N.A., Martinovski, G., Rice, B.T., Craig, M.J., Varsos, Z.S., Roca, H. and Pienta, K.J. (2009). The chemokine CCL2 increases prostate tumor growth and bone metastasis through macrophage and osteoclast recruitment. *Neoplasia*, *11*(11), pp.1235-1242.

Moch, H., Cubilla, A. L., Humphrey, P. A., Reuter, V. E., & Ulbright, T. M. (2016). The 2016 WHO classification of tumours of the urinary system and male genital organs—part A: renal, penile, and testicular tumours. *European Urology*, *70*(1), 93-105.

Mortensen, M.S., Lauritsen, J., Gundgaard, M.G., Agerbæk, M., Holm, N.V., Christensen, I.J., von der Maase, H. and Daugaard, G. (2014). A nationwide cohort study of stage I seminoma patients followed on a surveillance program. *European Urology*, *66*(6), pp.1172-1178.

Mossadegh-Keller, N., Gentek, R., Gimenez, G., Bigot, S., Mailfert, S., & Sieweke, M. H. (2017). Developmental origin and maintenance of distinct testicular macrophage populations. *Journal of Experimental Medicine*, jem-20170829.

Mutzke, E., Chomyshyn, E., Nguyen, K. C., Blahoianu, M., & Tayabali, A. F. (2015). Phagocytosis-coupled flow cytometry for detection and size discrimination of anionic polystyrene particles. *Analytical Biochemistry*, *483*, 40-46.

Murphy, K., Weaver, C. (2017). Janeway's Immunobiology. New York: Garland Science.

Myrup, C., Wohlfahrt, J., Oudin, A., Schnack, T., & Melbye, M. (2010). Risk of testicular cancer according to birthplace and birth cohort in Denmark. *International Journal of Cancer*, *126*(1), 217-223.

Nakamura, R., Sene, A., Santeford, A., Gdoura, A., Kubota, S., Zapata, N., & Apte, R. S. (2015). IL10-driven STAT3 signalling in senescent macrophages promotes pathological eye angiogenesis. *Nature Communications*, *6*, 7847.

Nakanoma T, Nakamura K, Deguchi N, et al. Immunohistological analysis of tumour infiltrating lymphocytes in seminoma using monoclonal antibodies. *Virchows Archiv A Pathol Anat Histopathol* 1992 :**421**; 409 – 413. PMID:1455691.

Narita, D, Seclaman, E, Ursoniu, S, Ilina, R, Cireap, N, Anghel, A. (2011). Expression of CCL18 and interleukin-6 in the plasma of breast cancer patients as compared with benign tumor patients and healthy controls. *Romanian J Morphol Embryol.* 2011;52(4)1261–1267.

Netto, G.J., Nakai, Y., Nakayama, M., Jadallah, S., Toubaji, A., Nonomura, N., Albadine, R., Hicks, J.L., Epstein, J.I., Yegnasubramanian, S. and Nelson, W.G. (2008). Global DNA hypomethylation in intratubular germ cell neoplasia and seminoma, but not in nonseminomatous male germ cell tumors. *Modern Pathology*, *21*(11), p.1337.

Ocaña-Guzman, R., Torre-Bouscoulet, L., & Sada-Ovalle, I. (2016). TIM-3 regulates distinct functions in macrophages. *Frontiers in Immunology*, *7*, 229.
O'shea, J. J., & Murray, P. J. (2008). Cytokine signaling modules in inflammatory responses. *Immunity*, 28(4), 477-487.

Palucka, K., & Banchereau, J. (1999). Dendritic cells: a link between innate and adaptive immunity. *Journal of Clinical Immunology*, *19*(1), 12-25.

Park, E. K., Jung, H. S., Yang, H. I., Yoo, M. C., Kim, C., & Kim, K. S. (2007). Optimized THP-1 differentiation is required for the detection of responses to weak stimuli. *Inflammation Research*, *56*(1), 45-50.

Pérez, CV, Theas, MS, Jacobo, PV, Jarazo-Dietrich, S, Guazzone, VA, Lustig, L. (2013). Dual role of immune cells in the testis-protective or pathogenic for germ cells? *Spermatogenesis* 2013;3:e23870-I-e23870-12.

Pöllänen, P., & Maddocks, S. (1988). Macrophages, lymphocytes and MHC II antigen in the ram and the rat testis. *Journal of Reproduction and Fertility*, *82*(2), 437-445.

Pöllänen, S., & Söder, O. (1993). Role of transforming growth factor β in testicular immunosuppression. *Journal of Reproductive Immunology*, *24*(2), 123-137.

Postow, M. A., Callahan, M. K., & Wolchok, J. D. (2015). Immune checkpoint blockade in cancer therapy. *Journal of Clinical Oncology*, *33*(17), 1974.

Pyle, L. C., & Nathanson, K. L. (2016). Genetic changes associated with testicular cancer susceptibility. In *Seminars in Oncology* (Vol. 43, No. 5, pp. 575-581). WB Saunders.

Rajpert-De Meyts, E. (2006). Developmental model for the pathogenesis of testicular carcinoma in situ: genetic and environmental aspects. *Human Reproduction Update*, *12*(3), 303-323.

Rajpert-De Meyts, E., McGlynn, K. A., Okamoto, K., Jewett, M. A., & Bokemeyer, C. (2016). Testicular germ cell tumours. *The Lancet*, *387*(10029), 1762-1774.

Redpath, S. A., van der Werf, N., Cervera, A. M., MacDonald, A. S., Gray, D., Maizels, R. M., & Taylor, M. D. (2013). ICOS controls Foxp3+ regulatory T-cell expansion, maintenance and IL-10 production during helminth infection. *European Journal of Immunology*, 43(3), 705-715.

Richiardi, L, Bellocco, R, Adami, HO, Torrång, A, Barlow, L, Hakulinen, T, Rahu, M, Stengrevics, A, Storm, H, Tretli, S, Kurtinaitis, J, Tyczynski, JE, Akre, O. (2004). Testicular cancer incidence in eight northern European countries: secular and recent trends.*Cancer Epidemiol Biomarkers* Prev13(12): 2157–2166.
Rival, C., Lustig, L., Iosub, R., Guazzone, V. A., Schneider, E., Meinhardt, A., & Fijak, M. (2006). Identification of a dendritic cell population in normal testis and in chronically inflamed testis of rats with autoimmune orchitis. *Cell and Tissue Research*, *324*(2), 311.

Roca, H., Varsos, ZS., Sud, S., Craig, MJ., Ying, C., Pienta, KJ. (2009). CCL2 and interleukin-6 promote survival of human CD11b+ peripheral blood mononuclear cells and induce M2-type macrophage polarization.*J Biol Chem.*284(49):34342–34354.

Romieu-Mourez, R., François, M., Boivin, M. N., Stagg, J., & Galipeau, J. (2007). Regulation of MHC class II expression and antigen processing in murine and human mesenchymal stromal cells by IFN-γ, TGF-β, and cell density. *The Journal of Immunology*, *179*(3), 1549-1558.

Ryder, M., Ghossein, RA., Ricarte-Filho, JC., Knauf, JA., Fagin, JA. (2008). -$I0ncreased density of tumor-associated macrophages is associated with decreased $masurvival in advanced thyroid cancer. *Endocr Relat Cancer*.15:1069- 74, doi: 10.1677/ERC-08-0036.

Sabatos, C.A., Chakravarti, S., Cha, E., Schubart, A., Sánchez-Fueyo, A., Zheng, X.X., Coyle, A.J., Strom, T.B., Freeman, G.J. & Kuchroo, V.K. (2003). Interaction of Tim-3 and Tim-3 ligand regulates T helper type 1 responses and induction of peripheral tolerance. *Nature Immunology*, *4*(11), p.1102.

Sanz-Rodriguez, F., Fernandez, L.A., Zarrabeitia, R., Perez-Molino, A., Ramirez, J.R., Coto, E., Bernabeu, C., Botella, L.M. (2004). Mutation analysis in Spanish patients with hereditary hemorrhagic telangiectasia: deficient endoglin up-regulationin activated monocytes. *Clin. Chem*. 50, 2003–2011.

Scarlett, U.K., Rutkowski, M.R., Rauwerdink, A.M., Fields, J., Escovar-Fadul, X., Baird, J., Cubillos-Ruiz, J.R., Jacobs, A.C., Gonzalez, J.L., Weaver, J., & Fiering, S. (2012). Ovarian cancer progression is controlled by phenotypic changes in dendritic cells. *Journal of Experimental Medicine*, pp.jem-20111413.

Scarpino, S., Stoppacciaro, A., Ballerini, F., Marchesi, M., Prat, M., Stella, M.C., Sozzani, S., Allavena, P., Mantovani, A. & Ruco, L.P. (2000). Papillary carcinoma of the thyroid: hepatocyte growth factor (HGF) stimulates tumor cells to release chemokines active in recruiting dendritic cells. *The American Journal of Pathology*, *156*(3), pp.831-837.

Schaer, D. J., Boretti, F. S., Schoedon, G., Schaffner, A. (2002). Induction of the CD163-dependent haemoglobin uptake by macrophages as a novel antiinflammatory action of glucocorticoids. *Br. J. Haematol*. 119: 239–243.

Schlecker, E., Stojanovic, A., Eisen, C., Quack, C., Falk, C. S., Umansky, V., & Cerwenka, A. (2012). Tumor-infiltrating monocytic myeloid-derived suppressor cells mediate CCR5-dependent recruitment of regulatory T cells favoring tumor growth. *The Jou/rnal of Immunology*, 1201018.

Schraml, BU & Reis e Sousa, C. (2015). Defining dendritic cells. *Curr Opin Immunol* 2015; 32: 13-20.
Schraufstatter, I U, Zhao, M, Khaldoyanidi, S K, DiScipio, R G (2012). The chemokine CCL18 causes maturation of cultured monocytes to macrophages in the M2 spectrum. *I Immunology*, 135, 287–298.

Schreiber, R. D., Old, L. J., & Smyth, M. J. (2011). Cancer immunoediting: integrating immunity's roles in cancer suppression and promotion. *Science*, *331*(6024), 1565-1570.

Schutyser, E., Struyf, S., & Van Damme, J. (2003). The CC chemokine CCL20 and its receptor CCR6. *Cytokine & Growth Factor Reviews*, *14*(5), 409-426.

Shieh, Y. S., Hung, Y. J., Hsieh, C. B., Chen, J. S., Chou, K. C., & Liu, S. Y. (2009). Tumor-associated macrophage correlated with angiogenesis and progression of mucoepidermoid carcinoma of salivary glands. *Annals of Surgical Oncology*, *16*(3), 751.

Sica A, Saccani A, Mantovani A (2002) Tumor-associated macrophages: a molecular perspective. *Int Immunopharmacol* 2:1045–1054.

a) Sica, A, Allavena, P, Mantovani, A (2008). Cancer related inflammation: The macrophage connection. *Cancer Letters*. Volume 267, Issue 2, Pages 204–215.

b) Sica, A., Larghi, P., Mancino, A., Rubino, L., Porta, C., Totaro, M.G., Rimoldi, M., Biswas, S.K., Allavena, P. and Mantovani, A., (2008). Macrophage polarization in tumour progression. In *Seminars in Cancer Biology* (Vol. 18, No. 5, pp. 349-355). Academic Press.

Sica, A, Schioppa, T, Mantovani, A, Allavena, P. (2006). Tumour-associated macrophages are a distinct M2 polarised population promoting tumour progression: potential targets of anti-cancer therapy. *European Journal of Cancer*;42:717-27, doi: 10.1016/j.ejca.2006.01.003.

Sica, A. & Mantovani, A. (2012). Macrophage plasticity and polarization: *in vivo* veritas. *The Journal of Clinical Investigation* 122, 787–795.

Sierra-Filardi, E., Nieto, C., Domínguez-Soto, Á., Barroso, R., Sánchez-Mateos, P., Puig-Kroger, A., López-Bravo, M., Joven, J., Ardavín, C., Rodríguez-Fernández, J.L. & Sánchez-Torres, C., (2014). CCL2 shapes macrophage polarization by GM-CSF and M-CSF: identification of CCL2/CCR2-dependent gene expression profile. *The Journal of Immunology*, p.1302821.

Skakkebæk, N. E., Meyts, R. D., & Main, K. M. (2001). Testicular dysgenesis syndrome: an increasingly common developmental disorder with environmental aspects: Opinion. *Human Reproduction*, *16*(5), 972-978.

Skinner, M. K., & Moses, H. L. (1989). Transforming growth factorβ gene expression and action in the seminiferous tubule: Peritubular cell-Sertoli cell interactions. *Molecular Endocrinology*, *3*(4), 625-634.

Sluijter, B., van den Hout, M. F., Koster, B. D., vn Leeuwen, P. A., Schneiders, F. L., van de Ven, R., & van der Eertwegh, A. J. (2015). Arming the melanoma SLN through local administration of CpG-B and GM-CSF: recruitment and activation of BDCA3/CD141+ DC and enhanced cross-presentation. *Cancer Immunology Research*,(5):495-505.

Smiraglia, D. J., Szymanska, J., Kraggerud, S. M., Lothe, R. A., PeltomaÈki, P., & Plass, C. (2002). Distinct epigenetic phenotypes in seminomatous and nonseminomatous testicular germ cell tumors. *Oncogene*, *21*(24), 3909.

Soria, G., & Ben-Baruch, A. (2008). The inflammatory chemokines CCL2 and CCL5 in breast cancer. *Cancer Letters*, *267*(2), 271-285.

Steensberg A., Fischer C.P., Keller C., Møller K., Pedersen B.K. IL-6 enhances plasma IL-1ra, IL-10, and cortisol in humans. *Am. J. Physiol. Endocrinol. Metab*., 285: E433-E437, 2003.

Steinman, R. M., & Hemmi, H. (2006). Dendritic cells: translating innate to adaptive immunity. *From Innate Immunity to Immunological Memory* (pp. 17-58). Springer, Berlin, Heidelberg.

Stout, R. D., Jiang, C., Matta, B., Tietzel, I., Watkins, S. K., & Suttles, J. (2005). Macrophages sequentially change their functional phenotype in response to changes in microenvironmental influences. *The Journal of Immunology*, *175*(1), 342-349.

Streilein, J. W. (1995). Unraveling immune privilege. *Science*, *270*(5239), 1158-1160.

Szarek, M., Bergmann, M., Konrad, L., Schuppe, H. C., Kliesch, S., Hedger, M. P., & Loveland, K. L. (2018). Activin A target genes are differentially expressed between normal and neoplastic adult human testes: clues to gonocyte fate choice. *Andrology*. 2018 Oct 13. doi: 10.1111/andr.12553.

Tran Janco, JM., Lamichhane, P., Karyampudi, L., Knutson, KL. (2015). Tumor-Infiltrating Dendritic Cells in Cancer Pathogenesis. *J. Immunology* 194:2985-2991.

Tung, K. S., & Teusher, C. (1995). Mechanisms of autoimmune disease in the testis and ovary. *Human Reproduction Update*, *1*(1), 35-50.

Ueno, T., Toi, M., Saji, H., Muta, M., Bando, H., Kuroi, K., Koike, M., Inadera, H., Matsushima, K. (2000). Significance of macrophage chemoattractant protein-1 in macrophage recruitment, angiogenesis, and survival in human breast cancer. *Clin Cancer Res*.6:3282-3289.

Urban, J. L., Shepard, H. M., Rothstein, J. L., Sugarman, B. J., & Schreiber, H. (1986). Tumor necrosis factor: a potent effector molecule for tumor cell killing by activated macrophages. *Proceedings of the National Academy of Sciences*, *83*(14), 5233-5237.

Ushida, H., Kawakami, T., Minami, K., Chano, T., Okabe, H., Okada, Y., & Okamoto, K. (2012). Methylation profile of DNA repetitive elements in human testicular germ cell tumor. *Molecular Carcinogenesis*, *51*(9), 711-722.

Van Beek, J. J., Wimmers, F., Hato, S. V., de Vries, I. J. M., & Skold, A. E. (2014). Dendritic cell cross talk with innate and innate-like effector cells in antitumor immunity: implications for DC vaccination. *Critical Reviews™ in Immunology*, *34*(6).

Van Elsas, A., Hurwitz, A. A., & Allison, J. P. (1999). Combination immunotherapy of B16 melanoma using anti–cytotoxic T lymphocyte–associated antigen 4 (CTLA-4) and granulocyte/macrophage colony-stimulating factor (GM-CSF)-producing vaccines induces rejection of subcutaneous and metastatic tumors accompanied by autoimmune depigmentation. *Journal of Experimental Medicine*, *190*(3), 355-366.

Veglia F. & Gabrilovich D. I. (2017). Dendritic cells in cancer: the role revisited. *Current Opinion in Immunology*, *45*, 43-51.

Vianello, E., Dozioa, F., Arnaboldia, M.G., Marazzia, C., Martinellia, J., Lamontb, L., Tacchinia, A., Sigrünerc, G., Schmitzc, M.M., Romanelli, M. C. (2016). Epicardial adipocyte hypertrophy: Association with M1-polarization and toll-like receptor pathways in coronary artery disease patients. *Nutrition, Metabolism and Cardiovascular Diseases*.Volume 26, Issue 3, March 2016, Pages 246–253.

Wang, M., Fijak, M., Hossain, H., Markmann, M., Nüsing, R. M., Lochnit, G., Hartmann, M. F., Wudy, S. A., Zhang, L., Gu, H., Konrad, L., Chakraborty, T., Meinhardt, A., Bhushan, S. (2017). Characterization of the Micro-Environment of the Testis that Shapes the Phenotype and Function of Testicular Macrophages. *J Immunol*, 1700162; DOI: https://doi.org/10.4049/jimmunol.1700162.

Wang, J., Wreford, N.G., Lan, H.Y., Atkins, R., Hedger, M.P. (1994). Leukocytepopulations of the adult rat testis following removal of the leydig cells bytreatment with ethane dimethane sulfonate and subcutaneous testosteroneimplants. *Biol. Reprod*. 51, 551–561.

Walton KL, Johnson KE, Harrison CA. (2017). Targeting TGF-β Mediated SMAD Signaling for the Prevention of Fibrosis. *Front Pharmacol*.8:461. doi: 10.3389/fphar.2017.00461.

Weagel, E., Smith, C., Liu, G. P., Robison, R., & O'Neill, K. (2015). Macrophage polarization and its role in cancer. *J. Clin. Cell Immunol*, *6*, 338.

Wei YQ, Hang ZB, Liu KF. In situ observation of inflammatory cell-tumour cell interaction in humans seminomas (germinomas): light, electron microscopic and immunohistochemical study. *Hum Pathol* 1992 :**23**; 421 – 428. PMID:1563744.

Wermann, H., Stoop, H., Gillis, A.J., Honecker, F., van Gurp, R.J., Ammerpohl, O., Richter, J., Oosterhuis, J.W., Bokemeyer, C. & Looijenga, L.H. (2010). Global DNA methylation in fetal human germ cells and germ cell tumours: association with differentiation and cisplatin resistance. *The Journal of Pathology*, *221*(4), pp.433-442.

Winnall, WR., Muir, JA. & Hedger, MP. (2011). Rat resident testicular macrophages have an alternatively activated phenotype and constitutively produce interleukin-10 in vitro. *Journal of Leukocyte Biology,* 90 133-143.

Wynn, T. A., Chawla, A., & Pollard, J. W. (2013). Macrophage biology in development, homeostasis and disease. *Nature*, *496*(7446), 445.

Xia, Y., Shen, S., Verma, IM. (2014). NF-κB, an active player in human cancers. *Cancer Immunology Research*. 2014;2(9):823-830. doi:10.1158/2326-6066.CIR-14-0112.

Yang, L., & Zhang, Y. (2017). Tumor-associated macrophages: from basic research to clinical application. *Journal of Hematology & Oncology*, *10*(1), 58.

Yasukawa, H., Ohishi, M., Mori, H., Murakami, M., Chinen, T., Aki, D., & Hirano, T. (2003). IL-6 induces an anti-inflammatory response in the absence of SOCS3 in macrophages. *Nature Immunology*, *4*(6), 551.

Yoshimura, A., Mori, H., Ohishi, M., Aki, D., & Hanada, T. (2003). Negative regulation of cytokine signaling influences inflammation. *Current Opinion in Immunology*, *15*(6), 704-708.

Young, J. C., Jaiprakash, A., Mithraprabhu, S., Itman, C., Kitazawa, R., Looijenga, L. H. J., & Loveland, K. L. (2011). TCam-2 seminoma cell line exhibits characteristic foetal germ cell responses to TGF-beta ligands and retinoic acid. *International Journal of Andrology*, *34*(4pt2), e204-e217.

Yuan, R., Chen, Y., He, X., Wu, X., Ke, J., Zou, Y., Cai, Z., Zeng, Y., Wang, L., Wang, J., & Fan, X. (2013). CCL18 as an independent favorable prognostic biomarker in patients with colorectal cancer. *Journal of Surgical Research*, *183*(1), pp.163-169.

Zhang, B., Yao, G., Zhang, Y., Gao, J., Yang, B., Rao, Z., & Gao, J. (2011). M2-polarized tumor-associated macrophages are associated with poor prognoses resulting from accelerated lymphangiogenesis in lung adenocarcinoma. *Clinics*, *66*(11), 1879-1886.

Zhang, F., Wang, H., Wang, X., Jiang, G., Liu, H., Zhang, G., Wang, H., Fang, R., Bu, X., Cai, S. and Du, J. (2016). TGF-β induces M2-like macrophage polarization via SNAIL-mediated suppression of a pro-inflammatory phenotype. *Oncotarget*, *7*(32), p.52294.

Zhang, X., Blenis, J., Li, H. C., Schindler, C., Chen-Kiang, S. (1995). Requirement of serine phosphorylation for formation of STAT-promoter complexes. *Science*, *267*(5206), 1990-1994.

Zhao, S., Zhu, W., Xue, S., Han, D. (2014). Testicular defense systems: immune privilege and innate Immunity. *Cellular & Molecular Immunology* 11, 428–437.

Zheng, W., Chen, J., Liu, C., Zhou, J., Zhu, C., Li, M., Fan, L., Duan, Y., Li, X. (2016). Immature CD11c+ myeloid dendritic cells with inflammatory and regulatory cytokine profile in human seminoma. *Int J Clin Exp Pathol 2016*;9(3):2803-2819.

10 ACKNOWLEDGEMENTS

I am very glad that I made the decision to be a part of the IRTG. I was able to make incredeable experiences during the last three years. Thus, I would like to thank for all of this opportunities I got.

I want to thank my supervisor Prof. Martin Bergmann, for his trust, knowledge and support during this hard time of my PhD. I learnt a lot about testicular histology and without him I never would have this knowledge in this area.

I want to thank Prof. Hans-Christian Schuppe for his great interest in my project, the interesting disscusions and his great willingness to help and support me in all stages of my PhD.

A big thank you to Daniela Fietz. During a PhD there are a lot of up and downs and Dani was always supportive and helpful, in a scientific way but also in a private way. Thank you, Dani!

Thank you to Prof. Kate Loveland, my Australian supervisor who has an impressive knowledge in reproductive biology and a supportive attitude. Consequently, I benefit from Kates expertise and knowledge. I also would like to thank Kate for all the scientifical discussions. I was able to learn from Kate and sometimes I feel like that I have her critical thinking in my mind. Thank you, Kate!

I would like to thank Prof. Tina Trenczek and PD Dr. Ellen Kauschke who showed me how interesting biology is. Both of them were always supportive and maybe without them I wouldn’t be here.

Thank you to Prof. Mark Hedger and Bruce Loveland for their professional help at different stages during this PhD.

I would like to thank all of my friends who were always supportive. A special thanks to Marco and my Australian roommates, Anthony and Melina.

Lastly, I want to thank my mother and sister for being incredibly supportive.

11 PUBLICATIONS

PUBLISHED ORIGINAL WORK

Loveland K, Klein B, **Pueschl D**, Indumathy S, Bergmann M, Loveland B, Hedger M and Schuppe HC. Cytokines in Male Fertility and Reproductive Pathologies: Immunoregulation and Beyond. Front. Endocrinol.doi: 10.3389/fendo.2017.00307

MANUSCRIPTS IN PROGRESS

Pueschl D, Klein B, Indumathy S, Klieschl S, Hedger M, Loveland K, Bergmann M, Schuppe H-C. Neoplasia in human testis: Evidence of functional polarization of macrophages and dendritic cells. Submission planned in November 2018.

Pueschl D, Hedger M, Loveland K, Bergmann M, Schuppe H-C. Testicular cancer: the functional role of Macrophage and Dendritic cell subsets. Review for Journal of Endocrinology (JOE). Submission planned in November 2018.

Pueschl D, Hedger M, Bergmann M, Schuppe H-C, Loveland K. Tumour cells influence macrophage polarization into immunosuppressive M2 macrophages. Submission planned in November 2018.

Indumathy S, **Pueschl D**, Schuppe H-C, Bergmann M, Da Silva N, Hickey MJ, Hedger M, Loveland K. Delineating the testicular leukocyte population in the adult mouse testis and the macrophage population during postnatal development. In preparation.

CONFERENCE ABSTRACTS

2018:

24-26 Oct., 2018 9th Copenhagen Workshop on Testicular Germ Cell Cancer, Copenhagen, Denmark (poster)
28th June-1th July, 2018 ASRI Annual Meeting American Society Reproductive Immunology, Shanghai, China (received ASRI Travel Award) (talk)

2017:

29th Nov, 2017 IRTG–CRH Melbourne Reproductive Health and Biology Workshop 2017, Clayton, Australia (talk)
27th Oct., 2017 10th Melbourne Cell and Developmental Biology Meeting, Melbourne, Australia (poster)
17-20 Sep, 2017 ASRI Annual Meeting American Society Reproductive Immunology, Chicago, USA (poster)
27-30 Aug, 2017 Annual Scientific Meetings of the Endocrine Society of Australia and the Society for Reproduction Biology 2017, Perth, (received Hudson Travel Award) (talk)
4th May, 2017 CRH “Immunology in Reproduction”, Hudson Institute, Clayton, Australia (talk)
15-17 Feb, 2017 50th Annual Conference of Physiology and Pathology of Reproduction and 42th Mutual Conference of Veterinary and Human Reproductive Medicine, Munich, Germany (talk)

2016:

20-21 Sep, 2016 9th GGL Annual Conference, Giessen, Germany (poster)
21-23 Sep, 2016 9th European Congress of Andrology, Rotterdam, Netherlands, (poster)
08-10 Sep, 2016 DGA conference, 28th Annual Conference of German Association of Andrology, Saarbrücken, Germany (talk)
11-15 Jun, 2016 19th European Testis workshop, St. Malo, France (talk)

12 DECLARATION

I declare that I have completed this dissertation single-handily without the unauthorized help of a second party and only with the assistance acknowledged therein. I have appropriately acknowledged and cited all text passages that are derived verbatim from or are based on the content of published work of others, and all information relating to verbal communications. I consent to the use of an anti-plagiarism software to check my thesis. I have abided by the principles of good scientific conduct laid down in the charter of the Justus Liebig University Giessen „Satzung der Justus-Liebig-Universität Gießen zur Sicherung guter wissenschaftlicher Praxis“ in carrying out the investigations described in the dissertation.

Ich erkläre: Ich habe die vorgelegte Dissertation selbstständig und ohne unerlaubte fremde Hilfe und nur mit den Hilfen angefertigt, die ich in der Dissertation angegeben habe. Alle Textstellen, die wörtlich oder sinngemäß aus veröffentlichten oder nicht veröffentlichten Schriften entnommen sind, und alle Angaben, die auf mündlichen Auskünften beruhen, sind als solche kenntlich gemacht. Bei den von mir durchgeführten und in der Dissertation erwähnten Untersuchungen habe ich die Grundsätze guter wissenschaftlicher Praxis, wie sie in der „Satzung der Justus-Liebig-Universität Giessen zur Sicherung guter wissenschaftlicher Praxis“ niedergelegt sind, eingehalten.